issn 0424-7116
An open-access journal by the German Quaternary Association
Editor-in-chief: Christopher Lüthgens

E&G

Quaternary Science Journal

Eiszeitalter und Gegenwart

Special issue

Geoarchaeology of the Nile Delta

Guest editors: Julia Meister, Eva Lange-Athinodorou and Tobias Ullmann

Copernicus Publications
The Innovative Open Access Publisher

E&G Quaternary Science Journal

An open-access journal of the German Quaternary Association

E&G Quaternary Science Journal (EGQSJ) is an interdisciplinary open-access journal published by the German Quaternary Association (DEUQUA) since 1951, and it is one of the longest-running journals related to Quaternary research. EGQSJ publishes peer-reviewed articles and express reports, as well as thesis abstracts related to Quaternary geology, paleo-environments, paleo-ecology, soil science, paleo-climatology, geomorphology, geochronology, archaeology, and geoarchaeology focussing on, but not limited to, research from central Europe.

Copernicus Publications
The Innovative Open Access Publisher

Copernicus Publications
Bahnhofsallee 1e
37081 Göttingen
Germany

Phone: +49 551 90 03 39 0
Fax: +49 551 90 03 39 70

publications@copernicus.org
https://publications.copernicus.org

Printed in Germany.
Schaltungsdienst Lange o.H.G.

ISSN 0424-7116

Published by Copernicus GmbH (Copernicus Publications) on behalf of the German Quaternary Association (DEUQUA).

Image credit:
Temple of Bastet at ancient Bubastis, located in the suburbs of Zagazig, southeastern Nile Delta, by Eva Lange-Athinodorou (26 March 2012)

E&G
Quaternary Science Journal
An open-access journal of the German Quaternary Association
https://www.eg-quaternary-science-journal.net/

E&G Quaternary Science Journal
An open-access journal of the German Quaternary Association
https://www.eg-quaternary-science-journal.net/

E&G Quaternary Science Journal
An open-access journal of the German Quaternary Association
https://www.eg-quaternary-science-journal.net/

Advisory board

Copernicus Publications
The Innovative Open Access Publisher

Editorial Support

Natascha Töpfer
editorial@copernicus.org

Publication Production

Sarah Schneemann
production@copernicus.org

E&G Quaternary Sci. J., 70, 187–190, 2021
https://doi.org/10.5194/egqsj-70-187-2021

Open Access E&G Quaternary Science Journal

Preface

Preface: Special issue "Geoarchaeology of the Nile Delta"

Julia Meister[1], **Eva Lange-Athinodorou**[2], **and Tobias Ullmann**[1]

[1]Chair of Physical Geography, Institute of Geography and Geology, University of Würzburg, 97074 Würzburg, Germany
[2]Chair of Egyptology, Institute for Ancient Studies, University of Würzburg, 97070 Würzburg, Germany

Correspondence: Julia Meister (julia.meister@uni-wuerzburg.de)

Relevant dates: Received: 9 June 2021 – Revised: 30 June 2021 – Accepted: 2 July 2021 – Published: 23 July 2021

How to cite: Meister, J., Lange-Athinodorou, E., and Ullmann, T.: Preface: Special issue "Geoarchaeology of the Nile Delta", E&G Quaternary Sci. J., 70, 187–190, https://doi.org/10.5194/egqsj-70-187-2021, 2021.

1 Geoarchaeology of the Nile Delta: research context and emerging fields

The Egyptian Nile Delta is the largest delta system in the Mediterranean region, covering about 24 000 km^2. As the most fertile region in North Africa, it is nowadays heavily used for agriculture and is home to about 60 million inhabitants. Today, there are only two estuarine branches in the Nile Delta (the Rosetta and Damietta branches), while for antiquity there are textual descriptions of up to seven major Nile branches that flowed through the delta. Major ancient Egyptian cities are found only in their immediate vicinity as these waterways were of great importance for intra-Egyptian traffic and trade, as well as for the availability of water. In addition, settlements were often built on their embankments for protection against the seasonal Nile floods. The Holocene dynamics of the ancient river network, therefore, influenced the ancient settlement activity in the Nile Delta (Butzer, 2002). However, these branches have been silted up or canalized and are usually no longer recognizable in the modern landscape, while the historical data allow for only a rough estimate of the former river courses and their chronology. Hence, the reconstruction of Holocene delta environments plays a central role in the study of human–environment interactions in ancient Egypt, and researchers working on this topic recognized the importance of the large river branches early on.

A pioneer in this field was Manfred Bietak who reconstructed the river courses of the eastern delta on the basis of the contour maps of the Survey of Egypt (Bietak, 1975). In the following years, the geoarchaeological survey of the Amsterdam University Expedition continued this line of research in the northeastern delta with more detailed investigations on the early historical periods of ancient Egypt (van den Brink et al., 1986; van Wesemael, 1988; de Wit, 1993). At the same time, the geological exploration, especially of the northern delta, progressed through the extensive drilling campaigns of the Mediterranean Basin Program of the Smithsonian Institute from 1985 to 1994, analysing a total of 87 boreholes on- and offshore. This project generated large amounts of new data on the Late Pleistocene and Holocene delta evolution (e.g. Coutellier and Stanley, 1987; Stanley and Warne, 1993; Stanley et al., 1996, 2004). Further on, the team of Jürgen Wunderlich (Goethe University Frankfurt) established a project on the Holocene development of the western Nile Delta, building a bridge between geography, geoarchaeology, and Egyptology (Wunderlich, 1988, 1989; Andres and Wunderlich, 1991). This project is still ongoing in cooperation with Robert Schiestl (University of Munich) and the German Archaeological Institute (DAI) in Cairo (Ginau et al., 2017, 2019, 2020; Altmeyer et al., 2021). In recent years further geoarchaeological ventures evolved in the Nile Delta. To name two, the "Delta Survey" of the Egypt Exploration Society has created a database available online of all visited tells throughout the delta, which is continually updated (Wilson and Grigoropoulos, 2009; Spencer, 2016), and it is also worth mentioning that there is the ongoing geoarchaeological exploration of the sacred landscape of Bubastis being carried out by the University of Würzburg (Lange-Athinodorou et al., 2019; Ullmann et al., 2019, 2020).

2 The contributions to this volume

This special issue includes primarily studies presented at the DFG-funded (German Research Foundation) international workshop “Geoarchaeology of the Nile Delta: Current Research and Future Prospects”, which took place in Würzburg in November 2019, pooling geoarchaeological case studies from different regions of the Nile Delta. Encompassing the broad interdisciplinary audience of the meeting, the nine articles in this special issue report on current geoarchaeological research projects in the Nile Delta and the application of innovative methods and approaches in this context, reflecting the wide range of current developments and challenges in geoarchaeological research in this region.

The study of Altmeyer et al. (2021) presents results on geophysical, stratigraphic, and pXRF surveys in the surroundings of the site Kom el-Gir in the northwestern Nile Delta. The synthesis of these investigations allows for a comprehensive reconstruction of a former fluvial network in the immediate surroundings of this site and confirms previous studies that suggested a larger Nile branch in this region.

The study of Crépy and Boussac (2021) investigates the palaeohydrology of ancient Lake Mareotis in the northwestern Nile Delta near the Mediterranean coast of Egypt, precursor of the modern Mariut lagoon, which acted as a gateway between the Nile valley and the Mediterranean Sea in ancient times. To reconstruct the extension of the western lake(s) at different periods, this study is based on the reassessment of geoarchaeological data and the analysis of early scholars’ accounts, maps, and satellite images. The data show that Lake Mareotis experienced a drawdown in its western part during the 1st millennium BCE, followed by the formation of several distinct lakes and building activities in emerging areas during the Hellenistic period. During the 2nd century CE several canals were dug to connect the sites of the western wadi Mariut to the eastern part of the Mariut basin, leading to a reconfiguration of the lake(s).

Based on the assumption that lake-level changes, connections with the Nile and the sea, and possible high-energy events considerably controlled the human occupation history of ancient Lake Mareotis, the study of Flaux et al. (2021) reconstructs the lake’s hydrology in historical times using faunal remains, geochemistry, and geoarchaeological indicators of relative lake-level changes. The data show both an increase in Nile sediment inputs to the basin during the 1st millennia BCE and CE and a lake-level rise of ca. 1.5 m during the Roman period. A high-energy deposit may explain an enigmatic sedimentary hiatus previously documented in the chronostratigraphy of the lake sediments.

The article of Khaled (2021) points out that the vast and fertile agricultural lands of the Nile Delta formed the backbone of the economy of the Old Kingdom. Foodstuffs and a wide variety of goods that were produced in this area were mandatory for the conduction of royal building projects like, for example, the erection of pyramids at the royal cemeteries in Sakkara, Giza, and other sites. To establish unhindered access to these resources, an effective administrative system came into place, based on the territorial distribution of the delta into districts, the so-called nomes. In these nomes, agricultural units (“domains”) produced, collected, and delivered agricultural products for the needs of the royal household. New pictorial and written evidence from the causeway of the pyramid of King Sahure at Abusir provides us with fresh information on the territorial administration of the Nile Delta in the 5th dynasty.

For a long time, ancient Egyptian texts and descriptions of Greek and Roman historiographers were the only available sources of information about water bodies as parts of the sacred landscape of temples in the Nile Delta. The recent introduction and application of geoarchaeological methods in archaeological projects, however, led to an unprecedented accumulation of new geophysical, sedimentological, and archaeological data which can be utilized to identify and locate lakes, canals, and river branches in close vicinity to the temple areas. The study of Lange-Athinodorou (2021) reviews the available geoarchaeological information on the temples of the cities of Buto, Sais, and Bubastis, which were home to important goddesses acknowledged all over Egypt, and compares these with the information coming from textual sources. The combined results allow for reconstructions of the most elemental parts of the sacred landscapes of those shrines, their role in religious and daily life activities, and their surrounding hydro-geography and natural landscapes.

In the absence of geoarchaeological indications, Schiestl (2021) applied a combined analysis of historical sources, satellite imagery, and the TanDEM-X digital elevation model to investigate the Butic Canal, a waterway that crossed the northern Nile Delta in a transversal way during Roman times. The detection of debris from the excavation of the canal, which became visible as a linear elevated feature in the digital elevation model, allowed for the identification of the eastern section of the canal. The discovery is of relevance as this artificial watercourse resulted from the need for a more economic and less time-consuming transportation route through the delta, and it was a manifestation of imperial investments in the infrastructure of the eastern part of the Roman Empire.

The study of Stanley and Wedl (2021) addresses the question of how climate and environmental changes affected the societies of Ancient Egypt. By examining marine sediments in the Levantine Basin, they were able to demonstrate reduced depositional accumulation rates and altered compositional attributes of the sediment facies mainly from 2300 to 2000 BCE. These effects were presumably triggered by displaced climatic belts leading to decreased rainfall and lower Nile flows, as well as modified oceanographic conditions. As a result agricultural production probably decreased significantly, possibly leading to a changed social, political, and economic situation that could have promoted the disintegration of the political system at the end of the Old Kingdom.

The study of Ullmann et al. (2020) analyses Landsat remote sensing data, acquired between 1985 and 2019 for the entire Nile Delta, to detect surface anomalies that are potentially related to buried near-surface palaeogeographical features. Using the normalized difference wetness index calculated for months with low and high evapotranspiration, anomalies in the immediate surroundings of several Pleistocene sand hills ("geziras") and tells of the eastern delta were identified. This approach allowed them to map the potential near-surface continuation of these geziras and the indication of buried river branches in the northern and eastern Nile Delta.

The paper of Wilson and Ghazala (2021) investigates the embedding of the ancient city of Sais (Sa el-Hagar) within the surrounding natural landscape of the western-central Nile Delta and explores the possibility that certain features of the landscape influenced the choice of the settlement location. By combining geological, geophysical, remote sensing, and archaeological data, this study aims to describe and reconstruct the deltaic environs and hydro-geography of Sais. A special focus lies on the question of if research can determine the specific nature of human interactions with the landscape, i.e. if human occupants reacted in a proactive or reactive manner. The study shows that over a period of several millennia (i.e. from around 4000 BCE to the modern day) the settlement at Sais occupied several locations in the immediate environs of a moving Nile branch. Ultimately, the positive effects of the local hydrography led to the establishment of a capital city in the 7th century BCE.

3 Current challenges and future research

The aforementioned emerging fields of geoarchaeological research are accompanied by several challenges. These include the rapid expansion of modern settlements due to the rapidly growing population, leading to overbuilding and thus the endangerment of archaeological sites. In addition, the continuing sea-level rise is gradually submerging the coastal regions of the Nile Delta. In order to quickly advance research and to generate as much data as possible in the relatively short time remaining, as well as to further develop the field of geoarchaeology in the Nile Delta, the cooperation of existing projects and the establishment of new projects in close collaboration with the Ministry of State for Antiquities of Egypt is therefore all the more important in the coming years. Moreover, the application and further development of interdisciplinary methods and models have a key position in this process.

Code and data availability. Information provided throughout the text is available in previously published studies by authors cited throughout the text and listed in the references.

Author contributions. The manuscript was prepared by JM, ELA, and TU.

Disclaimer. Publisher's note: Copernicus Publications remains neutral with regard to jurisdictional claims in published maps and institutional affiliations.

Special issue statement. This article is part of the special issue "Geoarchaeology of the Nile Delta". It is a result of the workshop "Geoarchaeology of the Nile Delta: Current Research and Future Prospects", Würzburg, Germany, 29–30 November 2019.

Acknowledgements. We gratefully thank all authors for their contributions to this special issue. We also kindly thank Hans von Suchodoletz and one anonymous reviewer for constructive comments and suggestions.

Financial support. This open-access publication was funded by Julius-Maximilians-Universität Würzburg.

Review statement. This paper was edited by Hans von Suchodoletz and reviewed by one anonymous referee.

References

Altmeyer, M., Seeliger, M., Ginau, A., Schiestl, R., and Wunderlich, J.: Reconstruction of former channel systems in the northwestern Nile Delta (Egypt) based on corings and electrical resistivity tomography (ERT), E&G Quaternary Sci. J., 70, 151–164, https://doi.org/10.5194/egqsj-70-151-2021, 2021.

Andres, W. and Wunderlich, J.: Late Pleistocene and Holocene Evolution of the Eastern Nile Delta and Comparisons with the Western Delta, in: Von der Nordsee bis zum Indischen Ozean. Ergebnisse der 8. Jahrestagung des AK Geographie der Meere und Küsten, 13.–15. Juni 1990, Düsseldorf, edited by: Brückner, H. and Ratdke, U., Stuttgart, 121–130, 1991.

Bietak, M.: Tell el-Dab'a II, Der Fundort im Rahmen einer archäologisch-geographischen Untersuchung über das ägyptische Ostdelta, Austrian Academy of Sciences Press, Wien, 1975.

Butzer, K. W.: Geoarchaeological implications of recent research in the Nile Delta, in: Egypt and the Levant: Interrelations from the 4th through the Early 3rd Millennium BCE, edited by: van den Brink, E. C. M. and Levy, T. E., Leicester University Press, London, New York, 83–97, 2002.

Coutellier, V. and Stanley, D. J.: Late Quaternary stratigraphy and paleogeography of the eastern Nile Delta, Egypt, Mar. Geol., 77, 257–275, https://doi.org/10.1016/0025-3227(87)90116-2, 1987.

Crépy, M. and Boussac, M.-F.: Western Mareotis lake(s) during the Late Holocene (4th century BCE–8th century CE): diachronic evolution in the western margin of the Nile Delta and evidence for the digging of a canal complex during the early Roman period, E&G Quaternary Sci. J., 70, 39–52, https://doi.org/10.5194/egqsj-70-39-2021, 2021.

de Wit, H. E.: The evolution of the eastern Nile Delta as a factor in the development of human culture, in: Environmental change and human culture in the Nile Basin and Northern Africa until the second millennium B.C, edited by: Krzyżaniak, L., Kobusiewicz, M., and Alexander, J., Poznan Archaeological Museum, Poznań, 305–320, ISBN 978-83-900434-1-8, 1993.

Flaux, C., Giaime, M., Pichot, V., Marriner, N., el-Assal, M., Guihou, A., Deschamps, P., Claude, C., and Morhange, C.: The late Holocene record of Lake Mareotis, Nile Delta, Egypt, E&G Quaternary Sci. J., 70, 93–104, https://doi.org/10.5194/egqsj-70-93-2021, 2021.

Ginau, A., Schiestl, R., Kern, F., and Wunderlich, J.: Identification of historic landscape features and settlement mounds in the Western Nile Delta by means of remote sensing time series analysis and the evaluation of vegetation characteristics, J. Archaeol. Sci. Rep., 16, 170–184, https://doi.org/10.1016/j.jasrep.2017.09.034, 2017.

Ginau, A., Schiestl, R., and Wunderlich, J.: Integrative geoarchaeological research on settlement patterns in the dynamic landscape of the northwestern Nile delta, Quat. Int., 511, 51–67, https://doi.org/10.1016/j.quaint.2018.04.047, 2019.

Ginau, A., Steiniger, D., Hartmann, R., Hartung, U., Schiestl, R., Altmeyer, M., Seeliger, M., and Wunderlich, J.: What settlements leave behind – pXRF compositional data analysis of archaeological layers from Tell el-Fara’in (Buto, Egypt) using machine learning, Palaeogeogr. Palaeocl., 546, 109666, https://doi.org/10.1016/j.palaeo.2020.109666, 2020.

Khaled, M. I.: Nomes of Lower Egypt in the early Fifth Dynasty, E&G Quaternary Sci. J., 70, 19–27, https://doi.org/10.5194/egqsj-70-19-2021, 2021.

Lange-Athinodorou, E.: Implications of geoarchaeological investigations for the contextualization of sacred landscapes in the Nile Delta, E&G Quaternary Sci. J., 70, 73–82, https://doi.org/10.5194/egqsj-70-73-2021, 2021.

Lange-Athinodorou, E., El-Raouf, A. A., Ullmann, T., Trappe, J., Meister, J., and Baumhauer, R.: The sacred canals of the Temple of Bastet at Bubastis (Egypt): New findings from geomorphological investigations and Electrical Resistivity Tomography (ERT), J. Archaeol. Sci. Rep., 26, 101910, https://doi.org/10.1016/j.jasrep.2019.101910, 2019.

Schiestl, R.: A new look at the Butic Canal, Egypt, E&G Quaternary Sci. J., 70, 29–38, https://doi.org/10.5194/egqsj-70-29-2021, 2021.

Spencer, J.: The Delta Survey, 2009–2015, Egypt Exploration Society, Excavation Memoir 112, London, 31 pp., ISBN 978 0 85698 225 5, 2016.

Stanley, D. J. and Warne, A. G.: Nile Delta: Recent Geological Evolution and Human Impact, Science, 260, 628–634, https://doi.org/10.1126/science.260.5108.628, 1993.

Stanley, D. J., McRea, J. E., and Waldron, J. C.: Nile Delta drill core and sample database for 1985–1994: Mediterranean Basin (MEDIBA) Program, Smithson. Contrib. Mar. Sci., 1–428, https://doi.org/10.5479/si.01960768.37.1, 1996.

Stanley, J., Warne, A., and Schnepp, G.: Geoarchaeological Interpretation of the Canopic, Largest of the Relict Nile Delta Distributaries, Egypt, J. Coast. Res., 203, 920–930, https://doi.org/10.2112/1551-5036(2004)20[920:GIOTCL]2.0.CO;2, 2004.

Stanley, J.-D. and Wedl, S. E.: Significant depositional changes offshore the Nile Delta in late third millennium BCE: relevance for Egyptology, E&G Quaternary Sci. J., 70, 83–92, https://doi.org/10.5194/egqsj-70-83-2021, 2021.

Ullmann, T., Lange-Athinodorou, E., Göbel, A., Büdel, C., and Baumhauer, R.: Preliminary results on the paleo-landscape of Tell Basta /Bubastis (eastern Nile delta): An integrated approach combining GIS-Based spatial analysis, geophysical and archaeological investigations, Quat. Int., 511, 185–199, https://doi.org/10.1016/j.quaint.2017.12.053, 2019.

Ullmann, T., Nill, L., Schiestl, R., Trappe, J., Lange-Athinodorou, E., Baumhauer, R., and Meister, J.: Mapping buried paleogeographical features of the Nile Delta (Egypt) using the Landsat archive, E&G Quaternary Sci. J., 69, 225–245, https://doi.org/10.5194/egqsj-69-225-2020, 2020.

van den Brink, E. C. M., van Wesemael, B., and Dirksz, P.: A geoarchaeological survey in the north-eastern Nile Delta, Mitteilungen Dtsch. Archäol. Inst. Abt. Kairo, 43, 7–31, 1986.

van Wesemael, B.: The relation between natural landscape and distribution of archaeological remains in the Northeastern Nile Delta, in: The archaeology of the Nile Delta, Egypt: problems and priorities, in: Proceedings of the seminar held in Cairo, 19–22 October 1986, on the occasion of the fifteenth anniversary of the Netherlands Institute of Archaeology and Arabic Studies in Cairo, edited by: van den Brink, E. C. M., Amsterdam, 125–139, 1988.

Wilson, P. and Ghazala, H.: Sandhills, sandbanks, waterways, canals and sacred lakes at Sais in the Nile Delta, E&G Quaternary Sci. J., 70, 129–143, https://doi.org/10.5194/egqsj-70-129-2021, 2021.

Wilson, P. and Grigoropoulos, D.: The West Nile Delta Regional Survey, Beheira and Kafr El-Sheikh Provinces, Egypt Exploration Society, Excavation Memoir 86, London, 490 pp., ISBN 978 0 85698 194 4, 2009.

Wunderlich, J.: Investigations on the development of the Western Nile Delta in Holocene times, in: The archaeology of the Nile Delta, Egypt: problems and priorities, Proceedings of the seminar held in Cairo, 19–22 October 1986, edited by: van den Brink, E. C. M., Amsterdam, 251–257, 1988.

Wunderlich, J.: Untersuchungen zur Entwicklung des westlichen Nildeltas im Holozän, Marburger Geographische Gesellschaft, Marburg/Lahn, ISBN 978-3-8835-3038-3, 1989.

E&G Quaternary Sci. J., 70, 151–164, 2021
https://doi.org/10.5194/egqsj-70-151-2021

Open Access E&G Quaternary Science Journal

Research article

Reconstruction of former channel systems in the northwestern Nile Delta (Egypt) based on corings and electrical resistivity tomography (ERT)

Marina Altmeyer[1], Martin Seeliger[1], Andreas Ginau[1], Robert Schiestl[2], and Jürgen Wunderlich[1]

[1]Department of Physical Geography, Goethe University Frankfurt, Frankfurt a. M., 60438, Germany
[2]Department of Ancient History, Ludwig Maximilian University of Munich, Munich, 80539, Germany

Correspondence: Marina Altmeyer (marina.altmeyer@gmx.de)

Relevant dates: Received: 30 September 2020 – Revised: 30 March 2021 – Accepted: 16 April 2021 – Published: 18 June 2021

How to cite: Altmeyer, M., Seeliger, M., Ginau, A., Schiestl, R., and Wunderlich, J.: Reconstruction of former channel systems in the northwestern Nile Delta (Egypt) based on corings and electrical resistivity tomography (ERT), E&G Quaternary Sci. J., 70, 151–164, https://doi.org/10.5194/egqsj-70-151-2021, 2021.

Abstract: The current state of research about ancient settlements within the Nile Delta allows the hypothesizing of fluvial connections to ancient settlements all over the Nile Delta. Previous studies suggest a larger Nile branch close to Kom el-Gir, an ancient settlement hill in the northwestern Nile Delta. To contribute new knowledge to this little-known site and prove this hypothesis, this study aims at using small-scale paleogeographic investigations to reconstruct an ancient channel system in the surroundings of Kom el-Gir. The study pursues the following: (1) the identification of sedimentary environments via stratigraphic and portable X-ray fluorescence (pXRF) analyses of the sediments, (2) the detection of fluvial elements via electrical resistivity tomography (ERT), and (3) the synthesis of all results to provide a comprehensive reconstruction of a former fluvial network in the surroundings of Kom el-Gir. Therefore, auger core drillings, pXRF analyses, and ERT were conducted to examine the sediments within the study area. Based on the evaluation of the results, the study presents clear evidence of a former channel system in the surroundings of Kom el-Gir. Thereby, it is the combination of both methods, 1-D corings and 2-D ERT profiles, that derives a more detailed illustration of previous environmental conditions which other studies can adopt. Especially within the Nile Delta which comprises a large number of smaller and larger ancient settlement hills, this study's approach can contribute to paleogeographic investigations to improve the general understanding of the former fluvial landscape.

Kurzfassung: Der derzeitige Stand der Forschung über antike Siedlungen im Nildelta erlaubt es, Hypothesen fluvialer Verbindungen zu antiken Siedlungen im gesamten Nildelta aufzustellen. Frühere Studien deuten auf einen größeren Nilarm in der Nähe des Kom el-Girs, einem antiken Siedlungshügel im nordwestlichen Nildelta, hin. Um neue Erkenntnisse zu dieser wenig bekannten Stätte zu gewinnen und diese Hypothese zu beweisen, zielt diese Studie auf kleinräumige paläogeographische Untersuchungen zur Rekonstruktion eines antiken Kanal-/Rinnensystems in der Umgebung des Kom el-Girs ab. Die Studie verfolgt: (1) die Identifizierung von Sedimentationsmilieus mittels stratigraphischer und pXRF-

Analysen, (2) den Nachweis fluvialer Strukturen mittels elektrischer Widerstandsmessung (ERT) und (3) die Synthese aller Ergebnisse, um eine umfassende Rekonstruktion eines ehemaligen fluvialen Netzwerkes in der Umgebung des Kom el-Girs zu erstellen. Dazu wurden Rammkernsondierungen, pXRF-Analysen und elektrische Widerstandsmessungen (ERT) durchgeführt, um die Sedimente innerhalb des Untersuchungsgebietes zu beschreiben. Die Auswertung der Ergebnisse zeigt deutliche Hinweise auf ein ehemaliges Kanal-/Rinnensystem in der Umgebung des Kom el-Girs. Dabei ist es die Kombination beider Methoden, der 1D-Bohrungen und 2D-ERT-Profile, die eine detailliertere Darstellung früherer Umweltbedingungen ermöglicht und die von anderen Studien übernommen werden kann. Besonders im Nildelta mit seiner großen Anzahl kleinerer und größerer antiker Siedlungshügel, kann der Ansatz dieser Studie in weiteren paläogeographischen Untersuchungen Anwendung finden, um das allgemeine Verständnis ehemaliger Flusslandschaften zu verbessern.

1 Introduction

The Nile Delta (Fig. 1) has been settled and cultivated since the Neolithic period as the earliest known archeological remains within the delta from ca. 4530 BCE reveal (Butzer, 2002). The connection of ancient settlements to former Nile branches is considered an essential factor for the vitality of a settlement to supply people and animals with fresh water, to irrigate fields, or as a connection to the transport system (Bietak, 1975; Lange et al., 2016; Schiestl, 2018; Ginau et al., 2019). Therefore, elevated levees or relict dunes near watercourses offered favorable conditions to settle due to the combination of assured protection from the annual Nile flood while providing access to water supply (Wunderlich, 1989; El Gamili et al., 2001; Schiestl, 2018). Based on a high-resolution TanDEM-X image, Ginau et al. (2019) presented the first detailed illustration of a former fluvial landscape (Fig. 2) in the regional context of the northwestern Nile Delta. Kom el-Gir (KeG), an ancient settlement site in the area of interest (Figs. 2, 3), presumably represents a favored place with a hypothesized connection to a larger former Nile branch (Schiestl, 2019). To prove this assumption, this study aims to explore the subsurface sediments in the surroundings of KeG to obtain a comprehensive view of the paleoenvironmental conditions in this area. In this context, core drillings are widely adopted for scientific investigations into paleoenvironmental reconstructions (Marriner et al., 2012; Pint et al., 2015; Morhange et al., 2016; Seeliger et al., 2018). In addition to core drillings, electrical resistivity tomography (ERT) offers great opportunities for near-subsurface investigations in general (Toonen et al., 2018; Wunderlich et al., 2018) and was previously applied within the Nile Delta (El Gamili et al., 1994, 2001).

Therefore, the study applies a combination of methods to

1. identify and classify sedimentary environments (e.g., riverbed/channel, floodplain) via coring followed by portable X-ray fluorescence (pXRF) analyses of sampled sediments
2. detect fluvial elements (e.g., channel, levee, floodplain) along transects via electrical resistivity tomography (ERT)
3. interpret and correlate all results to combine the point-like coring data with the two-dimensional data of the ERT in order to derive a reconstruction of a former channel system.

2 Study area

2.1 Geographical setting

KeG is located in the northwestern Nile Delta, approx. 20 km south of Lake Burullus and 16 km east of the Rosetta branch (Figs. 1, 2). It represents a former settlement hill with a present-day extent of approx. 20 ha and a maximum elevation of ca. 5 m above the Nile Delta floodplain.

The lithology of the Nile Delta floodplain is characterized by alluvial accumulations dominated by late Neo-Nile deposits (Bilqas Formation), which are overlying the Pre-Nile sediments (Mit Ghamr Formation) at greater depths (Rizzini et al., 1978; Pennington et al., 2017; Gebremichael et al., 2018). Today's uppermost deposits, the so-called Nile mud, represent aggrading clastic sediments that mainly originated as Nile alluvium from the Ethiopian Highlands during the Holocene. Within the delta, the predominantly clayey and silty sediments reach a thickness of 10–15 m (Andres and Wunderlich, 1986; Wunderlich, 1988, 1989; Woodward et al., 2015; Ginau et al., 2019). These sediments overlie deposits, which mainly consist of fine to medium sands. They are distinguished from the overlying sediments by lighter colors and the appearance of a post-sedimentary lime formation within the upper section. This lime formation was dated by Wunderlich (1989) and verified the sedimentation during the Pleistocene (Wunderlich, 1989; El Gamili et al., 1994).

2.2 Historical background of KeG

Recent investigations of the *kom*'s area and pottery from the surface and from corings on the site date the settlement from

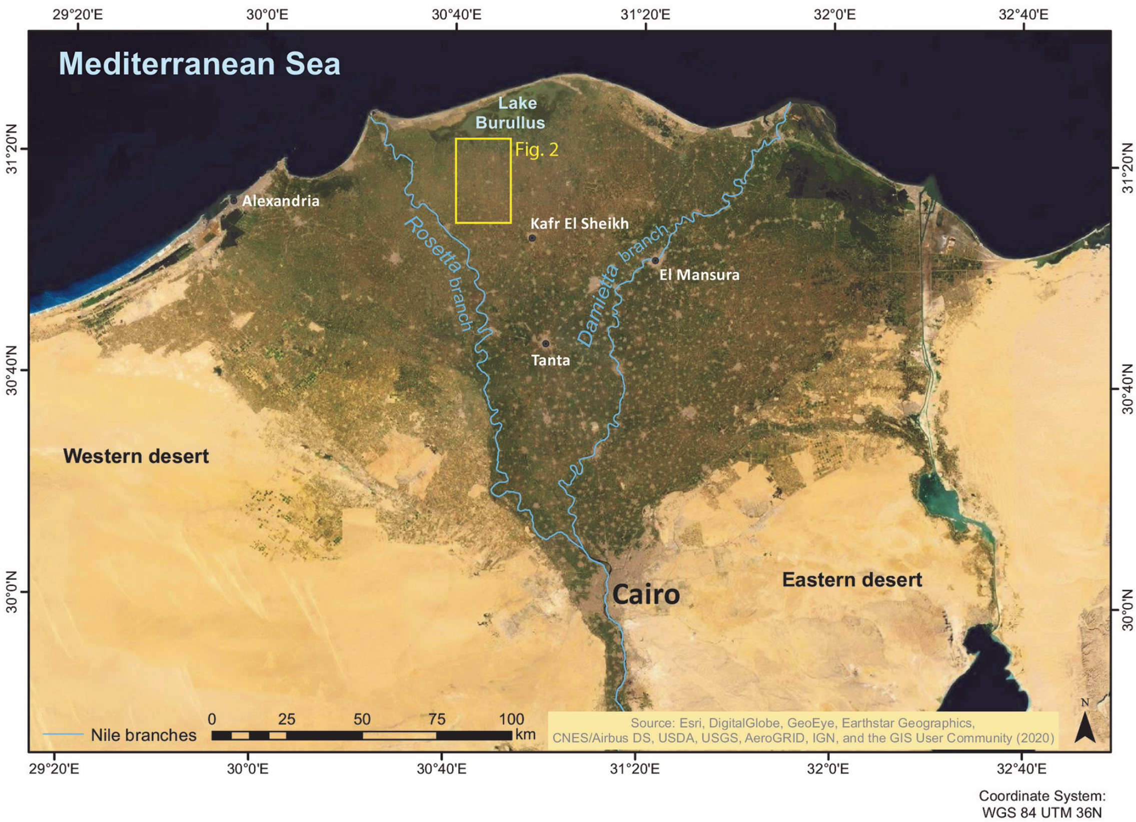

Figure 1. Regional area of interest (yellow frame) located in the northwestern Nile Delta.

the Ptolemaic (late 4th–1st century BCE) to the Late Roman period (4th–7th century CE) (Schiestl, 2012; Schiestl and Herbich, 2013; Schiestl, 2019). Investigations via magnetic prospection further revealed a densely occupied settlement covered with buildings 8 to 10 m wide as well as additional bigger enclosures. Those are interpreted as a temple enclosure and a Late Roman fort (Schiestl and Rosenow, 2016). Within the Nile Delta, it is the first archeological evidence for the existence of a Roman fort (Schiestl and Herbich, 2013; Schiestl, 2015, 2019). As transport by ship was common during those days, the presumed function and given knowledge about the founding of former settlements support the hypothesis that KeG was connected to a substantial watercourse (Ginau et al., 2019; Schiestl, 2019).

3 Material and methods

To combine and correlate the results of all applied methods, lateral and vertical changes in the subsurface sediment stratigraphy were investigated performing auger core drillings, followed by pXRF analyses of the core sediments as well as electrical resistivity tomography (ERT) measurements.

3.1 Geoarcheological fieldwork

Auger core drillings were performed using a vibracorer (Wacker EH 23/230) with open steel auger heads of 8, 6, and 5 cm diameter and 1 m length. The drillings reached a maximum depth of 11 m. These recorded the Holocene sedimentary sequence, which normally has a thickness of less than 10 m (Wunderlich and Andres, 1991). The positions of each drilling location to the north and east of KeG (Fig. 3) were based on prior investigations of Ginau et al. (2019) and measured using a global navigation satellite system (Topcon GR-5, accuracy of ≤ 2 cm in all three dimensions). The altitude given in m a.s.l. (meters above recent sea level) is based on the local reference system, established by the German Archaeological Institute (in German, Deutsches Archäologisches Institut – DAI) and its excavation team of Buto (Ginau et al., 2019). Retrieved sediments were lithologically described via grain size and lime content (10 % HCl) estimations according to German soil classification (Ad-Hoc-AG Boden, 2005). In addition to this, color (Munsell soil color charts) and special findings (ceramic fragments, mollusks, shell fragments, charcoal, plant remains, etc.) were documented. Based on the specific sedimentological characteristics of the core material, bulk samples for laboratory analyses were taken from the open sediment cores.

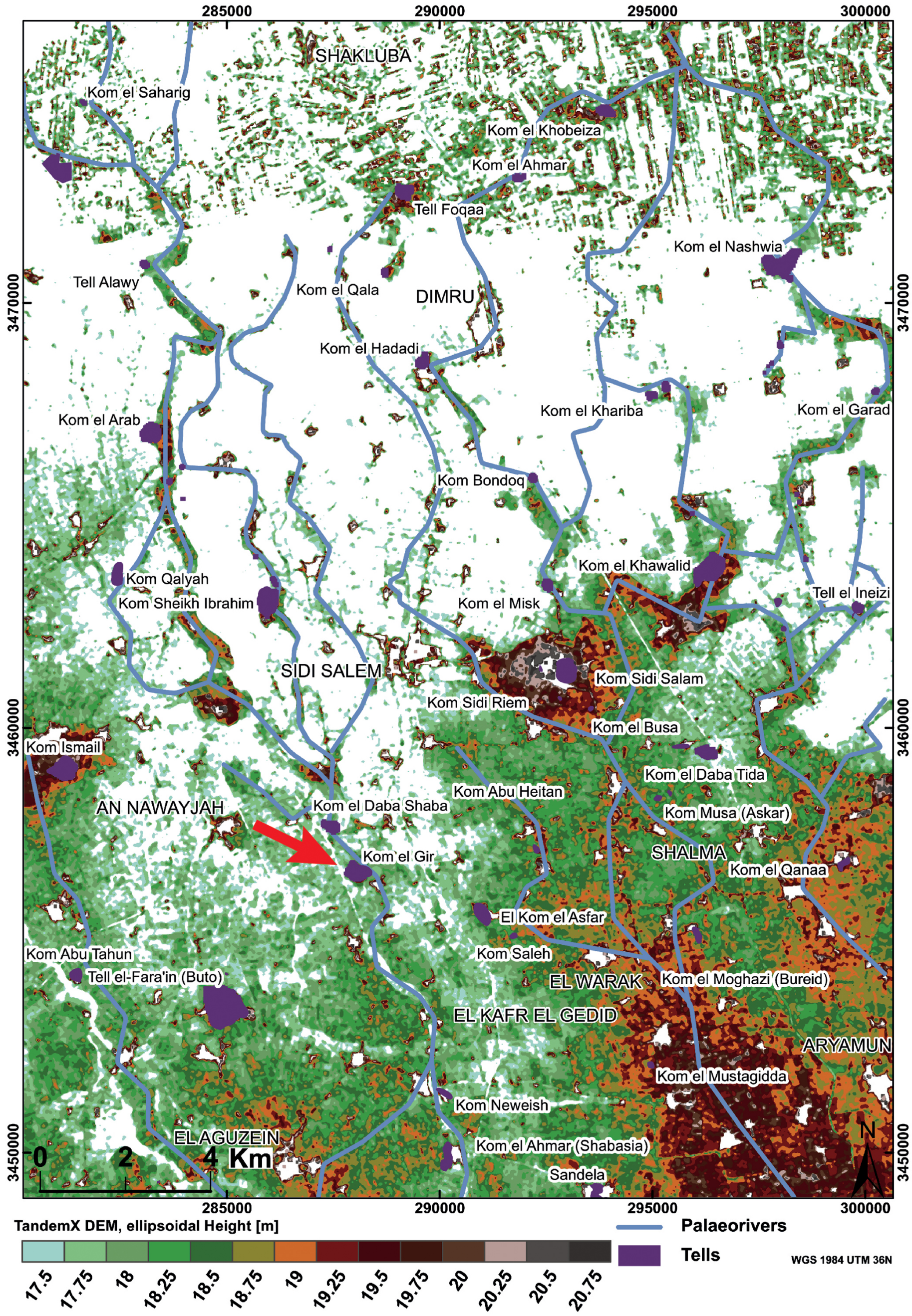

Figure 2. TanDEM-X image of the regional area of interest in the northwestern Nile Delta. The red arrow highlights Kom el-Gir (Ginau et al., 2019; German Aerospace Center).

3.2 Geochemical analysis via pXRF

All sample preparation procedures for the subsequent pXRF analyses adhered to a standardized process flow to reduce the influences on the samples, especially due to missing laboratory facilities and equipment on-site. For each core sample, a reduced sediment mass representing a mix of the overall sample was dried in an oven at 100 °C for at least 12 h. To produce a homogenous, fine-grained powder, the dried samples were ground in an agate mortar. Through this approach, the results of the conducted pXRF analysis are representative and a true achievement of the respective geochemical signals of the sample is ensured. The ground sample powder was packed into a special XRF plastic cylinder and coated with a 4 µm thick XRF foil that allows the best penetration of the fluorescence radiation (Ginau et al., 2019). The sediment samples were analyzed using a Niton XL3t 980-He portable XRF (pXRF) device equipped with an Ag anode.

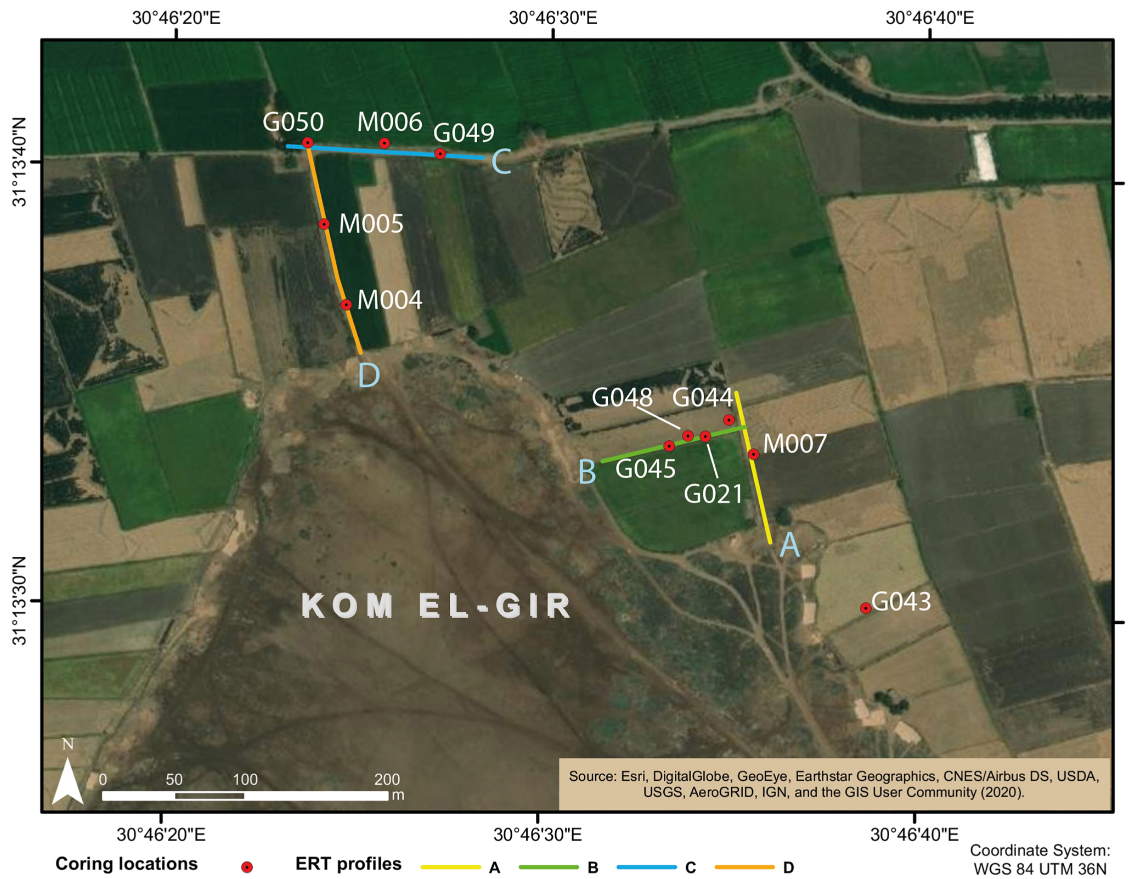

Figure 3. Locations of performed corings and ERT profiles within the study area located north and northeast of KeG.

The measurements were performed under standardized conditions using a measurement chamber. According to testing and calibration within prior research work, the measurement parameters were set to 180 s using the AllGeo mode that combines the soil and mining mode of the device. During measurements, helium was induced into the detector unit of the device. The application of helium allows the reduction of the measurement times and preserves the necessary precision for the detection of light elements such as phosphor (Ginau et al., 2020).

3.3 Data analysis

In addition to the applied methods performed on-site, possible sources of error were considered in order to prepare and analyze the sampled data. Therefore, zero values or values below the limit of detection (LOD), which occur due to the inaccurate precision of the measurement method, were excluded according to the calculated detection limits of Ginau et al. (2020). Based on relevant literature and given geochemical signals used in paleoenvironmental studies (Kern et al., 2019), specific elements or element ratios were selected as potential proxies (Table 1).

3.4 Electrical resistivity tomography (ERT)

In total, four profiles (100–150 m length) of electrical resistivity measurements reaching from the edges of KeG into the adjacent fields were made employing a multi-electrode setup with 24 electrodes using Lippmann 4point light HP equipment. This was considered the appropriate method to detect lateral facies changes down to sounding depths of ca. 10 m. The resistivity distribution was determined by inversions according to the Levenberg–Marquardt algorithm. The profiles were placed alongside the positions of recently performed corings (Fig. 3) to correlate the results of both applied methods. Profiles A–C are presented in Fig. 5, whereas profile D was excluded due to problems during the measurements.

4 Results

To investigate the study area, seven corings were performed in the northern and northeastern surroundings of KeG (Fig. 3). Due to the small extent of the study area and resulting resemblance of the retrieved core sediments, coring M006 is presented exemplarily in detail (Fig. 4).

Table 1. Selected elements used as geochemical proxies.

Element	Proxy for	Corresponding references
Zr	terrigene influence	Eckert (2014)
Fe, Al	fluvial influence (strongly enriched in Blue Nile draining), terrigenous origin	Vött et al. (2002), Revel et al. (2010), Eckert (2014), Pint et al. (2015), Pennington et al. (2019)
Fe, S	reducing/anoxic conditions	Revel et al. (2010), Eckert (2014), Martinez-Ruiz et al. (2015), Pennington et al. (2019), Emmanouilidis et al. (2020)
Ca	eolian deposit	Woronko (2012)
Cu	anthropogenic influence	Pint et al. (2015), Delile et al. (2018)
Element ratio		
Ca/Fe	dominating terrestrial (or fluvial) influences (in favor of iron)	Pint et al. (2015)
Ca/Ti	relative contributions of eolian (in favor of Ca) vs. fluvial (in favor of Ti) input	Vött et al. (2002), Blanchet et al. (2015), Pint et al. (2015), Castañeda et al. (2016), Pennington et al. (2019)
Cu/Zn	nature of river sediments (natural watercourses vs. human-constructed canals)	Ginau et al. (2019)

4.1 Coring M006

M006 (31.22794° N, 30.773801° E; 2.178 m a.s.l., depth: 11 m) is situated approx. 135 m north of the northern edge of the present-day *kom* area (Figs. 3, 4). The lowermost sediments between 11.00 and 6.00 m b.s. (meters below modern surface) are made of well-sorted silty medium sand, associated with ceramic fragments and mica. The pXRF values of this section reveal strongly fluctuating Ca/Fe and Ca/Ti ratios and Fe and Al concentrations. The S concentration of the lowermost section is around 250 ppm with an increasing trend towards upper sections. The Cu/Zn ratio shows strong fluctuations between 0.0 and 2.0 while the Zr concentration fluctuates around 320 ppm up to ca. 3.00 m b.s.

Between 6.00 and 2.70 m b.s., the sediment sequence shows alternating layers (mm–cm) of silty fine sand and medium sand. The intercalation of fS and mS shows more fluctuations in the element ratios with a high peak (2.7 for Ca/Fe and 9.0 for Ca/Ti) in favor of Ca at approx. 4.50 m b.s. Fe and Al concentrations remain fluctuating before values reveal a gradual increasing trend from 4.00–2.70 m b.s. After an S peak of 500 ppm, the values gradually decrease with a few anomalies. Only within the upper fS unit is no S concentration detected. The Cu/Zn ratio as well as Zr further fluctuates until 3.00 m b.s. where the Zr concentration begins to increase gradually.

Within the overlying material (2.70–1.70 m b.s.), silty fine sand dominates the sediment sequence. The Ca/Fe and Ca/Ti ratios consistently range around 0.5 (Ca/Fe) and 3.0 (Ca/Ti), while the Fe and Al concentrations are generally high with a gradual increase towards the upper sediment section. In contrast to lower core sections, the Cu/Zn ratio shows slightly fewer variations and weaker amplitudes. At 1.90 m b.s., the Zr concentration reaches its maximum of approx. 680 ppm within the uppermost Ufs unit.

Between 1.70 and 1.00 m b.s., silty fine sand within the lower section gradually transitions into fine sandy silt towards the upper parts. In contrast to underlying sections, these sediments reveal a medium lime content of c1–c3. Between 2.00 and 0.30 m b.s., the S concentration ranges around 0 and 350 ppm.

The uppermost material (1.00–0.30 m b.s.) consists of clay intercalated by silty clay, showing decreasing Ca/Fe and Ca/Ti ratios in favor of Ca, while Fe and Al concentrations gradually increase. The Zr concentration reveals gradually decreasing values around 240 ppm.

4.2 ERT profiles

The ERT profiles measured the electrical resistivity of the subsurface sediments over a length of 100–150 and 8–10 m depth with a total resistivity range from less than 2.5 Ωm to approx. 40.0 Ωm (Figs. 3, 5).

The lowest resistivity (<2.5–10.0 Ωm) was predominantly measured within the topmost subsurface sediments, partially reaching into deeper surface areas and occurring as lenses (Fig. 5a, b). Medium values of electrical resistivity (10.0–20.0 Ωm) are observed within various profile areas. They are present within middle profile sections as well as within near-tell areas. Sediments of higher electrical resistivity (20.0–40.0 Ωm) are predominantly located below the top layer of low resistivity and within deeper profile sections. They

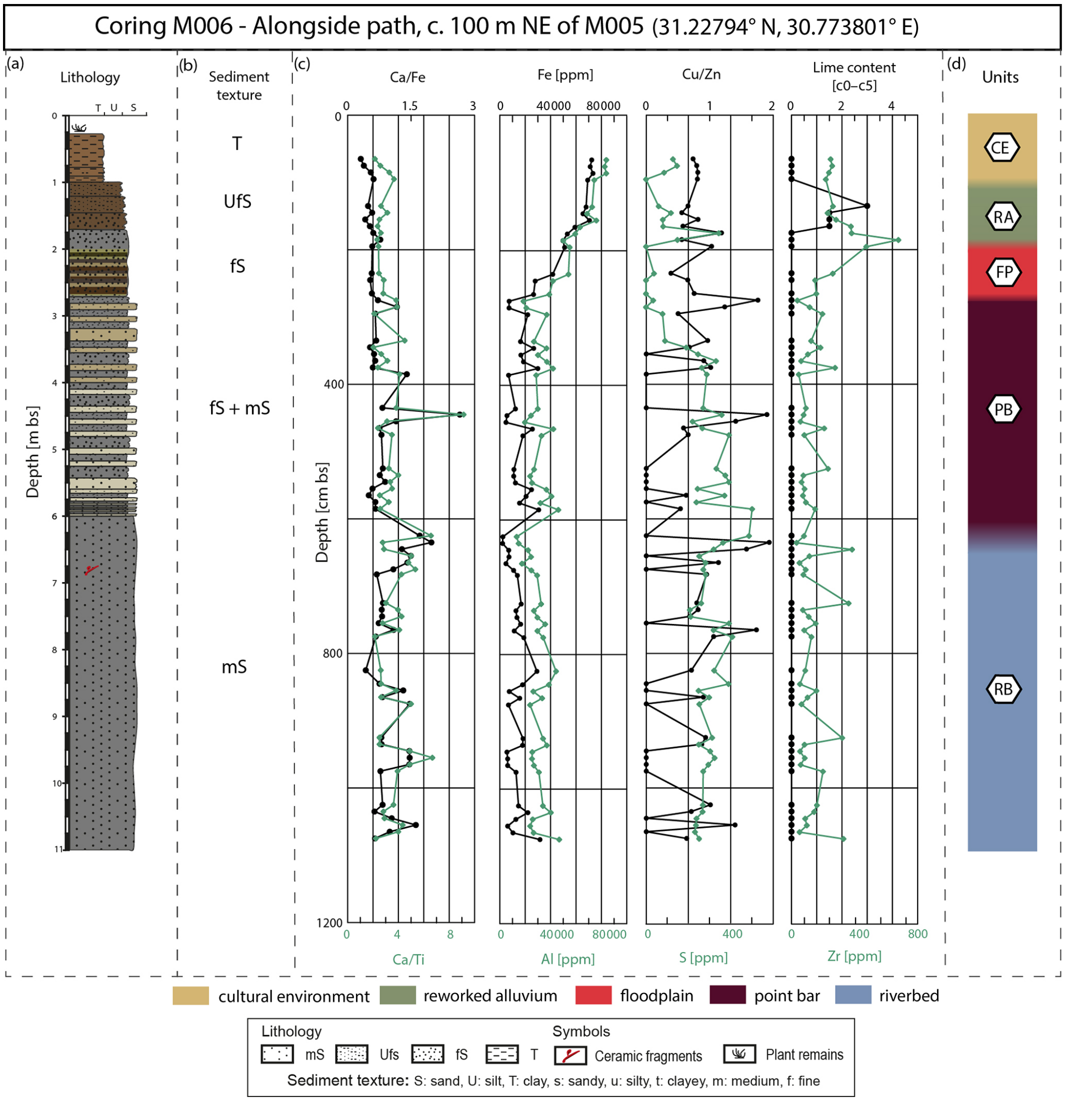

Figure 4. Lithostratigraphy **(a)** and sediment texture **(b)** as well as pXRF results of selected proxies **(c)** for coring M006. For unit interpretation **(d)** see Sect. 5.

mainly occur as depressions representing channel-like features.

4.3 ERT profile C

In addition to coring M006 (Fig. 4), ERT profile C (Fig. 5c), which includes the coring site of M006, is exemplarily described in detail. The modeled ERT image is subdivided into three sections, showing distinct differences in electrical resistivity of the sediments. The material of the uppermost 1.50 m b.s. reveals low to medium resistivity values (5.0–11.0 Ωm), reaching further down to 4.00 m b.s. within the western profile part. Sediments below this layer reveal high electrical resistivity (20.0–40.0 Ωm), almost visible over the entire profile length and depth. Only between profile meters 20 and 50 does the material within the lowermost 2 m possess lower resistivity values around 10.0 Ωm. Besides, the material of high resistivity is sharply defined by sediments with medium (15.0–16.0 Ωm) resistivity. The boundary of medium values is visible in the top transition area and lower-lying parts.

5 Discussion

5.1 Interpretation and discussion of core data

5.1.1 Classification of sedimentary units

Based on the coring results, eight distinct units (Fig. 6) are identified that represent the sedimentary environments in which the sediments once accumulated or that predominantly influenced them.

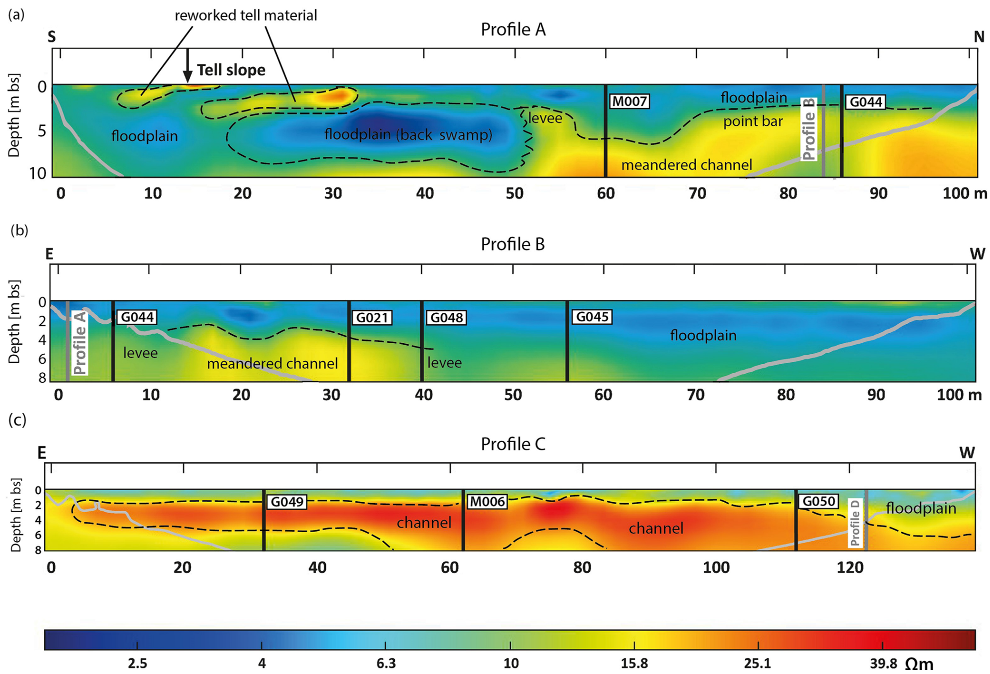

Figure 5. Modeled ERT images of **(a)** profile A, **(b)** profile B, and **(c)** profile C with identified subsurface channel elements. The color scale visualizes the resistivity of the subsurface sediments, ranging from blue, representing low resistivity to red, representing high resistivity. Further features such as locations of several corings conducted in this area are also indicated. The grey lines mark the boundaries of uncertain result reliability towards the start and end of the profile. For profile location see Fig. 3.

- *Unit BA (basement).* The dark grey to whitish colored fine to medium sands (Fig. 6a, b) with partially horizontal color shifts to greenish and yellowish hues indicate former fluvial origin. Studies of regional sediments show that those deposits are usually overlain by peat or organic-rich layers and reveal elevated lime concentrations within upper parts (Wunderlich, 1989; Ginau et al., 2019).

- *Unit LE (levee).* The yellowish-brown coarser sandy sediments are intercalated with thin, fine-grained dark brown loam layers (Fig. 6d). Those sediment alternations are interpreted as a result of flood events with gradually decreasing flow velocities within areas adjacent to channels. The periodical flood sediments accumulated as darker and fine-grained layers in between the sandy deposits, shaping elevated overbank structures (Wunderlich, 1989; Toonen et al., 2012; El Bastawesy et al., 2020). A trend of increasing sediment accumulation is also reflected by gradually increasing Zr concentrations, which mainly originate from erosional processes, reflecting the terrigenous character of the sediments (Eckert, 2014). Furthermore, alternating flood and drought phases are reflected by intense fluctuations in the Cu/Zn ratio (Ginau et al., 2019).

- *Unit RB (riverbed).* The grey-colored material (Fig. 6e) with partially greenish to dark olive hues varies between fine-grained sediments and coarse sand, associated with findings of ceramic fragments, pebbles, or mollusks which serve as proxies for a former channel environment (Giaime et al., 2018; Ginau et al., 2019). The Ca/Ti and Ca/Fe ratios in favor of Ti and Fe, additionally indicate former fluvial conditions (Pint et al., 2015; Castañeda et al., 2016; Croudace et al., 2019; Pennington et al., 2019). Fe with its terrigenous origin is strongly enriched in the sediments transported by the Blue Nile, possibly fed by erodible Fe-rich silicate rocks present within the Ethiopian drainage basin (Revel et al., 2010; Ménot et al., 2020). Continuous fluctuations in the measured pXRF data underline the fluvial nature of this unit. The geochemical variability reveals changing streamflow conditions associated with alternating floods and droughts (Stanley et al., 2003; Ginau et al., 2019).

- *Unit PB (point bar).* The dark greenish-grey as well as light whitish coarser sediments are strongly laminated with dark grey to greyish-brown silts (Fig. 6c). The elements and associated ratios show a similar geochemical variability to those of unit RB. Fluctuations within the Fe and Al concentrations as well as the Cu/Zn ratio indicate the accumulation within a fluvial system (Stanley et al., 2003; Ginau et al., 2019). The visible lamination of the sand section with silty strata highlights changing hydrodynamics (Vött et al., 2002; Goiran et al., 2014).

Figure 6. Exemplary core sediments corresponding to the different sedimentary units. Selected sediments of the coring material representing the identified units. **(a, b)** unit basement, **(c)** unit point bar, **(d)** unit levee, **(e)** unit riverbed, **(f, g)** unit reworked alluvium, **(h, i)** unit floodplain, **(j)** unit cultural debris, and **(k)** unit cultural environment.

The Ca/Fe and Ca/Ti ratios show peaks towards Ca, indicating predominantly eolian input at certain intervals (Woronko, 2012; Blanchet et al., 2015; Pint et al., 2015; Pennington et al., 2019). Partially present high S concentrations reflect the existence of reducing conditions, detectable within silty sediments corresponding to phases of low-energy flow or stagnant water (Goiran et al., 2014; Martinez-Ruiz et al., 2015).

- *Unit FP (floodplain).* The light brown to greenish-grey and dark grey varying sediments range from clay to coarser sand (Fig. 6h, i). The small-scale layering of multiple accumulated sections of silty clay and medium sand indicates a change in the energetic environmental conditions caused either by variations in sediment load and flood height or by alternating channel courses and associated marginalizing energetic conditions. The fluctuating Cu/Zn ratio reflects phases of floods and droughts (Stanley et al., 2003; Ginau et al., 2019). A partially elevated lime content, the Ca/Ti ratio in favor of Ca, and plant remains support the assumption that sediments were accumulated within an area of dominating eolian input during dryer periods (Woronko, 2012; Pint et al., 2015). During warm and dry periods without flood events, ascendant water mobilization possibly led to Ca precipitation (Vött et al., 2002; Pennington et al., 2019). The fine-grained material is partially rich in organics characterized by a distinct sulfidic smell and a blackish color, which developed due to the existence of a long-lasting brackish water body (Wunderlich, 1989; Ginau et al., 2019). Coarser sediments either were accumulated within close distance of an active channel or can be interpreted as crevasse splays, transported over longer distances from the stream course due to the higher streamflow velocity of flood events (Wunderlich, 1989; Toonen et al., 2012; Ginau et al., 2019).

- *Unit CD (cultural debris).* The red-brick-colored composition of brick and ceramic fragments (Fig. 6j) shows distinct boundaries of under- and overlying sediments. Although, the unit can be clearly distinguished visually, differences in its geochemistry compared to the overlying reworked alluvium (see unit RA) are not detectable.

- *Unit RA (reworked alluvium).* The dark yellowish-brown clayey to fine sandy material (Fig. 6f, g) represents the Nile alluvium characteristic for this region (Wunderlich, 1989; Ginau et al., 2019). High element loadings of Fe and Al, indicating that the deposited sediments are fluvially transported material with a terrigenous origin, underline the presumed source (Revel et al., 2010; Eckert, 2014; Pint et al., 2015; Pennington et al., 2019). The unit contains cultural components such as charcoal, ceramic, and brick fragments that presumably influenced the sediment's geochemistry and altered the geochemical signal, leading to differing geochemical distributions and elemental loadings compared to those of a floodplain area without human influences. Thus, the sediments of this unit rather show steady to gradual element distributions. The visible gradual increase in element loadings, such as Fe and Al, without severe geochemical distinctions, further indicate anthropogenic influences (Ginau et al., 2017, 2019; Pennington et al., 2019).

- *Unit CE (cultural environment).* The dark greyish-brown sediments composed of varying amounts of clay, silt, and fine sand (Fig. 6k) are predominantly formed by human activity. A high quantity of anthropogenic remains such as ceramic or brick fragments, charcoals, mortar, and plastic bags among other findings such as plant remains, lime concretions, and pebbles are present.

5.1.2 Interpretation of coring M006

The results of core M006 (Fig. 4) lead to a differentiation of five units (Fig. 7). The lowermost unit (11.00–6.00 m b.s.) is represented by unit RB. The presence of a ceramic fragment embedded within coarse sand underlines a sediment transport by a turbulent flow (Goiran et al., 2014). The overlying sediments (6.00–2.80 m b.s.) are attributed to unit PB. A visible lamination within the sediment texture and the coarse material underlines this interpretation. The material above (2.80–2.00 m b.s.) is identified as unit FP. The existence of fine sand and the number of color differences within the sediments suggest a fluvial origin, presumably with minor distance to the actual channel stream (Toonen et al., 2020). The sediments above (2.00–1.25 m b.s.) are transitioning into unit RA. Although no anthropogenic remains are visible, increasing Fe and Al concentrations and the depth of the unit within the drilling core indicate anthropogenic influences. The uppermost material (1.25–0.00 m b.s.) predominantly shows strongly enriched Fe and Al concentrations without the presence of ceramic fragments or other remains as well. Nevertheless, it is to be identified as unit CE, considering the core location and implied influences of human activity.

5.2 Interpretation of ERT profile C

The images of all three ERT profiles (Fig. 5) reveal clear indicators for buried channel features. Specifically, the resistivity distribution of profile C (Fig. 5c) shows two deep structures with high values (at 55–70 and 80–120 m), presumably representing relict riverbeds as channel sediments contain fine to coarser sand (Ginau et al., 2019). A zone of medium resistivity values (at 70–80 m) in lower-profile sections leads to the interpretation of a sand/point bar between the two channels.

Lower hydrodynamics within such stream-protected areas entail dominating accumulation processes. An alternating streamflow leads to the deposition of sediments with varying grain sizes. The lithological character of the deposits most likely reveals laminations of coarse and fine-grained sediments (Wunderlich, 1989; Goiran et al., 2014; Toonen et al., 2018). Thus, due to the portions of coarse-grained material, the electrical resistivity potentially reveals higher values as well. High ERT values above this presumed sand/point bar indicate overlying channel deposits. Therefore, a first channel construction with two branches and a corresponding sand bar in between is assumed. A potential increasing discharge may have initiated the extending of these streams into one wider channel (channel Ia) that also incorporates the area between 10–50 m (Fig. 5c). However, the eastern half of the profile may also represent a floodplain close to the detected channel. The slightly decreasing electrical resistivity towards the eastern profile end may correspond to the decrease in the mean deposit grain size with distance to an active stream (Toonen et al., 2020). Following this idea, a corresponding floodplain on the western edge at approx. 120–140 m is to be expected.

5.3 Channel-network reconstruction

The obtained data distinctively reveal evidence of buried channel elements embedded in the subsurface sediments of the study area. The core sediments of M006 and the ERT profile C reveal the presence of coarse sand sequences that reach from near-surface areas (approx. 3.00 m b.s.) to deeper sections. These deep-reaching coarse deposits could only have been accumulated within a stream course with high hydrodynamics and flow velocity (Wunderlich, 1989; Goiran et al., 2014). Further corings (M004, M005) in this area also comprise coarse-grained sediments within deeper sections that are classified as unit RB according to their lithology and pXRF data (Fig. 7). In addition to this, M004 incorporates a preserved FP unit below the riverbed section, indicating lower hydrodynamics, which only partially eroded these floodplain deposits. Therefore, it is to be assumed that the location of coring M004 represents marginal areas of the former channel environment. The identified sedimentary units (unit PB and unit FP) within upper sections of M004 and M005 indicate the channel relocation towards the north. Thereby, the interpretations of the ERT profile C lead to the assumption that this profile cuts the former channel nearly orthogonally, indicating the presence of an additional stream.

This presumption is revised with the aid of the topographic map of the *Survey of Egypt* (Fig. 8) that presents contour lines in this area. At the considered location, the contour lines are narrower, which indicates a slightly steeper slope (Fig. 8). A potentially increasing flow energy of the channel may have initiated a further discharge course. Within deeper sections of the ERT profile, two identified depressions suggest the first initiation of two smaller streams before extending into one larger stream. Based on the ERT and coring results, revealing near-surface locations of these channel elements, it is assumed that the channel (channel Ia) silted up later than the channel incorporating M004 and M005 (channel Ib).

The northeast-located corings and ERT measurements also reveal evidence of a former channel (channel II).

Based on the interpretation of the ERT profiles A and B (Fig. 5a, b), the stream is interpreted as a smaller side channel. Although the dimensions of the defunct paleochannel cannot be drawn with certainty, the interpretations of the results lead to this schematic reconstruction (Fig. 8). In consideration of the corings G044 and G048, the pXRF data of the sediments furthermore indicate a low-energy stream. They also align with additional results by Ginau et al. (2019), concluding there was a former channel (coring G21 Fig. 5b) in the eastern surroundings of KeG. Based on its infill comprising loamy fine sand, the authors attributed the stream to a low-energy domain that also revealed characteristics of a natural channel (Ginau et al., 2019). In addition to this, the existent RB units within the performed corings transitioning into FP units and the thickness of these sections suggest an earlier siltation than in the northern channel.

The applied multi-proxy approach allowed the small-scale reconstruction of a former channel system within the study area. However, the sole use of a pXRF approach may be problematic as the Nile Delta sediments possess strong conformities regarding their chemical composition. This can be explained by the consistent sources of the Nile sediments, which did not vary due to climate fluctuations or human in-

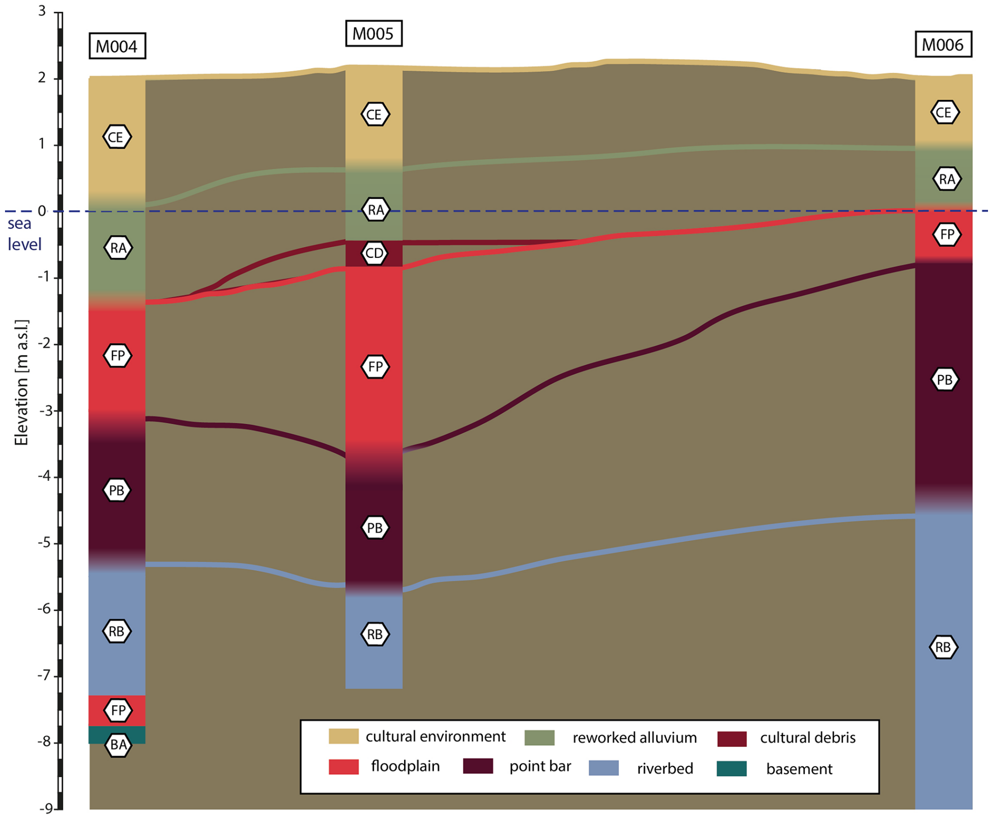

Figure 7. Identified units of coring M004, M005, and M006 representing the environmental evolution in this part of the study area. Corings are presented schematically; for core locations see Fig. 3.

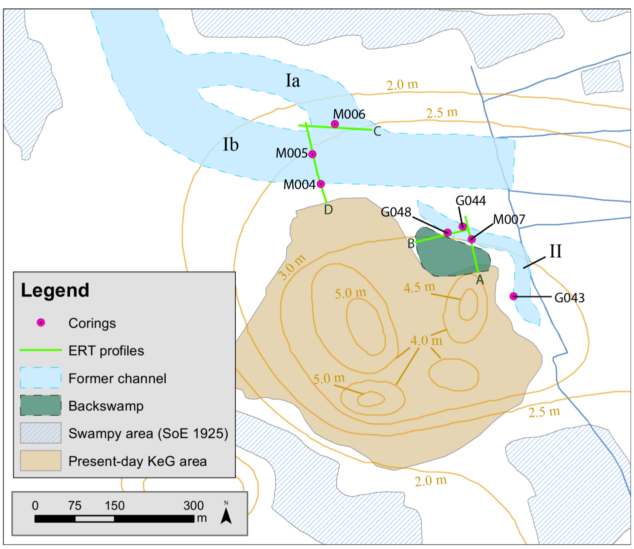

Figure 8. Reconstructed channel systems in the northern and northeastern surroundings of KeG. Based on topographic map of the *Survey of Egypt* from 1925 (scale 1 : 25 000).

fluences. Thus, the pXRF values within this study are only to be considered in combination with the lithological sediment description. However, additional studies may further develop this multi-proxy approach and add more sedimentary and geochemical analyses to the state of research.

6 Conclusion

Through the pXRF analyses of the coring material, eight sedimentary environments are classified that provide subsequent insights into the evolution of the coring sites and former environmental conditions of the study area.

These analyses and the ERT images reveal clear evidence for deposits of defunct channels in the area close to KeG. While deep-reaching sandy deposits in the northern research area represent a former stream (channel Ia, Ib) with high hydrodynamics, the northeast-located sediments show only features of a smaller channel (channel II) with lower flow velocity. In summary, by combining pXRF analyses, lithology, and ERT measurements, a comprehensive small-scale reconstruction of a former fluvial network was elaborated in the area northeast of KeG. Therefore, combining these methods yields a massive benefit in answering the assumptions of Schiestl (2019) about the Nile Delta's fluvial landscape. The used approach may be a choice for investigations of several other settlement hills in the nearby area (Fig. 2).

Although the pXRF analyses and ERT measurements provide no indications of the width of the former streams, topographic maps and current satellite images suggest a framework for the potential dimensions of at least one of the identified channels by the arrangement of fields southeast of KeG. Furthermore, due to a lack of dating facilities, it is not possible to relate the channels to each other or the period of their activity. In this context, future research may provide improved reconstructions and extended insights regarding this topic and the illustrated channel network as well as its dimensions. Datings, microfossil analyses, and further multi-proxy approaches may contribute additional knowledge about the channel system and their activity periods.

Data availability. The TanDEM-X digital elevation model is used with the permission of the German Aerospace Center (DLR), based on the data requested via the proposal (DEM_HYDR1426) by Andreas Ginau, Robert Schiestl, Jürgen Wunderlich, Eva Lange-Athinodorou, and Tobias Ullmann.

All further data generated during this study are included in this article or are available from the corresponding author upon request.

Author contributions. MA, MS, and JW designed this study. All authors performed the fieldwork, mainly comprising drilling, sediment sampling, and leveling the coring locations via GNSS. AG, MA, and MS carried out the pXRF analyses. MA wrote the first draft of the manuscript that was later improved by all co-authors. MA created all figures. JW acquired the funding for this research. RS provided the archeological and historical background for this paper.

Competing interests. The authors declare that they have no conflict of interest.

Special issue statement. This article is part of the special issue "Geoarchaeology of the Nile Delta". It is a result of the workshop "Geoarchaeology of the Nile Delta: Current Research and Future Prospects", Würzburg, Germany, 29–30 November 2019.

Acknowledgements. The fieldwork was conducted as part of the regional survey around Buto (Tell el-Fara'in), with a particular focus on Kom el-Gir. This project is undertaken under the auspices of the Cairo Department of the German Archaeological Institute (DAI). We thank Viktor Nawa and Mona Maier-Rotter for performing the ERT measurements. Thanks to the entire DAI team, especially the first director of the DAI Cairo Department Stephan Seidlmayer for his hospitality and support during the field campaigns. We thank the Egyptian Ministry of State for Antiquities for their assistance and support of our work in the field and for granting the research permits. Furthermore, we thank the two anonymous reviewers for their valuable comments.

Financial support. This study was funded by the Deutsche Forschungsgemeinschaft (DFG, German Research Foundation) (grant no. 392434407).

This open-access publication was funded by the Goethe University Frankfurt.

Review statement. This paper was edited by Tobias Ullmann and reviewed by two anonymous referees.

References

Ad-Hoc-AG Boden: Bodenkundliche Kartieranleitung, Bundesanstalt für Geowissenschaften und Rohstoffe in Zusammenarbeit mit den Staatlichen Geologischen Diensten, 5, Hannover, Germany, 2005.

Andres, W. and Wunderlich, J.: Untersuchungen zur Paläogeographie des westlichen Nildeltas im Holozän, Marburger Geographische Schriften, 100, 117–131, 1986.

Bietak, M.: Tell el-Dab'a II: Der Fundort im Rahmen einer archäologisch-geographischen Untersuchung über das ägyptische Ostdelta, Verlag d. Österr. Akademie d. Wissenschaft, Vienna, Austria, 1975.

Blanchet, C. L., Contoux, C., and Leduc, G.: Runoff and precipitation dynamics in the Blue and White Nile catchments during the mid-Holocene: A data-model comparison, Quaternary Sci. Rev., 130, 222–230, https://doi.org/10.1016/j.quascirev.2015.07.014, 2015.

Butzer, K. W.: Geoarchaeological Implications of Recent Research in the Nile Delta, in: Egypt and the Levant. Interrelations from the 4th throught the early 3rd Millennium B.C.E., New Approaches to Anthropological Archaeology, edited by: van den Brink, E. C. M. and Levy, T. E., Leicester University Press, London/New York, 83–97, 2002.

Castañeda, I. S., Schouten, S., Pätzold, J., Lucassen, F., Kasemann, S., Kuhlmann, H., and Schefuß, E.: Hydroclimate variability in the Nile River Basin during the past 28,000 years, Earth Planet. Sc. Lett., 438, 47–56, https://doi.org/10.1016/j.epsl.2015.12.014, 2016.

Croudace, I. W., Löwemark, L., Tjallingii, R., and Zolitschka, B.: Current perspectives on the capabilities of high resolution XRF core scanners, Quatern. Int., 514, 5–15, https://doi.org/10.1016/j.quaint.2019.04.002, 2019.

Delile, H., Goiran, J. P., and Blichert-Toft, J.: The contribution of geochemistry to ancient harbor geoarcheology: The example of Ostia Antica, Quaternary Sci. Rev., 193, 170–187, https://doi.org/10.1016/j.quascirev.2018.06.019, 2018.

Eckert, S.: The past and present trace metal budget of the Black Sea: a comparison of the Holocene and Eemian marine ingression, PhD thesis, Carl von Ossietzky Universität, University Oldenburg, Germany, 120 pp., 2014.

El Bastawesy, M., Gebremichael, E., Sultan, M., Attwa, M., and Sahour, H.: Tracing Holocene channels and landforms of the Nile Delta through integration of early elevation, geophysical, and sediment core data, The Holocene, https://doi.org/10.1177/0959683620913928, 2020.

El Gamili, M. M., Shaaban, F. F., and El-Morsi, O. A.: Electrical resistivity mapping of the buried stream channel of the Canopic Branch in the Western Nile Delta, Egypt, J. Afr. Earth Sci., 19, 135–148, https://doi.org/10.1016/0899-5362(94)90046-9, 1994.

El Gamili, M. M., Ibrahim, E. H., Hassaneen, A. R. G., Abdalla, M. A., and Ismael, A. M.: Defunct Nile Branches Inferred from a Geoelectric Resistivity Survey on Samannud area, Nile Delta, Egypt, J. Archaeol. Sci., 28, 1339–1348, https://doi.org/10.1006/jasc.2001.0761, 2001.

Emmanouilidis, A., Messaris, G., Ntzanis, E., Zampakis, P., Prevedouros, I., Bassukus, D. A., and Avramidis, P.: CT scanning, X-ray fluorescence: Non-destructive techniques for the identification of sedimentary facies and structures, Revue de micropaléontologie, 67, 100410, https://doi.org/10.1016/j.revmic.2020.100410, 2020.

Gebremichael, E., Sultan, M., Becker, R., El Bastawesy, M., Cherif, O., and Emil, M.: Assessing land deformation and sea encroachment in the Nile Delta: a radar interferometric and inundation modeling approach, J. Geophys. Res.-Sol. Ea., 123, 3208–3224, https://doi.org/10.1002/2017JB015084, 2018.

Giaime, M., Morhange, C., Marriner, N., López-Cadavid, G. I., and Artzy, M.: Geoarchaeological investigations at Akko, Israel: New insights into landscape changes and related anchorage locations since the Bronze Age, Geoarchaeology, 33, 641–660, https://doi.org/10.1002/gea.21683, 2018.

Ginau, A., Schiestl, R., Kern, F., and Wunderlich J.: Identification of historic landscape features and settlement mounds in the Western Nile Delta by means of remote sensing time series analysis and the evaluation of vegetation characteristics, J. Archaeol. Sci.: Reports, 16, 170–184, https://doi.org/10.1016/j.jasrep.2017.09.034, 2017.

Ginau, A., Schiestl, R., and Wunderlich J.: Integrative geoarchaeological research on settlement patterns in the dynamic landscape of the northwestern Nile delta, Quatern. Int., 511, 51–67, https://doi.org/10.1016/j.quaint.2018.04.047, 2019.

Ginau, A., Steiniger, D., Hartmann, R., Hartung, U., Schiestl, R., Altmeyer, M., Seeliger, M., and Wunderlich, J.: What settlements leave behind – pXRF compositional data analysis of archaeological layers from Tell el-Fara'in (Buto, Egypt) using machine learning, Palaeogeogr. Palaeocl., 546, 109666, https://doi.org/10.1016/j.palaeo.2020.109666, 2020.

Goiran, J. P., Salomon, F., Mazzini, I., Bravard, J. P., Pleuger, E., Vittori, C., Boetto, G., Christiansen, J., Arnaud, P., Pellegrino, A., Pepe, C., and Sadori, L.: Geoarchaeology confirms location of the ancient harbour basin of Ostia (Italy), J. Archaeol. Sci., 41, 389–398, https://doi.org/10.1016/j.jas.2013.08.019, 2014.

Kern, O. A., Koutsodendris, A., Mächtle, B., Christanis, K., Schukraft, G., Scholz, C., Kotthoff, U., and Pross, J.: XRF core scanning yields reliable semiquantitative data on the elemental composition of highly organic-rich sediments: Evidence from the Füramoos peat bog (Southern Germany), Sci. Total Environ., 697, 134110, https://doi.org/10.1016/j.scitotenv.2019.134110, 2019.

Lange, E., Ullmann, T., and Baumhauer, R.: Remote sensing in the Nile Delta: spatio-temporal analysis of Bubastis/Tell Basta, Egypt and the Levant, 26, 377–392, available at: https://www.jstor.org/stable/44243959 (last access: 10 August 2020), 2016.

Marriner, N., Flaux, C., Kaniewski, D., Morhange, C., Leduc, G., Moron, V., Chen, Z., Gasse, F., Empereur, J. Y., and Stanley, J.-D.: ITCZ and ENSO-like pacing of Nile delta hydro geomorphology during the Holocene. Quaternary Sci. Rev., 45, 73–84, https://doi.org/10.1016/j.quascirev.2012.04.022, 2012.

Martinez-Ruiz, F., Kastner, M., Gallego-Torres, D., Rodrigo-Gámiz, M., Nieto-Moreno, V., and Ortega-Huertas, M.: Paleoclimate and paleoceanography over the past 20,000 yr in the Mediterranean Sea Basins as indicated by sediment elemental proxies, Quaternary Sci. Rev., 107, 25–46, https://doi.org/10.1016/j.quascirev.2014.09.018, 2015.

Ménot, G., Pivot, S., Bouloubassi, I., Davtian, N., Hennekam, R., Bosch, D., Ducassou, E., Bard, E., Migeon, S., and Revel, M.: Timing and stepwise transitions of the African Humid Period from geochemical proxies in the Nile deep-sea fan sediments, Quaternary Sci. Rev., 228, 106071, https://doi.org/10.1016/j.quascirev.2019.106071, 2020.

Morhange, C., Giaime, M., Marriner, N., abu Hamid, A., Bruneton, H., Honnorat, A., Kaniewski, D., Magni, F., Porotov, A. V., Wante, J., Zviely, D., and Artzy, M.: Geoarchaeological evolution of Tel Akko's ancient harbor (Israel). J. Archaeol. Sci., 7, 71–81, https://doi.org/10.1016/j.jasrep.2016.03.046, 2016.

Pennington, B. T., Sturt, F., Wilson, P., Rowland, J., and Brown, A. G.: The fluvial evolution of the Holocene Nile Delta, Quaternary Sci. Rev., 170, 212–231, https://doi.org/10.1016/j.quascirev.2017.06.017, 2017.

Pennington, B. T., Hamdan, M. A., Pears, B. R., and Sameh, H. I.: Aridification of the Egyptian Sahara 5000–4000 cal BP revealed from x-ray fluorescence analysis of the Nile Delta sediments at Kom al-Ahmer/Kom Wasit, Quatern. Int., 514, 108–118, https://doi.org/10.1016/j.quaint.2019.01.015, 2019.

Pint, A., Seeliger, M., Frenzel, P., Feuser, S., Erkul, E., Berndt, C., Klein, C., Pirson, F., and Brückner, H.: The environs of Elaia's ancient open harbour-a reconstruction based on macrofaunal evidence, J. Archaeol. Sci., 54, 340–355, https://doi.org/10.1016/j.jas.2014.06.011, 2015.

Revel, M., Ducassou, E., Grousset, F. E., Bernasconi, S. M., Migeon, S., Révillon, S., Mascle, J., Murat, A., Zaragosi, S., and Bosch, D.: 100,000 years of African monsoon variability recorded in sediments of the Nile margin, Quaternary Sci. Rev., 29, 1342–1362, https://doi.org/10.1016/j.quascirev.2010.02.006, 2010.

Rizzini, A., Vezzani, F., Cococcetta, V., and Milad, G.: Stratigraphy and sedimentation of a Neogene – Quaternary section in the Nile Delta area (ARE), Mar. Geol., 27, 327–348, https://doi.org/10.1016/0025-3227(78)90038-5, 1978.

Schiestl, R.: Investigating ancient settlements around Buto, Egyptian Archaeology, 40, 18–20, 2012.

Schiestl, R.: Landschaftsarchäologie und regionale Siedlungsnetzwerke um den Fundplatz Tell el-Fara'in, Gouvernorat Kafr esch-Scheich. Die Arbeiten des Jahres 2012, e-Forschungsberichte, 1, 11–13, available at: https://www.dainst.org/documents/10180/727267/eFB2015-1_Schiestl_Buto.pdf/cff14d7c-eb23-4be5-bde9-911156900701 (last access: 31 May 2021), 2015.

Schiestl, R.: Gouvernorat Kafr esch-Scheich, Ägypten. Landschaftsarchäologie und regionale Siedlungsnetzwerke um den Fundplatz Tell el-Fara'in (Buto) im Nildelta. Die Arbeiten des Jahres 2018, e-Forschungsberichte 2018, 2, 44–46, available at: https://publications.dainst.org/journals/index.php/efb/article/view/2149 (last access: 24 May 2021), 2018.

Schiestl, R.: Gouvernorat Kafr esch-Scheich, Ägypten. Landschaftsarchäologie und regionale Siedlungsnetzwerke um den Fundplatz Tell el-Fara'in im Nildelta und Untersuchungen am antiken Fundplatz Kom el-Gir. Die Arbeiten des Jahres 2018 und Frühjahres 2019, e-Forschungsberichte, 2, 51–55, https://doi.org/10.5282/ubm/epub.69238, 2019.

Schiestl, R. and Herbich, T.: Kom el-Gir in the western Delta, Egyptian Archaeology, 42, 28–29, 2013.

Schiestl, R. and Rosenow, D.: Prospektion am Kom el-Gir: eine Einführung in eine neue Siedlung des Deltas, Mitteilungen des Deutschen Archäologischen Instituts, Abteilung Kairo, 72, 169–196, 2016.

Seeliger, M., Pint, A., Frenzel, P., Weisenseel, P. K., Erkul, E., Wilken, D., Wunderlich, T., Başaran, S., Bücherl, H., Herbrecht, M., Rabbel, W., Schmidts, T., Szemkus, N., and Brückner, H.: Using a multi-proxy approach to detect and date a buried part of the Hellenistic City Wall of Ainos (NW Turkey), Geosciences, 8, 357, https://doi.org/10.3390/geosciences8100357, 2018.

Stanley, J. D., Krom, M. D., Cliff, R. A., and Woodward, J. C.: Short contribution: Nile flow failure at the end of the Old Kingdom, Egypt: strontium isotopic and petrologic evidence, Geoarchaeology, 18, 395–402, https://doi.org/10.1002/gea.10065, 2003.

Toonen, W. H. J., Kleinhans, M. G., and Cohen, K. M.: Sedimentary architecture of abandoned channel fills, Earth Surf. Proc. Land., 37, 459–472, https://doi.org/10.1002/esp.3189, 2012.

Toonen, W. H. J., Graham, A., Pennington, B. T., Hunter, M. A., Strutt, K. D., Barker, D. S., Masson-Berghoff, A., and Emery, V. L.: Holocene fluvial history of the Nile‘s west bank at ancient Thebes, Luxor, Egypt, and its relation with cultural dynamics and basin-wide hydroclimatic variability, Geoarchaeology, 33, 273–290, https://doi.org/10.1002/gea.21631, 2018.

Toonen, W. H. J., Munoz, S. E., Cohen, K. M., and Macklin, M. G.: High-Resolution Sedimentary Paleoflood Records in Alluvial River Environments: A Review of Recent Methodological Advances and Application to Flood Hazard Assessment, in: Palaeohydrology, Geography of the Physical Environment, edited by: Herget, J. and Fontana, A., Springer, Cham, Switzerland, https://doi.org/10.1007/978-3-030-23315-0_11, 213–228, 2020.

Vött, A., Handl, M., and Brückner, H.: Rekonstruktion holozäner Umweltbedingungen in Arkanien (Nordwestgriechenland) mittels Diskriminanzanalyse von geochemischen Daten, Geologica et Palaeontologica, 36, 123–147, 2002.

Woodward, J., Macklin, M., Fielding, L., Millar, I., Spencer, N., Welsby, D., and Williams, M.: Shifting sediment sources in the world‘s longest river: A strontium isotope record for the Holocene Nile, Quaternary Sci. Rev., 130, 124–140, https://doi.org/10.1016/j.quascirev.2015.10.040, 2015.

Woronko, B.: Late-Holocene dust accumulation within the ancient town of Marea (coastal zone of the South Mediterranean Sea, N Egypt), Quatern. Int., 266, 4–13, https://doi.org/10.1016/j.quaint.2011.09.010, 2012.

Wunderlich, J.: Investigations on the development of the western Nile Delta in Holocene times, in: The Archaeology of the Nile Delta: Problems and Priorities, edited by: van den Brink, E. C. M., Neth. Found. Archaeol. Res. Egypt, Amsterdam, the Netherlands, 251–257, 1988.

Wunderlich, J.: Untersuchungen zur Entwicklung des westlichen Nildeltas im Holozän, Marburger Geographische Schriften, 114, Marburg/Lahn, Germany, 1989.

Wunderlich, J. and Andres, W.: Late Pleistocene and Holocene evolution of the western Nile delta and implications for its future development, in: Von der Nordsee bis zum Indischen Ozean, Erdkundliches Wissen, edited by: Brückner, H. and Radtke, U., Franz Steiner Verlag, Stuttgart, Germany, 105–120, 1991.

Wunderlich, T., Fischer, P., Wilken, D., Erkul, E., Mecking, R., Günther, T., Heinzelmann, M., Vött, A., and Rabbel, W.: Constraining electric resistivity tomography by direct push electric conductivity logs and vibracores: An exemplary study oft he Fiume Morto silted riverbed (Ostia Antica, western Italy), Geophysics, 83, B87–B103, https://doi.org/10.1190/geo2016-0660.1, 2018.

E&G Quaternary Sci. J., 70, 39–52, 2021
https://doi.org/10.5194/egqsj-70-39-2021

Open Access E&G Quaternary Science Journal

Research article

Western Mareotis lake(s) during the Late Holocene (4th century BCE–8th century CE): diachronic evolution in the western margin of the Nile Delta and evidence for the digging of a canal complex during the early Roman period

Maël Crépy[1] **and Marie-Françoise Boussac**[2]

[1]UMR5133 Archéorient and UMR5189 HiSoMA, Maison de l'Orient et de la Méditerranée, CNRS, Lyon 69007, France
[2]UMR7041 ArScAn, Université Paris Nanterre, 21 allée de l'Université, 92023 Nanterre, France

Correspondence: Maël Crépy (crepy.mc@gmail.com)

Relevant dates: Received: 25 September 2020 – Revised: 7 December 2020 – Accepted: 17 December 2020 – Published: 28 January 2021

How to cite: Crépy, M. and Boussac, M.-F.: Western Mareotis lake(s) during the Late Holocene (4th century BCE–8th century CE): diachronic evolution in the western margin of the Nile Delta and evidence for the digging of a canal complex during the early Roman period, E&G Quaternary Sci. J., 70, 39–52, https://doi.org/10.5194/egqsj-70-39-2021, 2021.

Abstract: Lake Mareotis (modern Mariut), located near the Mediterranean coast of Egypt west of the Nile Delta, is bordered by ancient sites dating from the New Kingdom (end of the 2nd millennium BCE) to the Medieval period (8th century CE), the most famous one being Alexandria. In its western part (wadi Mariut), several sites are equipped with harbour structures, but they also have structures contemporaneous with them that are not compatible with the lake level required for the operation of the harbour. Between the 1990s and 2010, several sedimentological studies tried to solve this paradox without completely succeeding. To go further, this study is based on the reassessment of geoarchaeological data and on the analysis of early scholars' accounts (1800–1945), maps (1807–1958) and satellite photographs (Corona). It allows us to reconstruct the extension of the lake(s) at different periods in wadi Mariut. During the 1st millennium BCE, the Mariut lagoon experienced a drawdown in its western part, and several distinct lakes formed, followed by building operations in some emerged areas during the Hellenistic period (332–30 BCE). During the early Roman period (30 BCE–284 CE), the digging of several canals in the 2nd century CE to connect the sites of the wadi Mariut to the eastern part of the Mariut basin reconfigured the lake(s).

Kurzfassung: Der Mareotis-See (mod. Mariut), nahe der ägyptischen Mittelmeerküste, westlich des Nildeltas, liegt an antiken Siedlungen, die vom Neuen Reich (Ende des zweiten Jt. v. Chr.) bis ins Mittelalter (8. Jh. n. Chr.) datieren; die berühmteste ist Alexandria. In seinem westlichen Teil (Wadi Mariut) sind mehrere Siedlungen mit Hafenanlagen angelegt, enthalten aber auch zeitgenössische Gebäude, die mit dem Seespiegel unvereinbar sind und die für das Funktionieren der Häfen in Betracht gezogen werden müssen. Zwischen den 1990er Jahren und 2010 wurden mehrere Studien, die sich auf die Sedimentologie stützten, auf diese Frage angewandt, ohne dieses Paradox vollständig zu lösen. Um noch einen Schritt weiter zu gehen, stützt sich diese Studie auf die Neubewertung geoarchäologischer Daten, und zwar auf Analyse von Berichten früher Gelehrter (1800–1945), Karten (1807–1958) und Satellitenfotos (Corona). Sie ermöglicht es, die Ausdehnung des Sees/der Seen zu verschiedenen Zeiten im Wadi Mariut zu rekonstruieren. Während des ersten Jt. v. Chr. erlebte die Lagune in ihrem westlichen Teil eine Absenkung, gefolgt von Bauarbeiten in neu entstandenen Gebieten während der hellenistischen Periode (332–30 v. Chr.). Durch das Graben mehrerer Kanäle im 2. Jh. n. Chr., um die Siedlungen mit dem östlichen Teil des Mariut-Beckens zu verbinden, wurden der See bzw. die Seen neu gestaltet.

1 Introduction and objectives

Lake Mariut, ancient Mareotis (Fig. 1), is a lagoon that polarised the human occupation of Egypt's north-western margins during antiquity. The region developed mainly after the foundation of Alexandria in 332 BCE (Fraser, 1972), although earlier occupation is archaeologically evidenced since the New Kingdom at Plinthine (Boussac et al., 2015; Boussac and Redon, 2021) and Kom Bahig (Empereur, 2018). Agricultural lands and towns, such as Taposiris on the north shore (Boussac, 2015) and Marea (Pichot, 2012) on the southern one, flourished until the Arab-Muslim conquest, which was followed in the 7–8th centuries CE by a reconfiguration of the territory and the abandonment of many settlements (Décobert, 2002). During all periods, the human occupation of the region has been closely linked to the lake (Blue and Khalil, 2011).

Strabo (∼ 60 BCE–∼ 20 CE) mentions a very large lake (Strabo, 2015:17, 14) of major economic importance (Strabo, 2015:17, 7). Later, accounts by travellers from the 6th century CE to 1798 (Sennoune, 2015), maps (Awad, 2010) and sedimentological data (Flaux, 2011) indicate significant fluctuations of the lake levels and positions (including phases of desiccation). At the beginning of the French expedition to Egypt (1798–1801), the lake area was dry (Le Père, 1825).

If one focuses on the wadi Mariut (western part of the Mariut basin; Fig. 1), the presence at some Hellenistic and/or Roman sites of harbour structures close to remains that are incompatible with the vicinity of a lake (e.g. amphora workshops) and dating back to the same periods constitutes a geoarchaeological paradox. How can this paradox be solved? Did the lake levels shift at high frequency during this period? Have several independent lakes of small extent coexisted in the Mariut basin? Should a major water engineering work be considered?

This geoarchaeological study, undertaken within the French mission at Taposiris Magna and Plinthine (dir. M.-F. Boussac and then B. Redon), aims to assess, through a composite method, the western extension of the Mareotis lake(s) in wadi Mariut from the 4th century BCE to the 8th century CE.

2 General settings and previous studies

2.1 Geomorphic settings

Lake Mariut lies at the interface between three geomorphological systems: the Mediterranean littoral, the Nile Delta and the Libyan desert. During the Holocene, distinct morphogenetic processes have influenced its evolution: climate change and the evolution of the Nile floods (Macklin et al., 2015), sea level rise (Dalongeville and Fouache, 2005), wind erosion (Woronko, 2012; Crépy, 2021), subsidence (Pennington et al., 2017), and neotectonics (Stanley, 2003), to which must be added the impact of human activities (Flaux et al., 2012).

The lagoon, whose water level is currently controlled by means of pumps and a canal to the Mediterranean Sea located at Al Max (in the vicinity of Alexandria), occupies parts of a depression, some areas of which are below mean sea level. This depression consists of two distinct areas (Fig. 1). To the east, its edges slope gently, and no significant topographical features separate it from the now-drained Abukir lagoon to the north-east, the delta to the east, the desert to the west and the agricultural lands of Al Buhayrah to the south. In the western part, often called wadi Mariut or Mariut valley, the depression stretches from east to west and is bordered by two steeply sloping calcarenite ridges separating it from the Mediterranean Sea in the north and from another depression in the south.

2.2 Archaeological and historic settings (∼ 1000 BCE–∼ 1000 CE)

The archaeology of the western part of Lake Mareotis (wadi Mariut) has been investigated since the beginning of the 20th century (e.g. De Cosson, 1935). From the beginning of the 1st millennium BCE to the end of the 1st millennium CE, the following dynamics of occupation have been demonstrated: from the New Kingdom (∼ 1580–∼ 1077 BCE), occupation on high points on the northern and southern banks of the valley (Boussac et al., 2015; Empereur, 2018; Nenna et al., 2020); from the Saite Period (664–525 BCE) at the latest, agricultural development (wine) attested to in Plinthine on the northern bank (Redon et al., 2017); during the Hellenistic period (332–30 BCE), urban development in sectors located lower down on both banks and on Mariut island (Blue and Khalil, 2011; Boussac, 2015); and from the early Roman

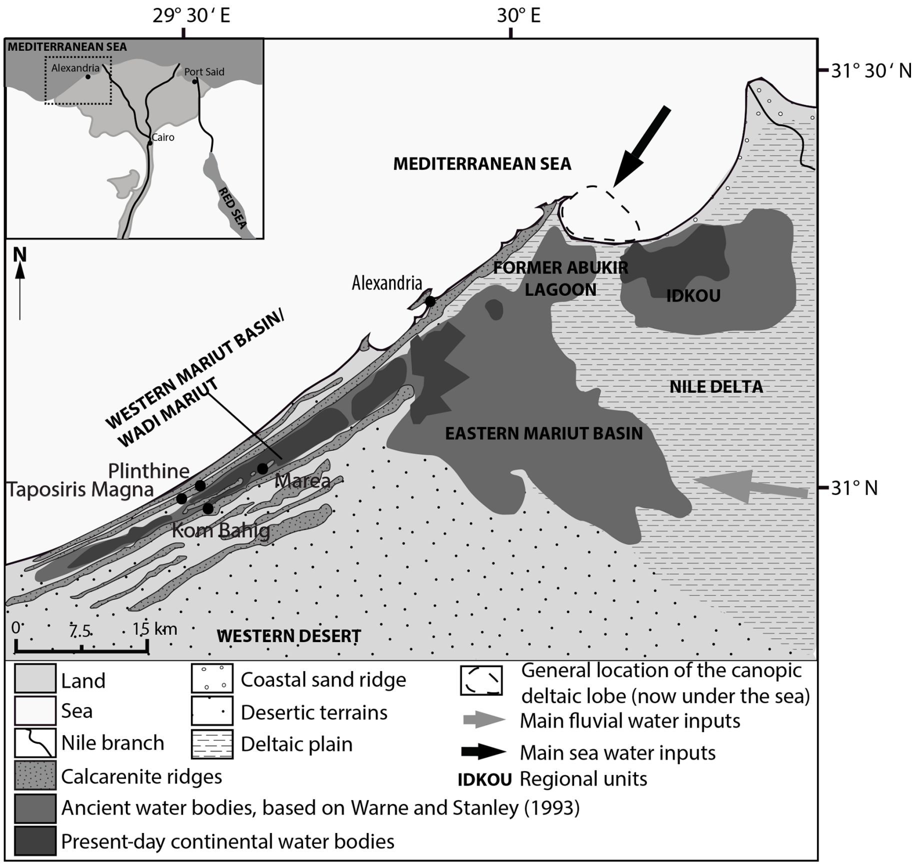

Figure 1. Main geomorphic units in the Mariut area, based on Flaux (2011).

period (30 BCE–284 CE) to the Arab-Islamic conquest (mid-7th century CE), increasing harbour and economic development (including wine export) (Décobert, 2002; Blue and Khalil, 2011; Boussac and El-Amouri, 2010; Dzierzbicka, 2018; Pichot and Simony, 2021). The Hellenistic and Roman periods are characterised by structures occupying areas that are very close to the current shores of the lake (or even in the present lake) and located at altitudes much lower than the remains of other periods, suggesting that the lake levels were lower during these periods or that the geometry of the lake was different. This has been demonstrated at Taposiris and on Mariut island (Blue and Khalil, 2011; Flaux, 2012).

2.3 Previous geomorphological and geoarchaeological studies

2.3.1 Holocene history of the Mariut lagoon

The calcarenite ridge separating the Mariut depression and the Mediterranean Sea, as well as the ridge delimiting the wadi Mariut to the south, predate the Holocene (El Asmar and Wood, 2000) and have durably limited the extension of the lagoon. The Holocene shifts of the lagoon were therefore mainly conditioned by the balance between sea level variations, subsidence, and the Nile's liquid and solid inputs, the latter being determined by climatic conditions and human activities in its watershed.

During the Holocene, the evolution of the Mariut region (Table 1) has been established by the work of Clément Flaux mainly thanks to data from the eastern part of the Mariut but also from Taposiris and from the southern bank of the wadi Mariut (Flaux et al., 2011; Flaux, 2011, 2012). From the early Roman period (30 BCE–284 CE), the evolution of the lagoon has been linked to the filling in of the Canopic branch (Fig. 1; Bernand, 1970; Hairy and Sennoune, 2009) and to the sinking of its deltaic lobe below sea level around the 8th century CE (Stanley et al., 2001).

2.3.2 A geoarchaeological paradox

This general environmental pattern cannot be directly applied to the wadi Mariut; on the one hand, subsidence is strong in the eastern part of the Mariut depression but very weak in wadi Mariut (Pennington et al., 2017), and on the other hand, marine and Nilotic water inputs both originate from the east (Fig. 1). Moreover, in wadi Mariut, Pleistocene outcrops are not uncommon and the Pleistocene–Holocene boundary is generally close to the topographic surface, so less sedimentation occurred during the Holocene (Flaux, 2012).

Table 1. Holocene evolution of the Mariut region based on Flaux et al. (2011) and Flaux (2011, 2012).

Period	Status	Main causes
∼ 9000–∼ 7000 BCE	Coastal deltaic plain periodically flooded by the Nile	Nile Delta progradation
∼ 6000–∼ 5500 BCE	Lagoon sedimentation	Holocene marine transgression
∼ 5500–∼ 2800 BCE	Lagoon closed to marine influences	Nile Delta progradation
∼ 2800–∼ 1200 BCE	Marine influence and hydrological instability	Climatic aridification and reduced Nile flow
∼ 1000 BCE–∼ 200 CE	Lagoon more subject to the Nilotic influence than to the maritime one and anthropogenic disturbances	Canopic branch defluviation and anthropogenic activities
∼ 200–∼ 800 CE	Brackish lagoon dominated by nilotic inputs	To be determined
∼ 800–∼ 1200 CE	Sebkha	Nile defluviation and canal siltation

Sedimentological and physico-chemical analyses have been interpreted as evidence of a large extension of the Mariut lagoon westward between ∼ 4000 BCE and ∼ 1200 CE even beyond the present limits of the lake (Warne and Stanley, 1993). A generally high water level in antiquity has also been assumed for Taposiris (Tronchère, 2010; Tronchère et al., 2014).

A lot of ancient harbour infrastructure has been prospected (Blue and Khalil, 2011) but also Hellenistic and Roman remains submerged or located close to the current shores of the lagoon, including amphora workshops (Empereur and Picon, 1998; Flaux, 2012). Their underground kilns make them incompatible with their proximity to the lake and high water levels. However, the operation of the few ports and sites bordering the lake studied in more detail implies relatively high water levels, for the Roman period at least, for example at Taposiris (Boussac and El Amouri, 2010) or on Mariut island (Flaux, 2012).

The archaeological remains and the environmental data from wadi Mariut thus present a geoarchaeological paradox to be solved. Not only do the environmental and archaeological data not converge, but even the archaeological data seem to contradict each other unless we consider a variability in water levels of high frequency, several independent lakes or water engineering on the scale of the wadi Mariut, whose remains have not yet been highlighted.

2.3.3 Illustration of the geoarchaeological paradox: Taposiris harbour

The lake complex of Taposiris (Fig. 2), investigated since 1998 by the French mission at Taposiris Magna and Plinthine, consists of a dug or deepened canal bordered to the south by an artificial sedimentary levee on which warehouses are lined up and to the north, at its eastern end, by dredging material. A bridge that connects the bank to the artificial levee is dated to early Roman times, more specifically to the 2nd century CE (Boussac and El Amouri, 2010). The artificial levee and the dredged material cover Hellenistic remains (2nd–1st century BCE), part of which is below the present water surface (Boussac and El-Amouri, 2010). To the east, a stone pier from the late Roman period (4th century CE) closes the port complex. The swamp located to the north, which could suggest a harbour basin, was already a swamp during antiquity (Flaux, 2012).

The chronological sequence is as follows (Boussac and El-Amouri, 2010; Boussac, 2015):

- urban development during the 2nd–1st century BCE;
- building of an artificial levee during the 2nd century CE;
- raising of the artificial levee after the 4th century CE;
- installation of the eastern pier around the 4th century CE;
- abandonment of the area after the 7th century CE.

3 Material and methods

Carrying out a geoarchaeological study in wadi Mariut is complex due to the lack of analysis equipment and to Egyptian legislation prohibiting the export of samples. Moreover, urbanisation and agricultural development in the region in the 20th century has considerably altered the topography and sedimentary formations of the region (quarries, salt ponds, etc.). We therefore used a combination of methods to overcome these obstacles.

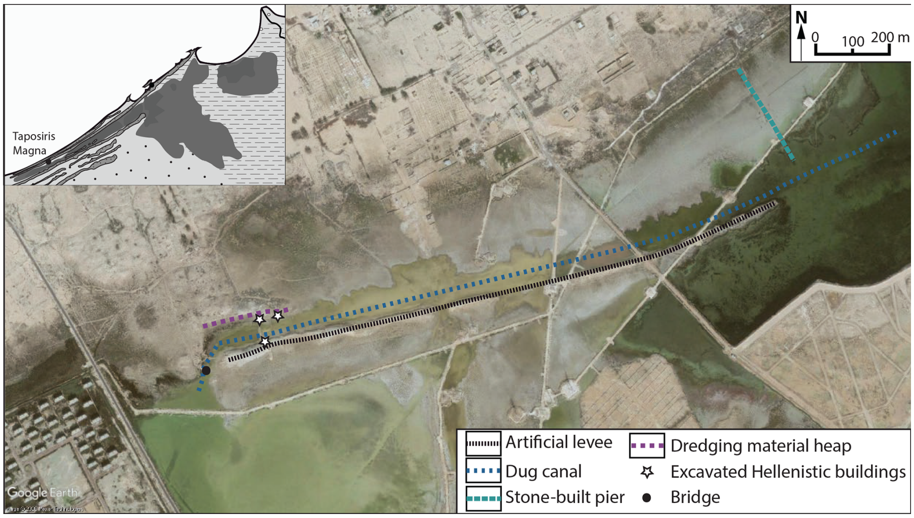

Figure 2. Harbour of Taposiris. Base map image: © Google Earth Pro November 2009.

3.1 Reassessment of geoarchaeological data

We reassessed and crossed three types of data that led researchers to reconstruct a large extension of Lake Mareotis in wadi Mariut:

- sedimentological, biological and physico-chemical data (available in Tronchère, 2010; Tronchère et al., 2014; Warne and Stanley, 1993);
- archaeological data, in particular the distribution of sites (from Blue and Khalil, 2011 and Boussac, 2015);
- historical data, through an analysis of two sources frequently used in the study of the region (Strabo, 2015:17; Jacotin, 1818).

3.2 Early scholars' accounts (1800–1945)

A total of 11 early western scholars' contributions (Chabrol and Lancret, 1829; De Cosson, 1935; El Falaki, 1872; Le Père, 1823, 1825, 1829; Jacotin, 1824; Oliver, 1945; Reclus, 1885; Rennell, 1800; St John, 1849) have been selected and studied to recover data erased over time. They describe a period during which human activities were less developed than today and provide additional elements on archaeology, completing the data concerning the distribution of the sites and the topography.

3.3 Maps (1807–1958)

Eight maps (Table 2) have been analysed to identify the topography of the lands currently flooded and the vanished archaeological sites and to characterise the recent evolution of the extension of the lake.

3.4 Corona photographs

Three declassified satellite photographs from the Corona programme (Table 3) were acquired free of charge on EarthExplorer (https://earthexplorer.usgs.gov/, last access: 22 January 2021).

They allow us to evaluate the topography of the now-flooded areas and to observe the region before its current development. Moreover, they help us to escape the subjectivity of early scholars and the bias of cartographic surveys in swampy areas and to observe the terrain from the sky to identify macrostructures.

4 Results and interpretation

4.1 Reassessment of geoarchaeological data

4.1.1 Sedimentological data: playa, lake or lakes?

Two studies led to the reconstruction of a large extension of Lake Mareotis in its western part: Warne and Stanley (1993) at the regional scale and Tronchère (2010) and Tronchère et al. (2014) around Taposiris. The first study (Warne and Stanley, 1993) was based on the analysis of sedimentary cores and revealed the presence of a lagoon dominated by fluvial inputs throughout wadi Mariut and up to Taposiris in the west $\sim$ 2500–$\sim$ 2000 years ago. If only the regional scale and major trends are considered, these conclusions are correct, although a reassessment is needed at the local scale and is made possible by the rigour of Warne and Stanley (1993) in presenting their data. At the scale of wadi Mariut, the data highlight three points:

- on several isopleth maps (Fig. 3), the Nilotic influence does not appear (verdine/glauconite) or appears very slightly (mica, heavy minerals) in the western part of wadi Mariut, and other parameters strongly differentiate it (gypsum, foraminifera);

- the Holocene sedimentary column represents less than 2.5 m in most of wadi Mariut;

- in the western part of wadi Mariut, the only facies that can be linked to a lagoon are "lagoon margin mud" facies whose composition could just as well correspond to playa or semi-playa deposits (as described by Embabi, 2004, and by Crépy, 2016).

The continuity of the lagoon up to Taposiris is therefore not established by Warne and Stanley's data (1993) which show, in contrast, that at least one basin has undergone a specific evolution (Fig. 3).

Data from Tronchère (2010) and Tronchère et al. (2014) at local scale led to the reconstruction of a lake or lagoon reaching Taposiris during the whole Holocene (the alteration layer of the calcarenite substratum was dated to 40 254–38 032 cal BCE[1]). However, the very small quantity of ostracods found (some samples were totally free of them) and the granulometric data do not go in this direction. The laser granulometry curves are all multimodal, which Tronchère (2010) attributed to a sampling bias. The presence of recurrent aeolian modes (loess: 10–20 µm; dune sand: 100–200 µm; according to Tsoar and Pye, 1987) mixed with other modes would rather indicate a palustrine environment influenced by desert dynamics (e.g. playa or sebkha margin). To sum up, the sedimentological data are more likely to correspond to marshy or immersed areas disconnected from the Mariut lagoon.

4.1.2 Historical data: some necessary precautions

Strabo's Book 17 (Strabo, 2015:17) and Jacotin's map (1818) are often used to study Lake Mareotis' extension during antiquity. According to the ancient geographer, the lake measured, in his time, 150 stadia (∼ 27.75 km) or more in width and less than 300 stadia (∼ 55.5 km) in length (Strabo, 2015:17, 14). These measurements have generally been interpreted in light of the current state of the lake, and the orientation has often been used as follows: 300 stadia from the north-east to south-west and 150 stadia from the north-west to south-east. However, there is no indication of this orientation in Strabo's text, and data on the Holocene evolution of the Nile Delta and on subsidence in the eastern Mariut basin would rather fit with an opposite orientation, especially if one takes into account a Nilotic influence.

Jacotin's map (1818) has sometimes been used as a reference state of ancient Mariut (e.g. Tronchère et al., 2014) even if the limits of the lake have been drawn after a British military operation, as mentioned on the map, "Cuts made by the English to flood Lake Mareotis (19 Germinal An 9–19 April 1801)". The lake on the map corresponds to a state when it was directly connected to the Aboukir lagoon, itself open to the sea, and therefore at a much higher level than the maxima during most of the studied period (4th century BCE–8th century CE) when the Canopic deltaic lobe used to be an obstacle to links with the Mediterranean Sea (Stanley et al., 2001).

4.1.3 Archaeological data

The spatio-temporal distribution of the sites could seem relevant to draw the ancient shores of the lake. However, two obstacles prevent the proper exploitation of the survey results (e.g. Blue and Khalil, 2011; Picon and Empereur, 1998). In the absence of underwater surveys, the distribution of sites is incomplete and draws a shoreline corresponding to the limit of the lake at the time of the survey (even if Blue and Khalil, 2011, also mentioned some underwater remains, they saw from the land), and surface surveys are not sufficient to give an exhaustive chronology of the sites. However, the following observations can be made thanks to the Hellenistic and Roman amphora workshops of Mariut island and Borg el Arab (surveyed by Empereur and Picon, 1998, and Blue and Khalil, 2011; Fig. 4). The altitude of their kilns shows that the lake must have been located within more restricted limits or at a lower level than today in this part of wadi Mariut. The kilns of this area are indeed located below the top of the phreatic water table induced by the current lake. Similar levels inferred for antiquity would thus hinder their use. Likewise, the Hellenistic quarter of the lower town of Taposiris is incompatible with the present level of the lagoon (Flaux, 2012)

4.2 Early scholars' accounts (1800–1945)

4.2.1 Limits of the lake(s)

Before the flooding in 1801, low areas of the Mariut depression could fill with water after rainfall (Chabrol and Lancret, 1829; Le Père, 1825) and form small independent lakes, for example southwest of Taposiris (St John, 1849). At the peak of the flood, the western limit of the water would have been located at the level of the so-called Arabs' tower (Jacotin, 1824) or 1000 m east of Taposiris (Le Père, 1829) or about 500 m east of the Arabs' tower (Fig. 5). W. G. Browne, at the end of the 18th century, saw no reason to consider a lake that would have been more than 1 or 1.5 leagues (∼ 4.83 or ∼ 7.25 km) from Alexandria in the past based on the observation of the ground and the topography (Rennell, 1800).

4.2.2 Data on archaeological remains

Early scholars mention remains that have now disappeared, such as walls and canals in wadi Mariut (Chabrol and Lancret, 1829), as well as levees or small dikes (now under wa-

[1] Calibration by M. Crépy with OxCal using IntCal20 calibration curve based on raw data from Tronchère et al. (2014).

Table 2. Maps used in this study.

Date	Author	Link
1807	Arrowsmith	https://gallica.bnf.fr/ark:/12148/btv1b530669569/ (last access: 22 January 2021)
1818	Jacotin	https://gallica.bnf.fr/ark:/12148/btv1b531569998/ (last access: 22 January 2021)
1827	Coste	https://gallica.bnf.fr/ark:/12148/btv1b8491814n/ (last access: 22 January 2021)
1850	St John	https://gallica.bnf.fr/ark:/12148/btv1b53136219p/ (last access: 22 January 2021)
1866	El Falaki	https://gallica.bnf.fr/ark:/12148/btv1b10101071m/ (last access: 22 January 2021)
1910	Survey of Egypt	https://www.davidrumsey.com/luna/servlet/detail/ RUMSEY~8~1~317305~90086593:Sheet-47-Bahig (last access: 22 January 2021)
1942	AMS	http://legacy.lib.utexas.edu/maps/ams/egypt/ txu-pclmaps-oclc-6559596-el-hammam.jpg (last access: 22 January 2021)
1958	AMS	http://legacy.lib.utexas.edu/maps/ams/north_africa/ txu-oclc-6949452-nh35-8.jpg (last access: 22 January 2021)

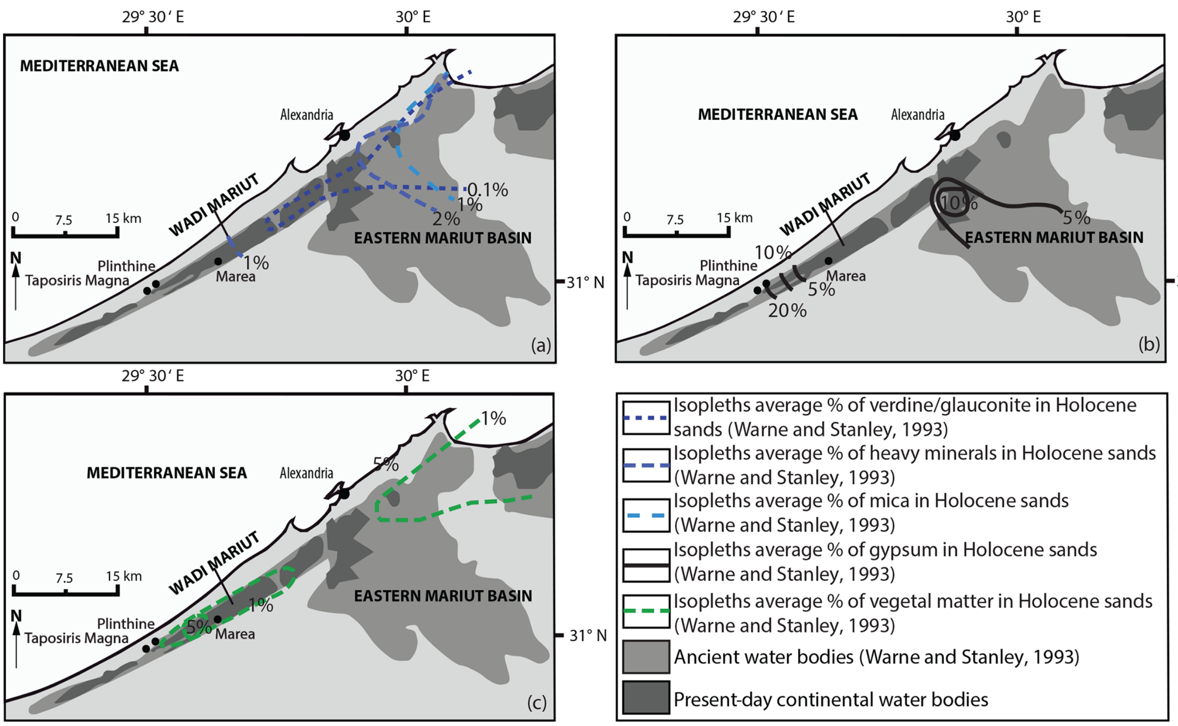

Figure 3. (a) Isopleths (based on Warne and Stanley, 1993) recording the Nile's influence on the Mariut basin. **(b)** Isopleths (based on Warne and Stanley, 1993) indicating high evaporation processes during the Holocene in the western part of wadi Mariut. **(c)** Isopleths (based on Warne and Stanley, 1993) emphasising specific local dynamics in wadi Mariut.

Figure 4. Amphora workshops in the area (base map image: © Google Earth Pro).

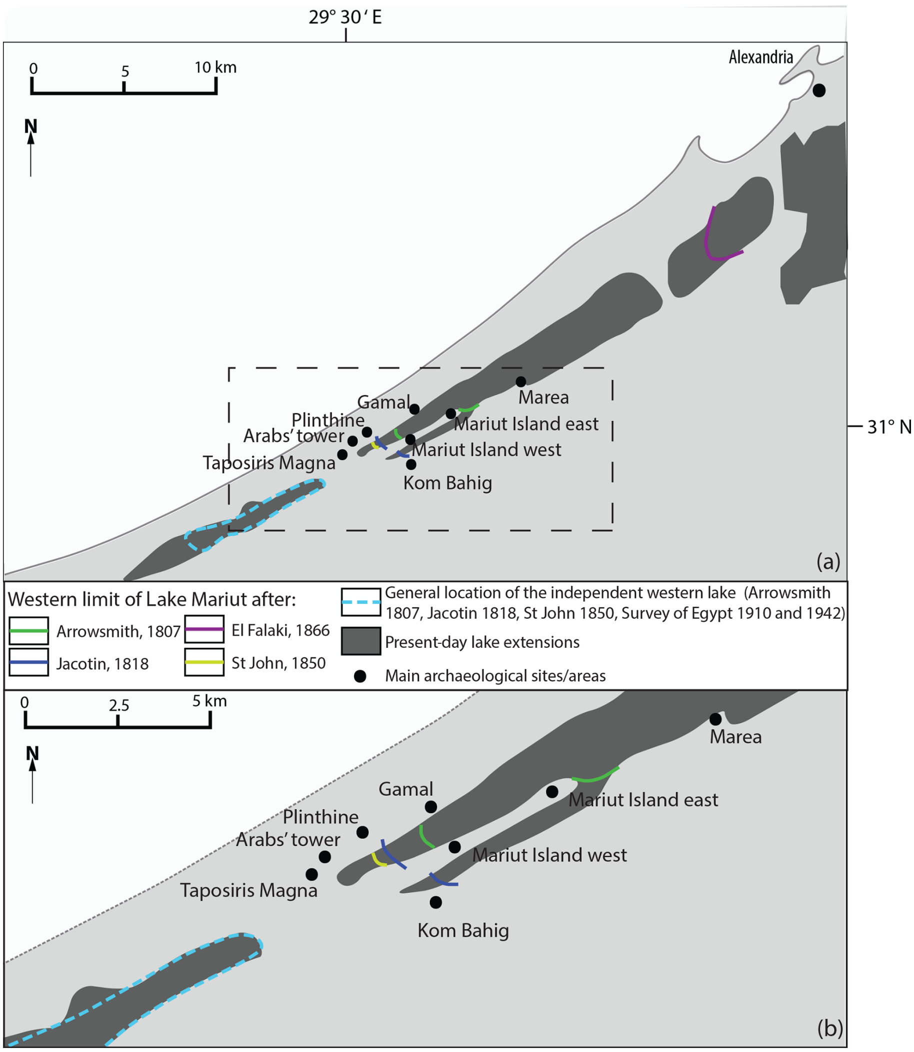

Figure 5. Limit of the lakes according to old maps. **(a)** Regional scale. **(b)** More local scale.

Table 3. Corona photographs used in this study.

Corona ID	Acquisition (mm/yyyy)
DS1016-2088DF007	01/1965
DS1109-2171DF010	03/1970
DS1111-2167DA024	08/1970

ter) which were spanned by small bridges and crossed the wadi Mariut (Le Père, 1823). El Falaki (1872) even mentions entire sites (destroyed by modern construction) extending over 9 km north-east of Taposiris, thus offering a counterpart on the north bank to the succession of sites still visible on the south bank (Blue and Khalil, 2011; Pichot and Simony, 2021). Because of the presence of underwater remains, some early scholars speculated that the lake was completely or partially desiccated during part of antiquity without specifying a precise period (e.g. Reclus, 1885).

4.2.3 Data on Taposiris artificial levee

Some early scholars described the harbour complex of Taposiris, bringing two pieces of information that have now been erased. The west–east artificial levee of Taposiris was doubled by an ancient causeway (De Cosson, 1935), and a second canal dug across the wadi Mariut from north to south linked Taposiris harbour to a dock on the south side of the valley and was doubled with a causeway located on the sedimentary levee forming the west bank of the canal (Oliver, 1945).

4.3 Maps (1807–1958)

4.3.1 Extension of the lake(s)

For all but one (St John, 1850) of the studied maps, the lake did not reach the Arabs' tower even in the periods following the flood of 1801 (Fig. 5). Wadi Mariut is often depicted as being occupied exclusively by marshes (El Falaki, 1866; on a smaller area, Survey of Egypt, 1910, 1942) or being completely dry (AMS, 1958). The boundaries of the lake, whether dried up (Coste, 1827) or in water (Arrowsmith, 1807; Jacotin, 1818), extend farther to the east-south-east in its eastern part than to the west in wadi Mariut, which is in favour of a reinterpretation of the measurements given by Strabo (cf. Sect. 4.1.2). Finally, a small independent lake or marsh is drawn to the west of Taposiris (Fig. 5) in five out of six maps covering this sector (Arrowsmith, 1807; Jacotin, 1818; St John, 1850; Survey of Egypt, 1910, 1942).

4.3.2 Subaquatic topography

One map (AMS, 1958) gives an insight into the now-flooded topography of the bottom of wadi Mariut; the western part of wadi Mariut includes several closed basins whose elevations are below mean sea level and are separated by topographic thresholds and higher areas.

4.3.3 Mention of ruins and remains

The ruins are numerous on both banks of wadi Mariut, as well as on islands and even in the marshy part at its bottom (El Falaki, 1866). To the south of Taposiris and near Kom Bahig, a map (St John, 1850) shows the remains of catacombs and an excavation on the opposite bank. Many dikes, causeways or bridges are also indicated (Jacotin, 1818); there is one causeway between Marea and Sidi Kirayr and a second between Gamal and Mariut island, and elements of dikes or causeways are represented at Taposiris. Finally, the dug canal of the port of Taposiris appears clearly on two maps; El Falaki (1866) indicates in addition to this canal, which he extends to the west, a second canal towards the south in accordance with the descriptions of Oliver (1945; cf. Sect. 4.2.3), and Arrowsmith (1807) roughly draws the shape of the west–east canal and designates it as "Remains of an ancient canal from the Nile". Unfortunately, travellers' descriptions do not make it possible to assess precisely the dating of the remains, but the low occupation of the area from the end of the 7th century CE (Décobert, 2002) until at least the end of the 18th century (Hairy and Sennoune, 2009) makes an ancient dating very likely. Moreover, concerning the canals, neither the books of Coste (1878) and Linant de Bellefonds (1873), who worked on agricultural projects in the region, nor the topographical maps of the 20th century mention the canals, which confirms that they were not made in the 19th or 20th centuries.

4.4 Corona photographs: canals in wadi Mariut

In the photographs used, the levels and extent of the lake are lower than they are today as the agricultural projects that now bring in large amounts of surplus irrigation water were still in their initial stages. In the photograph of August 1970 in particular, the level is very low because of summer evaporation and scarce rainfall, whereas it is higher in the two other ones (March 1970 and January 1965). In the photographs, it appears that in the western part of wadi Mariut, several of the closed basins are linked by two large canals or channels (the longest being more than 12 km) joined to the west of Gamal. From there, a unique canal extends discontinuously up to the artificial levee of Taposiris and further south-west and then west from the Roman bridge of Taposiris where it ends in the small lake mentioned in maps and accounts (Fig. 6). The maximal width of the two joint canals is around 80 m. They border some depressions which could have been harbour basins as they are located close to sites including ancient piers (Fig. 6). The north–south canal (reported by El Falaki, 1866; Oliver, 1945) is also visible.

Some shorter, narrow canals branch to the two main ones and join sites to the south. It is difficult to determine whether

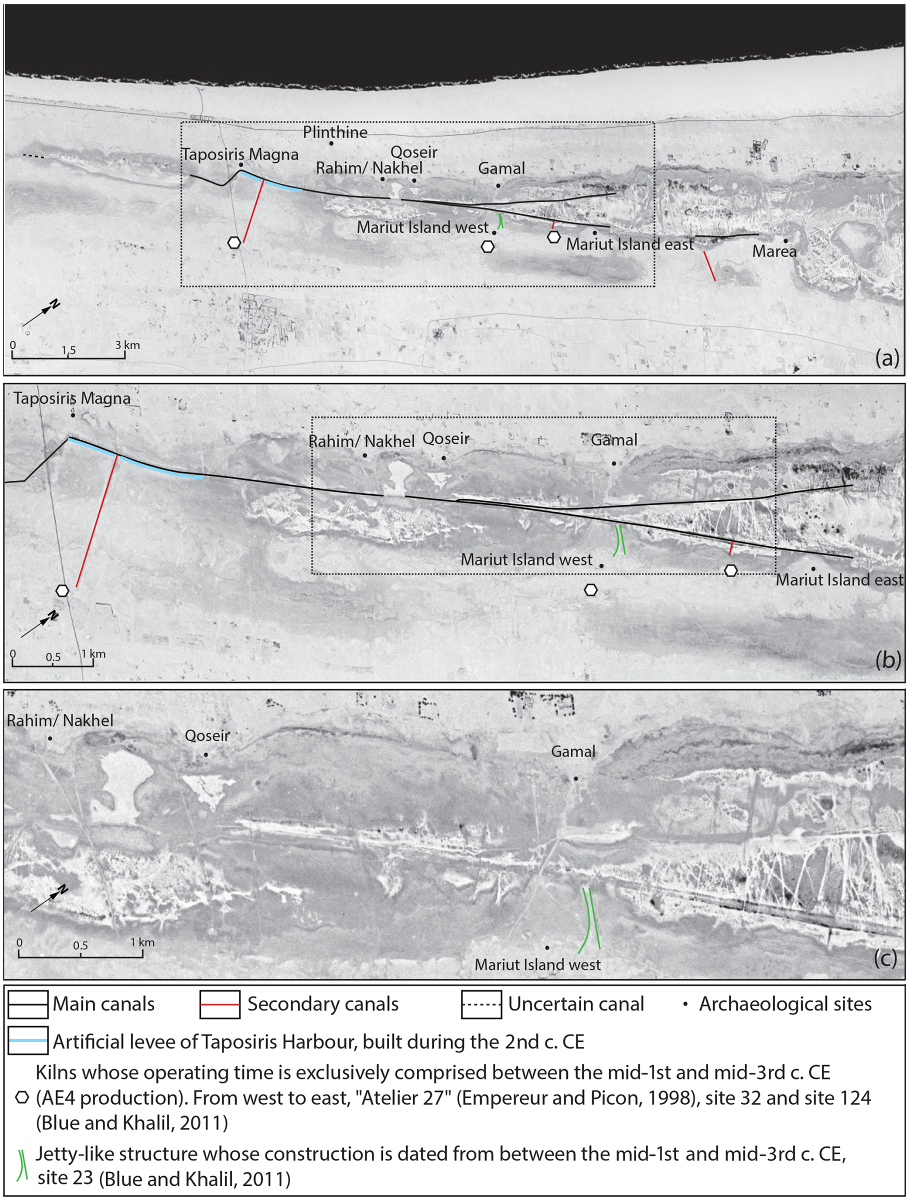

Figure 6. Corona photograph DS1111-2167DA024 (USGS). **(a)** Canal from Marea to the west of Taposiris. **(b)** Focus on the central area. **(c)** Details of the canals.

these canals were deepened channels in flooded areas or if they were canals dug in dry or marshy areas. However, the shapes of the banks of rubble along some parts of the two main canals indicate digging in an environment dry enough for the rubble to remain despite the high proportions of silt and clay at the bottom of wadi Mariut.

5 Discussion

5.1 Solving the paradox: lakes and canals

The combination of all these elements shows that for certain periods of the Holocene, there was not a unique Mariut lake but several lakes occupying closed depressions (cf. Sects. 4.1, 4.2, 4.3.2, 4.4) which could be filled by rainfall. The creation of canals (cf. Sect. 4.4) made it possible to connect them by crossing the topographic thresholds (cf. Sect. 4.3.2). In this way, it was possible to have harbour infrastructures without a continuous stretch of water. These canals are connected to the Taposiris harbour canal, whose digging is firmly dated to the 2nd century CE, and they border several sites that were occupied during the same period, including three amphora kilns whose construction is dated between the mid-1st and the mid-3rd centuries CE (Fig. 6). It is therefore probable that the canals were built during the

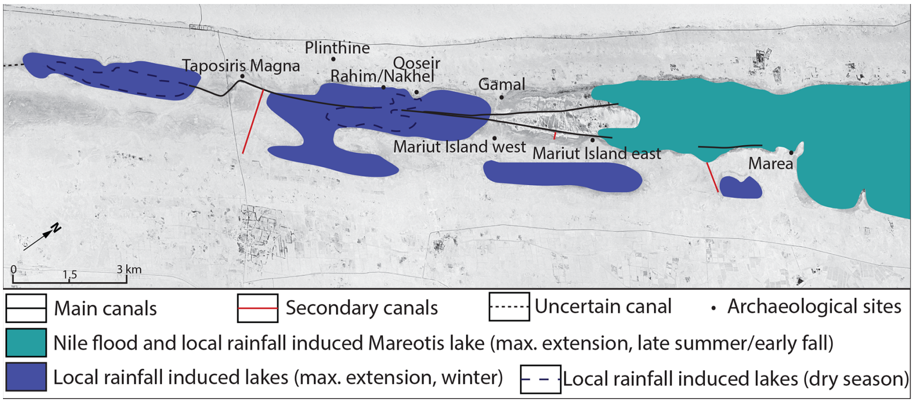

Figure 7. Corona photograph DS1111-2167DA024 (USGS). Proposed extension of the lakes in wadi Mariut during the Hellenistic and early Roman period. Coloured patches correspond to maximum extensions.

Roman period as a harbour complex including several sites (including Taposiris, Mariut island, Marea, etc.). Under these conditions, it becomes easier to understand how Roman harbours could have been in the direct vicinity of Roman amphora kilns; it was not an extensive lake with a highly developed underground water table but smaller basins connected to each other by canals. This interpretation pattern is fully consistent with previously published sedimentological data (e.g. Warne and Stanley, 1993; Tronchère, 2010; Tronchère et al., 2014; Flaux, 2012). Obviously, the chronology will have to be refined by fieldwork at the scale of the wadi Mariut. The magnitude of the works raises a question: for what reasons were canals and at least one bridge built? This article alone cannot provide a complete answer, but it is likely that in an Egyptian climatic context dominated by hyper aridity, the agricultural opportunities offered by the Mediterranean winter rainfall and the natural concentration of surface water in wadi Mariut justified the efforts in connection with the export of local agricultural productions (e.g. wine).

5.2 New hypothesis on Mareotis lake(s) evolution

During the first part of the period under study (first half of the 1st millennium BCE), the archaeological remains were mainly found in high areas, which could lead to the assumption of high lake levels compatible with the palaeoenvironmental data (from Flaux, 2012), but the lack of archaeological excavations calls for caution. In contrast, it is clear that during the Hellenistic and early Roman periods, the water levels were lower, and the extension of the water was smaller (Fig. 7) thanks to the presence of numerous sites incompatible with a single large lake. This reduction can be explained both by the progradation of the Canopic lobe closing off the Bay of Aboukir and the connection to the sea (Flaux, 2012) and by the canal of Alexandria, depriving the lake of part of the Nile flood to the benefit of the city's water supply. The urban and agricultural development of this period could therefore partly explain the ruins mentioned by the early scholars and the maps at the bottom of the wadi Mariut, which are located in some of the topographic threshold areas separating the closed depressions. However, flooding during intense rainfall or an exceptional Nile flood cannot be excluded.

During the Roman period, the digging of the canal artificially re-established the connectivity between the lakes of the wadi Mariut and linked all the sites to Lake Mareotis proper in the east and thus to Alexandria, the Nile and the Mediterranean, contributing to the economic growth of the region. Finally, the construction of the stone jetty at Taposiris after the 4th century CE, which includes a fish pond, as well as the raising of the levee after the 4th century CE (Boussac and El Amouri, 2010), seems to indicate a rise in the water level which could be linked to the gradual subsidence of the Canopic branch (Stanley et al., 2001) or greater Nile floods. This rise has also been demonstrated near Marea (Pichot and Flaux, 2015). Our study does not allow us to know more, but that of Flaux (2011) indicates a severe drying up as early as the 9th century CE.

6 Conclusion and perspectives

This article returns to a subject already addressed by classical sedimentological methods of geoarchaeology. This type of data alone, although obviously necessary to study past environments, was not sufficient to solve the paradox of the wadi Mariut. Combining it with geohistorical sources (Corona photographs, maps, accounts of early scholars) allows for new interpretations. They provide a complementary vision of the spatial organisation, landscapes and environmental dynamics prior to the profound changes in this region since the 1980s.

They allow for the development of a model of the evolution of the wadi Mariut from the beginning of the Hellenistic period (late 4th century BCE) to the beginning of the Medieval period (8th century CE). The lake first experienced a period of drying up followed by urban and agricultural development, including in some sectors of the bottom of the wadi Mariut. During the Roman period in the 2nd century CE, a system composed of large canals was set up, linking independent basins to each other and to the large Lake Mareotis (the lake actually described by Strabo) in the east. After the 4th century CE, higher water levels are likely, before drying up in the 9th century CE (Flaux, 2012). Refining and completing this chronology and this model, as well as studying the canals in detail (possible locks, variability of water levels, etc.) now requires us to go back to the field and start new coring and excavations. It is also a starting point for a new analysis of regional economy and history.

Data availability. The reassessed sedimentological datasets are available in the articles cited in the paper. All the maps are available free of charge on online platforms (last access: 22 January 2021): http://legacy.lib.utexas.edu/maps/ams/egypt/txu-pclmaps-oclc-6559596-el-hammam.jpg (AMS, 1942), http://legacy.lib.utexas.edu/maps/ams/north_africa/txu-oclc-6949452-nh35-8.jpg (AMS, 1958), https://gallica.bnf.fr/ark:/12148/btv1b530669569/ (Arrowsmith 1807), https://gallica.bnf.fr/ark:/12148/btv1b8491814n/ (Coste, 1827), https://gallica.bnf.fr/ark:/12148/btv1b10101071m (El Falaki, 1866), https://gallica.bnf.fr/ark:/12148/btv1b531569998/f42.item (Jacotin, 1818), https://gallica.bnf.fr/ark:/12148/btv1b53136219p/ (St John, 1850), https://www.davidrumsey.com/luna/servlet/detail/RUMSEY~8~1~317305~90086593:Sheet-47-Bahig (Survey of Egypt 1910). These URLs are also indicated in the References. Most of the traveller or early scholar accounts used in this paper are available free of charge on online platforms (last access: 22 January 2021): https://gallica.bnf.fr/ark:/12148/bpt6k28016p/f1.item.r=descriptiondel{'}egypte (Chabrol and Lancret, 1829; Le Père, 1829), https://books.google.fr/books?id=yWo3AQAAMAAJ&printsec=frontcover&hl=fr#v=onepage&q&f=false (Coste, 1878), https://gallica.bnf.fr/ark:/12148/bpt6k280140.r=descriptionel{'}egypte (Jacotin, 1824), https://gallica.bnf.fr/ark:/12148/bpt6k2991761/f9.item.r=dictionnaire%20des%20d%C3%A9couvertes%20mou%20-%20pat (Le Père, 1823), https://gallica.bnf.fr/ark:/12148/bpt6k28013n.r=descriptiondel{'}egypte (Le Père, 1825), https://books.google.de/books?id=tepYAAAAYAAJ&printsec=frontcover&hl=fr#v=onepage&q&f=false (Linant de Bellefonds, 1873), https://archive.org/details/geographicalsys00renn/page/n7/mode/2up (Rennell, 1800), https://archive.org/details/adventuresinliby00stjo/page/n7/mode/2up (St John, 1849). These URLs are also indicated in the References. Corona photographs are available free of charge at https://earthexplorer.usgs.gov/ (USGS, 2021) using the following Corona ID (also provided in Table 3): DS1016-2088DF007, DS1109-2171DF010, DS1111-2167DA024.

Author contributions. MC carried out the reassessment of sedimentological, archaeological and historical data, as well as the collection and analysis of maps, early scholars' accounts, and Corona photographs. MFB contributed to the reassessment of the archaeological and historical data, as well as to the collection of maps and early scholars' accounts. MC took charge of the writing of the paper, MFB amended and approved it.

Competing interests. The authors declare that they have no conflict of interest.

Special issue statement. This article is part of the special issue "Geoarchaeology of the Nile Delta". It is a result of the workshop "Geoarchaeology of the Nile Delta: Current Research and Future Prospects", Würzburg, Germany, 29–30 November 2019.

Acknowledgements. This study has been done as part of the French mission at Taposiris Magna and Plinthine with the kind authorisation of the Egyptian Ministry of Antiquities. We thank Bérangère Redon and Ninon Blond for their suggestions. We thank the anonymous referee and Judith Bunbury for their reviewing works. We warmly thank the editors of this special issue and the organisers of the workshop "Geoarchaeology of the Nile Delta: Current Research and Future Prospects".

Financial support. This research was funded by the French Institute of Oriental Archaeology (IFAO), HiSoMA (MOM) and the French Ministry of Foreign Affairs. The open-access publication was partly funded by DEUQUA and partly by the Shelby White and Leon Levy Program for Archaeological Publications.

Review statement. This paper was edited by Julia Meister and reviewed by Judith Bunbury and one anonymous referee.

References

AMS: El Hammam 88/42, available at: http://legacy.lib.utexas.edu/maps/ams/egypt/txu-pclmaps-oclc-6559596-el-hammam.jpg (last access: 22 January 2021), 1942.

AMS: Burg El Arab, Serie P-502, available at: http://legacy.lib.utexas.edu/maps/ams/north_africa/txu-oclc-6949452-nh35-8.jpg (last access: 22 January 2021), NH35-8, 1958.

Arrowsmith, A.: Map of Lower Egypt, available at: https://gallica.bnf.fr/ark:/12148/btv1b530669569/ (last access: 22 January 2021), 1807.

Awad, I.: A Study of the Evolution of the Maryut Lake through Maps, in: Lake Mareotis Conference: Reconstructing the past, Universities of Southampton and Alexandria, Alexandria, Egypt, 2008, edited by: Blue, L. and Khalil, E., Archaeopress, Oxford, UK, 11–33, 2010.

Bernand, A.: Le Delta égyptien d'après les textes grecs. 1 – les confins libyques, IFAO, Le Caire, 1970 (in French).

Blue, L. K. and Khalil, E.: A multidisciplinary approach to Alexandria's economic past: The Lake Mareotis research project, Archaeopress, Oxford, UK, 2011.

Boussac, M.-F.: Recent works at Taposiris and Plinthine, Bulletin de la Société archéologique d'Alexandrie, 49, 189–217, 2015.

Boussac, M.-F. and El-Amouri, M.: The lake structures at Taposiris, in: Lake Mareotis Conference: Reconstructing the past, Universities of Southampton and Alexandria, Alexandria, Egypt, 2008, edited by: Blue, L. and Khalil, E., 87–105, Archaeopress, Oxford, UK, 2010.

Boussac, M.-F. and Redon, B.: L'intégration des confins nord-ouest de l'Égypte du Nouvel Empire à l'époque ptolémaïque. À propos des découvertes archéologiques récentes à Plinthine et Taposiris Magna (côte méditerranéenne, région du lac Mariout), in: Western borders and margins of Egypt from Antiquity to the Middle Ages, edited by: Boussac, M.-F., Dhennin, S., Redon, B., Somaglino, C., and Tallet, G., IFAO press, in press, 2021 (in French).

Boussac, M.-F., Dhennin, S., and Redon, B.: Plinthine et la Maréotide Pharaonique, BIFAO, 115, 15–35, 2015 (in French).

Chabrol, G. and Lancret, M. A.: Notice topographique sur la partie de l'Egypte comprise entre Rahmanyeh et Alexandrie, et sur les environs du lac Mareotis, available at: https://gallica.bnf.fr/ark:/12148/bpt6k28016p/f1.item.r=descriptiondel'egypte (last access: 22 January 2021), in: Description de l'Égypte, C.L.F. Pancoucke, Paris, France, 18, 2, 3–28, 1829 (in French).

Coste, P.-X.: Carte de la Basse-Égypte dédiée à Mohammed Aly Pacha, available at: https://gallica.bnf.fr/ark:/12148/btv1b8491814n/ (last access: 22 January 2021), vice Roi, 1827.

Coste, P.-X.: Mémoires d'un artiste. Notes et Souvenirs de voyages (1817–1877), available at: https://books.google.fr/books?id=yWo3AQAAMAAJ&printsec=frontcover&hl=fr#v=onepage&q&f=false (last access: 22 January 2021), Marseille, Cayer et Cie, Marseille, France, 1878 (in French).

Crépy, M.: Géomorphologie et environnement du site de la nécropole de Plinthine, in: La nécropole hellénistique de Plinthine, IFAO press, Le Caire, in press, 2021 (in French).

Crépy, M.: Les Paysages du vent: géohistoire et géoarchéologie de la dépression de Kharga (désert Libyque, Égypte) du cinquième siècle avant notre ère à nos jours, PhD thesis, Université Lumière Lyon 2, France, Université de Lyon, 2 December 2016, available at: https://hal.archives-ouvertes.fr/tel-01490559/document (last access: 23 March 2017), 2016 (in French).

Dalongeville, R. and Fouache, E.: Les variations de la ligne de rivage en mer Méditerranée orientale du Pléistocène supérieur et de l'Holocène récent: réflexions, Paleo, 31, 27–38, https://doi.org/10.3406/paleo.2005.4781, 2005 (in French).

De Cosson, A.: Mareotis, Country Life Ltd., London, UK, 1935.

Décobert, C.: Maréotide médiévale. Des Bédouins et des chrétiens, Alexandrie Médiévale, 2, 139–148, 2002 (in French).

Dzierzbicka, D.: Oinos, Production and import of wine in Graeco-roman Egypt, JJP Suppl. 31, University of Warsaw, Warsaw, Poland, 2018.

El-Asmar, H. M. and Wood, P.: Quaternary shoreline development: the northwestern coast of Egypt, Quaternary Sci. Rev., 19, 1137–1149, https://doi.org/10.1016/S0277-3791(99)00097-9, 2000.

El-Falaki, M. B.: Carte des environs d'Alexandrie, available at: https://gallica.bnf.fr/ark:/12148/btv1b10101071m (last access: 22 January 2021), Erhard, Paris, France, 1866.

El-Falaki, M. B.: Mémoire sur l'antique Alexandrie, Bianco-Luno, F.-S. Mulhe, Copenhague, Denmark, 1872 (in French).

Embabi, N. S.: The geomorphology of Egypt: landforms and evolution, 1st Ed., Egyptian Geographical Society, Cairo, Egypt, 2004.

Empereur, J.-Y.: New data concerning the foundation of Alexandria, in: Hellenistic Alexandria, edited by: Zerefos, C. and Vardinoyannis, M., Archaeopress, Athens, Greece, 3–12, 2018.

Empereur, J.-Y. and Picon, M.: Les ateliers d'amphores du lac Mariout, Bulletin de Correspondance Hellénique, 33, 75–79, 1998 (in French).

Flaux, C.: Connexion de la région lagunaire d'Alexandrie au Nil depuis 2 000 ans: entre contrôle anthropique et forçage naturel, Méditerranée, 117, 73–79, https://doi.org/10.4000/mediterranee.5935, 2011 (in French).

Flaux, C.: Paléo-environnements littoraux Holocène du lac Maryut, nord-ouest du delta du Nil, Égypte, PhD thesis, Aix-Marseille, France, 2012 (in French).

Flaux, C., Morhange, C., Marriner, N., and Rouchy, J.-M.: Bilan hydrologique et biosédimentaire de la lagune du Maryût (delta du Nil, Egypte) entre 8 000 et 3 200 ans cal. B.P., Geomorphologie, 17, 261–278, https://doi.org/10.4000/geomorphologie.9474, 2011.

Fraser, P.M.: Ptolemaic Alexandria, Clarendon Press, Oxford, UK, 1972.

Flaux, C., El-Assal, M., Marriner, N., Morhange, C., Rouchy, J.-M., Soulié-Märsche, I., and Torab, M.: Environmental changes in the Maryut lagoon (northwestern Nile delta) during the last ∼ 2000 years, J. Archaeol. Sci., 39, 3493–3504, https://doi.org/10.1016/j.jas.2012.06.010, 2012.

Hairy, I. and Sennoune, O.: Le canal d'Alexandrie: la course au Nil, in Du Nil à Alexandrie: Histoire d'eaux, edited by: Hairy, I., Harpocrates Publishing, Alexandria, Egypt, 2009.

Jacotin, P.: Carte topographique de l'Égypte et de plusieurs parties des pays limitrophes, available at: https://gallica.bnf.fr/ark:/12148/btv1b531569998/f42.item (last access: 22 January 2021), Dépôt général de la Guerre, Paris, France, 1818.

Jacotin, P.: Mémoire sur la construction de la carte de l'Egypte, available at: https://gallica.bnf.fr/ark:/12148/bpt6k280140.r=descriptionel'egypte (last access: 22 January 2021), in: Description de l'Egypte, 17, 437–652, C.L.F. Pancoucke, Paris, France, 1824 (in French).

Le Père, G.: Nome Maréotique, in: Dictionnaire des Découvertes, available at: https://gallica.bnf.fr/ark:/12148/bpt6k2991761/f9.item.r=dictionnaire%20des%20d%C3%A9couvertes%20mou%20-%20pat (last access: 22 January 2021), 12, Louis Colas, Paris, France, 214–222, 1823 (in French).

Le Père, G.: Extrait d'un Mémoire sur les lacs et les déserts de la Basse Egypte, available at: https://gallica.bnf.fr/ark:/12148/bpt6k28013n.r=descriptiondel'egypte (last access: 22 January 2021), in: Description de l'Egypte, 16, 199–227, Panckoucke, Paris, France, 1825 (in French).

Le Père, G.: Mémoire sur la partie occidentale de la province de Bahyreh, connue anciennement sous le nom de nome maréotique, available at: https://gallica.bnf.fr/ark:/12148/bpt6k28016p/f1.item.r=descriptiondel'egypte (last access: 22 January 2021), in: Description de l'Egypte, 18, 29–57, Panckoucke, Paris, France, 1829 (in French).

Linant de Bellefonds, L. M. A.: Mémoires sur les principaux travaux d'utilité publique exécutés en Egypte, available at: https://books.google.de/books?id=tepYAAAAYAAJ&printsec=frontcover&hl=fr#v=onepage&q&f=false (last access: 22 January 2021), Arthus Bertrand, Paris, France, 1873 (in French).

Macklin, M. G., Toonen, W. H. J., Woodward, J. C., Williams, M. A. J., Flaux, C., Marriner, N., Nicoll, K., Verstraeten, G., Spencer, N., and Welsby, D.: A new model of river dynamics, hydroclimatic change and human settlement in the Nile Valley derived from meta-analysis of the Holocene fluvial archive, Quaternary Sci. Rev., 130, 109–123, https://doi.org/10.1016/j.quascirev.2015.09.024, 2015.

Nenna, M. D., Simony, A., Machinek, K., Soukiassian, G., Pichot, V., Awad, I., Séguier, R., Abdelaziz, M., Elsayed, M., Hairy, I., and Soubias, P.: Alexandrie (actions du Centre d'études alexandrines), Bulletin archéologique des Écoles françaises à l'étranger, Égypte, https://doi.org/10.4000/baefe.1094, 2020 (in French).

Oliver, F. W.: Dust-Storms in Egypt and Their Relation to the War Period, as Noted in Maryut, 1939–45, Geogr. J., 106, 26, https://doi.org/10.2307/1790101, 1945.

Pennington, B. T., Sturt, F., Wilson, P., Rowland, J., and Brown, A. G.: The fluvial evolution of the Holocene Nile Delta, Quaternary Sci. Rev., 170, 212–231, https://doi.org/10.1016/j.quascirev.2017.06.017, 2017.

Pichot, V.: La Maréotide: région fertile de la chôra d'Alexandrie, carrefour du commerce, in Quartiers artisanaux en Grèce ancienne, Une perspective méditerranéenne, edited by Esposito, A. and Sanidas, G., Presses Universitaires du Septentrion, Lille, France, 81–104, 2012 (in French).

Pichot, V. and Flaux, C.: Les fours à amphores du Haut-Empire du site d'Akadémia (Maréotide): campagne de fouille et carottages 2014, BCE 25, 259–276, 2015 (in French).

Pichot, V. and Simony, A.: An archaeological map of the Mareotid: initial results regarding the evolution of occupation in the region, in: Western borders and margins of Egypt from Antiquity to the Middle Ages, edited by: Boussac, M.-F., Dhennin, S., Redon, B., Somaglino, C., and Tallet, G., IFAO press, in press, 2021.

Reclus, E.: L'Afrique Septentrionale. Le Bassin du Nil, Hachette et cie, Paris, France, 1885 (in French).

Redon, B., Vanpeene, M., and Pesenti, M.: "La vigne a été inventée dans la ville égyptienne de Plinthine". À propos de la découverte d'un fouloir saïte à Kôm el-Nogous (Maréotide), Bulletin de l'Institut français d'archéologie orientale, 116, 303–323, https://doi.org/10.4000/bifao.440, 2017 (in French).

Rennell, J.: The Geographical System of Herodotus, available at: https://archive.org/details/geographicalsys00renn/page/n7/mode/2up (last access: 22 January 2021), W. Bulmer, London, UK, 1800.

Sennoune, O.: Alexandrie dans les récits de voyage, VIe–XVIIIe siècles, L'Harmattan, Paris, France, 2015 (in French).

Stanley, J.-D.: Nile delta margin: failed and fluidized deposits concentrated along distributary channels / La marge du delta du Nil: concentration de dépôts fracturés et fluidisés le long des paléochenaux fluviatiles, Geomorphology, 9, 211–226, https://doi.org/10.3406/morfo.2003.1186, 2003.

Stanley, J.-D., Goddio, F., and Schnepp, G.: Nile flooding sank two ancient cities, Nature, 412, 293–294, https://doi.org/10.1038/35085628, 2001.

St John, B.: Adventures in the Libyan Desert, available at: https://archive.org/details/adventuresinliby00stjo/page/n7/mode/2up (last access: 22 January 2021), Putnam-John Murray, New York-London, 1849.

St John, B.: Map to Illustrate a Journey from Alexandria (Egypt) to The Oasis of Siwah, available at: https://gallica.bnf.fr/ark:/12148/btv1b53136219p/ (last access: 22 January 2021) Housselin, Paris, France, 1850.

Strabo: Géographie, Livre XVII, 1re partie: l'Égypte et l'Éthiopie nilotique, text edited and translated by Laudenbach, B., Les Belles Lettres, Paris, France, 2015.

Survey of Egypt: Mudiriyet El-Beheira, available at: https://www.davidrumsey.com/luna/servlet/detail/RUMSEY~8~1~317305~90086593:Sheet-47-Bahig (last access: 22 January 2021), Sheet of the 1:50,000 series, Bahîg V-VI N.W., 1910.

Tronchère, H.: Approche paléoenvironnementale de deux sites archéologiques dans le delta du Nil: Avaris et la branche Pélusiaque, Taposiris et le lac Mariout, PhD thesis, Lumière Lyon 2, Lyon, France, 2010 (in French).

Tronchère, H., Millet, B., Goiran, J.-P., Carbonel, P., Djerbi, H., Vera, R., Torab, M., Elassal, M., and Callot, Y.: Geoarchaeological results from the harbor of Taposiris and implications concerning the construction of the harbor, AEundL, 22–23, 383–394, https://doi.org/10.1553/s383, 2014.

Tsoar, H. and Pye, K.: Dust transport and the question of desert loess formation, Sedimentology, 34, 139–153, https://doi.org/10.1111/j.1365-3091.1987.tb00566.x, 1987.

US Geological Survey (USGS): EarthExplorer, available at: https://earthexplorer.usgs.gov/, last access: 22 January 2021.

Warne, A. and Stanley, J.-D.: Late Quaternary Evolution of the Northwest Nile Delta and Adjacent Coast in the Alexandria Region, Egypt, J. Coastal Res., 9, 26–64, 1993.

Woronko, B.: Late-Holocene dust accumulation within the ancient town of Marea (coastal zone of the South Mediterranean Sea, N Egypt), Quaternary Int., 266, 4–13, https://doi.org/10.1016/j.quaint.2011.09.010, 2012.

E&G Quaternary Sci. J., 70, 93–104, 2021
https://doi.org/10.5194/egqsj-70-93-2021

Open Access E&G Quaternary Science Journal

Research article

The late Holocene record of Lake Mareotis, Nile Delta, Egypt

Clément Flaux[1], Matthieu Giaime[2,a], Valérie Pichot[3], Nick Marriner[4], Mena el-Assal[5], Abel Guihou[6], Pierre Deschamps[6], Christelle Claude[6], and Christophe Morhange[6]

[1]Mosaïques Archéologie, Cournonterral, 34660, France
[2]Department of Geography, Durham University, Durham DH1 3LE, UK
[3]CEAlex, CNRS, USR3134, Alexandria, Egypt
[4]Chrono-Environnement, CNRS-UFC, UMR 6249, Besançon, 25000, France
[5]Department of Geography, Faculty of Humanities, King Khalid University, Abha, 62529, Saudi Arabia
[6]Aix Marseille Univ, CNRS, IRD, INRAE, Coll France, CEREGE, Aix-en-Provence, 13090, France
[a]present address: Institute of Environmental Science and Technology (ICTA-UAB), Universitat Autònoma de Barcelona, Bellaterra, 08193 Catalonia, Spain

Correspondence: Clément Flaux (c.flaux@mosaiquesarcheologie.com)

Relevant dates: Received: 28 August 2020 – Revised: 8 February 2021 – Accepted: 17 February 2021 – Published: 8 April 2021

How to cite: Flaux, C., Giaime, M., Pichot, V., Marriner, N., el-Assal, M., Guihou, A., Deschamps, P., Claude, C., and Morhange, C.: The late Holocene record of Lake Mareotis, Nile Delta, Egypt, E&G Quaternary Sci. J., 70, 93–104, https://doi.org/10.5194/egqsj-70-93-2021, 2021.

Abstract: Lake Maryut (northwestern Nile Delta, Egypt) was a key feature of Alexandria's hinterland and economy during Greco-Roman times. Its shores accommodated major economic centers, and the lake acted as a gateway between the Nile valley and the Mediterranean. It is suggested that lake-level changes, connections with the Nile and the sea, and possible high-energy events considerably shaped the human occupation history of the Maryut. To reconstruct Lake Maryut hydrology in historical times, we used faunal remains, geochemistry (Sr isotopic signature of ostracods) and geoarcheological indicators of relative lake-level changes. The data show both a rise in Nile inputs to the basin during the first millennia BCE and CE and a lake-level rise of ca. 1.5 m during the Roman period. A high-energy deposit, inferred from reworked radiocarbon dates, may explain an enigmatic sedimentary hiatus previously attested to in Maryut's chronostratigraphy.

Kurzfassung: In griechisch-römischer Zeit spielte der Maryut-See (nordwestliches Nil-Delta, Ägypten) eine wirtschaftliche Schlüsselrolle im Hinterland von Alexandria. An seinen Ufern befanden sich wichtige Wirtschaftszentren und der See fungierte als Bindeglied zwischen dem Niltal und dem Mittelmeer. Es ist zu vermuten, dass Schwankungen des Seespiegels, Verbindungen zum Nil und zum Mittelmeer und mögliche Hochenergieereignisse die menschliche Besiedlungsgeschichte des Maryut-Sees beachtlich geprägt haben. Um die Hydrologie des Maryut-Sees in historischer Zeit zu rekonstruieren, untersucht diese Studie Faunenreste, geochemische (Sr-Isotopensignaturen von Ostrakoden) und geoarchäologische Indikatoren, die relative Schwankungen des Seespiegels anzeigen. Die Ergebnisse zeigen sowohl einen Anstieg der Nileinträge in den See während des ersten Jahrtausends v. Chr. und n. Chr. als auch einen Anstieg des Seespiegels um ca. 1,5 m während der Römerzeit. Ein Hochenergieereignis, ausgewiesen durch umgelagerte ^{14}C Alter, könnte die Ursache eines rätselhaften Hiatus in den Profilen sein, der zuvor in der Chronostratigraphie des Maryut-Sees nachgewiesen wurde. (*Abstract was translated by Martin Seeliger.*)

1 Introduction

Lake Mareotis, precursor of the modern Maryut lagoon located just south of Alexandria (Egypt), constituted a dense traffic waterway during antiquity (Empereur, 1998), straddling the northwestern Nile Delta. Extensive archeological surveys have shed new light on the intense occupation of its shores between the 4th century BCE and the 7th century CE (Blue and Khalil, 2010). An archeological synthesis at the scale of the western delta has demonstrated that paleowaterways and the overall hydraulic configuration shaped the geography of ancient settlements (Wilson, 2012). Our knowledge and representation of the ancient water network is primarily based upon historical statements, in particular Strabo (Strabo, XVII, 1, 7; translation Yoyotte et al., 1997), according to whom Lake Mareotis was connected to the Nile through several canals on its southern and eastern sides. Lake-level oscillations were then mediated by Nile floods. Nonetheless, this vision furnishes a static view of the lake, whose shores were occupied for a period of 1000 years or more, as recently underscored at Kom el-Nogous close to Taposiris Magna (Fig. 1), occupied during the New Kingdom (Redon et al., 2017). Following Stanley (2019) quoting Butzer (1976, p. 56), "it has become difficult to ignore the possibility that major segments of ancient Egyptian history may be unintelligible without recourse to an ecological perspective." We suggest that this statement resonates strongly with the human occupation history of Lake Mareotis, as originally perceived by De Cosson (1935).

Lake Mareotis is part of the coastal belt of the Nile Delta, spread over a structural boundary which separates Pleistocene coastal sandstone ridges to the west and northwest from the Holocene Nile Delta to the east and southeast (Fig. 1). This situation at the deltaic margin made it very sensitive to hydrological changes, modulated by Holocene relative sea-level changes (e.g., Goiran et al., 2018) and Nile flow modifications (e.g., Sun et al., 2019). We have previously exploited Lake Mareotis sedimentary archives in order to reconstruct its Holocene history (Flaux et al., 2011, 2012, 2013, 2017), aiming to elucidate the ancient geography and hydrology of the lake. The marine transgression of the area is dated to 7.5 ka cal BP. Nile inputs then became progressively predominant in Maryut's hydrology (7–5.5 ka cal BP) in the context of the African Humid Period (AHP). Between 5.5 and 2.8 ka cal BP, the end of the AHP is translated by a progressive hydrological shift from a Nile-dominated to a marine-dominated lagoon. A hiatus in Maryut's sedimentary record precludes investigating the lagoon system between 2.8 and 1.7 ka cal BP. The final phase from 1.7 to 0.2 ka cal BP was characterized by dominant freshwater inputs except between 1.1 to 0.7 ka cal BP, when a Maryut relative lowstand and seawater intrusion are attested. New biosedimentological, geochemical, radiocarbon and geoarcheological data have helped to shed new light on the evolution of Lake Mareotis' water budget during historical times. In particular, this paper aims to better constrain hydrological conditions of the lake during the Greco-Roman period and probe the sedimentary hiatus previously described within the lake sequence (Goodfriend and Stanley, 1996; Flaux et al., 2012).

2 Materials and methods

This study is based on sedimentary sequences retrieved from archeological structures and Lake Maryut. All localities have been benchmarked relative to mean sea level (tide-gauge data from Alexandria taken in 1906) using a differential GPS.

Akadémia and Kôm de la Carrière are two Roman archeological sites lying on the southwestern waterfront of Lake Maryut (Fig. 1). At Akadémia, one sedimentary core was taken from a flooded kiln chamber (core AKA19; 30°59′16.74″ N 29°40′23.56″ E). Another core (AKA12; 30°59′12.31″ N 29°40′07.68″ E; WGS84 coordinate system) was retrieved from the sedimentary filling of a water-wheel well (Egyptian sakieh). Cores were taken in 2015 using a percussion corer Cobra TT and relevant sediment samples were extracted for wet sieving and binocular observation of the sand fraction. The base of the kiln chamber is used as an upper limit of the water table and the base of the well as a lower one. The chronology of both structures, based on their archeological dating (Pichot and Flaux, 2015; Pichot, 2017), shows the evolution of the water-table elevation, related to the adjacent Lake Maryut base level.

At Kôm de la Carrière eight sedimentary cores were collected in 2015 from a ancient silted quarry (Fig. 2). Core AMR-3 (31°01′07.15″ N, 29°44′07.27″ E; WGS84 coordinate system), drilled in the center of the basin, underwent sediment grain size and ostracod analyses at Durham University. We used wet sieving to quantify the sediment texture, including the coarse fraction (>2 mm), sand fraction (50 µm–2 mm) and silty-clay fraction (<50 µm). Ostracods were picked from the >125 µm fraction using a binocular microscope and identified to species level (Athersuch et al., 1989). The core chronology is based on three radiocarbon dates (Table 1), as well as ceramics studied at the Centre d'Etudes Alexandrines (CEAlex; CNRS, Alexandria).

The stratigraphy of Maryut lagoon's southeastern basin was investigated using the new sedimentary section M83, collected in 2014 from the section of a drain crossing the for-

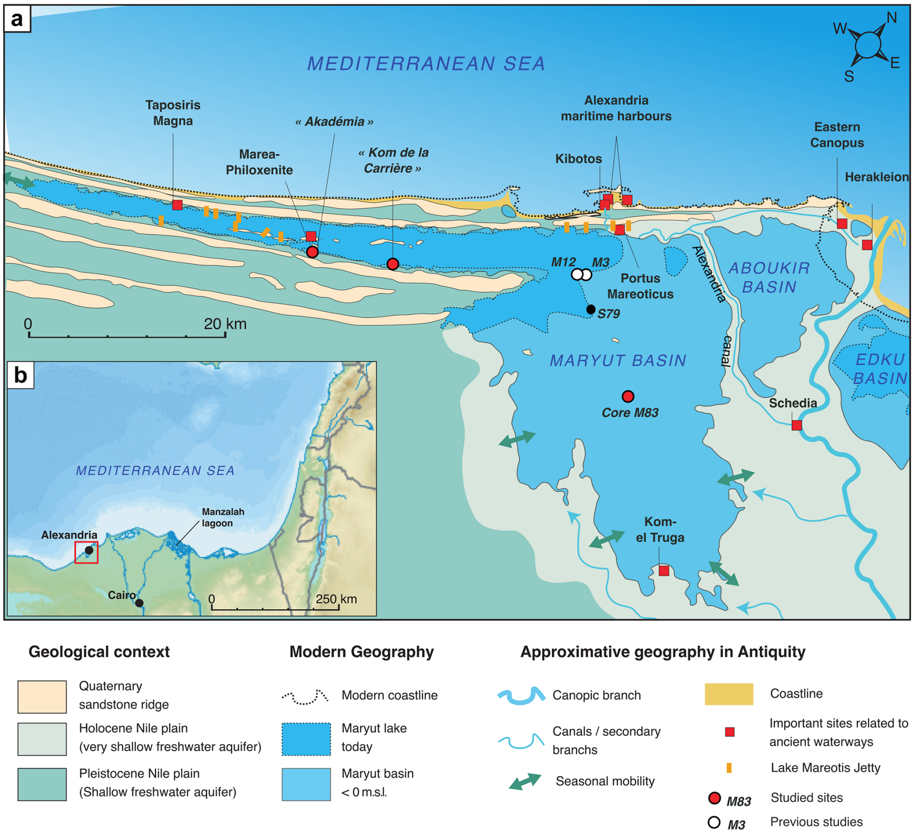

Figure 1. **(a)** Geomorphological map of Lake Mareotis at the northwestern edge of the Nile Delta. **(b)** Location of the study area along the southeastern Mediterranean Sea.

mer lagoon bottoms, now cultivated (Fig. 1; 31°2′39.24″ N, 30°2′21.52″ E; WGS84 coordinate system). A continuous set of 66 samples, each 2 cm thick, was taken from a 1.4 m thick sequence. Bio-sedimentary analyses were undertaken at CEREGE (CNRS, France). We used wet sieving to quantify the sediment texture (including the coarse fraction (>2 mm), sand fraction (50 µm–2 mm) and silty-clay fraction (<50 µm). Ostracods were picked from the >125 µm fraction using a binocular and identified to species level (Athersuch et al., 1989). Sorted mollusk shells were assigned to ecological assemblages according to modern faunal groups observed on the Nile coast (Bernasconi and Stanley, 1994). Magnetic susceptibility measurements were undertaken using a Bartington MS2 magnetic susceptibility meter and are reported as mass-specific magnetic susceptibility in SI units (10^{-8} m^3 kg^{-1}). Strontium isotopes were measured on ostracod valves for 29 samples (ca. 30 when available; Table 2). Reinhardt et al. (1998) analyzed Sr isotopic ratios on surface and subsurface shell samples taken from Manzala lagoon in the eastern Nile Delta and showed that this proxy could be used to reconstruct the recent desalinization of the lagoon, attributed to increasing Nile inflow from the modern irrigation system. Similar results were obtained from the modern northwestern Nile coast (Flaux, 2012, vol. III, p. 13–20) and applied to Maryut's Holocene sedimentary archives (Flaux et al., 2013). For the ^{87}Sr / ^{86}Sr analyses of section M83, we selected the euryhaline ostracod *Cyprideis torosa* due to the species' wide tolerance to hydrological changes (Frenzel and Boomer, 2005). Clean shells were selected and washed with Milli-Q water and then dissolved in a 3 N HNO_3 solution. Sr separation and purification techniques used Sr Spec resin following the procedure modified by Pin et al. (1994). Sr isotopic measurements were performed with a NEPTUNE+ Multicollector ICP-MS at CEREGE. A total of 13 replicate analyses of the NBS 987 standard yielded a ^{87}Sr / ^{86}Sr ratio of 0.710264 ± 0.000023 (2σ), providing a standard error of ±32 ppm (parts per million). The chronology of core M83 is based on seven radiocarbon dates (Table 1).

3 Geoarcheological indicators

3.1 Sediment record from a silted quarry at Kôm de la Carrière

The Kôm de la Carrière site is located on the southwestern shore of Lake Maryut (Fig. 1) at the foothill of a Pleistocene ridge mostly made of poorly consolidated aeolian oolitic carbonate sands (Gebel Maryut ridge; El Asmar and Wood,

Table 1. Radiocarbon data from the Kôm de la Carrière site (core AMR-3) and section M83. The ^{14}C activity was calibrated using the software Calib 8.2 (http://calib.org, last access: February 2021) and the IntCal20 curve (Reimer et al., 2020). No reservoir age correction was applied to radiocarbon ages (see discussion in Flaux et al., 2012, p. 3497). Extracted collagen was used for the bone sample Poz-88215.

Laboratory code	Conventional ^{14}C age	Error	Material	Calibrated BCE/CE (*IntCal20; 2σ*)
Poz-114734	111.84 pMC	0.54 pMC	Plant remains	Recent
Poz-114735	1050	80	Plant remains	774–1198 CE
Poz-114736	2205	30	Organic sediment	371–175 BCE
Beta - 406936	130	30	Charcoal	1673–1942 CE
Poz-89003	2310	50	*Bittium reticulatum* shell	537–203 BCE
Poz-89004	2465	30	*Bittium reticulatum* shell	760–418 BCE
Poz-88215	>46.000	–	Burnt bone fragment	>45 700 BCE
SacA 16171	2655	30	*Cerastoderma* valve	898–788 BCE
Poz-88214	1195	30	Organic residue	706–950 CE
Poz-89005	1845	30	*Bittium reticulatum* shell	122–308 CE

Table 2. Sr isotope data from the ostracod *Cyprideis torosa* extracted in section M83.

Sample depth below the surface (cm)		Sr isotopic ratio		
		Cyprideis torosa number of valves	$^{87}Sr / ^{86}Sr$	StdErr (abs)
2	4	31	0.7088923	6.8995×10^{-06}
6	8	32	0.7086547	7.1254×10^{-06}
10	12	32	0.7086056	7.3353×10^{-06}
16	18	30	0.7089906	6.8555×10^{-06}
22	24	25	0.7088767	8.4143×10^{-06}
32	34	32	0.7090380	7.2522×10^{-06}
36	38	37	0.7090952	5.6228×10^{-06}
40	42.5	29	0.7090651	7.8184×10^{-06}
45	46	28	0.7084412	7.0303×10^{-06}
50	52	32	0.7085629	6.9299×10^{-06}
54	56	33	0.7083908	6.9392×10^{-06}
58	60	46	0.7083415	6.1782×10^{-06}
66	68	38	0.7084961	7.3548×10^{-06}
68	70	29	0.7086069	7.2733×10^{-06}
74	76	23	0.7085054	7.3531×10^{-06}
78	80	26	0.7086150	6.7636×10^{-06}
82	84	23	0.7087141	7.1005×10^{-06}
86	88	16	0.7084723	6.7583×10^{-06}
92	94	20	0.7086781	6.4997×10^{-06}
98	100	23	0.7083944	8.8246×10^{-06}
102	104	26	0.7086270	7.0049×10^{-06}
108	110	26	0.7081114	7.7709×10^{-06}
110	112	25	0.7087512	0.00002
114	116	25	0.7087348	4.73×10^{-06}
116	118	30	0.7089914	6.9982×10^{-06}
118	120	38	0.7089995	4.94×10^{-06}
122	123	34	0.7090287	1.83×10^{-05}
126	128	17	0.7090530	4.57×10^{-06}
130	135	57	0.7086334	4.68×10^{-06}

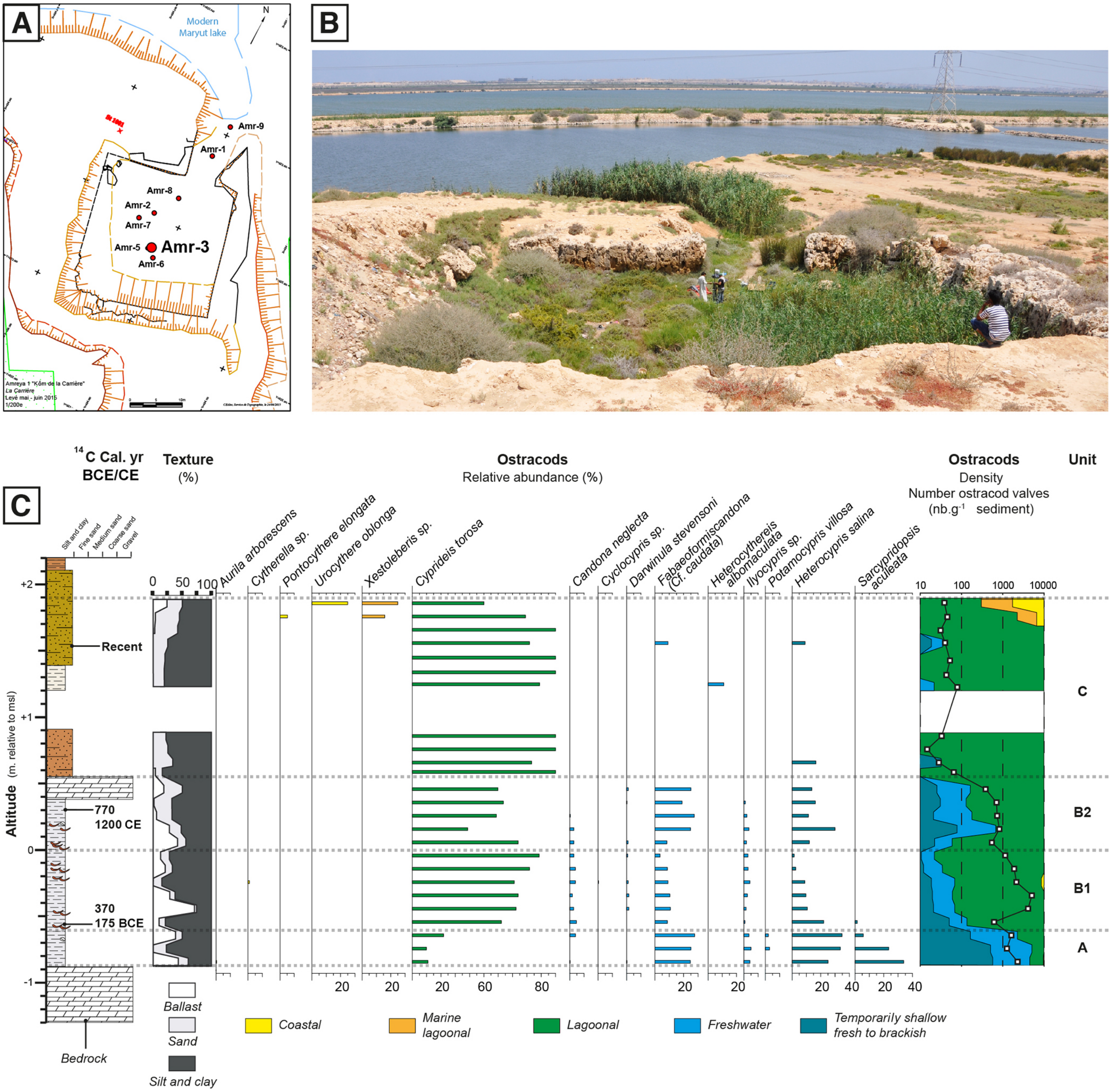

Figure 2. Kôm de la Carrière archeological site. Map **(a)** and photograph **(b)** of the silted quarry open toward Lake Maryut (© CEAlex archive). The quarry was hypothetically used as a lake harbor. Eight cores were taken from the silted quarry to test this hypothesis. Stratigraphy and ostracod species and assemblages of core AMR-3 are given in **(c)**.

2000). This bedrock has been carved in the form of a box-shaped quarry opening onto Lake Maryut (Fig. 2), which led El-Fakharani (1991) to suggest that this structure was later used as a protected harbor in ancient times. Core AMR-3 was taken from the silted quarry in order to test this hypothesis. Three main units were elucidated along the sedimentary sequence.

Unit A is composed of light gray silts and clays (56 %). The sand and gravel fractions respectively represent 17 % and 27 % of the sediment texture. The ostracods comprise an association of freshwater to brackish (86 %) and lagoonal (14 %) species. *Heterocypris salina* and *Sarcypridopsis aculeata*, indicative of temporary fresh to brackish water environments, constitute 52 % of the ostracod assemblage. The density is <1000 valves per 10 g of sediment.

Unit B comprises 63 % silts and clays, 17 % sands, and 20 % gravels. The gravels fraction is dominated by ceramic fragments. There is no color change in relation to unit A. The unit is dated between 370–175 cal BCE and 775–1200 cal CE (1050 ± 80 BP) (Table 1; Fig. 2).

The study of the ostracods allowed us to divide unit B into two subunits. Subunit B1 shows a high density of ostracods (between 530 and 4800 valves for 10 g of sediment). The ecology shows that lagoonal (*C. torosa*) ostracods dominate this assemblage (75 % of the valves). The remaining 25 % comprise freshwater (*Fabaeformiscandona* cf. *caudata*, *Candona neglecta*, *Iliocypris* sp.) and fresh to brackish water species (*Heterocypris salina*). In subunit B2 the faunal density is lower and never exceeds 800 valves per 10 g of sediment (mean density = 511 valves for 10 g of sediment). Fresh to brackish water species represent 45 % of the faunal assemblage, and *C. torosa* is still dominant with 55 % of the identified valves.

Unit C is sandier (27 %), but silts and clays still dominate the total texture (70 %). The gravels represent (3 %) of the sediment aggregate. The faunal density is very low with a maximum density of around 75 valves for 10 g of sediment in the middle of the unit. *C. torosa* is also dominant in this unit, comprising 93 % of the valves. Freshwater species are sporadically present in some samples and represent up to 5 % of the total assemblage.

3.2 Sediment record from a kiln firing chamber and a sakieh well at Akadémia

Akadémia is located on the southwestern shore of Lake Maryut, close to the ancient site of Marea-Philoxenite, ca. 8 km southwest of Kôm de la Carrière (Fig. 1) on the piedmont of the same Gebel Maryut Pleistocene ridge. Archeological remains at Akadémia are composed of an amphora workshop (kilns, activity level and a big waste dump) and a wine press from the 2nd century CE and hydraulic structures from the 5th to early 7th century CE. The plan view of one of the amphora kilns shows a semi-buried circular structure 12.65 m in outside diameter and 7.7 m in inside diameter. The firing chamber of the amphora kiln was cored in order to probe its volume and infilling (core AKA19; Fig. 3). The base of the firing chamber was found 4 m below the oven floor at 0.6 m below msl (mean sea level). The first deposit is a composite, comprising eight layers, 0.1 to 10 cm thick, of ashen and char sediments intercalated with silty sands and fragments of fired clay bricks. This first deposit translates the kiln activity. It is mainly overlain by fragments of fired clay bricks within a sandy silt matrix, related to the abandonment and the infilling stage of the structure. Four well-defined layers of clayey silts, 5–10 cm thick and including a few specimens of the freshwater ostracod *Ilyocypris* sp., were intercalated in the coarse sedimentary infilling.

Core AKA12 retrieved the infilling of a sakieh well found on the western part of Akadémia and is dated to the 5th to early 7th centuries CE (Fig. 3). The sequence is 3.8 m thick. At the base, unit A is made of alternating fine to coarse oolitic sand layers, including a few shell fragments and aeolianite gravels corresponding to the upper altered bedrock. The first depositional layer in the well comprises hydromorphic clayey sandy silts (unit B) with a few specimens of the freshwater ostracod *Candona sp.* and potsherd fragments. Unit C is broadly made up of a conglomerate of gravels and pebbles within a brown silty-sand matrix. This unit C, 1.5 m thick, likely derived from the abandonment and partial destruction of the sakieh's structure. The latter was stabilized during the last deposition of unit D, characterized by homogeneous yellowish brown silty sands. The well's base was found at 0.6 m below msl, while an estimate for the sakieh's hydraulic wheel diameter and position (Pichot and Empereur, 2013, Annexe IV, p. 88) shows that the water level in the sakieh's well when in use was around 1 m above msl (Fig. 3).

4 Sediments from section M83 (Fig. 4)

4.1 Unit A: the Maryut marine lagoon

The upper unit A comprises an alternation of shell-rich and dark mud layers deposited at the centimetric scale. Shell-rich layers comprise very abundant shell fragments and well-preserved and abundant gastropods, mollusks and ostracod valves, the latter sometimes still in connection. Species density is high and diversity low, dominated by *Hydrobia ventrosa* (50 %–95 %), followed by *Cerastoderma glaucum*, *Loripes lacteus*, *Bittium reticulatum* and *Abra* sp. The ostracod assemblage appears monospecific, represented by the ubiquist, euryhaline and opportunist species *Cyprideis torosa* (Frenzel and Boomer, 2005). The $^{87}Sr/^{86}Sr$ values of *Cyprideis torosa* valves taken from this unit are around 0.7090 except one sample close to 0.7086. The upper unit A ends with the deposition of a 4 cm thick layer almost exclusively composed of shell fragments from the same species as the unit A assemblage.

4.2 Units B and C: reworked Lake Mareotis muds?

Unit B is 0.8 m thick and comprises homogeneous silty clays (90 %–95 % of the bulk sediment), dark gray to brown, with a lumpy structure. Gypsum dominates the composition of the sand fraction mainly in discoidal lenticular forms. In sectional view, fine white gypsum was observed in the form of nodules and a mycelium-like morphology. Macrofauna and microfauna are scarce in this unit, but nonetheless the gastropods *Planorbis planorbis* and the ostracod *Ilyocypris* sp. are present, indicators of lightly brackish conditions, together with lagoonal and marine lagoonal species. These low-brackish conditions are confirmed by the $^{87}Sr/^{86}Sr$ signature that decreases significantly to 0.70805 at the base of the unit, although the whole facies is characterized by important fluctuations ranging between 0.70805 and 0.7087

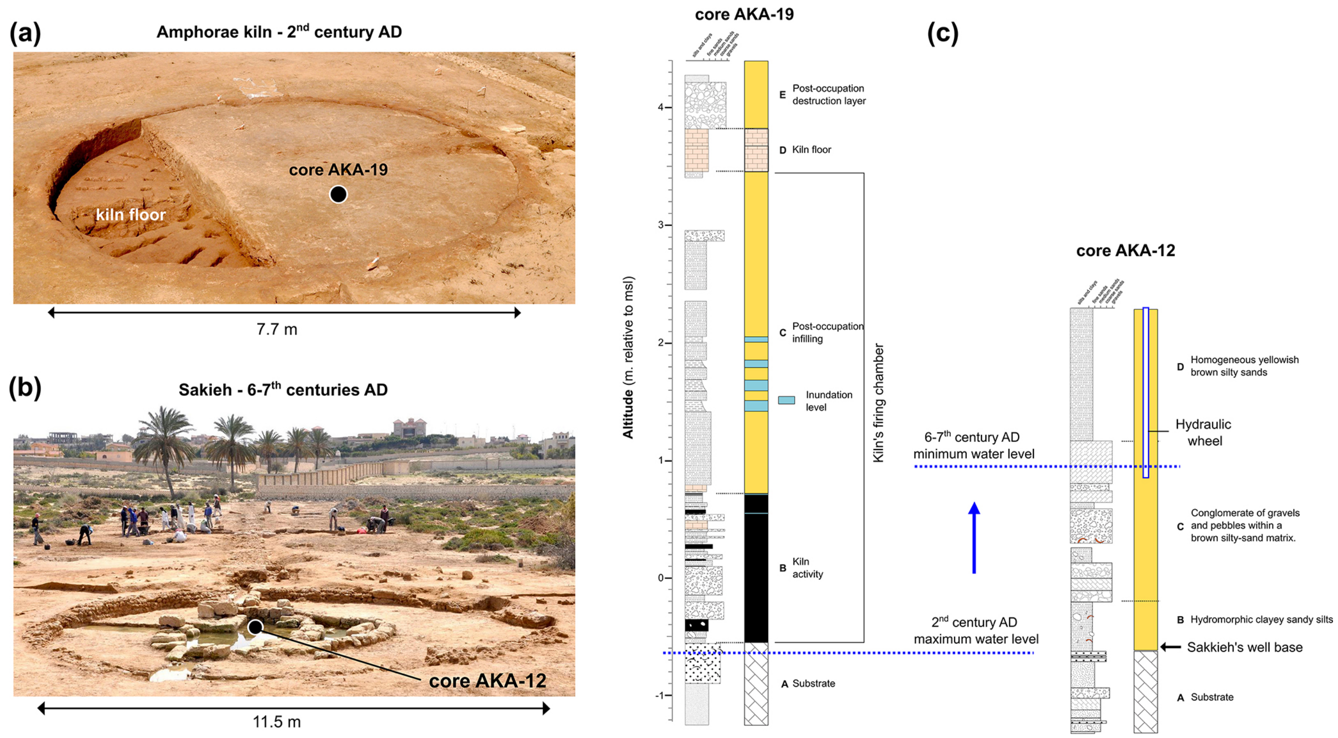

Figure 3. Akadémia archeological site. **(a)** A 2nd century CE amphora kiln. **(b)** A 5th to early 7th century CE sakieh (Egyptian water wheel) 500 m westward from the kiln. Both structures are located at ca. 150 m from the modern lakeshores in a similar configuration at the foothill of a Pleistocene coastal ridge covered by late Quaternary aeolian sands. **(c)** Comparison between cores AKA-19 and AKA-12 stratigraphies. The water table must have been below the kiln chamber during its use, then above the lower water wheel, showing a rise between the 2nd to the 5th century CE.

(Fig. 4). The transition between units A and B is characterized by a decrease in the faunal density and Sr isotope ratio and a sudden increase in magnetic susceptibility from 0 to $70 \times 10^{-8}\,m^3\,kg^{-1}$.

The next unit C comprises compact dark gray clayey silts with a lumpy structure. There is a rich gypsum layer with a pseudo-mycelium structure. Macrofauna density remains are just a few individuals per 100 g of dry sediment, although it peaks to >10 individuals towards the lower half of the unit, dominated by lightly brackish species (*Planorbis planorbis* and *Bellamya* sp.); *Cyprideis torosa* density increases rapidly from tens to hundreds of individuals from the base of unit C then decreases to tens of individuals per gram of sediments. The $^{87}Sr / ^{86}Sr$ ratio in unit C ranges between 0.7083 and 0.70855.

Radiocarbon data from units B and C show great inconsistency (Fig. 4). Three samples, taken from the base of unit B, display ages ranging from 900 BCE to 950 CE. A shell from the middle of unit B was dated to 760–420 BCE, while a burnt bone taken from the same level dates to late Pleistocene times (>45 700 BCE; Fig. 4). Lastly, the upper unit C was dated from 540 to 200 BCE. Such a discrepancy, coupled with age inversions, suggests that units B and C consist of reworked muds. Given the macrofauna and $^{87}Sr / ^{86}Sr$ and ^{14}C data, these muds were mostly reworked from lightly brackish lake bottoms deposited between the first millennium BCE and the first millennium CE.

4.3 Unit D: Lagoon regression

The lower and upper interfaces of unit D were sharply defined. The facies shows an increase in fine-sand inputs that reach ca. 50 % of the sediment bulk. Sands are dominated by quartz minerals. A laminated structure is partially preserved with alternations of sand-rich and mud-rich infra-millimetric layers. The faunal assemblage is characterized by the return of lagoonal species sensu stricto and an increase in *Cyprideis torosa* densities up to several thousand individuals per gram of dry sediment. Three $^{87}Sr / ^{86}Sr$ values display a narrow range between 0.709 and 0.7091 and signal the return of marine-dominated conditions.

4.4 Unit E: final lagoon stage

Unit E provides the last record of section M83. The sand fraction, dominated by quartz minerals, decreases to 25 %–50 % in the lower half and 10 %–25 % in the upper part. The unit contains a few individuals of lagoonal shells (*Hydrobia* sp. and *Cerastoderma glaucum*). The $^{87}Sr / ^{86}Sr$ ratio comprises

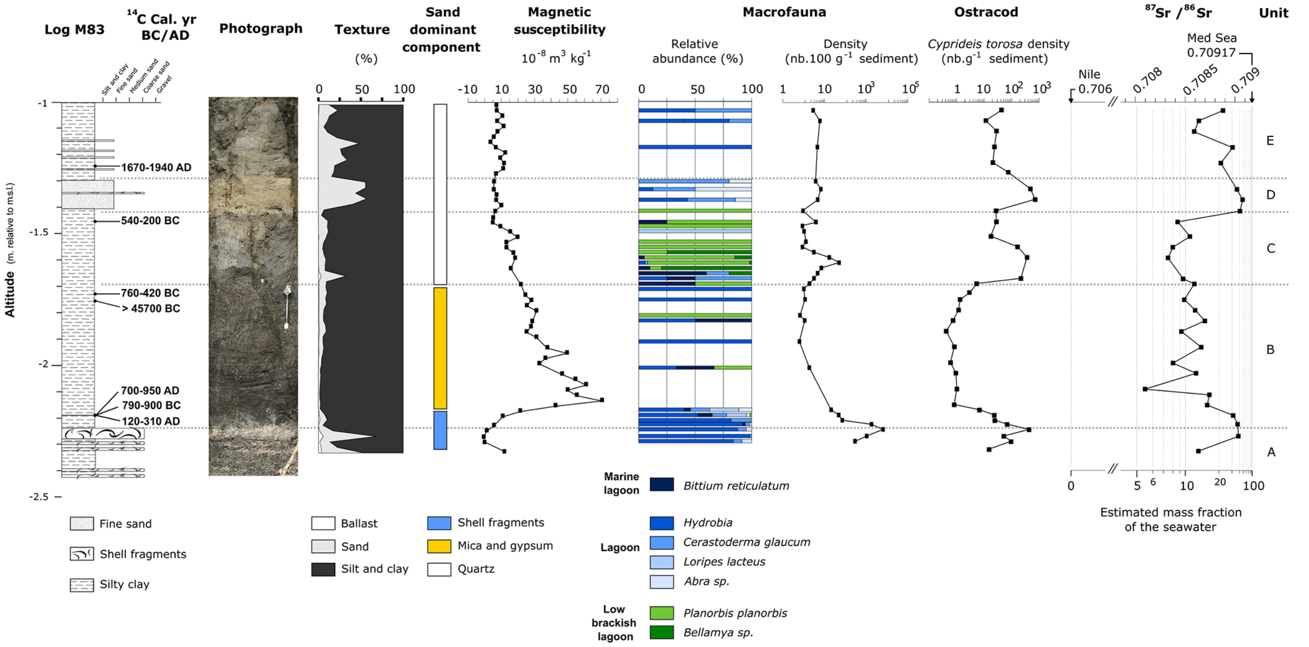

Figure 4. Multi-proxy analysis of section M83 taken from southeastern Lake Maryut (Fig. 1). The mass fraction of seawater was estimated via a two-component mixing equation using modern seawater and Nile river water $^{87}Sr / ^{86}Sr$ signatures (details in Reinhard et al., 1998 and Flaux et al., 2013)

a wider range between 0.7086 and 0.709, indicating a fluctuating water budget from fluvial to marine dominated. A charcoal sample was radiocarbon dated to the modern period, in agreement with historical accounts from the 16th to the 18th centuries CE, which describe, from year to year, alternating lacustrine, lagoonal and salt marsh landscapes in the Maryut basin (Flaux et al., 2012).

5 Lake Mareotis' contrasting sedimentary record

5.1 Lake Mareotis desalinization during the first millennium BCE and Roman water-level rise

Mixed sediments deposited in section M83 have nevertheless recorded, according to fauna and $^{87}Sr / ^{86}Sr$, dominant Nile inputs to Maryut's water budget for a broad period spanning the first millennium BCE to the first millennium CE. This assessment is confirmed by lagoonal to freshwater ostracods found in core AMR-3 taken in a sheltered context in relation to Maryut's southeastern central basin, i.e., the semi-closed inundated quarry located along the western Maryut margin (Fig. 2). These data show that Lake Mareotis was connected to the Nile. Geoarcheological data at Akadémia and Kôm de la Carrière confirm and refine hydrological conditions in Greco-Roman times.

At Akadémia, the kiln and the sakieh lie 500 m from each other in a similar geomorphological context at the foothill of a Pleistocene coastal ridge covered by late Quaternary aeolian sands (El-Asmar and Wood, 2000) ca. 150 m from the modern Lake Maryut shoreline. The base of the kiln's firing chamber lies at a similar depth to the base of the sakieh well, suggesting a rise in the water table between the 2nd (kiln activity) and the 5th to early 7th (sakieh activity) centuries CE, which is in accordance with clayey silt layers including a few specimens of the freshwater ostracod *Ilyocypris* sp., translating stagnant water after the inundation of the firing chamber posterior to its use (Fig. 3). In light of estimates for the sakieh's hydraulic wheel diameter and position (Pichot and Empereur, 2013, Annexe IV, p. 88), a minimum rise in the water table of 1.5 m is inferred (Fig. 3). Because the water table, given the shoreline context of the site and the porosity of loose sediments that compose the substrate of both structures, is probably controlled by the base level of Lake Maryut, it is suggested that Akadémia's remains have recorded a rise in Lake Mareotis' level during Roman times.

The study at Kôm de la Carrière has revealed that the quarry was excavated before or at the beginning of the Hellenistic period at a time when the level of the lake was below mean sea level (msl), given that it is not possible to extract the stones below shallow water (Fig. 2). Following a subsequent rise in water level, the quarry was transformed into a lightly brackish to freshwater basin connected to Lake Mareotis (unit A) and maybe used as a protected harbor. Alternatively, the quarry could have been excavated while disconnected from the lake before the excavation of a canal towards the lake. However, the great porosity of the bedrock, made of poorly consolidated fine to coarse sand layers, and the proximity of the lake go against this hypothesis. Our chronological framework shows that the onset of sedimentation is not much earlier than 370–195 cal years BCE (terminus post quem), which is consistent with excavations and archeological surveys undertaken upon the adjacent Kôm, showing an occupation spanning the Greco-Roman period (Pichot, 2017). Moreover, the basin silted during or after the late Roman period and later, as suggested by late Roman sherds discovered in most of the cores drilled into the silted quarry. Ostracod assemblages from this silting stage (units B1 and B2) comprise 25 % freshwater (*Fabaeformiscandona* cf. *caudata*, *Candona neglecta*, *Iliocypris* sp.) and fresh to brackish water species (*Heterocypris salina*), demonstrating important freshwater inputs, although *Cyprideis torosa* dominates the assemblages and attests to important variations in salinity, possibly related to seasonal Nile floods, in particular in subunit B1. Units B2 and C were deposited between 0 and 1.9 m above msl (Fig. 2), suggesting that Lake Maryut was disconnected from the sea at the time of deposition and mainly supplied by Nile inflow.

Geoarcheological indicators therefore suggest that (1) Lake Mareotis was a lightly brackish lagoon and (2) its level increased by at least ca. 1.5 m between the 2nd and the 5th centuries CE and lay above msl. Late Pleistocene stiff muds lying below Holocene sediments (Chen and Stanley, 1993) represent a relatively impermeable substratum that could have favored the water-level rise and stabilization above msl. It is not clear, however, whether the lake level stabilized above msl or was a seasonal high level linked to the Nile flood. More data are required to better document the dating and nature of this hydrological change, which is crucial for the interpretation of lakeshore archeological sites. For example, the lake-level rise could partially explain the apparent abandonment of Lake Mareotis' southwestern waterfront during the 3rd–4th centuries CE (Pichot, 2017).

5.2 Origin of reworked sediments in section M83: a tsunamite?

M83 chronological framework records a mixed sediment layer (units B and C) deposited between two non-reworked laminated facies (units A and D). The lower unit A is composed of shell-rich layers with a marine $^{87}Sr\,/\,^{86}Sr$ signature (Fig. 4) intercalated with mud layers. This biofacies is widely attested across Maryut sedimentary archives (Warne and Stanley, 1993; Goodfriend and Stanley, 1996; Flaux et al., 2011, 2012, 2013) and formed within a marine lagoon whose deposition ended at the beginning of the first millennium BCE. The upper unit D comprises aeolian sands alternating with muds (unit D), which is consistent with the lake's drying up stage recorded through evaporitic crust dated from the end of the 1st millennium CE (Flaux et al., 2012). Consistently, units B and C show ^{14}C datings from the 1st millennia BCE and CE, but the ages are completely reworked within these units, and a sample of late Pleistocene age was incorporated into the sediment matrix. This facies presents (i) dating inversions, (ii) incoherent juxtaposition of marine lagoonal, lagoonal and lightly brackish faunistic assemblages (unit B), (iii) heterogeneous Sr isotopic ratios (0.70805 and 0.7087), (iv) abrupt changes in the magnetic susceptibility signature of the sediments at the base of the unit B, and (v) a broken shell layer observed at the interface between units A and B (Fig. 4). These elements may suggest that units B and C resulted from the reworking of Lake Mareotis mud bottoms reworked by a high-energy event. At the lake scale, previous chronologies have highlighted an enigmatic sedimentary hiatus. For instance, in core M12, located in the deeper central part of the lake (Fig. 1), the shell-rich facies (identical to M83's unit A) is directly overlain by a gypsum-rich facies (consistent with M83's unit D), meaning that sediments from the first millennium BCE to the first millennium CE are missing (Flaux et al., 2012 and 2013). In section M3, the upper shelly facies dated from the beginning of the first millennium BCE is overlain by lightly brackish muds from the 2nd–3rd centuries CE (Flaux et al., 2012). Radiocarbon dates from section M83 suggest that sediments may have been reworked from the northern deeper part of the basin and were redeposited southeastwards. Goodfriend and Stanley (1996) previously described reworked sediments in core S79 (location in Fig. 1). Faunal assemblages and ^{14}C and $\delta^{13}C$ analyses of shells from the upper 2 m of the sequence show a mixed layer composed of younger freshwater (*Corbicula* sp., 855 uncal BP) and older reworked lagoonal (*Cerastoderma* sp., 3900 uncal BP) species. The scenario means that the tsunami wave would have overflowed above the coastal ridge (5 m high above msl in its lower parts) and across the urban topography of Alexandria, then eroded lake-bottom sediments finally redeposited towards the southeast. In section M83, the shell fragment layer capping unit A and mixed marine to low-brackish species from unit B could have resulted from tsunami wave trains, while dominant lightly brackish fauna in unit C would translate as backwash flow from lake margins. M83's hypothetical tsunamite would have been formed some 20 km from the sea (Fig. 1). Mega-tsunami sediment imprints can be found several kilometers from the coast (Scheffers and Kelletat, 2003), and reworked silt and clays found at site M83 may represent the distal sediment plume.

According to historical sources, eight tsunamis or high-energy marine events struck the coast of Alexandria during antiquity (Goiran, 2012). Previous research has focused on their sedimentological signatures in cores from Alexandria's ancient maritime harbors. Goiran et al. (2005) identified a coarse deposit with older reworked dates, mixed fauna and coarse sediment inputs, including shock impacts on quartz grains (Goiran, 2012). Radiocarbon dates framing the coarse deposit suggest that it has recorded the tsunami wave that hit Alexandria in 811 or 881 CE (Goiran, 2012). Stanley and Bernasconi (2006) observed a possible tsunamite facies with mixed fauna and slump-like sediment strata. Overall, both studies identified, in several coastal sequences of Alexandria's eastern harbor, a centennial- to millennial-scale sedimentary hiatus, as in some of the Lake Mareotis' sequences. It remains, however, difficult to link ancient processes to missing sediments. In Lake Mareotis, section M83 may have recorded mixed sediment reworked from the lake bottoms. The younger reworked age is chronologically consistent with the high-energy event, providing a terminus post quem to 700–950 cal CE. In core M12, given that the gypsum-rich layer following the sedimentary hiatus was dated between the 9th and the 12th centuries CE (Flaux et al., 2012), the 811 or 881 CE tsunami wave may have impacted not only Alexandria's coastal waterfront (Goiran, 2012) but also its southern lakeside. In section M3, however, the sedimentary hiatus spans a shorter period, up to the 2nd–3rd centuries CE, meaning that an older tsunami would have eroded these lake bottoms. Three tsunamic layers deposited during the last 2000 years were found within coastal lagoons protected by 2–20 m high dunes on the northwestern coast of Egypt (Salama et al., 2018).

Alternatively, recurrent gypsum in pseudo-mycelium form observed in units B and C, as well as their lumpy sediment structure and dark color likely related to higher organic input, suggests the development of pedogenic features at site M83. Soil development would necessarily imply that Lake Mareotis retreated from this area and would likely derive from the lake-level lowstand previously recorded after evaporitic deposits in sequences M3 and M12 between the 9th to the 12th centuries CE (Flaux et al., 2012). Soil biological activity or agricultural plowing could also explain reworking dating along units B and C. Although this alternative hypothesis does not explain the enigmatic sedimentary hiatus recorded from the deeper part of the lake, it shows that the tsunami hypothesis requires deeper investigation. Synolakis and Fryer (2001) and Marriner et al. (2017) caution that every coastal enigma does not necessarily have a tsunami explanation.

6 Conclusion

Lake Mareotis was densely occupied during Greco-Roman times. The present contribution aims to better constrain hydrological conditions of the lake during this period. Faunal remains, the Sr isotopic signature of ostracods and geoarcheological indicators of lake levels show both a rise in Nile inputs to the basin during the first millennia BCE and CE and a lake-level rise of ca. 1.5 m during the Roman period. Such changes highlight a complex co-evolution of Alexandria's lakeside occupation history and Nile flow changes, the latter being divided into fluctuating distributaries at the delta scale that were furthermore diverted by irrigation and drainage networks (e.g., Blouin, 2006). From a forward-looking viewpoint, the Alexandria canal (see location in Fig. 1) may have played a crucial role in the evolution of Lake Mareotis' water budget: (1) it has partially diverted the Canopic Nile flow towards the delta's western margin, and (2) it has disconnected the lake from the Aboukir lagoon and thus from the sea, favoring Lake Mareotis' desalinization and allowing its level to rise above msl, as observed at Akadémia and Kôm de la Carrière archeological sites. In any case, desalinization of the northwestern Nile Delta margin could have been key in the development of human occupation in this area during the first millennium BCE. At this time, Lake Mareotis became the natural conveyor for drainage and irrigation water. Since the Hellenistic period at least, there was increasing management of the water system around Lake Mareotis, a process which was accelerated during the Roman period (Pichot, 2017) and may have played a significant role in driving lake-level changes.

Lake Mareotis' configuration was transformed by the 9th century CE from a high-level, hypohaline coastal lake to a sebkha. While we previously related this environmental change to the progressive silting up of the Canopic branch and northwestern delta irrigation system, our new results instead highlight an environmental change related to the impact of possible high-energy event(s). A reconstruction of Lake Mareotis history requires new approaches and perspectives (Crépy and Boussac, 2021).

Data availability. All data generated during this study are included in this article or are available from the corresponding author upon request.

Author contributions. CF, MG, VP, NM, MeA, AG, PD, CC and CM conceived the study and wrote the paper. CF, VP, NM, CM and MeA performed fieldwork and provided chronostratigraphies. MG performed ostracod analyses. CF, AB, PP and CC performed Sr isotopes analyses.

Competing interests. The authors declare that they have no conflict of interest.

Special issue statement. This article is part of the special issue "Geoarchaeology of the Nile Delta". It is not associated with a conference.

Acknowledgements. We thank Hélène Mariot for taking care of CEREGE's clean lab. Matthieu Giaime acknowledges the support of the Institute of Advanced Studies and the Department of Geography at Durham University. We thank two anonymous referees for constructive comments on an earlier version of the manuscript. We thank Martin Seeliger for kindly translating the abstract into German.

Financial support. This research has been supported by the ANR (France) (grant no. ANR-12-SENV-0008-03), the Investissement d'Avenir (France) (grant no. EQUIPEX ASTER-CEREGE), and the Durham Junior Research Fellowship (grant no. 609412).

Review statement. This paper was edited by Julia Meister and reviewed by two anonymous referees.

References

Athersuch, J., Horne, D. J., and Whittaker, J. E.: Marine and Brackish Water Ostracods (Superfamilies Cypridacea et Cytheracea): Keys et Notes for the Identification of the Species, Brill Archive, New Work, USA, 1989.

Bernasconi, M. P. and Stanley, D. J.: Molluscan biofacies and their environmental implications, Nile delta lagoons, Egypt, J. Coast. Res., 10, 440–465, 1994.

Blouin, K.: Homme et milieu dans le nome mendésien à l'époque romaine (1er au 6e s.), PhD thesis, University of Nice Sophia Antipolis, France and University of Laval, Québec, Canada, 558 pp., 2006 (in French).

Blue, L. and Khalil, E. (Eds.): Lake Mareotis: Reconstructing the Past, Proceedings of the International Conference on the Archaeology of the Mareotic Region, Bar International Series 2113, Oxford, England, 2010.

Butzer, K. W.: Early Hydraulic Civilization in Egypt, University of Chicago Press, Chicago, USA, 1976.

Chen, Z. and Stanley, D. J.: Alluvial stiff muds (late Pleistocene) underlying the lower Nile delta plain, Egypt: petrology, stratigraphy and origin, J. Coast. Res., 9, 539–576, 1993.

Crépy, M. and Boussac, M.-F.: Western Mareotis lake(s) during the Late Holocene (4th century BCE–8th century CE): diachronic evolution in the western margin of the Nile Delta and evidence for the digging of a canal complex during the early Roman period, E&G Quaternary Sci. J., 70, 39–52, https://doi.org/10.5194/egqsj-70-39-2021, 2021.

De Cosson, A.: Mareotis, Being a Short Account of the History of Ancient Monuments of the North-western Desert of Egypt and of Lake Mareotis, Country Life Ltd., London, USA, 1935.

El-Asmar, H. M. and Wood, P.: Quaternary shoreline development: the northwestern coast of Egypt, Quaternary Sci. Rev., 19, 1137–1149, https://doi.org/10.1016/S0277-3791(99)00097-9, 2000.

El-Fakharani, F. A.: The Kibotos of Alexandria, Studi Miscellanei, 28, 21–28, 1991.

Empereur, J.-Y.: Alexandrie redécouverte. Fayard, Paris, 254 pp., 1998.

Flaux, C.: Holocene Coastal Palaeo-environment of Maryut Lake in the Northwestern Nile delta, Egypt, PhD thesis, Aix-Marseille University, Marseille, France, 413 pp., 2012.

Flaux, C., Morhange, C., Marriner, N., and Rouchy, J.-M.: Bilan hydrologique et biosédimentaire de la lagune du Maryût (delta du Nil, Egypte) entre 8000 et 3200 ans cal. B.P., Géomorphologie, 3, 261–278, https://doi.org/10.4000/geomorphologie.9474, 2011.

Flaux, C., El-Assal, M., Marriner, N., Morhange, C., Rouchy, J.-M., Soulié-Märsche, I., and Torab, M.: Environmental changes in the Maryut lagoon (northwestern Nile delta) during the last 2000 years, J. Archaeol. Sci., 39, 3493–3504, https://doi.org/10.1016/j.jas.2012.06.010, 2012.

Flaux, C., Claude, C., Marriner, N., and Morhange, C.: A 7500 years strontium isotope record from the northwestern Nile delta (Maryut lagoon, Egypt), Quaternary Sci. Rev., 78, 22–33, https://doi.org/10.1016/j.quascirev.2013.06.018, 2013.

Flaux, C., El-Assal, M., Shaalan, C., Marriner, N., Morhange, C., Torab, M., Goiran, J.-P., and Empereur, J.-Y.: Geoarchaeology of Portus Mareoticus: Ancient Alexandria's lake harbour (Nile Delta, Egypt), J. Archaeolog. Sci. 13, 669–681, https://doi.org/10.1016/j.jasrep.2017.05.012, 2017.

Frenzel, P. and Boomer, I.: The use of ostracods from marginal marine, brackish waters as bioindicators of modern and Quaternary environmental changes, Palaeogeogr. Palaeocl., 225, 68–92, 2005.

Goiran, J.-P.: Caractérisation d'un dépôt de tsunami dans le port antique d'Alexandrie par l'étude exoscopique des quartz: apports et limites de la méthode, in: Archéosismicité & Tsunamis en Méditerranée, Approches croisées, edited by: Rébé-Marichal, I., Laurenti, A., Boehm, I., and Goiran, J.-P., Editions APS, Perpignan, France, 157–190, 2012 (in French).

Goiran, J.-P., Marriner, N., Morhange, C., Abd El-Maguid, M., Espic, K., Bourcier, M., and Carbonel, P.: Évolution géomorphologique de la façade maritime d'Alexandrie (Egypte) au cours des six derniers millénaires, Méditerranée, 104, 61–65, https://doi.org/10.4000/mediterranee.2132, 2005 (in French).

Goiran, J.-P., Vittori, C., Noirot, B., and Torab, M.: Relative Sea Level Variations at Alexandria (Nile Delta, Egypt) over the Last Millennia: Archaeological Implications for the Ancient Harbour, Verlag der Österreichischen Akademie der Wissenschaften, Wien, 2018.

Goodfriend, G. A. and Stanley, J.-D.: Reworking and discontinuities in Holocene sedimentation in the Nile delta: documentation from amino acid racemization and stables isotopes in mollusks shells, Mar. Geol., 129, 271–283, https://doi.org/10.1016/0025-3227(96)83348-2, 1996.

Marriner, N., Kaniewski, D., Morhange, C., Flaux, C., Giaime, M., Vacchi, M., and Goff, J.: Tsunamis in the geological record: Making waves with a cautionary tale from the Mediterranean, Sci. Adv., 3, 10, https://doi.org/10.1126/sciadv.1700485, 2017.

Pichot, V.: Aux portes d'Alexandrie. Le développement de la Maréotide hellénistique et romaine, PhD thesis, Lyon 2 Lumière University, Lyon, France, 1391 pp., 2017 (in French).

Pichot, V. and Empereur, J.-Y.: Rapport de la campagne de fouille juin–août 2013 sur le site d'Akadémia (Égypte), Rapport pour le Ministère de l'Europe et des affaires étrangères, CEAlex, Alexandria, Egypt, 102 pp., 2013 (in French).

Pichot, V. and Flaux, C.: Les fours à amphores du Haut-Empire du site d'Akadémia (Maréotide): campagne de fouille et carottages 2014, Bulletin de liaison de la Céramique Égyptienne (BCE), 25, 259–276, 2015 (in French).

Pin, C., Briot, D., Bassin, C., and Poitrasson, F.: Concomitant separation of strontium and samarium-neodymium for isotopic analysis in silicate samples, based on specific extraction chromatography, Anal. Chim. Acta, 298, 209–217, 1994.

Redon, B., Vanpeene, M., and Pesenti, M.: La vigne a été inventée dans la ville égyptienne de Plinthine, A propos de la découverte d'un fouloir saïte à Kôm el-Nogous (Maréotide), Bulletin de l'Institut français d'archéologie orientale (BIFAO), 116, 303–323, https://doi.org/10.4000/bifao.440, 2017 (in French).

Reimer, P., Austin, W., Bard, E., Bayliss, A., Blackwell, P., Bronk Ramsey, C., Butzin, M., Cheng, H., Edwards, R. L., Friedrich, M., Grootes, P. M., Guilderson, T. P., Hajdas, I., Heaton, T. J., Hogg, A. G., Hughen, K. A., Kromer, B., Manning, S. W., Muscheler, R., Palmer, J. G., Pearson, C., van der Plicht, J., Reimer, R. W., Richards, D. A., Scott, E. M., Southon, J. R., Turney, C. S. M., Wacker, L., Adolphi, F., Büntgen, U., Capano, M., Fahrni, S. M., Fogtmann-Schulz, A., Friedrich, R., Köhler, P., Kudsk, S., Miyake, F., Olsen, J., Reinig, F., Sakamoto, M., Sookdeo, A., and Talamo, S.: The IntCal20 Northern Hemisphere Radiocarbon Age Calibration Curve (0–55 cal kBP), Radiocarbon, 62, 725–757, https://doi.org/10.1017/RDC.2020.41, 2020.

Reinhardt, E. G., Stanley, J.-D., and Patterson, R. T.: Strontium isotopic paleontological method as a high-resolution paleosalinity tool for lagoonal environments, Geology, 26, 1003–1006, 1998.

Salama, A., Meghraoui, M., El Gabry, M., Maouche, S., Hussein, M. H., and Korrat, I.: Paleotsunami deposits along the coast of Egypt correlate with historical earthquake records of eastern Mediterranean, Nat. Hazards Earth Syst. Sci., 18, 2203–2219, https://doi.org/10.5194/nhess-18-2203-2018, 2018.

Scheffers, A. and Kelletat, D.: Sedimentologic and geomorphologic tsunami imprints worldwide – a review, Earth-Sci. Rev., 63, 83–92, 2003.

Stanley, J.-D.: Egypt's Nile Delta in Late 4000 Years BP: Altered Flood Levels and Sedimentation, with Archaeological Implications, J. Coast. Res., 35, 1036–1050, https://doi.org/10.2112/JCOASTRES-D-19-00027.1, 2019.

Stanley, J.-D. and Bernasconi, M. P.: Holocene Depositional Patterns and Evolution in Alexandria's Eastern Harbor, Egypt, J. Coast. Res., 22, 283–297, https://doi.org/10.2112/04-0348.1, 2006.

Sun, Q., Liu, Y., Salem, A., Marks, L., Welc, F., Ma, F., Zhang, W., Chen, J., Jiang, J., and Chen, Z.: Climate-induced discharge variations of the Nile during the Holocene: Evidence from the sediment provenance of Faiyum Basin, north Egypt, Global Planet. Change, 172, 200–210, 2019.

Synolakis, C. and Fryer, G. J. : Review of: Tsunami: The underrated hazard, EOS, 82, 588, https://doi.org/10.1029/01EO00342, 2001.

Warne, A. G. and Stanley, D. J.: Late Quaternary evolution of the northwest Nile delta and adjacent coast in the Alexandria region, Egypt, J. Coast. Res., 9, 26–64, 1993.

Wilson, P.: Waterways, settlements and shifting power in the northwestern Nile Delta, Water Hist., 4, 95–117, https://doi.org/10.1007/s12685-012-0053-z, 2012.

Yoyotte, J., Charvet, P., and Gompertz, S.: Strabon, le voyage en Egypte, un regard romain, Nil Edition, Paris, France, 1997.

E&G Quaternary Sci. J., 70, 19–27, 2021
https://doi.org/10.5194/egqsj-70-19-2021

Open Access E&G Quaternary Science Journal

Research article

Nomes of Lower Egypt in the early Fifth Dynasty

Mohamed Ismail Khaled

Ministry of Antiquities, University of Würzburg, Würzburg, Germany

Correspondence: Mohamed Ismail Khaled (mohamed.khaled@uni-wuerzburg.de)

Relevant dates: Received: 8 July 2020 – Revised: 4 November 2020 – Accepted: 17 November 2020 – Published: 15 January 2021

How to cite: Khaled, M. I.: Nomes of Lower Egypt in the early Fifth Dynasty, E&G Quaternary Sci. J., 70, 19–27, https://doi.org/10.5194/egqsj-70-19-2021, 2021.

Abstract: Having control over the landscape played an important role in the geography and economy of Egypt from the predynastic period onwards. Especially from the beginning of the Old Kingdom, we have evidence that kings created new places (funerary domains) called *ḥw.t* (centers) and *njw.t* (*Ezbah*) for the equipment of the building projects of the royal tomb and the funerary cult of the king, as well as to ensure the eternal life of both kings and individuals. Kings used these localities in order to do so, and they oftentimes expanded the border of an existing nome and created new establishments. Consequently, these establishments were united or divided into new nomes. The paper discusses the geography of Lower Egypt and the associated royal domains in the early Fifth Dynasty based on the new discoveries from the causeway of Sahura at Abusir.

Kurzfassung: Die geographische Unterteilung des Landes als Voraussetzung des Zugriff auf die Ressourcen des Landes spielte für die Wirtschaft Ägyptens und königliche Bauprojekte seit der prädynastischen Zeit eine wichtige Rolle. Um die landwirtschaftliche Nutzung des Landes auszuweiten und diesen Zugriff gleichzeitig zu sichern, begründeten die ägyptischen Könige Wirtschaftsanlagen (Grabdomänen) an schon bestehenden oder neu geschaffenen Siedlungen. Da sich der größte Teil der agrarisch nutzbaren Fläche im Delta befand, wurde im Laufe der Zeit auch das bestehende Gausystem dieses Gebietes mehrfach verändert. Das Papier erörtert die Geographie des Deltas in der frühen fünften Dynastie auf der Grundlage neuer Entdeckungen vom Aufweg des Pyramidenbezirkes des Sahure in Abusir (*Abstract was translated by Eva Lange-Athinodorou.*).

1 Introduction

The term nome is a territorial division in ancient Egypt; it comes from the ancient Greek word νομός, nomós. The term was used when the Greek language was common in Egypt, and this made the Greek historian adapt the term nome to identify the large lists of depictions of nomes with its divisions that are depicted in the late Greco-Roman temples. They usually take the shape of personified male or female figures, and they sometimes carry offerings; above their head is the sign of the nome that they represent, which is depicted on a standard.

In 1907–1908, Ludwig Borchardt carried out the principal exploration of the pyramid complex of Sahura, the second king of the Fifth Dynasty (2490–2475 BCE). Here, he discovered a large number of decorated wall reliefs which until today are considered the most complete example of a decorative program of a royal pyramid complex from the Old Kingdom. His publication still remains the most important source of information about the monument (Borchardt, 1910, 1913).

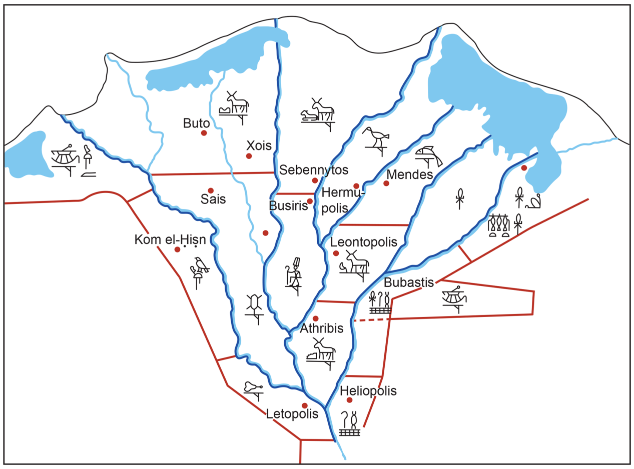

Figure 1. The map of the delta showing the distribution of nomes during the Fifth Dynasty based on the work of Helck (1974), redrawn by Svenja Dirksen based on Helck (1974).

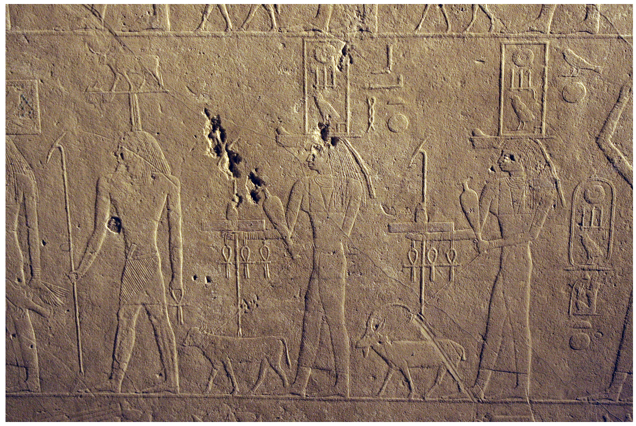

Figure 2. Depiction of the 10th nome of Lower Egypt from a newly discovered block from the causeway of Sahura (photo by Martin Frouz).

Figure 3. Depiction of the western part of the seventh nome of Lower Egypt from a newly discovered block from the causeway of Sahura (photo by Martin Frouz).

The decoration of the south wall of the southern portico of the side entrance to the king's pyramid temple shows different nomes from Lower Egypt in the form of a procession of the personifications of nomes and funerary domains of Sahura. Reflecting the physical geography of Egypt, the scene is divided symmetrically into a southern and a northern section. Unfortunately, only fragments depicting female personifications (most probably from Upper Egypt) were found by Borchardt (1913, 45–46, 106–109, plate 28).

On the opposite north wall of the side entrance, the personifications of Lower Egypt are depicted (Borchardt, 1913, 46, 109–111, plate 31). The scene shows two male and one female bearer of the nomes. The males wear a long wig, necklace and false beard tied to the long wig by means of straps. They also wear a short kilt. Their right hand holds a *wꜣś* scepter, while the loosely hanging left hand carries an *ꜥnḫ* sign. On a fragment published by Borchardt (1913, 42, 105, plate 26), the symbol of the first nome can be seen on the head of the male figure; a complete relief depicting the 10th and 11th nomes of Lower Egypt was also found by Borchardt (1913, 41, 105, plate 31). The female nome personification wears a long wig with a lappet falling over her left shoulder, which hangs down to the top of her long tight-fitting dress held up by shoulder straps that expose her right breast. She wears a broad collar consisting of several layers of beads and a tight choker necklace, bracelets and anklets. Her right hand holds a *wꜣś* scepter, while the loosely hanging left hand carries an *ꜥnḫ* sign. On the head of the female figure is the symbol of the 16th nome of Lower Egypt. Two female bearers of the *ḥwt* type, representing the centers that the king created in each Egyptian nome, follow each of these figures.

The recent excavation by the Supreme Council of Antiquities (SCA) along the upper part of the north wall of Sahura's causeway revealed the most complete example of an Old Kingdom procession of funerary domains. The domains are represented as both the *ḥwt* and *nỉwt* types. However, the majority are of the *nỉwt* type, and there are only six figures of the *ḥwt* type. In addition to the domains, the 10th nome and western part of the seventh nome of Lower Egypt are represented (Khaled, 2008, 101, 131–132). The procession of the funerary domains of Sahura's causeway ends with an additional section which shows a group of fecundity figures in four registers with each register containing three figures. This list represents the northern borders (subdivision) of the nomes depicted in the procession, representing what is called the pehou (*pḥww*) list, i.e., a list of the names of the backwaters of each nome (Khaled, 2018, 235–42).

The depiction of the nome as a male figure occurs for the first time in the pyramid temple of Sahura, and, as in the case of Userkaf, only the standard of the nome is attested (Labrousse and Lauer, 2000, 85–86, Fig. 133a, b). Afterwards, this method of depiction became standard in the royal

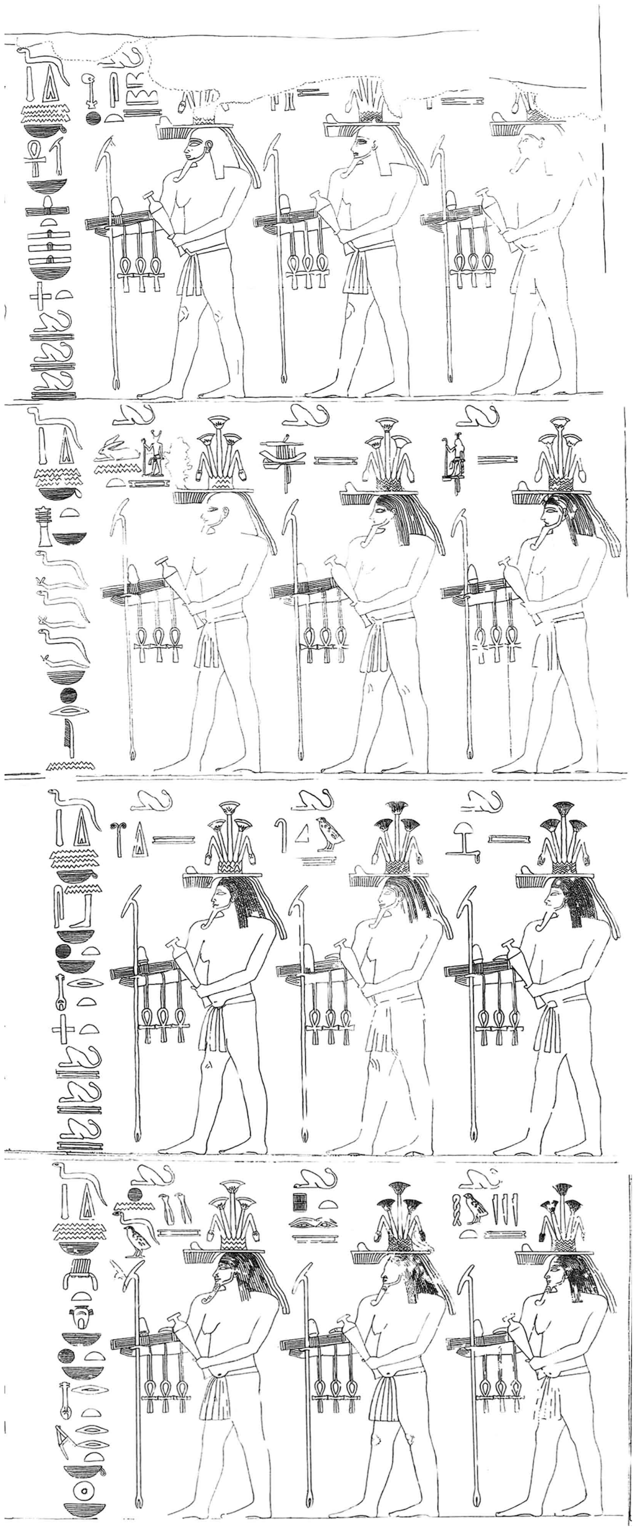

Figure 4. The earliest list of pehou from a newly discovered block from the causeway of Sahura drawn by Jolana Malátková based on the photo of Martin Frouz.

decorative programs of Sahura's successors. What remains unclear is the depiction of a female personification of a nome in the same scenes, which opens a new debate on the attestation of nomes in the form of males and females. Of course, this leads to the suggestion that the depiction of these figures is found only in scenes from the pyramid temple as female personifications as nomes have not yet been discovered in the recently excavated scenes from the causeway. Future exploration of the remaining blocks should clarify this unresolved dilemma.

Additional scenes of nomes are attested on an alabaster altar in the open courtyard on which offerings were presented to the deceased king. These scenes consist of the personifications of male and female figures representing the nomes of Egypt (Megahed, 2014, 58).

1.1 Nomes of Lower Egypt in the Old Kingdom

The late Greco-Roman temples introduced Egyptology to the list of nomes with their division by *mr*, "canal", *ww*, "farmland", and *pḥw.w*, "swamp" (Gauthier, 1935; Helck, 1974; Leitz, 2014, 69–126, plate 1b). They usually take the shape of personified male or female figures, and they sometimes carry offerings. Above their head is the sign of the nome that they represent, which is depicted on a standard.

Jacquet-Gordon (1962, 113) believed that the lists of the nomes from the Old Kingdom to the New Kingdom are different in several aspects from the standard list of later periods. She added that the reasons behind such changes are vague, and they were perhaps due to some administrative requirements.

The new discovery from the northern wall of the causeway of Sahura presents two more nomes of Lower Egypt in addition to the already known Lower Egyptian nomes depicted on the walls of the pyramid temple. Furthermore, the abovementioned so-called pehou list, which brings up the rear of the procession of the funerary domains of Sahura, represents the northern border of the Lower Egyptian nomes. It is the only example of the listing of pehou areas from the Old Kingdom.

Comprehensive information regarding the nomes of Lower Egypt during the Old Kingdom can be derived from different sources. First, there are the royal monuments, such as pyramid complexes belonging to Snefru, Userkaf and Sahura, or the solar temple of Niuserra where nearly complete lists of Lower Egyptian nomes are attested (von Bissing, 1955, 319–38; Kees, 1956, 33–40; Nuzzolo, 2018, 188–198; Seyfried, 2019, 39–42, plates 1–3). Second, there are non-royal tombs where several other nomes from the delta also occur. Nevertheless, only the symbol of the nomes was depicted on a standard. These are usually portrayed within the procession of the funerary domains, referring to the location of the domains that follow. Most of them are incorporated with a royal name. However, in a few cases, nomes also are attested with some private names in the non-royal tombs, such as the tomb of Nikaura (L.G. 87; G 8158), which is attributed to the reign of Khafra (Jacquet-Gordon, 1962, 219–221), and the tombs of Akhethotep and Ptahhotep II (D 64), which are attributed to the reign of Djedkara (Griffith and Davies, 1900, 8–9, plate 13; Baer, 1960, 75 [161]; Strudwick, 1985, 88 [50]; Harpur, 1987, 274 [400]). The tomb of Kairer is attributed to the reign of Unas and Teti (Jacquet-Gordon, 1962, 428–429). The tomb of Sabu/Ibebi (E1, 2+ H3) dates back to the reign of Teti (Baer, 1960, 118 [402]; Strudwick, 1985, 128 [113]; Harpur, 1987, 216–217; El-Khadragy, 2005, 169–199, plates 16–19). The tomb of Khnumenti (G 2374) was created in the reign of Teti (Jacquet-Gordon, 1962, 310–312; Brovarski, 2001, 122–123, plate 92, Fig. 87a). The tomb of Hesi is attributed to the reign of Pepi I (Kanawati and Abder-Raziq, 1999, 13:42, plate 62); however, Silverman (2000, 1–13; Kloth, 2002, 25–26) attributed it to the reign of Teti. Correspondingly, the tomb of Mehou dates to the reign of Pepi I (Baer, 1960, 83 [202]; Strudwick, 1985, 101–102 [69]; Harpur, 1987, 274 [424]), while Altenmüller (1998, 202–205), on the other hand, dates the tomb to the reign of Teti.

Furthermore, nomes are sometimes attested in the autobiography and the titles of the high officials who were in charge of such nomes in the delta; for example, in the biographical inscription of Metjen (tomb: L.S. 6) (Goedicke, 1966, 1–71) and Pehernefer (Junker, 1939, 63–84).

In addition to the nomes attested in the royal annals on the Palermo stone, the Abusir Papyri and other written documents are useful here as will be shown in the following survey.

1.1.1 The first nome

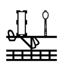

Royal complexes: the first nome of Lower Egypt has been attested in the pyramid complex of Sahura (Borchardt, 1913, 42, 105, plate 26). A possible likeness of the same depiction was found in the "room of the seasons" in the solar temple of Niuserra at Abu Ghurab.

However, it is not clear since it does not appear on top of a standard like the other nomes (von Bissing, 1955, 321, plates 3, 4; Nuzzolo, 2018, 188–198; Seyfried, 2019, plate 3).

Administrative titles, royal annals, etc.: the first nome has appeared in the royal annals of Sahura on the Palermo stone (Wilkinson, 2000, 160–161).

Non-royal tombs: the first nome has appeared in the tomb of Akhethotep (D 64) with a private domain incorporated with his name; however, the nome is not depicted on a standard.

1.1.2 The second nome

Royal complexes: the second nome of Lower Egypt has been depicted in the pyramid complex of Userkaf (Labrousse and Lauer, 2000, 88, Doc. 62, Fig. 134a–b).

Administrative titles, royal annals, etc.: the second nome has been attested in the biographical inscription of Metjen. Also, it occurs in the Abusir Papyri in an administrative title (Posener-Kriéger, 1976, 595).

Non-royal tombs: the second nome appears in the tombs of Akhethotep (D 64) on a standard in front of two Hwt centers incorporated with the name of king Isesi, of Ptahhotep II with a private name of a domain, of Sabu/Ibebi with a domain with the name of king Teti, of Khnumenti with the names of both kings Unas and Teti, and of Hesi with the name of king Teti.

1.1.3 The third nome

Royal complexes: the third nome of Lower Egypt has been attested in the "room of the seasons" in the solar temple of Niuserra at Abu Ghurab.

Administrative titles, royal annals, etc.: the third nome can be found in the biographical inscription of Metjen.

Non-royal tombs: the third nome occurs in the procession of the funerary domains of the tombs of Akhethotep (D 64) on a standard followed by two domains incorporated with the name of Isesi and his queen Setibhor (Megahed, 2011, 616–634; Megahed et al. 2019, 44), of Ptahhotep II and also incorporated with the name of queen Setibhor, of Kairer with the name of Teti, of Sabu/Ibebi with the name of Teti, of Khnumenti with the name of Teti, of Hesi with the name of Teti, and of Mehou incorporated with the names of Isesi, Unas and Teti in addition to a private domain incorporated with his name.

1.1.4 The fourth and fifth nomes

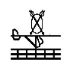

Royal complex: both the fourth and fifth nomes of Lower Egypt have been attested in the pyramid complex of Niuserra (Jacquet-Gordon, 1962, 155), as well as in the "room of the seasons" in the solar temple of Niuserra at Abu Ghurab.

Administrative titles, royal annals, etc.: the fourth and fifth nomes have occurred in the biographical inscription of Metjen. Also, they have been attested in an administrative title in the Abusir Papyri of the Fifth Dynasty (Posener-Kriéger, 1976, 594).

Non-royal tombs: the fourth and fifth nomes have appeared in the tomb of Khnumenti preceding a domain incorporated with the name of Teti. Also, they can be found in the tomb of Hesi above a name of a domain incorporated with the name of Teti.

1.1.5 The sixth nome 

Royal complex: the sixth nome of Lower Egypt has been attested in the pyramid complex of Userkaf (Labrousse and Lauer, 2000, 87–88, DOC. 61 A–C, Fig. 133a, b). Another depiction can be seen in the "room of the seasons" in the solar temple of Niuserra at Abu Ghurab in addition to the last available attestation of this nome in the time of the Old Kingdom in the pyramid complex of Unas (Labrousse and Moussa, 2002, 97–98 Doc. 107, Fig. 139, plate 19a.).
Administrative titles, royal annals, etc.: the sixth nome has occurred in the biographical inscription of Metjen.
Non-royal tombs: the sixth nome has appeared in the tomb of Hesi above a name of a domain incorporated with the name of Teti.

1.1.6 The seventh nome (west) 

Royal complex: the seventh nome of Lower Egypt has been attested on the newly discovered blocks from the northern side of the causeway of Sahura. Also, it has appeared in the pyramid complex of Unas, but it is worth noting that Jacquet-Gordon marked it as the 11th nome of Lower Egypt (Jacquet-Gordon, 1962, 173). Labrousse and Moussa (2002, 98–99 Doc. 108, Fig. 140), on the other hand, believed that this nome is the eighth Lower Egyptian nome. However, based on our new list, we can conclude now that the seventh nome (west) is the best candidate since the same nome is attested in the procession of domains in the non-royal tombs incorporated with the name of Unas. In contrast, the eighth nome with the name of Unas never occurs.
Non-royal tombs: the seventh nome (west) appears in the tomb of Akhethotep (D 64) on a standard followed by eight domains, two of which are in the form of Hwt incorporated with the name of Niuserra, while the rest are depicted in the form of *nỉwt* incorporated with the name of Userkaf (once, possibly twice through reconstruction) and Isesi (four times). It is also noteworthy that the writing of the name in the tomb shows a different writing for the sign for the west, Z 11 in Gardiner's sign list (Gardiner, 1957). Also, the name has been attested in the tomb of Kairer preceding the name of two domains incorporating the names of Unas and Teti. In the tomb of Khnumenti, it appears incorporated with the name of Teti and, in the tomb of Hesi, with the name of Teti. Finally, it can be seen in the tomb of Mehou incorporated with the birth names of Niuserra (Ini), Unas and Teti.

1.1.7 The seventh/eighth nome (harpoon) 

Royal complex: the seventh and eighth nome of Lower Egypt has been attested in the "room of the seasons" in the solar temple of Niuserra at Abu Ghurab.
Administrative titles, royal annals, etc.: the name of the seventh/eighth nome has appeared in the biographical inscription of Metjen. The name of the harpoon nome is also attested on Ostracon Leiden J 427 (Goedicke, 1968, 27).
Non-royal tombs: the name of the seventh/eighth nome has been attested three times in the tomb of Ptahhotep II (D 64) incorporated with the name of Sahura followed by a domain in the form of Hwt and with the names of Ikauhor and Isesi, followed by domains in the form of *nỉwt*.

1.1.8 The eighth nome 

Royal complex: the eighth nome of Lower Egypt has been attested in the pyramid complex of Pepi II as a sign on a standard preceding two domains in the form of Hwt (Jéquier, 1940, plate 25).
Non-royal tombs: the name of the eighth nome has been attested in the tomb of Mehou incorporated with the name of Isesi.

1.1.9 The ninth nome 

Royal complex: the ninth nome of Lower Egypt has never been attested in any royal complexes of the Old Kingdom; however, it appeared as a name of a pehou from the newly discovered blocks from the causeway of Sahura (Khaled, 2018, 238–239, Fig. 1).
Administrative titles, royal annals, etc.: the name of the ninth nome has been attested in the biographical inscription of Pehernefer (Junker, 1939, 68 Nr. 24). Also, it occurred in the royal annals of Sahura on the Palermo stone (Wilkinson, 2000, 160–161).
Non-royal tombs: the ninth nome has been attested twice in the procession of the funerary domains in the tomb of Ptahhotep II (D 64) incorporated with the names of Userkaf and the sanctuary of Nekhen Osiris. It also appeared in the tomb of Kairer with the name of Teti preceding a domain in the form of Hwt and in the tomb of Hesi incorporated with the names of Unas and Teti. Finally, it can be found in the tomb of Mehou incorporated with the name of Teti.

1.1.10 The 10th nome 

Royal complex: the 10th nome of Lower Egypt has been attested in the pyramid complex of Sahura (Borchardt, 1913, 42, 105, plate 31), as well as in the newly discovered blocks from the northern side of the causeway of Sahura. The same depiction can be found in the "room of the seasons" in the solar temple of Niuserra at Abu Ghurab.
Administrative titles, royal annals, etc.: the name of the 10th nome has occurred in the royal annals of Sahura on the Palermo stone (Wilkinson, 2000, 160–161).
Non-royal tombs: The 10th nome has occurred twice in the procession of the funerary domains in the tomb of Ptahhotep II (D 64) incorporated with the names of Snefru and the birth

name of Neferirkara (Kakai); unfortunately, the nome sign is destroyed so that only the rear part of the bull can still be seen. Jacquet-Gordon (1962, 401, 13) reconstructed this nome as the 12th nome; however, based on this present study, it is apparent that this nome is either the 10th or 11th Lower Egyptian nome. Also, the name of the 10th nome has been attested in the tomb of Hesi incorporated with the name of Unas and Teti. Moreover, the same depiction of the bull alone on a standard is depicted in the tomb of Mehou with two domains incorporated with the name of Teti. Jacquet-Gordon (1962, 424, 25) reconstructed this nome as the 12th nome. At any rate, it is far more likely that this depiction also shows the 10th nome since the name of the domain is similar to the name of the domain in the tomb of Hesi.

1.1.11 The 11th nome 

Royal complex: the attestation of the 11th nome of Lower Egypt has occurred in the pyramid complex of Sahura (Borchardt, 1913, 42, 105, plate 31). The nome has also been attested in the pyramid complex of Niuserra (Borchardt, 1907, plate 14), as well as in the "room of the seasons" in the solar temple of Niuserra at Abu Ghurab.
Administrative titles, royal annals, etc.: the 11th nome has occurred in an administrative title in the Abusir Papyri (Posener-Kriéger, 1976, 594).
Non-royal tombs: the 11th nome has been attested in the tomb of Akhethotep (D 64) incorporated with the name of Djedfra, as well as in the tomb of Ptahhotep II with the name of Isesi. This depiction also occurred in the tomb of Sabu/Ibebi with the name of Teti. Jacquet-Gordon (1962, 417, 2) was confused because the bull was depicted alone on a standard, and she preferred to identify it as the 12th nome. Correspondingly, the recent publication by El-Khadragy followed Jacquet-Gordon, Still, the current study shows that this is in fact the 11th Lower Egyptian nome as a recent publication of the tomb of Hesi shows a similar name for the domain of Teti located in the 11th nome.

1.1.12 The 12th nome 

Non-royal complex: the 12th nome of Lower Egypt has been attested in the royal complexes, namely in the "room of the seasons" in the solar temple of Niuserra at Abu Ghurab.
Administrative titles, royal annals, etc.: the name of the 12th nome has occurred in the biographical inscription of Pehernefer (Junker, 1939, 6).
Non-royal tombs: the 12th nome has been attested in the tomb of Ptahhotep II with a domain incorporated with the name of Isesi. Furthermore, the name of the 12th nome has also been attested in the tomb of Hesi incorporated with the name of Teti.

1.1.13 The 13th nome 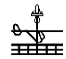

The depiction of the 13th nome has not been attested in any royal complex from the Old Kingdom. The 13th and 14th nomes were both most probably united until the end of the Fifth Dynasty; consequently, both of them were split into two separate nomes after that time (Fischer, 1959, 129–142; Jacquet-Gordon, 1962, 110; Altenmüller, 1998, 124).
Non-royal tombs: the 13th nome has been attested in the tomb of Sabu/Ibebi incorporated with the name of Teti. The same nome has occurred in the tomb of Hesi with the name of Teti, as well as in the tomb of Mehou with the names of Unas and Teti, which could serve as proof that the nome was divided during the reign of Unas as this is the oldest attestation.

1.1.14 The 13th/14th nome (east nome) 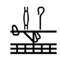

Royal complex: the two nomes have been attested before the division in the pyramid complex of Snefru (Fakhry, 1961, 50. Fig. 24); they are also depicted on the alabaster altar of Niuserra (Borchardt, 1907, plate 14).
Administrative titles, royal annals, etc.: the nome has been documented in the autobiography of the official Nesutnefer (Junker, 1938, 172–175, Abb. 27).
Non-royal tombs: the two nomes have occurred before their division in the tomb of Sabu//Ibebi in the procession of his funerary domains incorporated with the names of Khafra and Isesi. This also serves as proof that, until the time of the Isesi, there was no splitting up of the 13th and 14th nomes.

1.1.15 The 14th nome 

Royal complex: the 14th nome of Lower Egypt has been attested in the pyramid complex of Sahura (Borchardt, 1913, 42, 105, plate 26). Another possible depiction comes from the pyramid complex of Niuserra (von Bissing, 1955, 321, plates 3, 4).
Non-royal tombs: the 14th nome has occurred in the tomb of Khnumenti with the name of Teti. Also, it occurred in the tomb of Hesi with the name of Teti. This could serve as proof that the division was already completed during the reign of Teti.

1.1.16 The 15th nome 

Royal complex: the 15th nome of Lower Egypt has been attested in the "room of the seasons" in the solar temple of Niuserra at Abu Ghurab.
Administrative titles, royal annals, etc.: the nome has also been documented in the autobiography of the official Sehetepu, however, in opposition to Montet (1946, 219–220) who reads it as a name of the god Thoth.

Non-royal tombs: the 15th nome has occurred in the tomb of Kairer with the names of Unas and Teti, as well as in the tomb of Sabu/Ibebi with the names of Unas and Teti. Finally, in the tomb of Mehou, the nome precedes a number of domains of Kaki, Isesi, Unas, queen Seshseshet and Teti in addition to the name of prince Ptahshepses.

1.1.17 The 16th nome 

Royal complex: the 16th nome of Lower Egypt has been attested in the royal complexes in the pyramid complex of Sahura (Borchardt, 1913, 42, 105, plate 31).
Administrative titles, royal annals, etc.: the nome has also been documented in the autobiography of the official Metjen.
Non-royal tombs: the 16th nome has occurred in the tomb of Nikaura with the name of Khafra, as well as in the tomb of Khnumenti with the name of Teti. Finally, in the tomb of Mehou the name is attested with the name of Teti and the royal mother Seshseshet.

2 Conclusions

From the current study, it is apparent that, during the reign of Niuserra, Lower Egypt had its complete division and number of nomes; in addition, the changes in the administration of high regional officials outside the Memphite region serve as other evidence of expanding the land of the delta (Willems, 2014, 20–23). As Helck mentioned, the delta contained 16 nomes by the Fifth Dynasty (Helck, 1974, 199–203). On the other hand, one can observe that the delta had only 12 nomes in the time of Sahura at the beginning of the Fifth Dynasty. Some are attested in his pyramid temple and causeway, while the others are mentioned in the non-royal tombs. Other nomes already occur prior to Sahura's reign, such as the nomes of the delta mentioned in the autobiography of Metjen and also those attested with the names of Snefru, Khafra and Userkaf.

According to Helck, the fourth and fifth nomes of Lower Egypt were counted as one nome in the Old Kingdom (Helck, 1974, 158–163). Therefore, this paper proposes that the existing nomes of Lower Egypt in the time of Sahura were only 12 in number and include the 1st, 2nd, 3rd, 4th/5th and 6th and the west of the 7th, 8th, 9th, 10th, 11th, 13th/14th and 16th nomes. The new discovery of the pehou list from the causeway of Sahura somewhat confirms this number.

Scholars have already observed that the order of the nomes is not consistent, especially in the list of Niuserra in which the ninth nome is followed by the 12th and then the 11th and 10th nomes. Therefore, based on this observation, it is logical to accept variation in the names and their locations within the lists, which do not necessarily follow the numerical order of our modern view. However, it seems impossible to know the exact number of nomes, especially during the Old Kingdom, because these numbers were created according to later lists.

For example, the geographical location of the 16th nome of Lower Egypt depicted in the pyramid temple of Sahura is unknown, and this nome might have occupied the 12th position at the time of this king.

An important observation can be made, however, on the basis of the new data: the organization of the nomes was fluid in a way that the territory assigned to them and their borders was altered from time to time by the requirements of ancient Egyptian administration. The new reliefs from the causeway of Sahura at Abusir show how the kings were concerned about the geography of the country besides the important information that can be generated from the scenes that the territory of the delta was growing and expanding very quickly. Kings used to expand the borders of an existing nome and to create new establishments. Consequently, these establishments were united or divided into new nomes. (See above the division of the 13th and 14th nomes.) This could also serve as evidence for the changes in the names of the list of nomes. Of course, future excavation and discoveries will add more new information to the subject.

Data availability. All data relevant for this contribution are presented within the article itself (see Sects. 1 and 2).

Competing interests. The author declares that there is no conflict of interest.

Special issue statement. This article is part of the special issue "Geoarchaeology of the Nile Delta". It is a result of the workshop "Geoarchaeology of the Nile Delta: Current Research and Future Prospects", Würzburg, Germany, 29–30 November 2019.

Acknowledgements. This article was completed within the framework of the DFG project ID 389349558 (see https://gepris.dfg.de/gepris/projekt/389349558, last access: 8 July 2020). "Archäologie des ägyptischen Staates und seiner Wirtschaft im 3. Jahrtausend v. Chr.: eine neue Untersuchung des Sahurê-Aufwegs in Abusir".

Financial support. This open-access publication was funded by Julius-Maximilians-Universität Würzburg.

Review statement. This paper was edited by Eva Lange-Athinodorou and reviewed by two anonymous referees.

References

Altenmüller, H.: Die Wanddarstellungen Im Grab Des Mehu in Saqqara, Archäologische Veröffentlichungen 42, Mainz am Rhein, von Zabern, 1998.

Baer, K.: Rank and Title in the Old Kingdom: The Structure of the Egyptian Administration in the Fifth and Sixth Dynasties, Chicago: University of Chicago Press, 1960.

Borchardt, L.: Das Grabdenkmal Des Königs Ne-User-Re', Leipzig, Hinrichs'sche Buchhandlung, 1907.

Borchardt, L.: Das Grabdenkmal Des Königs S'ahu-Re. Leipzig: J. C. Hinrichs, 1910.

Borchardt, L.: Das Grabdenkmal Des Königs Sahu-Re: Abbildungsblätter, Leipzig: Hinrichs'sche Buchhandlung, 1913.

Brovarski, E.: The Senedjemib Complex. Pt. 1, [Ill.]: The Mastabas of Senedjemib Inti (G2370), Khnumenti (G2374), and Senedjemib Mehi (G2378), Giza Mastabas 7, Boston, Art of the Ancient World, Museum of Fine Arts, Boston, 2001.

Fakhry, A.: The Monuments of Sneferu at Dahshur II. The Valley Temple, Part I. The Temple Reliefs, Cairo: General Organization for Government Printing Offices, 1961.

Fischer, H. G.: Some Notes on the Easternmost Nomes of the Delta in the Old and Middle Kingdoms, in: Journal of Near Eastern Studies, 18, 129–42, 1959.

Gardiner, A. H.: Egyptian Grammar: Being an Introduction to the Study of Hieroglyphs, Third revised edition, London, Oxford University Press, 1957.

Gauthier, H.: Les Nomes d'Égypte Depuis Hérodote Jusqu'à La Conquête Arabe, Vol. 25. Mémoires de l'Institut d'Égypte, Le Caire: Imprimerie de l'Institut français d'archéologie orientale, 1935.

Goedicke, H.: Die Laufbahn Des MTn: in: Mitteilungen Des Deutschen Archäologischen Instituts, Abteilung Kairo, 21, 1–71, 1966.

Goedicke, H.: Four Hieratic Ostraca of the Old Kingdom, J. Egypt. Archaeol., 54, 23–30, 1968.

Griffith, F. Ll. and Davies, N. de G.: The Mastaba of Ptahhetep and Akhethetep at Saqqareh, Vol. 8–9. 2 vols. Archaeological Survey of Egypt, London, Egypt Exploration Fund, 1900.

Harpur, Y.: Decoration in Egyptian Tombs of the Old Kingdom: Studies in Orientation and Scene Content, Studies in Egyptology, London; New York: New York, NY, USA: KPI; Distributed by Methuen, Routledge & Kegan Paul, 1987.

Helck, W.: Die Altägyptischen Gaue, TAVO, B/5, Wiesbaden: Dr. Ludwig Reichert, 1974.

Jacquet-Gordon, H.: Les Noms Des Domaines Funéraires Sous l'Ancien Empire Égyptien. BdÈ 34, Caire: Institut Français d'Archéologie Orientale, 1962.

Jéquier, G.: Le Monument Funéraire de Pepi II: Tome 3. Les Approches Du Temple. Fouilles à Saqqarah, Le Caire: l'Institut francais d'archeologie orientale, 1940.

Junker, H.: Giza III: Bericht Über Die von Der Akademie Der Wissenschaften in Wien Auf Gemeinsame Kosten Mit Dr. Wilhelm Pelizaeus Unternommenen Grabungen Auf Dem Friedhof Des Alten Reiches Bei Den Pyramiden von Giza. Band III, Die Mastabas Der Vorgeschrittenen V. Dynastie Auf Dem Westfriedhof, Wien – Leipzig: Hölder-Pichler-Tempsky, 1938.

Junker, H.: PHrnfr, in: Zeitschrift Für Ägyptische Sprache Und Altertumskunde, 75, 63–84, 1939.

Kanawati, N. and Abder-Raziq, M.: The Teti Cemetery at Saqqara. Volume V: The Tomb of Hesi. Vol. 13. Australian Centre for Egyptology: Reports, Warminster: Aris & Phillips, 1999.

Kees, H.: Zu Den Gaulisten Im Sonnenheiligtum Des Neuserrê, in: Zeitschrift Für Ägyptische Sprache Und Altertumskunde, 81, 33–40, 1956.

El-Khadragy, M.: The Offering Niche of Sabu/Ibebi in the Cairo Museum, in: Studien Zur Altägyptischen Kultur, 33, 169–99, 2005.

Khaled, M. I.: The Old Kingdom Royal Funerary Domains: New Evidence from the Causeway of the Pyramid Complex of Sahure, PhD thesis, Prague: Charles University in Prague (PhD dissertation), 2008.

Khaled, M. I.: The Earliest Attested Pehou List in the Old Kingdom, in: The Art of Describing: The World of Tomb Decoration as Visual Culture of the Old Kingdom. Studies in Honour of Yvonne Harpur, edited by: Peter Jánosi and Hana Vymazalová, Prague: Charles University, Faculty of Arts, 235–247, 2018.

Kloth, N.: Die (Auto-) Biographischen Inschriften Des Ägyptischen Alten Reiches: Untersuchungen Zur Phraseolohgie Ung Entwicklung, SAK 8, Hamburg: Buske, 2002.

Labrousse, A. and Lauer, J. P.: Les Complexes Funéraires d'Ouserkaf et de Néferthétepès. BdE 130, Le Caire, Institut français d'archéologie orientale, 2000.

Labrousse, A. and Moussa, A. M.: La Chaussée Du Complexe Funéraire Du Roi Ounas. BdE 134, Le Caire: Institut francais d'archéologie orientale, 2002.

Leitz, C.: Geographische Soubassementtexte Aus Griechisch-Römischer Zeit Eine Hauptquelle Altägyptischer Kulttopographie, in: Altägyptische Enzyklopädien, Die Soubassements in Den Tempeln Der Griechisch-Römischen Zeit, Studien Zur Spätägyptischen Religion 7, Wiesbaden, I, 69–126, 2014.

Megahed, M.: The Pyramid Complex of Djedkare's Queen' in South Saqqara Preliminary Report 2010, in: Abusir and Saqqara in the Year 2010, edited by: Bárta, M., Coppens, F., and Krejčí, J., Prague, Czech Institute of Egyptology Faculty of Arts, Charles University in Prague, 616–634, 2011.

Megahed, M.: The Altar of Djedkare's Funerary Temple, from South Saqqara, in: Cult and Belief in Ancient Egypt: Proceedings of the Fourth International Congress for Young Egyptologists, 25–27 September 2012, Sofia, edited by: Lekov, T. and Buzov, E., Sofia: Bulgarian Institute of Egyptology, New Bulgarian University, 56–62, 2014.

Megahed, M., Hashesh, Z., Jánosi, P., and Vymazalová, H.: Djedkare-Isesis Pyramidenkomplex: Grabungskampagnen 2018, in: Sokar 38, 24–49, 2019.

Montet, P.: Tombeaux de La Ière et de La IVe Dynasties à Abou-Roach: Deuxième Partie, Inventaire Des Objets, in: Kêmi, 8, 157–227, 1946.

Nuzzolo, M.: The Fifth Dynasty Sun Temples: Kingship, Architecture and Religion in Third Millenium BC Egypt, Prague: Charles University Faculty of Arts, 2018.

Posener-Kriéger, P.: Les Archives Du Temple Funéraire de Néferirkare-Kakai (Les Papyrus d'Abousir): Traduction et Commentaire I-II. BdÈ 65, Caire: Institut Français d'Archéologie Orientale, 1976.

Seyfried, K. J.: Jahreszeitenreliefs Aus Dem Sonnenheiligtum Des Koenigs Ne-User-Re, 1st edition, Boston, MA, De Gruyter, 2019.

Silverman, D.: The Threat Formula and Biographical Text in the Tomb of Hezi at Saqqara, in: Journal of the American Research Center in Egypt, 37, 1–13, 2000.

Strudwick, N.: The Administration of Egypt in the Old Kingdom: The Highest Titles and Their Holders, Studies in Egyptology, London, KPI, 1985.

von Bissing, F. W.: La Chambre Des Trois Saisons Du Sanctuaire Solaire Du Roi Rathourès (Ve Dynastie) à Abousir, in: Annales Du Service Des Antiquités de l'Égypte, 53, 319–38, 1955.

Wilkinson, T.: Royal Annals of Ancient Egypt: The Palermo Stone and Its Associated Fragments, Studies in Egyptology, London, Kegan Paul International, 2000.

Willems, H.: Historical and Archaeological Aspects of Egyptian Funerary Culture: Religious Ideas and Ritual Practice in Middle Kingdom Elite Cemeteries, Culture and History of the Ancient Near East, volume 73, Leiden, Boston, Brill, 2014.

E&G Quaternary Sci. J., 70, 73–82, 2021
https://doi.org/10.5194/egqsj-70-73-2021

Open Access E&G Quaternary Science Journal

Research article

Implications of geoarchaeological investigations for the contextualization of sacred landscapes in the Nile Delta

Eva Lange-Athinodorou

Lehrstuhl für Ägyptologie, Julius-Maximilians-Universität Würzburg, Würzburg, 97070, Germany

Correspondence: Eva Lange-Athinodorou (eva.lange@uni-wuerzburg.de)

Relevant dates: Received: 2 July 2020 – Revised: 30 September 2020 – Accepted: 9 October 2020 – Published: 12 February 2021

How to cite: Lange-Athinodorou, E.: Implications of geoarchaeological investigations for the contextualization of sacred landscapes in the Nile Delta, E&G Quaternary Sci. J., 70, 73–82, https://doi.org/10.5194/egqsj-70-73-2021, 2021.

Abstract: Key elements of sacred landscapes of the Nile Delta were lakes, canals and artificial basins connected to temples, which were built on elevated terrain. In the case of temples of goddesses of an ambivalent, even dangerous, nature, i.e. lioness goddesses and all female deities who could appear as such, the purpose of sacred lakes and canals exceeded their function as a water resource for basic practical and religious needs. Their pleasing coolness was believed to calm the goddess' fiery nature, and during important religious festivals, the barques of the goddesses were rowed on those waters. As archaeological evidence was very rare in the past, the study of those sacred waters was mainly confined to textual sources. Recently applied geoarchaeological methods, however, have changed this situation dramatically: they allow in-depth investigations and reconstructions of these deltaic sacred landscapes. Exploring these newly available data, the paper presented here focuses on the sites of Buto, Sais and Bubastis, by investigating the characteristics of their sacred lakes, canals and marshes with respect to their hydrogeographical and geomorphological context and to their role in ancient Egyptian religion and mythology as well.

Kurzfassung: Heilige Gewässer verschiedener Art, d.h. Seen, Kanäle und künstliche Becken, verbunden mit auf erhöhtem Gelände befindlichen Tempelgebäuden, sind als Schlüsselelemente sakraler Landschaften des Nildeltas anzusehen. Im Falle von Tempeln von Göttinnen ambivalenter, ja gefährlicher Natur, wie Löwengöttinnen und allen anderen weiblichen Gottheiten, die als solche erscheinen konnten, ging die Funktion heiliger Seen und Kanäle über ihren Zweck als Wasserressource für grundlegende praktische und religiöse Bedürfnisse hinaus. Man glaubte, dass ihre angenehme Kühle die feurige Natur der Göttin beruhigte; auf den Gewässern fuhren auch die heiligen Barken, in denen die Göttinnen bei wichtigen religiösen Festen gerudert wurden. Da man bis vor relativ kurzer Zeit kaum über archäologische Belege verfügte, beschränkte sich das Studium dieser heiligen Gewässer hauptsächlich auf Textquellen. Die in neuerer Zeit verstärkt angewandten geoarchäologischen Methoden haben diese Situation jedoch dramatisch verändert und ermöglichen nun eingehende Untersuchungen und Rekonstruktionen dieser heiligen Landschaften des Nildeltas. Unter Einbeziehung dieser neu verfügbaren Daten konzentriert sich die hier vorgelegte Arbeit auf die heilige Landschaft von Buto, Sais und Bubastis, indem sie die Merkmale ihrer heiligen Seen, Kanäle und Sümpfe im Hinblick auf ihren hydrogeographischen und geomorphologischen Kontext sowie auf ihre Rolle in der altägyptischen Religion und Mythologie untersucht.

1 Introduction

Investigations of sacred landscapes occur at the very intersection of geomorphology and archaeology, where the methods and aims of both disciplines truly come together. The recent increase in geoarchaeological studies at several sites in the Nile Delta allows the reconstruction of important features of their respective palaeo-landscapes. In archaeology, the investigation of landscapes and their impact on human cultural history is well established (David and Thomas, 2016; on the different concepts of landscape in geoarchaeology cf. also Cordoba, 2020, p. 50).

The study of sacred landscapes represents a special branch of landscape archaeology, since sacred landscapes are essentially landscapes that are marked and mapped with mythological references and explanations. They were sometimes changed due to human activities or by additions of human material culture. In Egyptology, the term "sacred landscape" is oftentimes used for temple complexes and their nearby surroundings. Sometimes also waterways or land routes come into play, as they could connect two or more temples, thus widening the sacred landscape. For important Egyptian religious celebrations such as the so-called Opet festival as a well-known example, it was essential that the cult image of the god Amun travelled on his sacred barque from his main temple at Karnak to Luxor around 3 km to the south (Darnell, 2010). These travels took place on natural as well as on artificial waterways and land routes. These were the Nile and the canals connecting the temples to their surroundings and also their paved stone paths (dromoi) leading to their entrances (Geßler-Löhr, 1983, pp. 144–145; Boreik et al., 2017). Here and elsewhere, we can observe a most interesting process: at first, existing natural topographical features were exploited to conduct religious ceremonies. Subsequently, their requirements could then initiate the addition of artificial structures and perhaps even the changing of the natural landscape.

Turning now from the Nile Valley to the Nile Delta, what were the main constituents of a sacred landscape there? In the delta, temples and cemeteries were set on top of natural elevations (van den Brink, 1986, p. 12). In the eastern delta, these were the remains of deeply eroded massive Pleistocene sediments, accumulated by the vigorous Pre-Nile, the so-called *geziras* (Said, 1981, 1993). In the western delta, temples were built on elevations as well, which seem to be the result of different geomorphological processes, as became clear in the case of Buto (Wunderlich, 1989). Regardless of their geomorphological origin, *geziras* were the dominant feature of the vast alluvial plain of the delta. Other distinctive characteristics of this landscape were the manifold watercourses and marshlands with their stagnant waters. Therefore, a body of water, whether in the shape of a stream, canal, lake or pool, connected to an elevated temple formed the basic elements of a deltaic sacred landscape.

In the past, knowledge of the existence of sacred lakes or canals attached to or surrounding temple buildings was mainly based on religious texts with little additional archaeological evidence. The previously available record pointed to the existence of deltaic sacred landscapes at a number of sites. Of them, Buto (Geßler-Löhr, 1983, pp. 403–404) and Sais (Geßler-Löhr, 1983, pp. 233–240; Wilson, 2006, 2019, pp. 5, 17) in the western delta, Busiris in the central delta (Geßler-Löhr, 1983, pp. 437–438), and Tanis (Montet, 1966; Leclère, 2008, pp. 442–443) and Bubastis (Lange-Athinodorou et al., 2019) in the eastern delta were especially well known. At any rate, comparative studies of sacred lakes are still rare (Yoyotte, 1962; Sauneron, 1964; Geßler-Löhr, 1983; Tillier, 2010); in particular, studies on sacred lakes as elements of deltaic sacred landscapes do not exist at all.

Nowadays, evidence comes from a much wider variety of sources. In addition to textual and archaeological records, we have access to results of sedimentological analysis from core drillings, as well as from geoelectric and geomagnetic investigations. These now allow the investigation of the location, shape or course of sacred waters at temple sites. To date however, such comprehensive, multi-methodological approaches have only been applied to a relatively small number of delta sites with well-known large-temple districts. At present, Buto, Sais and Bubastis are the main sites that provide us with sufficient textual, archaeological and geoarchaeological material for a comparative analysis. Therefore, they represent the topics of the following case study, which will focus on the landscape surrounding the large temples of these cities. Moreover, the local main deities of these cities all belonged to the canon of the so-called dangerous goddesses; i.e. they all shared specific qualities, which influenced certain elements of their cults, temple buildings and their surroundings as well.

2 Buto

At Buto in the northwestern delta the sacred landscape refers to the temple of the goddess Wadjet, the main deity of the city, who also embodied the red crown of Lower Egypt. In this capacity, Wadjet was the northern counterpart to the goddess Nekhbet, the goddess of the white crown of Upper Egypt (Leclère, 2008, p. 198, remark no. 5).

2.1 Textual sources

A statue dating to the Middle Kingdom from Meidum mentions the goddess Wadjet with the epithet "lady of the *Isheru*" (Geßler-Löhr, 1983, p. 403). The Egyptian term *Isheru* usually designates horseshoe-shaped lakes or canals connected to or surrounding temples of goddesses, who were believed to display not only benevolent but also dangerous qualities (Sauneron, 1964, pp. 50–57; Geßler-Löhr, 1983, pp. 47, 401). To capture this ambivalent character, these Egyptian goddesses were imagined to appear as lionesses, primarily Sekhmet, Bastet, Shesemtet and other genuinely feline goddesses. In addition others, e.g. Hathor, Mut, Neith, Nekhbet and Wadjet, who usually appeared in a different, either anthropomorphic or zoomorphic, form (Tillier, 2010, pp. 167, 171–172; Lange-Athinodorou, 2019, pp. 554–561, 580–581) could also be imagined as lionesses. According to their predatory nature, lionesses were feared as wild and fiery. Possibly based on wildlife observations at natural water places were lions would rest, canals or lakes close to temples of lioness goddesses were believed to please the goddesses' wild nature. Therefore, locations surrounded by lakes or canals were considered the ideal setting for their cult.

Still, that the inscription on the above-mentioned statue really referred to a sacred lake or canal of the temple of Wadjet at Buto is not beyond all doubt. The reason for that uncertainty is that several temples all over Egypt had lakes called *Isheru* where Wadjet and other goddesses obtained subsidiary cults. The most famous *Isheru* lake was the horseshoe-shaped one at the temple of Mut at Karnak. However, the earliest attestations of the *Isheru* of the temple of Mut at Karnak date back to the 18th dynasty (ca. 1460 BCE). They are therefore much younger than the earliest records of the term *Isheru* (Yoyotte, 1962, pp. 101–103, 106; Geßler-Löhr, 1983, p. 412); one proof comes from a list of deities of Egypt receiving offerings from the king. Each deity is not only listed by name but also further specified by its cult place. There, the lioness goddess Sekhmet bears the epithet "Sekhmet in *Isheru*", with the name of the sacred water used as a toponym of its own (Mariette, 1869, T. I. Pl. 44.9). As the text comes from the temple of Seti I at Abydos one would date it to the New Kingdom (19th dynasty, ca. 1280 BCE). However, Yoyotte (1962) and Sauneron (1964) argue that the list is actually a copy from a much older template of the late Old Kingdom (6th dynasty, ca. 2260 BCE; Yoyotte, 1962, p. 105; Sauneron, 1964, p. 56.4; also Geßler-Löhr, 1983, p. 402). In addition, a block from the temple of Min at Koptos depicts Sesostris I (12th dynasty, 1919–1875 BCE) in front of the lioness goddess Bastet with the caption "Bastet, lady of the *Isheru*". Here, the use of the settlement determinative ⊗ in the writing shows again that this name was used as a toponym, yet its exact location remains unknown (Petrie, 1896, Pl. X.2; Geßler-Löhr, 1983, p. 404; Gomàa, 1987, p. 209). In the light of this unique evidence, it remains impossible to decide where the *Isheru* from the inscription on the statue from Meidum was located (cf. Yoyotte, 1962, pp. 99–101; Geßler-Löhr, 1983, p. 403; was it Memphis or Meidum?).

Specific information about sacred waters of the temple of Wadjet at Buto comes from an inscription at the temple of Mut at Karnak from the Ptolemaic Period (second–first century BCE). The text tells the story of an assemblage of the deities of Egypt at Buto where the gods and goddesses of the Ennead are ordered to dig out a canal for Wadjet: "the gods of the Ennead, as follows: 'you shall travel to the hill-country of Buto … were you shall dig out a canal for the mighty one. You shall draw its water with both of your hands [so?] her [temple?] is encircled by its canal because she is content in the great primeval ocean"' (Geßler-Löhr, 1983, p. 403; Sauneron, 1983, p. 20, Taf. X.11–13).

The Greek historian Herodotus (ca. 450 BCE) describes a lake at this temple: "In this way the shrine is for me the most marvellous of all things to see in this temple; the second place has an island called Chemmis. This lies in a deep and wide lake close to the temple at Buto, and the Egyptians say that it floats" (Hd. II. 156.1; Wilson, 2015, p. 221; Nesselrath, 2017, p. 194).

Thus the essential information provided by the texts is as follows:

1. There was a canal at the temple(?) of Wadjet at Buto in order to pacify her dangerous temper.
2. There was also a lake close to the temple with a floating vegetated island called Chemmis.

Chemmis is the Greek term for the Egyptian toponym *Akhbit* – "papyrus thicket of the bee", with "bee" as the heraldic animal designating the geographical area of the delta. *Akhbit* is well known from written sources, mostly of a mythological and religious background from the time of the Pyramid Texts (ca. 2350 BCE) onwards. There, it means the hiding place of the goddess Isis where she raised her infant son and crown prince Horus, in order to keep the god Seth, Horus' murderous uncle, from harming him. Gardiner (1944), who investigated all available textual references, discussed the possibility that the toponym *Akhbit* was used to designate not one but two different locations: the first site was an *Akhbit* in the temple district of Buto, as mentioned by Herodotus. This was probably an artificial replica of the mythological hideout of the young god Horus in the papyrus marshes, designed as a vegetated island set in a sacred lake. On the other hand, according to textual evidence that treats *Akhbit* as a real locality and not as a specific element within the temple precinct, the second was a natural landscape area with papyrus marshes, which inspired the mythos. However, this *Akhbit* would have to be localized in the vicinity of Buto as well (Gardiner, 1944, pp. 53–58).

2.2 Geoarchaeology

At Buto, the temple of Wadjet was located at the northeastern Kom B (Hartung et al., 2009, p. 184). In fact, not much

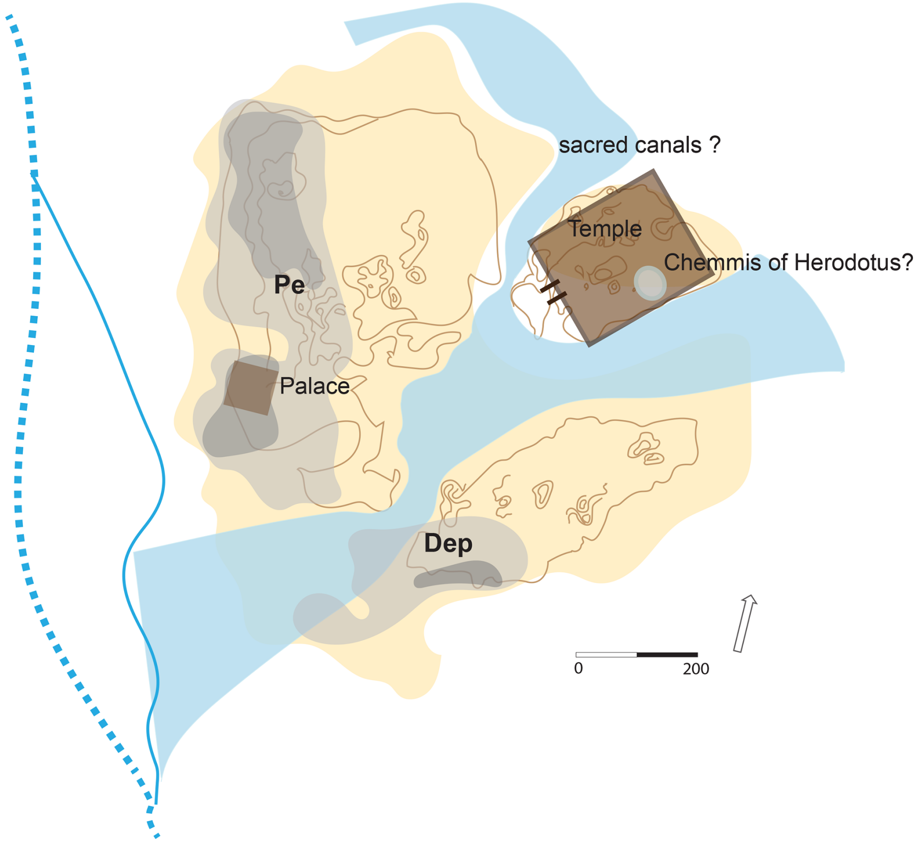

Figure 1. Topographic model of Buto with hypothetic course of the local canals at the temple. Topographic model after Hartung (2018, p. 102, Fig. 1).

survived of this building. Apparently, an enclosure wall of mud bricks of ca. 300 m by 200 m encircled the temple in the Late Dynastic Period. Its main entrance was on its western side (von der Way, 1999, p. 184; Leclère, 2008, pp. 205–208). Test trenches and drillings indicate the construction of a foundation made of sand in the Saite Period (seventh–sixth century BCE; Faltings et al., 2000, pp. 162–165). However, when looking at the elevation model of Buto (Hartung et al., 2009, p. 174, Abb. 27), a prominent depression between the northeastern, northwestern and southern parts of the tell, i.e. Kom A, B and C, is noticeable. One could speculate if this almost horseshoe-shaped depression could have formed a natural *Isheru*, presumably during the time of the inundation, when depressions were probably water-bearing.

At any case, a definitive answer could only be expected from the analysis of sediments of cores taken in that area. Although Hartung et al. (2009, p. 174, Abb. 27) conducted extensive drilling campaigns at the site, they focused mainly on the western stretch of the tell, leaving the area in question still unexplored. Interestingly, a single core drilling conducted by Faltings et al. (2000, pp. 167–168) in the eastern part of the temple precinct revealed green-greyish clayey mud with organic remains of plants, shells and fish bones, providing evidence of the former existence of a stagnant water body in this area.

Still ongoing is a long-term research programme on the natural landscape of the wider area around Buto. Based on core drillings and the digital and visual analysis of satellite imagery, Wunderlich (1989) detected massive peat layers to the north of Buto as far as Lake Burullus, indicating the former existence of a vast swampy area. These swamps originated from a belt of semi-marine lagoons, resulting from the marine transgression after the end of the last glacial period.

Figure 2 shows the extension of the consolidated *gezira* sands on which the settlement of Buto was founded and to its north the size and limits of the peat horizon to the north as attested by core drillings conducted by Wunderlich (1989). The peat horizon is the remnant of the above-mentioned semi-marine lagoon. C-14 datings on a number of test samples from the peat horizon (location indicated in Fig. 2) show that the lagoon belt moved inland to up to around 2 km north of Buto from 5050 to 4050 BCE. With the lowering of the sea level, the swamp dried up again from the fourth millennium BCE onwards (Wunderlich, 1989, pp. 106–110; Wunderlich and Ginau, 2014/2015, pp. 488–494).

Therefore, at the time of the beginning of the settlement at Buto in the second half of the fourth millennium BCE (Falt-

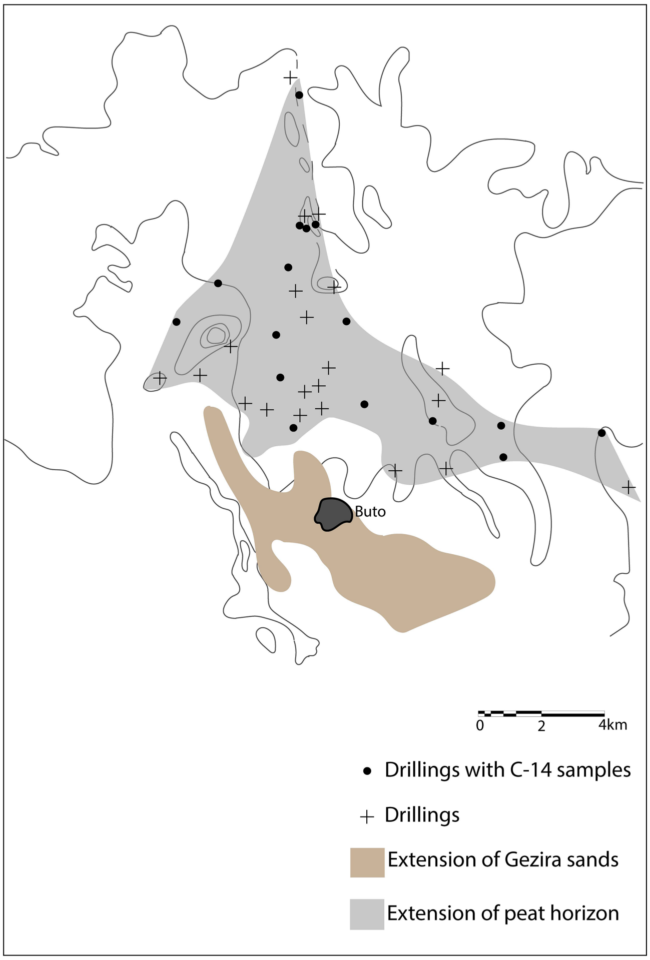

Figure 2. Geomorphology of Buto according to geophysical investigations, by courtesy of Jürgen Wunderlich (altered after Wunderlich, 1989, p. 108, Abb. 33).

ings, 1998, p. 373), the occupants of Buto could still explore large areas with open water surfaces and a dense vegetation of papyrus and other helophytes. Such a natural landscape would certainly match with the idea of the mythological papyrus marshes.

3 Sais

Sais was the main cult place of the goddess Neith, a goddess of deltaic origins (Wilson, 2006, pp. 2–3; Wilson, 2011, pp. 186–187), who since the earliest times belonged to the most important female deities of Egypt. As stated above, besides her anthropomorphic image often wearing the red crown of Lower Egypt, Neith could appear in the shape of a fearsome lioness goddess, sometimes associated with Sekhmet and Bastet (El-Sayed, 1982, p. 136).

3.1 Textual sources

Some important information concerning a lake at the temple of Neith at Sais under the reign of Amasis (570–526 BCE) comes from a biographical inscription on the dorsal pillar of the statue of an official named Horkhebi who states: "I dug a lake on the eastern side of the canal *ww*. [Its] length: 68 cubits, width: 65[?] cubits, lined with stone, with 8 staircases and walls around it [...] in it for Neith and the gods of the nome of Sais by order of the Dual king Amasis, son of Neith" (Geßler-Löhr, 1983, pp. 233–235).

The inscription on the statue of a woman from the early Ptolemaic Period usually cited in the literature amongst the textual evidence (Leclant and De Meulenaere, 1957, p. 36; Geßler-Löhr, 1983, p. 237; Zecchi, 1996, pp. 32–33; Wilson, 2019, p. 17) should be omitted as the reading of the group of signs in question is unsure and might refer to the offerings rather than to the lake.[1]

Herodotus describes the lake of the temple at Sais as follows: "Great stone obelisks stand in this sacred precinct, and a lake adjoins, beautifully lined with a crepidoma of stone all around; it is, as it seemed to me, as big as the lake at Delos, the so-called Circular Pond" (Hd. II. 170; Wilson, 2015, p. 228; Nesselrath, 2017, p. 200; also Wilson 2006, pp. 36–37).

These texts bear witness to the existence of a sacred lake in the precinct of the temple of Neith at Sais. The biographical inscription of Horkhebi provides some details on the dimensions and the location of the lake, which will be discussed below (Sects. 3.2 and 4).

3.2 Geoarchaeology

Similar to Buto, Sais was originally a twin tell, with the settlement started on two neighbouring *geziras*, to the west and east of a natural canal that evolved out of a lake between the two elevations (Wilson, 2006, pp. 203–204).

According to the drillings conducted by the team of Wilson (2006), an ancient water canal once flowed close to the eastern side of the so-called northern enclosure, an area to the north of the site. In this area to the north of the site was once located the temple of Sais, now completely destroyed. There might have been another palaeo-canal to the east, yet the traces found there indicate a more recent dating for this waterway (Wilson, 2006, pp. 177–204, 252–256).

On the eastern side of the northern enclosure, a possibly natural spring still flows. It may have already existed in ancient times. Wilson (2006) also reports the discovery of several limestone blocks at the site of this spring, which might have belonged to the lining of the sacred lake. According to her the spring could have been the source of the sacred lake of the temple (Wilson, 2006, p. 256). This fits well with the biographical text of Horkhebi cited above, who describes the

[1] My thanks go to Karl Jansen-Winkeln for his helpful comments on this text.

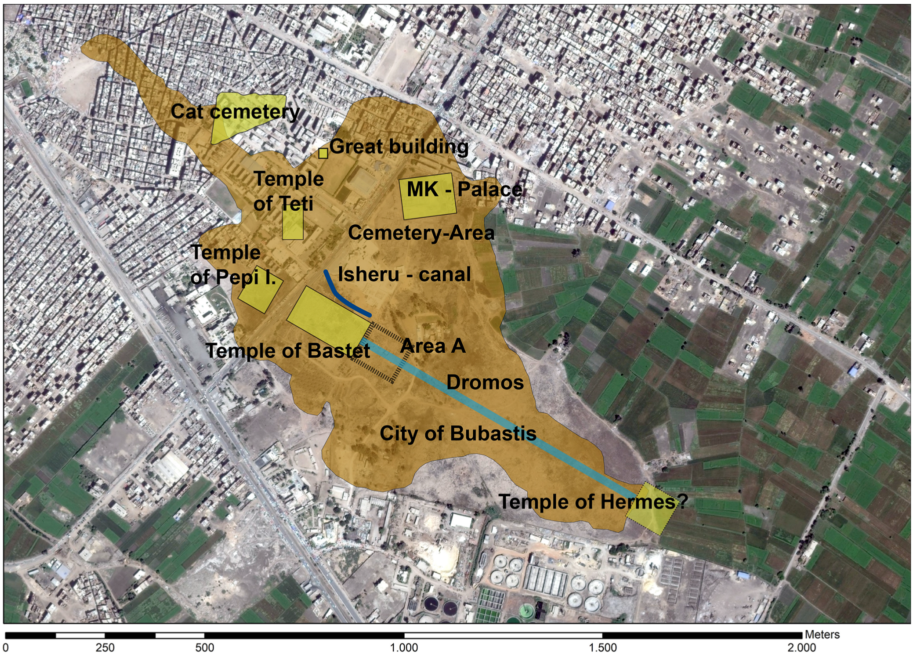

Figure 3. The course of the northern sacred canal at Bubastis according to the latest geophysical investigations. © Google Maps, modified by Eva Lange-Athinodorou.

construction of a sacred lake at the temple, more precisely an artificial water basin, lined with stone blocks and accessible via staircases leading down to the water.

4 Bubastis

Attestations for the cult of Bastet date back to the second dynasty (ca. 2850 BCE). If Bubastis was already the main cult place of this goddess in these early times is difficult to establish, as the earliest evidence of the cult of Bastet there dates back to the sixth dynasty only (Lange, 2016, pp. 310–313). We have, however, ample textual and archaeological evidence that she was the main goddess of Bubastis from then on until the time of the Roman emperors (Naville, 1891; de Wit, 1956, pp. 292–297).

4.1 Textual sources

The sacred waters of Bubastis appear prominently in the written record. Papyrus Brooklyn 47.218.84, a mythological compendium on the cities of the delta from the second part of the seventh century BCE, contains two references to it. The first says about the goddess, "She is on the pedestal of 'throwing down the enemies'. A falcon tames her, two hippo deities surround her, an *Henet* water is all around her, the length of which is . . . 7(?) (cubits and the width) 42 (cubits)" (pBrooklyn 47.218.84, IX.4; Meeks, 2006, p. 20). The term *Henet* that refers to the waters surrounding the temple of Bastet can generally designate various types of natural bodies of water, such as Nile branches, canals and lakes (Yoyotte, 1962, p. 88.4; Geßler-Löhr, 1983, p. 407, footnote 1348; Meeks, 2006, pp. 100–101).

Another paragraph in the same papyrus calling those waters *Isheru* informs us about the triumphal appearance of Bastet as the defeater of Seth in her sacred barque during her annual festival: "And they row her in the Oryx antelope on the *Isheru* at the moment as she saved the Udjat-Eye from him". (pBrooklyn 47.218.84, IX.7–8; Meeks, 2006, p. 20; Bohms, 2013, pp. 36–42). A very vivid depiction of this scene appears on the fragment of a stela from the Late Period. It was discovered at Bubastis at the cemetery of the cats, the sacred animals of the goddess (El-Sawi, 1977). Here we find all the elements described in the papyrus: the statue of the goddess in her shrine sitting in a barque, the stern of which is shaped like the head of an oryx antelope, the animal of Seth, representing the enemy she had subdued. Under the barque, zigzag lines indicate the water of the sacred canal as well (cf. also Geßler-Löhr, 1983, p. 407 and Fig. 74; Schorsch, 2015).

Herodotus describes the environments of the temple of Bastet at Bubastis in detail: "Except the entrance, the rest is an island. The canals, which come from the Nile, are not joining one another, but each one extends to the entrance of the temple; the one surrounds the one side, the other the other side and each one is 100 feet wide and shadowed by trees" (Hd. II. 138.1; Wilson, 2015, pp. 208–209; Nesselrath, 2017, p. 184).

The above-mentioned texts all come from the second part of the first millennium BCE. Still, how far the *Isheru* at Bubastis really dates back is unclear. The above-mentioned relief block (cf. Sect. 1.1) from the early 12th dynasty from Koptos names Bastet as the Lady of Isheru. Yet, the location of the *Isheru* mentioned on this block does not necessarily have to be at Bubastis, contrary to some attempts to locate it there (Sauneron, 1964, pp. 52, footnote 33; Yoyotte, 1962, pp. 103–104).

4.2 Geoarchaeology

Core drillings at Bubastis conducted by Ullmann et al. (2019, pp. 190, 195–197) revealed that the temple of Bastet sits on the elevated part of a NW–SE-oriented *gezira* of Pleistocene origin. Furthermore, it is possible that Bubastis, like Buto and Sais, was actually built not only on one elevation but also on a twin tell. In that case, the temple area was located on the southern mound, while the cemeteries were established at the northern one.

Recently, DCR soundings and ERT by Amr Abd el-Raouf pointed to the existence of a canal, close to the temple of Bastet. Core drillings and sediment analyses by Julia Meister corroborated those finds, placing a canal around 50–60 m to the north of the outer wall of the temple (Lange-Athinodorou et al., 2019). The results of the combined geophysical analysis led to the detection of around a 300 m length of a canal, its width measuring between 20 and 30 m (cf. Fig. 3; Lange-Athinodorou et al., 2019). This canal was most probably the northern part of the canal system that surrounded the temple, namely the *Isheru* or *Henet* of the Egyptian texts.

The dominant infill of the canal with fine-grained sediments as well as their high content of organic matter indicates that very slowly flowing water accumulated them. Parallel sediment laminations point to a periodic influx of fresh water, coming from a larger river, possibly a nearby Nile tributary. Eventually, the canal at the temple was cut off and became stagnant water, gradually silting up (Lange-Athinodorou et al., 2019, pp. 6–8, 11). A dating of the canal and its active periods is still difficult and must await further chronological analysis. However, the textual sources show that the canal system was existent at least in the time from the seventh to the fifth century BCE.

5 Discussion

The survey of the textual and geoarchaeological evidence represented in Sects. 1.1–3.2 allows some tentative reconstructions and comparisons of the lakes and canals in, around and nearby the temples of Buto, Sais and Bubastis with respect to their different hydrogeographic and geomorphological contexts. In addition, I will discuss the question as to whether the canals and lakes at those sites are of a natural or artificial origin.

For Buto, a text from the Ptolemaic Period at Karnak points to the existence of a sacred canal *around* the temple. By contrast, Herodotus refers to a "deep and wide" lake with an island somewhere close to the temple (cf. Sect. 1.1). As one can see in the case of Bubastis, Herodotus did differentiate between lakes and canals thoroughly. Therefore, the two texts might actually describe two distinct sacred waters at Buto: a probably horseshoe-shaped canal surrounding the temple mound and a lake within the temple enclosure wall. A drilling core in the eastern part of the temenos, south of the main axis of the temple, indicates that the sacred lake could have been somewhere in this area (cf. above Sect. 1.2). However, without further core drillings there is no way of determining its dimensions. Furthermore, no core drillings, sediment analyses and geoelectric soundings are available yet from the depression around the temple mound, where the canal of Wadjet could have flowed as described in the Ptolemaic text. Its existence in that vicinity is definitely a hypothesis worth testing by the means of geoarchaeological methods in the future. Another interesting, yet admittedly still unproven, possibility is that the palaeo-landscape with large marshlands to the north of Buto, as revealed by the geophysical survey there (cf. Sect. 2.1), might have inspired the mythos of the hiding of the child god Horus by his mother Isis in the papyrus thickets. In this process, the natural landscape, i.e. the marshlands called *Akhbit*, would have undergone a mythological interpretation and could later on be used as an ideal model providing the scenery for this specific mythos in Egyptian religious texts.

At Sais, we encounter a different situation. The texts unanimously describe a sacred lake, which Herodotus reports was established within the temenos area. The earlier text of Horkhebi adds its dimensions: the basin he built would have measured 35.63 m by 34.06 m, thus forming an almost square structure. Measuring 100 m by 70 m, the lake at Delos, which Herodotus uses for comparison, was, however, much larger (Nesselrath, 2017, p. 788, no. 264).

More complicated is the localization of the lake with regards to the canal of the name *ww* in Horkhebi's inscription. At first glance, one is inclined to identify this waterway with the palaeo-canal to the east of the temple area (cf. Sect. 2.2). Yet, as Wilson (2006, p. 257) points out, this poses problems, because Horkhebi clearly states, "I dug a lake on the *eastern* side of the canal *ww*" (emphasis added). The eastern side of the palaeo-canal is far outside of the temenos area. In this case, the artificial lake would have been nowhere within the enclosure wall of the temple, which seems to be very improbable. Moreover, the position of the spring, as the possible source of the lake, can be localized to the *west* of the palaeo-canal and hence doubtless well within the temple district (Wilson, 2006, p. 262, Fig. 8). Therefore, the *ww* canal should not be identified with the palaeo-canal to the east detected by core drillings. Rather, the *ww* canal was probably flowing somewhere to the west of the northern enclosure. The canal detected in this area is however a more recent structure.

More evidence is available for Bubastis: the main sacred body of water of the temple was doubtlessly a structure of two canals coming from a Nile branch. The temple mound therefore must truly have given the impression of an island, quite as Herodotus described it. As was shown above (Sect. 3.2), one of the paragraphs of Papyrus Brooklyn provides information on its dimensions: “an *Henet* water is all around her, the length of which is ... 7(?) (cubits and the width) 42 (cubits).” Unfortunately, the first specification in the papyrus is illegible. The width of the canal given by the ancient texts on the other hand is very close to the facts discovered by the geophysical analysis: the 42 cubits of Papyrus Brooklyn are a little more than 22 m. The description of Herodotus states 30 m for the width instead. These different statements of the dimensions in Papyrus Brooklyn and Herodotus might be explained by the fact that the canal was part of a dynamic hydrographic system. Its water level and dimensions therefore changed not only from season to season with the changing water volume of the Nile and its distributaries but also on a long-term scale. In Bubastis, another artificial basin might have also existed within the temple enclosure such as in Buto and Sais, but to date, there is no indication of it.

Finally, the question arises as to whether the sacred canals and lakes at Buto, Sais and Bubastis were of natural or artificial origin. In the case of the canals at Bubastis, the results of the geoarchaeological investigation do not yet allow a definitive answer. It is, however, conceivable that the natural hydrogeographic situation with two canals surrounding the elevated part of the *gezira* led to the founding of the temple of Bastet there. The main reasons for choosing this position were very probably the specific requirements of the cult of the lioness goddess (cf. Sect. 5; also Yoyotte, 1962, pp. 108–109). In later times, people might have artificially maintained the function of the canal as a navigable waterway by digging out accumulating sediments on a more or less regular basis. Regarding the canal around the temple mound at Buto, a similar situation is imaginable but awaits future investigations as well. The temple lake at Sais might have been based on a comparable process of enhancing a natural situation by artificial means: assumedly, a natural spring in the western part of the temenos area was the source of water that filled an artificial basin built of limestone blocks. Finally, whether the sacred lake within the temple of Wadjet was in any way similar to the one at Sais cannot be answered without further data.

The question remains around which reasons might have caused the specific connection of the horseshoe-shaped lakes and canals and the temples of goddesses. One answer lies in the geomorphological situation of the temple sites in the delta. Here, temples were built on elevations, while the depressions close to them would be at least seasonally water-bearing. In that case, a half-circular shape of the pool or canal would emerge as in the cases of Buto and Bubastis. As horseshoe-shaped lakes were preferred near temples of goddesses in the Nile Valley as well, several scholars argue that their natural prototypes might have been temporary fan-shaped lakes evolving on the estuaries of the wadis after seasonal rainfall. Such temporary lakes provided water for a variety of wildlife and therefore also attracted hunting lion prides (Tillier, 2010, p. 173, footnote 46). People would observe lionesses at those natural lakes not only hunting but also lovingly caring for their cubs. By analogy, people might have imagined that this kind of landscape was favourable for lioness goddesses as well. The water surrounding their temples would cool and calm their temper and bring out their positive, caring and protective nature. Therefore, locations surrounded by lakes or canals would have been thought to have been the ideal setting for their cult.

According to the narration of Herodotus, countless people celebrated festivals at Bubastis in honour of Bastet, which seem to have been ecstatic and orgiastic. The celebrations involved drunkenness and displays of many kinds of ecstatic activities like wild dancing and singing (Hd. II. 59.1–60.1; Wilson, 2015, pp. 161–162; Nesselrath, 2017, pp. 144–145). The already cited texts of Papyrus Brooklyn include a tale about Bastet, who saved the eye of Horus from Seth at Bubastis and was rowed on the sacred canals displaying her triumph over the enemy (cf. Sect. 3.1). This is actually the description of a river procession with a cult statue of Bastet in her barque shrine as the culmination of the festival. Surely, the appearance of the triumphant goddess would be the summit of a celebration passionately attended by the thousands of pilgrims who journeyed to her city every year to attend her festival.

6 Summary and conclusions

Elemental components of sacred landscapes at Buto, Sais and Bubastis were the canals and lakes in close proximity to the temples of the goddesses who were venerated in those cities. Geoarchaeological investigations not only bear witness to their existence but also indicate their dimensions and locations and help to reconstruct the hydrogeography and palaeolandscape they were connected to. So far, the analysis of the data gained by geoarchaeological methods leads to interesting results on the specifics of the lakes and canals at the three sites used as case studies: a sacred canal of the *Isheru* type and a sacred lake within the temple enclosure most probably defined the sacred landscape of Buto. At Sais, an existing sacred lake of possibly natural origin was enhanced for continuous use with an enclosure of stone blocks. The large *Isheru*-type canals of Bubastis enclosed the temple almost completely.

On the other hand, textual records are useful with regard to the understanding and reconstruction of the importance of sacred waters in the cult and the local mythology of Wadjet, Neith and Bastet. All of them were goddesses considered to be of an ambivalent nature: mighty, protecting and dangerous, the latter preferably to the enemies of the king; yet the rage of the goddesses could turn against even their admirers at any moment or, alternatively, into a peaceful calm temper (Lange-Athinodorou et al., 2019, pp. 554–561, 580–581). A canal system enclosing their temple or at least a lake close to the sanctuary was believed to be necessary to cool and please their unpredictable fiery temper.

Furthermore, the sacred canals were not only a tool to please and cool the mood of the goddesses; they were also a key element in the performance of their cults. The rich textual and pictorial evidence at Bubastis could be used as a role model of the events taking place on and around the sacred waters of Buto and Sais. Although there is no comparable textual evidence, it is well imaginable that Wadjet and Neith had festivals of their own with their barques appearing on their sacred canals and lakes during religious festivals. We know of such ceremonies at the temples of Sekhmet at Memphis, Mut at Karnak and Hathor at Dendera to name but a few (Geßler-Löhr, 1983, pp. 401–424; Tillier, 2010, pp. 170–171).

The results of the geophysical survey of the environs of Buto now widen the horizon much further. The evidence of a large palaeo-swamp north of Buto leads to the question as to whether human experience of this impressive landscape resulted in the concept of the papyrus marshes of *Akhbit* as the hiding place of Horus, a centrepiece of Egyptian mythology. If correct, this could highlight the cognitive process of connecting natural landscapes with mythological narratives: certain features of natural landscapes of the delta, even far from temple buildings, were incorporated into the imaginary sacred landscapes of the delta in ancient Egyptian minds.

Data availability. All relevant data and references are cited in this article.

Competing interests. The author declares that there is no conflict of interest.

Special issue statement. This article is part of the special issue "Geoarchaeology of the Nile Delta". It is a result of the workshop "Geoarchaeology of the Nile Delta: Current Research and Future Prospects", Würzburg, Germany, 29–30 November 2019.

Acknowledgements. I would like to thank the participants of the workshop for an interesting discussion, as well as the anonymous reviewers for their input.

Financial support. This open-access publication was funded by Julius-Maximilians-Universität Würzburg.

Review statement. This paper was edited by Becky Briant and reviewed by two anonymous referees.

References

Bohms, I.: Säugetiere in der altägyptischen Literatur, Ägyptologie 2, Lit-Verlag, Berlin, Münster, 2013.

Boreik, M., Gabolde, L., and Graham A.: Karnak's quaysides: evolution of the embankments from the Eighteenth Dynasty to the Graeco-Roman Period, in: The Nile: natural and cultural landscape in Egypt, edited by: Willems, H. and Dahms, J.-M., transcript, Bielefeld, 97–144, 2017.

Cordoba, C.: Geoarchaeology, The Human-Environmental Approach, I. B. Tauris, London, New York, Oxford, New Delhi, Sydney, 2020.

Darnell, J. C.: Opet festival, in: UCLA Encyclopedia of Egyptology online (1.1), edited by: Dieleman, J. and Wendrich, W., available at: https://escholarship.org/uc/item/4739r3fr (last access: 27 June 2020), 2010.

David, B. and Thomas, J.: Landscape archaeology: introduction, in: Handbook of landscape archaeology, edited by: David, B. and Thomas, J., Routledge, New York, 27–43, 2016.

De Wit, C.: Le rôle et le sens du lion dans l'Égypte ancienne, E.J. Brill, Leiden, 1951.

El-Sawi, A.: Preliminary report on Tell Basta excavations, Seasons 1969, 1970, 1971, Zeitschrift für Ägyptische Sprache und Altertumskunde, 104, 127–131, 1977.

El-Sayed, R.: La déesse Neith de Saïs, BdE 86, Institut français d'Archéologie orientale, Le Caire,1982 (in French).

Faltings, D., Ballet, P., Förster, F., French, P., Ihde, C., Sahlmann, H., Thomalsky, J., Thumshirn, C., and Wodzinska, A.: Zweiter Vorbericht über die Arbeiten in Buto von 1996 bis 1999, Mitteilungen des Deutschen Archäologischen Instituts, Abteilung Kairo, 56, 131–179, 2000 (in German).

Faltings, D.: Recent excavations in Tell El-Fara'in Buto: new finds and their chronological implications, in: Proceedings of the Seventh International Congress of Egyptologists, Cambridge, 3–9 September 1995, edited by: Eyre, C. J., Peeters, Leuven, 365–375, 1998 (in German).

Gardiner, A. H.: Horus the Behdetite, Journal of Egyptian Archaeology, 30, 23–60, 1944.

Geßler-Löhr, B.: Die heiligen Seen ägyptischer Tempel: ein Beitrag zur Deutung sakraler Baukunst im alten Ägypten, Hildesheimer Ägyptologische Beiträge, 21, Gerstenberg, Hildesheim, 1983.

Gomaà, F.: Die Besiedlung Ägyptens während des Mittleren Reiches II: Unterägypten und die angrenzenden Gebiete. Beihefte zum Tübinger Atlas des Vorderen Orients, Reihe B (Geisteswissenschaften) 66, Reichert, Wiesbaden, 1987.

Hartung, U., Ballet, P., Effland, A., French, P. G., Hartmann, R., Herbich, T., Hoffmann, H., Hower-Tilmann, E., Kitagawa, C., Kopp, P., Kreibig, W., Lecuyot, G., Lösch, S., Marouard, G., Zink, A., Nerlich, A., and Pithon M.: Tell el-Fara'in – Buto: 10, Vorbericht, Mitteilungen des Deutschen Archäologischen Instituts Kairo, 65, 83–190, 2009 (in German).

Hartung, U.: Recent investigations of Early Dynastic building structures at Tell el-Fara'in/Buto, in: Ancient Egyptian and ancient Near Eastern palaces, volume I: Proceedings of the conference on palaces in ancient Egypt, edited by: Bietak, M. and Prell, Silvia, London, UK, 12–14 June 2013, 101–112, 2018.

Lange, E.: The lioness goddess in the Old Kingdom Nile Delta: a study in local cult topography, in: Sapientia Felicitas: Festschrift für Günter Vittmann zum 29. Februar 2016, edited by: Lippert,

S. L., Schentuleit, M., and Stadler, M. A., CENiM, 14, 301–324, 2016.

Lange-Athinodorou, E.: Der "Tempel des Hermes" und die Pfeile der Bastet: zur Rekonstruktion der Kultlandschaft von Bubastis, in: En détail – Philologie und Archäologie im Diskurs, edited by: Brose, M., Dils, P., Naether, F., Popko, L., and Raue, D., De Gruyter, Berlin/Boston, Festschrift für Hans-Werner Fischer-Elfert 1, 549–585, https://doi.org/10.1515/9783110629705-025, 2019.

Lange-Athinodorou, E., Abd El-Raouf, A., Ullmann, T., Trappe, J., Meister, J., and Baumhauer, R.: The sacred canals of the temple of Bastet at Bubastis (Egypt): new findings from geomorphological investigations and Electrical Resistivity Tomography (ERT), J. Archaeol. Sci.-Rep., 26, 1–13, https://doi.org/10.1016/j.jasrep.2019.101910, 2019.

Leclant, J. and De Meulenaere, H.: Une statuette égyptienne à Délos, Kêmi 14, 34–42, 1957 (in French).

Leclère, F.: Les villes de Basse Égypte au Ier millénaire av. J.-C.: analyse archéologique et historique de la topographie urbaine, 2 vols. Bibliothèque d'étude 144, Institut français d'archéologie orientale, Le Caire, 2008 (French)

Mariette, A.: Abydos: description des fouilles exécutées sur l'emplacement de cette ville, Librairie A. Franck; Imprimerie nationale, Paris, 1869 (in French).

Meeks, D. : Mythes et légendes du Delta d'après le papyrus Brooklyn 47.218.84, Mémoires publiés par les membres de l'Institut français d'archéologie orientale 125, Institut Français d'Archéologie Orientale, Le Caire, 2006 (in French).

Montet, P.: Le lac sacré de Tanis, Académie des Inscriptions et Belles-Lettres (Extrait des Mémoires de l'Académie, Tome XLIV), Paris, 1966 (in French).

Naville, E: Bubastis (1887–1889), EEF 8, London, 1891.

Nesselrath, H.-G.: Herodot: Historien, Alfred Kröner Verlag, Stuttgart, 2017 (in German).

Petrie, W. M. F.: Koptos, Bernard Quaritch, London, 1896.

Said, R.: The geological evolution of the River Nile, Springer Verlag, New York, Heidelberg, Berlin, 1981.

Said, R.: The river Nile: geology, hydrology and utilization, Pergamon Press, Oxford, New York, Seoul, Tokyo, 1993.

Sauneron, S.: La porte ptolémaïque de l'enceinte de Mout à Karnak, Mémoires publiés par les membres de l'Institut français d'archéologie orientale, 107, Institut français d'archéologie orientale, Cairo, 1983 (French).

Sauneron, S.: Villes et légendes d'Égypte, Bulletin de l'Institut Français d'Archéologie Orientale (BIFAO), Cairo, 62, 33–57, 1964 (in French).

Schorsch, D.: Bastet goes boating, Bulletin of the Egyptological Seminar (BES), 19, 571–584, 2015.

Tillier, A.: Notes sur l'icherou, Égypte Nilotique et Méditerranéenne, 3, 167–176, 2010.

Ullmann, T., Lange-Athinodorou E., Göbel, A., Büdel, C., and Baumhauer, R.: Preliminary results on the paleo-landscape of Tell Basta/Bubastis (eastern Nile delta): an integrated approach combining GIS-based spatial analysis, geophysical and archaeological investigations, Quatern. Int., 511, 185–199, 2019.

van den Brink, E. C. M.: A geo-archaeological survey in the north-eastern Nile Delta, Mitteilungen des Deutschen Archäologischen Instituts, Abteilung Kairo, 43, 7–31, 1986.

von der Way, T.: Buto, in: Encyclopedia of the archaeology of ancient Egypt, edited by: Bard, K. and Shubert, S. B., London, 180–184, 1999.

Wilson, N. G.: Herodoti Historiae, Oxford University Press, Oxford, 2015.

Wilson, P.: Gateway to the underworld: the cult areas at Sais, Studies in Ancient Egypt and Sudan, 24, 341–364, 2019.

Wilson, P.: The survey of Saïs (Sa el-Hagar) 1997–2002, Egypt Exploration Society, Excavation Memoir 77, Egypt Exploration Society, London, 2006.

Wilson, P.: Sais I: The Ramesside-Third Intermediate Period at Kom Rebwa, Egypt Exploration Society, Excavation Memoir 98, Egypt Exploration Society, London, 2011.

Wunderlich, J.: Untersuchungen zur Entwicklung des westlichen Nildeltas im Holozän, Marburger geographische Schriften, Marburg/Lahn, Germany, 1989.

Wunderlich, J. and Ginau, A.: Paläoumweltwandel im Raum Tell el Fara'in/Buto: Ergebnisse und Perspektiven geoarchäologischer Forschung, Mitteilungen des Deutschen Archäologischen Instituts Kairo, 70–71, 485–497, 2014/2015 (in German).

Yoyotte, J.: Études géographiques, II: les localités méridionales de la région memphite et le "Pehou d'Héracléopolis", Revue d'égyptologie, 14, 75–111, 1962 (in French).

Zecchi, M.: A study of the Egyptian god Osiris Hemag. Archeologia e storia della civiltà egiziana e del vicino Oriente antico – Materiali e studi 1, La Mandragora, Imola, 1996.

E&G Quaternary Sci. J., 70, 29–38, 2021
https://doi.org/10.5194/egqsj-70-29-2021

Open Access E&G Quaternary Science Journal

Research article

A new look at the Butic Canal, Egypt

Robert Schiestl

Institute of Ancient History, Ludwig-Maximilians-University Munich, 80539 Munich, Germany

Correspondence: Robert Schiestl (robert.schiestl@lmu.de)

Relevant dates: Received: 24 August 2020 – Accepted: 2 November 2020 – Published: 26 January 2021

How to cite: Schiestl, R.: A new look at the Butic Canal, Egypt, E&G Quaternary Sci. J., 70, 29–38, https://doi.org/10.5194/egqsj-70-29-2021, 2021.

Abstract: The Butic Canal – a Roman period transversal route across the northern Nile Delta – was the longest artificial watercourse in the Nile Delta, yet it remains very poorly understood. To date, the canal has not yet been verified by archeological excavations. The route of the eastern section of the canal has been indirectly identified based on a linear elevated feature most likely representing earth from the excavation of the canal. This study combines the analysis of historical sources and remote sensing data, such as satellite imagery and the TanDEM-X digital elevation model, in order to discuss its date of construction, route, and functions. Based on the data of the digital elevation model, new constructional features are visible in the eastern delta providing the first detailed route of a Roman-era artificial watercourse in Egypt. It is suggested that the canal's construction is placed in the context of imperial investments in the infrastructure of the eastern part of the Roman empire.

Kurzfassung: Der Butische Kanal war eine römerzeitliche Querverbindung durch das nördliche Nildelta. Obwohl er die längste künstliche Wasserstraße des Deltas darstellt, ist unsere Kenntnislage über diesen Kanal sehr gering. Bis heute ist der Kanal nicht durch archäologische Ausgrabungen verifiziert. Der Verlauf eines Abschnitts des Kanals im östlichen Nildelta wurde indirekt durch eine lineare Struktur identifiziert, die höchstwahrscheinlich den Aushub des Kanals repräsentiert. Dieser Artikel kombiniert die Analyse historischer Quellen und Fernerkundungsdaten, wie Satellitenbilder und das TanDEM-X Digitale Höhemodell, um die Datierung, die Route und die Funktionen des Kanals zu diskutieren. Auf der Grundlage der Daten des Digitalen Höhenmodells sind im östlichen Delta bestimmte bauliche Merkmale des Kanals erstmals genauer erkennbar. Dadurch kann die erste detaillierte Route eines Abschnittes einer römerzeitlichen künstlichen Wasserstraße in Ägypten rekonstruiert werden. Es wird vorgeschlagen, die Errichtung des Kanals im Zusammenhang mit imperialen Infrastrukturprojekten in der Osthälfte des römischen Reiches zu verstehen.

1 Introduction

The *Boutikos potamos*, the Butic Canal, is named and described only in one ancient source, a 2nd century CE geographic treatise written in Greek by Ptolemy (Klaudios Ptolemaios, 4, 5, 44; Stückelberger and Graßhoff, 2006). The term *potamos* can refer to both natural and artificial watercourses (Bonneau, 1993). Here it is clearly an artificial watercourse spanning the Egyptian Nile Delta from west to east with a reconstructed length of about 185 to 200 km. Thus, it constitutes the longest man-made ancient watercourse in the delta, distinctly longer than the other major ancient delta canal which connected the Nile to the Red Sea (Cooper, 2009). Despite its size and unique route, very little is known about this canal. Recent discussions of the canal have addressed it in a wider delta perspective, looking at it in the context of trans-delta networks (Redon, 2018) but also including the course in a regional setting in the eastern delta (Blouin, 2014). To date, however, it has never been the topic of a specialized study. This holds true for the field of Egyptology, but also within the wider scope of ancient water technology (Wikander, 2000; Grewe, 2009) and Roman imperial construction, this watercourse finds no mention. While the Butic Canal does appear on maps of the Nile Delta (Ball, 1942; Bietak, 1975; Talbert, 2000; Wittke et al., 2007), the course is largely conjectural, attempting to place Ptolemy's description of the canal in the landscape. Its precise course, its date of construction, its period of activity, and its purpose(s) remain in discussion (Ball, 1942; Bietak, 1975; Yoyotte, 1987; Blouin, 2014; Redon, 2018) as does the question of its influence on the traffic, development, and economy of the delta. The background to this study is a survey which was conducted in the northwestern delta in the region of Buto (Tell el-Fara'in; Schiestl, 2012). For the surveyed area, see the yellow rectangle in Fig. 1. Traditionally, reconstructions of the course of the Butic Canal show it passing close to Buto and crossing the area surveyed. As the survey pursued, inter alia, a landscape archeological angle, the ancient land- and waterscapes were investigated using historic maps, satellite images, auger core drillings, and a digital elevation model (DEM). While this has resulted in much new information on the ancient water courses of the region (Ginau et al., 2019), no features were discerned which suggest themselves as a regional segment of the Butic Canal. Empirical evidence for this canal in the western delta remains elusive. In contrast, in the eastern delta, a linear elevated feature, still in parts extant between Mendes/Thmuis and Tanis (red rectangle on Figs. 1, 2a–c), has long been considered as evidence of the remains of the excavated earth of the Butic Canal. New data from the TanDEM-X digital elevation model provide new details of this feature which will be discussed in the following Sect. 4 in the context of the reconstruction of the route. This will be preceded by a discussion of the textual sources for the canal (Sect. 2) and the chronology (Sect. 3) and will be followed by an analysis of the functions of the canal (Sect. 5) and a summary of the main results (Sect. 6). Methodologically, this investigation combines ancient historical textual sources, archeological sources, and remote sensing information.

2 Textual evidence

There are two main textual sources describing a Roman period (30 BCE–7th century CE) transversal delta canal which are frequently considered as referring to the same system. The earlier one is an indirect reference in Flavius Josephus' History of the Jewish War (Jos. BI, IV, 11, 5). In 70 CE, during the reign of Vespasian, his son Titus moved troops from Alexandria to Judea in order to quell the Jewish uprising. Josephus describes how this was done: marching from Alexandria east to Nikopolis, the troops boarded ships there. They then sailed to the Mendesian nome as far as Thmuis. Here the army disembarked and continued on foot, the assumption being that the canal had ended at this point. No name for this west–east canal is, however, given, and geographic details for the course are lacking. The first leg of the journey was undertaken on a canal linking Nikopolis to Schedia on the Canopic branch of the Nile. While this canal's course has also not yet been archeologically verified, textual evidence exists which also provides a name, Agathos Daimon. In year 7 of Titus' reign (80/81), 14 stelae were erected along the Agathos Daimon canal documenting its repair (Zimmermann, 2003; Scheuble, 2009; Jördens, 2009). The name Agathos Daimon was later transferred to the Canopic branch, as evidenced by Ptolemy (5, 42–43). Further names, such as the Sebastos canal and the Philagrian canal, refer to the same or other canals linking the Canopic branch and Alexandria; they represent potential alternative routes taken by Titus and his soldiers (Jördens, 2009; Hairy and Senounne, 2011). Whether the canal used by Titus and his soldiers is an early, partial version of the Butic Canal (Ball, 1942; Bietak, 1975) or an entirely separate construction (Redon, 2018) is a matter of debate. The second source is the Geography by Ptolemy from the mid-2nd century CE (4, 5, 44; Stückelberger and Graßhoff, 2006). It is only here that the canal is actually named *Boutikos potamos*, and its course spans the entire width of the delta, running "parallel to the coast of the Mediterranean" and connecting the Canopic (= Agathodaemon) branch with the Thermuthiakos, Athribikos, Busiritikos, and Bubastikos branches.

3 Chronology

The two halves of the trans-delta canal, the western half from the Agathodaemon/Canopic branch to Thmuis and the eastern half from Thmuis to Pelusium, have individual biographies and are best analyzed separately. While the eastern half was not functional in Vespasian's time, there are textual and archeological arguments for the existence of earlier, pre-Roman versions (Blouin, 2014; Redon, 2018). A biographical inscription on the backpillar of a statue of the Ptolemaic official Pamerih from Tanis (Cairo, CG 687) from the 2nd century BCE references a journey from the region of Busiris in the central delta to Tanis in the eastern delta which is assumed to have been conducted on a canal (Zivie-Coche, 2004). Bietak (1975) proposed that the Butic Canal on this stretch replaced an earlier land route. A series of important towns in the eastern delta are aligned along roughly the same latitude, ca. 30° 57′, which suggests they were linked by a road or an earlier canal. The foundations of these towns range from the Predynastic Period at Mendes (late 4th millennium BCE), the New Kingdom at Baqlia/Hermopolis (mid-2nd

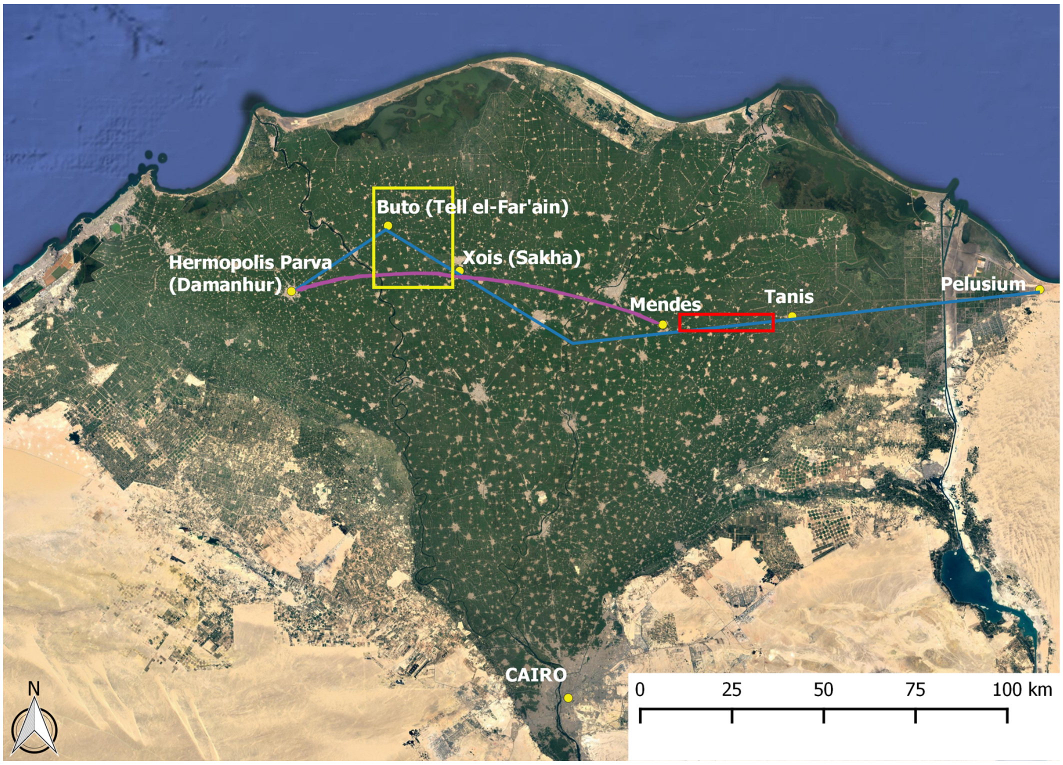

Figure 1. Nile delta, © Google Earth image. The blue line is the reconstruction of the Butic Canal by Talbert (2000), and the purple line is the reconstruction of the Butic Canal by Ball (1942). The rectangle outlined in red is the area enlarged in Fig. 2a–c, and the rectangle outlined in yellow is the area surveyed by the author.

millennium BCE), and the Third Intermediate Period at Tanis (11th century BCE), indicating a long tradition of trans-delta connections. This point is reinforced when we add a series of smaller, less well-known sites also located directly on this route (see Fig. 2c): Tell el-Dab^{c}a (EES 172, formerly known as Tell Qanan; Ball, 1942) was founded in the Predynastic Period, and Deir el-Hamra (EES 169) and El Tell el-Ahmar (EES 349) were founded in the Ptolemaic period. As few of these sites have been thoroughly investigated and published to date, in some cases the dating of their foundation may turn out to be earlier (dating information summarized on the Delta Survey web page: https://www.ees.ac.uk/delta-survey, last access: 3 August 2020). The eastern half thus seems to be older than the western but had fallen out of use by the later 1st century CE when Titus marched east. The western route used by Titus and his soldiers most likely made use of pre-existing canals which linked Nikopolis to the Canopic branch of the Nile and from that point on continued on a presumably new canal connecting the Canopic branch to the Mendesian branch. By the mid-2nd century CE, the eastern section, linking Mendes to Pelusium, had been reactivated or constructed anew, thus completing the trans-delta route and forming Ptolemy's Butic Canal. The date of construction is not known but probably falls between 70 CE and the mid-2nd century CE. This is a period of large-scale investment in Egyptian and Near-Eastern infrastructure (Sidebotham et al., 2000; Brun, 2018; Young, 2001), encompassing both the construction of public buildings, temples, canals, and roads and the foundation of a town (Antinoopolis), and it is suggested that the construction of the Butic Canal is to be placed in the context of such imperial building projects. A more detailed discussion of the chronology follows below in Sect. 5.

4 The route

A series of European maps from the late 16th century (Mercator, 1578, 1584; Ortelius, 1584, 1592; see Silotti, 1998) show the Butic Canal as a straight line crossing through the delta. These maps, however, are not the results of observations based on actual visits to Egypt but attempts at implementing Ptolemy's description. In some respects, this generation of maps is a step back in the accuracy of representing topographic realities as compared to earlier medieval maps (Haguet, 2018). Standard modern editions of historic maps show somewhat different routes while still also following Ptolemy's description. The route shown in blue in Fig. 1 follows that of Talbert's Barrington Atlas of the Greek and Roman World (Talbert, 2000) and the route shown in purple that of Ball (1942). Again, the eastern section and the western section are best discussed separately. The course in the

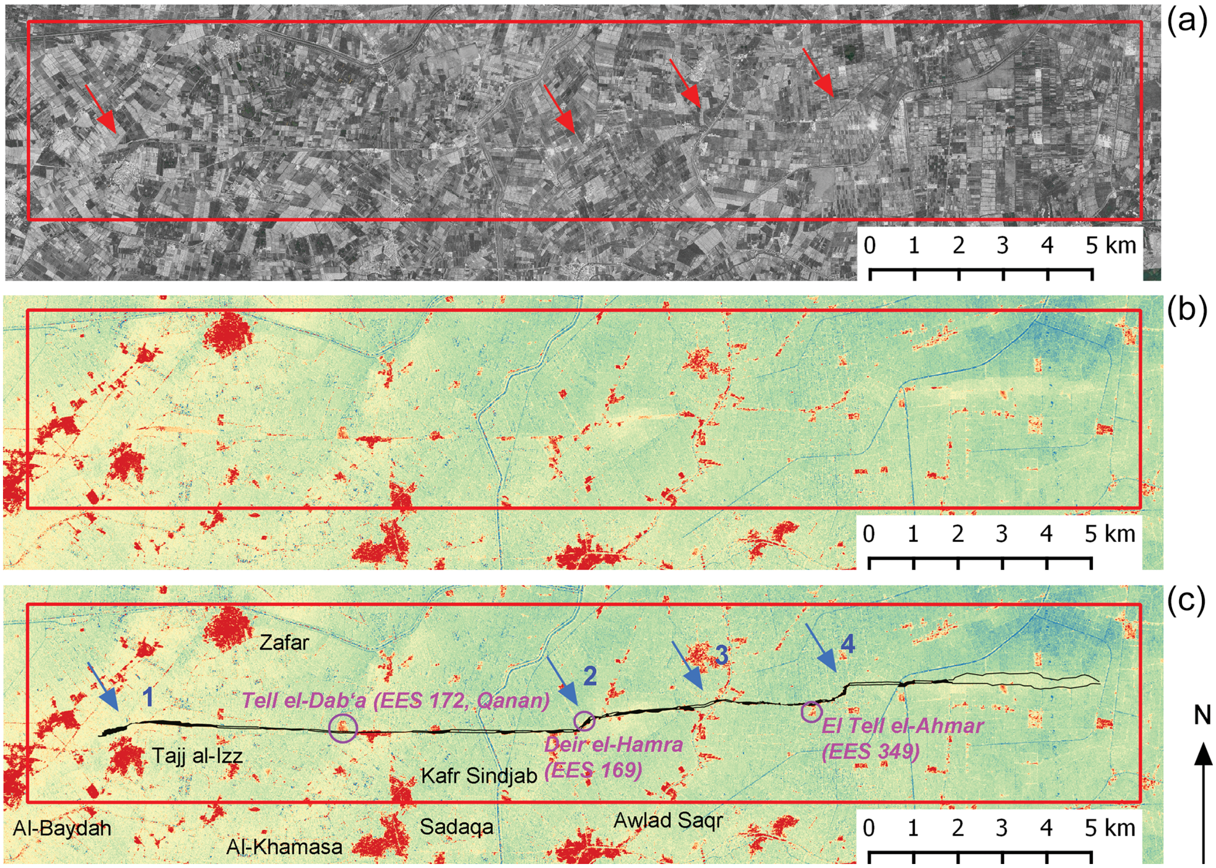

Figure 2. **(a)** Corona satellite image, 18 November 1968 (Corona Atlas of the Middle East, https://corona.cast.uark.edu, last access: 5 June 2020). **(b)** TanDEM-X digital elevation model of the area of investigation. TanDEM-X DEM courtesy of the German Aerospace Center (DLR). **(c)** TanDEM-X digital elevation model with the reconstructed course of the canal. TanDEM-X DEM courtesy of the German Aerospace Center (DLR). Names of ancient settlements shown in purple and modern names in black.

eastern part is based on an elevated feature which remains in parts still extant today. Compared to historic maps and older satellite imagery, such as the Corona image from 1968 (Fig. 2a), some details have been lost, but new data based on a digital elevation model (Fig. 2b) also provide new levels of detail in some areas. The information has been combined in Fig. 2c. This earthen linear feature, about 22 km long and of varying widths reaching a maximum of 140 m, is widely assumed to represent the excavated material from the canal (Bietak, 1975). As the canal itself has not been detected, its relationship to the elevated feature is a matter of debate; it has been suggested that the watercourse originally ran north (Holz et al., 1980) or south (Bietak, 1975) of this feature. A position in the middle seems to be suggested by some Corona satellite imagery and fits the common pattern of canals with dikes on both sides.

For the route of the western half, however, there is to date no archeological evidence. Neither historic maps, satellite images, nor the new digital elevation model provide comparable data to those in the eastern delta. Historic maps show some short stretches of west–east features south of Buto, which also find themselves reflected in the digital elevation model, but we lack any information on dating and function. These segments are not paired by the elevated features as in the eastern delta. The reasons for the very different data, or better lack thereof, in the western delta remain unclear. At this point, it cannot be stated whether the difference is caused by varying formation processes of the canals, lengths of use, or natural or man-made transformation processes post-abandonment. With the increased use of remote sensing data, the interruption or disappearance of hydrological features in the delta landscape has already been observed for various natural features (Ginau et al., 2019).

Talbert (2000; similar to Wittke et al., 2007) shows the western segment of the canal emerging from the Canopic branch at the town of Hermopolis Parva/Mikra, modern Damanhur, and turning northeast in order to reach Buto (Fig. 1, blue line). This is based on the assumption that, due to its name, it must have passed the city of Buto. From Buto, the course then turns in a southeastern direction reaching the area of Sebennytos, which lies roughly on the same latitude as Mendes/Thmuis and Tanis. This requires the canal to flow from a lower-lying region to a higher region. Based on the modern surface, the canal would have flowed from a region of currently about 2 m a.s.l. (meters above sea level), past the region of Xois, modern Sakha, at around 5–6 m a.s.l., to a region of about 6–7 m a.s.l. at Sebennytos, modern Samannud. All in all, the difference in height would have been around 5 m. We are missing, however, one fundamental piece of information: in which direction did the canal flow? The assumption west–east is suggested by the initial northeastern direction when branching off from the Canopic arm. The physical evidence in the eastern delta points in the same direction in that the canal displays a slightly northern shift moving east (Figs. 1 and 2, and discussion below). If the direction were reversed, that is from east to west, the canal would, following the blue route via Buto as shown in Fig. 1, be confronted with the same dilemma of having to flow uphill, albeit on a shorter stretch, namely from Buto to Hermopolis Parva/Damanhur. Overcoming differences in elevation in canals was technically possible in antiquity (Bockius, 2014). There is, however, a substantial effort involved, which begs the question of why such a route would be chosen. Was Roman Buto so significant it warranted such a detour? This seems unlikely, as Buto was neither a strategic, economic, or religious center of preeminent importance in this period. The region, however, was flourishing in Roman times. Two alternative scenarios emerge: firstly, the canal changes its direction of flow. In this scheme, in the western delta, the canal would flow from the west and from the east, in order to meet in Buto, where the water may have been redirected to northern distributaries. If this were the case, it would place Buto at the crucial junction and may explain naming the canal after this town. Secondly, a more southern course, minus the Buto detour, was chosen. If the town of Buto is no longer connected to the Butic Canal, how can the designation of Butic Canal then be explained? Butic does not necessarily refer to the town alone but is also applied to a larger region, the “land of Wadjet (Buto)”, which we find outlined in the Satrap Stela of the late 4th century BCE (Schäfer, 2011). Redon (2018) has recently added further Roman examples for the descriptor *Butikos* applied to different topographic features or goods which are located or produced on a regional level. For example, Strabo mentions a Butic lake (XVII, 1, 18) which most likely refers to the northern lagoon, the later Lake Burullus. Butic linen is mentioned by Pliny (HN, XIX, II, 14) as a product of the district. In short, the canal may have been named Butic for crossing the region of Buto without actually passing the town, as was recently also suggested by Redon (2018). Such a southern route would avoid the above-discussed problems of flowing “uphill”. Taking Ptolemy’s description of the canal “parallel to the coast line” literally, a curved shape would seem the most likely, as was already proposed by Ball (1942; see Fig. 1, purple route). In this way, the canal could remain on the same elevation while flowing west–east. For the eastern delta, new data are available in the form of a digital elevation model (DEM) which provides a greater level of detail (Fig. 2b and c). The DEM, based on the German satellite pair TanDEM-X, was acquired in cooperation with the German Aerospace Center in order to investigate the landscape in the survey area (Ginau et al., 2019). Due to the high resolution of the elevation information, it has been possible to use these data very successfully for the region north of Buto in order to reconstruct ancient watercourses based on the traces of elevated levees. No features, however, were detected which suggest themselves as being part of a west–east delta transversal route. In the eastern delta, the elevated linear feature appears clearly, and some new details emerge, which will be discussed in the following.

On the segment between Mendes/Thmuis and Tanis (Fig. 2c), four sharp bends, or “steps”, are detectable. They are designated, from west to east, steps 1–4. In such a step, the canal turns sharply in a northeastern direction and, after a length of between 480 and 843 m, turns right again in order to continue due east in a linear fashion. The distance between these steps is between 2.3 and 10.5 km. In this way, the canal is incrementally shifting slightly north: over the distance of 22 km, about 1 km. In steps 1, 2, and possibly 3, the steps coincide with an intersection with an elevated feature, most likely an ancient branch. These steps possibly served to support the crossing of branches, feeding them in and out of the canal. In Bietak’s reconstruction (1975), there are small branches crossing the canal in the area of steps 1 and 3. Between steps 1 and 2, east of Tell el-Dab^{c}a (EES 172), there is also an elevated feature crossing the canal, but there is no evidence for a step. This was possibly the levee of an old waterway which was no longer active. A similar stepped feature, albeit on a much smaller scale, was archeologically investigated in the middle of the Fossa Corbulonis, a 1st century CE Roman canal in the Netherlands (de Kort and Razczynski-Henk, 2014). This canal, which on average has a width of 12–15 m, narrows here to 4 m. The feature was interpreted as a portage, an area where the ship had to be taken out of the water and dragged over land, before being placed back in the canal. In the case of the Fossa Corbulonis, it was a measure to balance different levels of water. This does, upon first impression, not seem to be the case in the Butic Canal, but the definite function remains unclear. As the settlements are directly attached to the canal, these stepped features possibly served the purpose of redirecting the canal closer to some settlements. In between the steps, the canal runs along a mostly linear course. Notably, between steps 1 and 2, there is a slight southward shift of around 286 m between the top of step 1 and the base of step 2. With step 2, the course returns to its northward direction. This stretch of the canal provides the first detailed evidence of a Roman period artificial watercourse in the delta. Targeted archeological investigations and comparisons with other Roman period canals could supply crucial further understanding.

5 The function(s) of the canal

Apart from Josephus' description of the movement of troops on the "Titus Canal", the sources remain silent on the uses of the trans-delta route. The military purpose of the Titus Canal has been projected onto the later Butic Canal, comparing its construction to that of "Hitler's and Mussolini's highways" (Carrez-Maratray, 1999). Taking this analogy as a cue, it should be noted that current analysis of the program of the construction of highways by National Socialist Germany discusses them as tools of propaganda, embodying numerous ideas far more varied than those purely focused on strategic military deployment. A recent discussion shows how 1930s *Autobahnen* were conceived as a tool of healing a perceived rupture between landscape and technology. *Autobahnen* were deeply embedded in evolving concepts of landscape and in turn had a massive effect on the landscape (Zeller, 2007). Josephus' account itself raises questions for the strategic value of this route. Titus' journey was undertaken in three parts of distinctly different lengths: part 1, by ship from Nikopolis to Thmuis and continuing on land from Thmuis to Tanis, covered almost 200 km and was by far the longest; part 2, on land from Tanis to Herakleopolis Parva (Tell Belim), was about 28 km long; and part 3, from Herakleopolis Parva to Pelusium, was about 37 km long. Josephus writes that after arriving at Pelusium, the soldiers rested for 2 d (BI IV, 11, 5). Evidently reaching Jerusalem as fast as possible was not the main concern. It has been suggested that the journey by Titus was undertaken to test the strategic efficiency of the canal (Carrez-Maratray, 1999). The basic question remains: why bother creating such a watercourse parallel to the Mediterranean, in particular when the point of departure lay on the coast? One reason may have been the seasonality of sea travel, which due to weather conditions in the Mediterranean all but ceased in the winter. Between October, at the latest November, and March or April, large ships avoided traveling in the Mediterranean Sea. Additionally, entering and leaving Nile mouths presented challenges which made circumventing them attractive (Cooper, 2014). During this period, the transportation of goods switched to land routes or had to wait until spring. Titus' journey did indeed take place in winter. While the emperor Vespasian stayed in Alexandria and postponed his return to Rome until winter was over, Titus and his troops were sent off in the direction of Judea, with the siege of Jerusalem taking place in spring shortly before Passover (Jos. BI, IV, 11, 5; V, 3, 1; Schäfer, 2003). Thus, the canal created the strategic advantage of allowing transport by ship also in the winter. The Butic Canal itself, however, fell into the category of seasonal canals which were not operational year-round. Once the Nile was very low, they were dammed off and the dams were opened only after the peak of the flood. Such canals were active from September to the end of December/early January (Cooper, 2014). While the data on this are late antique, medieval, and modern, it seems likely that the same system was in place in Roman times. The period of activity falls into the period with no or only very dangerous sea travel, reducing this period to January to March and thus underscoring the value of an alternative provided by an artificial waterway. While the ancient sources remain silent on the Butic Canal's purpose, in other cases they supply an intriguing variety of reasons for the construction of waterways. The Fossa Corbulonis, connecting the Rhine and the Meuse in the Netherlands and being ca. 30 km in length, was built in the mid-1st century CE and has only recently been identified archeologically (de Kort and Raczinsky-Henk, 2014). According to Tacitus, it was built to keep troops busy and to provide a route to circumvent the dangers of the North Sea (Ann. XI, 18–20), while Cassius Dio (Hist Rom LXI 30, 4–6) provides another reason, namely that it could serve as a water management system. Seemingly inconsistent, these different purposes may reflect a blend of concepts, original functions, and eventual uses. In canals with long and complex biographies, primary purposes and later functions may vary fundamentally (Salomon et al., 2014). The Red Sea Canal, verifiably completed in the Persian period, certainly served the political purpose of binding Egypt, now a Persian province, closer to the Persian heartland. After the Persian domination over Egypt ended, the canal was rebuilt in the Ptolemaic period and later again in the Roman period with different functions, such as providing commercial links to the Red Sea, Arabia, and southern India, as well as a strategic role in Trajan's Parthian wars (Sijpesteijn, 1963; Reddé, 1986; Cooper, 2009). The canal also generated settlement development, with the foundation of a Ptolemaic harbor settlement adjoining the canal, and an opportunity to set up stelae extolling royal accomplishments along its path. While only Persian and Ptolemaic examples of such stelae survive from the Red Sea Canal, the erection of Roman stelae is very likely. If Titus had 14 stelae set up for the, in comparison, minor Agathos Daimon canal, discussed above in Sect. 2, the Roman Red Sea Canal and the Butic Canal provided greater opportunities for imperial self-presentations. That a canal was actually only re-excavated or repaired and not built from scratch is notably mentioned in Titus' stelae but not in the Persian or Ptolemaic stelae along the Red Sea Canal. Young (2001) considers the construction of the Red Sea Canal less an act "of economic policy and more as an act of euergetism". Roman roads – and canals by inference – are, as Kolb summed it up recently, "instrument and symbol of Roman rule" (Kolb, 2019). Imperial connectivity, in particular in the eastern part of the Roman empire, was greatly enhanced in the 2nd century CE. Such infrastructure measures also served travelers beyond the borders of the empire, as evidenced in Lucian's description of a journey of a young man in 170 CE sailing from Alexandria to Clysma thanks to the Red Sea Canal and continuing to India (Young, 2001). The Butic Canal was most likely also used for strategic purposes and provided a seasonal alternative to sea travel. Troops stationed in Egypt were moved to assist in eastern conflicts even prior to the Jewish uprising in 70 CE, for which the Titus Canal may have been built. Starting with an Armenian war of succession against Nero in 58–63, a pattern emerges during the 1st and 2nd centuries CE in which entire Egyptian legions or parts of them were involved in numerous conflicts in the east. The two main theaters of conflict were the wars with the Parthians and the Jewish uprisings in Judea. Movements of troops went in both directions, with the contingents leaving Nikopolis and eventually returning; occasionally other troops were shifted around (Mor, 2016). The Egyptian III legion, *Cyrenaica*, participated in Trajan's Parthian wars (Gilliam, 1966), and a vexillation of this legion was stationed in Jerusalem in 116 (Cotton, 2000, 353). For the suppression of the Jewish revolts in Egypt in 115–117 CE, troops were moved there to replace losses of soldiers (Gilliam, 1966). In the 130s CE, during the Bar Kokhba revolt, it is quite likely that the Egyptian XXII legion, *Deiotoriana*, was transferred to Judea (Millar, 1993; Eck, 1999). In this period, there was massive investment in road construction in the eastern provinces, particularly in Judea, which provided a military corridor between Egypt, Arabia, and Syria (Schäfer, 1990). However, the Judean road constructions under Hadrian took place in the years 120 and 129/30 CE prior to the Bar Kokhba revolt (Isaac, 1990). The building activities are thus not a strategic reaction to the unrest but are likely linked to the emperor's journey to Judea. Hadrian's visit to Egypt in 130–131 CE took him from Pelusium to Alexandria (Vita Hadriani, 14, 4; Cassius Dio, Hist Rom LXIX, 11.1; Sijpesteijn, 1969), but no information is provided on how this trip was undertaken (Halfmann, 1986; Birley, 2003). The Butic Canal possibly formed part of an imperial construction program linked to Hadrian's journey. It has been argued that Hadrian's visit to Egypt in 130 was his second, preceded by a visit in 117 shortly after his accession (Capponi, 2010). As in the trip of 130, Hadrian's entry to Egypt is suggested to have been from the east and continuing to Alexandria. This journey possibly fostered the plans to build an imperial canal, which may have been inaugurated on his second journey. Hadrian's visit(s) to Egypt were accompanied by the restoration of buildings and temples which formed part of an "imperial image campaign" (Capponi, 2010). The canal must have also had a major effect on the water system of the delta (Ball, 1942; Bietak, 1975; Blouin, 2008). The crossing branches of the Nile fed the canal, reducing the flow of water in these branches. It could, thus, have served as a sort of valve to regulate and distribute the Nile flood and may have been harnessed for irrigation purposes. The earthen dikes of the canal built across the delta plain would also have served to regulate the flood, as suggested by Bietak (1975). During Trajan's and Hadrian's reigns, low Nile floods are attested (Sijpesteijn, 1969; Pfeiffer, 2010) which may have been the reason for improvements to the canal-system undertaken during their reigns. The Butic Canal was possibly part of this scheme. Just as the date of the canal's opening remains unclear, so does the date of its demise. The very substantial elevated linear feature in the eastern half is probably the result of continued dredging over a longer time period, with the deposited earth thus creating a higher levee. Much of this may, however, have already accumulated during the canal's Pharaonic and Ptolemaic existence prior to the completion of the Roman Butic Canal. The lack of any trace of such a feature in the western section may reflect that part's shorter life use. By the early 4th century CE, the Butic Canal no longer seems to have been in use. The detailed travel log of Theophanes (Matthews, 2006), who in 320 CE traveled from Hermopolis in Middle Egypt to Antioch in Syria, crossed the delta from Thmuis to Tanis, and continued to Herakleopolis and to Pelusium on exactly the route covered by the Butic Canal. He did not, however, go by ship but on land, most likely in a horse drawn carriage. As he traveled in mid-March, this may have been due to seasonal reasons, when the low Nile made travel on canals all but impossible. The road traveled was likely on the dike of the Butic Canal. These elevated features provided the traditional placement for roads secure from the floods. In the eastern segment, from Thmuis to Pelusium, the route of a road crossing the delta shown on the tabula Peutingeriana (Talbert, 2010) concurs with that of the Butic Canal. The tabula Peutingeriana is a medieval copy of a map compiled in the late Roman period from mixed sources, some of which date to the early Roman period (Arnaud, 1990). It is very likely that this road was erected on the dike of the Butic Canal. On the stretch from Tanis to Pelusium, the remains of the Butic Canal may be depicted on the tabula Peutingeriana, with the road shown running parallel to a west–east watercourse (Redon, 2018). The full length of the Butic Canal most likely was not in existence very long. In contrast to other imperial prestige projects, canals required intense yearly maintenance lest they fall into disuse. The canal possibly fell apart into segments again, with an eastern part remaining in function and providing a local transportation route.

6 Conclusions

The Butic Canal was most likely created by reactivating existing canals: a Flavian section in the western delta and a possibly Pharaonic route in the eastern delta. Its route did not pass by the town of Buto but ran further south, crossing the region of Buto. Based on a digital elevation model, new features are clearly discernible in the eastern section of the canal. Four sharp bends, or steps, shift its course slightly north. These features possibly served to feed crossing watercourses in and out of the canal. The greatest artificial watercourse of Egypt was completed sometime between 70 CE and the mid-2nd century CE. It may have been built in connection with Hadrian's visit to Egypt and thus be considered less a strategic necessity than a representation of imperial rule. When traveling east from Alexandria by ship, the canal did provide a seasonal alternative to the Mediterranean route, which was to be avoided in the winter. It must have had a substantial impact on the waterscape of the delta and may have been an attempt at creating a new water management system. Whether this was entirely beneficial remains unclear, but the yearly maintenance required possibly outweighed the benefits and led to the abandonment of this cross-delta route. The canal's last traces may be found on the tabula Peutingeriana on which in the eastern delta a road is shown running parallel to a watercourse, quite likely on the dike of the Butic Canal. This study demonstrates the usefulness of new data, such as the TanDEM-X digital elevation model, used in combination with newly available data, such as the Corona satellite imagery, for the fields of archeology, landscape archeology, and geoarcheology of the Nile Delta.

Data availability. The TanDEM-X digital elevation model is used with the permission of the German Aerospace Center (DLR) and is based on the data requested via the proposal (DEM_HYDR1426) by Andreas Ginau, Robert Schiestl, Jürgen Wunderlich, Eva Lange-Athinodorou, and Tobias Ullmann. The TanDEM-X data are used within the framework of the agreement with the German Aerospace Center (DLR) and are not freely accessible.

Competing interests. The author declares that there is no conflict of interest.

Special issue statement. This article is part of the special issue "Geoarchaeology of the Nile Delta". It is a result of the workshop "Geoarchaeology of the Nile Delta: Current Research and Future Prospects", Würzburg, Germany, 29–30 November 2019.

Acknowledgements. I am grateful for the assistance of Andrea Squitieri in preparing the maps and for Henry Heitmann-Gordon and Janice Schiestl for helpful comments and for correcting my English. I am also grateful to the two anonymous reviewers for their valuable comments and suggestions.

Review statement. This paper was edited by Tobias Ullmann and reviewed by two anonymous referees, one of whom requested to be thanked anonymously in the Acknowledgements.

References

Arnaud, P.: L'origine, la date de rédaction et la diffusion de l'archétype de la Table de Peutinger, Bulletin de la Société Nationale des Antiquaires de France, 1988, 302–321, https://doi.org/10.3406/bsnaf.1990.9424, 1990 (in French).

Ball, J.: Egypt in the Classical Geographers, Survey of Egypt, Government Press, Cairo, Egypt, 1942.

Bietak, M.: Tell el-Dab^{c}a II. Der Fundort im Rahmen einer archäologisch-geographischen Untersuchung über das ägyptische Ostdelta, Untersuchungen der Zweigstelle Kairo des Österreichischen Archäologischen Instituts 1, Denkschriften der Gesamtakademie der Österreichischen Akademie der Wissenschaften 4, Austrian Academy of Sciences, Vienna, Austria, 1975 (in German).

Birley, A. R.: Hadrian's Travels, in: The Representation and Perception of Roman Imperial Power. Proceedings of the Third Workshop of the International Network Impact of Empire (Roman Empire, c. 200 B.C.–A.D. 476), Netherlands Institue in Rome, March 20–23, 2002, edited by: de Blois, L., Erdkamp, P., Hekster, O., de Kleijn, G., and Mols, S., J. C. Gieben, Amsterdam, 425–438, 2003.

Blouin, K.: De Mendès à Thmouis: hydrographie mobile, société mobile?, in: L'eau comme patrimoine−−de la Méditerranée à l'Amérique du Nord, edited by: Hermon, E., Presses de l'Université Laval, Québec, Canada, 107–128, 2008 (in French).

Blouin, K.: Triangular Landscapes. Environment, Society, and the State in the Nile Delta under Roman Rule, Oxford University Press, Oxford, United Kingdom, https://doi.org/10.1093/acprof:oso/9780199688722.001.0001, 2014.

Bockius, R.: Künstliche Schifffahrtswege. Wasserbau und hydrotechnische Einrichtungen im Altertum, in: Großbaustelle 793. Das Kanalprojekt Karls des Großen zwischen Rhein und Donau. Mosaiksteine. Forschungen am RGZM 11, edited by: Ettel, P., Daim, F., Berg-Hobohm, S., Werther, L., and Zielhofer, C., Verlag des Röm.-German. Zentralmuseums, Mainz, Germany, 87–94, 2014 (in German).

Bonneau, D.: Le régime administratif de l'eau du Nil dans l'Égypte grecque, romaine et byzantine, Probleme der Ägyptologie 8, Brill, Leiden, The Netherlands, 1993 (in French).

Brun, J.-P.: Chronology of the Forts of the Routes to Myos Hormos and Berenike during the Graeco-Roman Period, in: The Eastern Desert of Egypt during the Greco-Roman Period: Archaeological Reports, Paris: Collège de France, https://doi.org/10.4000/books.cdf.5239, 2018.

Capponi, L.: Hadrian in Jerusalem and Alexandria in 117, Athenaeum, 98, 489–501, 2010.

Carrez-Maratray, J.-Y.: Péluse et l'angle oriental du Delta égyptien aux époques grecque, romaine et byzantine ,Bibliothèque d'étude 124, Institut Français d'Archéologie Orientale, Cairo, Egypt, 403–404, 1999 (in French).

Cooper, J. P.: Egypt's Nile-Red Sea Canals: Chronology, Location, Seasonality and Function, in: Connected Hinterlands. Proceedings of the Red Sea Project IV Held at the University of Southampton September 2008, Society for Arabian Studies Monographs No. 8, BAR International Series 2052, edited by: Blue, L., Cooper, J. P., Thomas, R., and Whitewright, J., Archaeopress, Oxford, United Kingdom, 195–210, 2009.

Cooper, J.P.: The Medieval Nile: Route, Navigation, and Landscape in Islamic Egypt, American University in Cairo Press, Cairo, Egypt, 2014.

Cotton, H.: The Legio VI Ferrata, in: Les légions de Rome sous le Haut-Empire I, edited by: Le Bohec, Y., de Boccard, Lyon, France, 351–357, 2000.

De Kort, J.-W. and Raczynski-Henk, Y.: The Fossa Corbulonis between the Rhine and Meuse estuaries in the Western Netherlands, in: Roman canal studies, Water History 6/1, edited by: Salomon, F., Purdue, L., Goiran, J.-P., and Berger, J.-F., Springer, Berlin, Heidelberg, Germany, 51–71, https://doi.org/10.1007/s12685-014-0097-3, 2014.

Gilliam, J. F.: An Egyptian Cohort in A.D. 117, in: Bonner Historia Augusta-Colloquium 1964/1965, Bonn, 91–97, 1966.

Eck, W.: The Bar-Kokhba Revolt: The Roman Point of View, Journal of Roman Studies, 89, 76–89, 1999.

Ginau, A., Schiestl, R., and Wunderlich, J.: Integrative geoarchaeological research on settlement patterns in the dynamic landscape of the northwestern Nile delta, QI, 511, 51–67, https://doi.org/10.1016/j.quaint.2018.04.047, 2019.

Grewe, K.: Tunnels and Canals, in: The Oxford Handbook of Engineering and Technology in the Classical World, edited by: Oleson, J. P., Oxford University Press, Oxford, United Kingdom, 319–336, https://doi.org/10.1093/oxfordhb/9780199734856.013.0013, 2009.

Haguet, L.: Egypt and Maps, Or: What Early Modern Maps Are (Not) Telling Us about the History of Egyptology in Europe, in: Mapping Ancient Identities. Methodisch – kritische Reflexionen zu Kartierungspraktiken, Berlin Studies of the Ancient World 55, edited by: Grunwald, S., Hofmann, K. P., Werning, D. A., and Wiedemann, F., Edition Topoi, Berlin, Germany, 91–113, https://doi.org/10.17171/3-55, 2018.

Hairy, I. and Sennoune, O.: Le canal d'Alexandrie: la course au Nil, in: Du Nil à Alexandrie: histoires d'eaux, edited by: Hairy, I., Céntre d'Études Alexandrines, De Boccard, Alexandrie, 140–161, 2011 (in French).

Halfmann, H.: Itinera Principum. Geschichte und Typologie der Kaiserreisen im Römischen Reich, F. Steiner Verlag, Stuttgart, Germany, 1986 (in German).

Holz, R. K., Stieglitz, D., Hansen, D. P., and Ochsenschlager, E.: Mendes I, American Research Center in Egypt, Cairo, Egypt, 1980.

Isaac, B.: The Limits of Empire. The Roman Army in the East, Clarendon Press, Oxford, United Kingdom, 1990.

Jördens, A.: Statthalterliche Verwaltung in der römischen Kaiserzeit, Studien zum praefectus Aegypti, Historia Einzelschriften 175, Steiner, Stuttgart, Germany, 2009 (in German).

Kolb, A.: Via ducta – Roman Road Building: An Introduction to Its Significance, the Sources and the State of Research, in: Roman Roads. New Evidence - New Perspectives, edited by: Kolb, A., de Gruyter, Berlin, Boston, 3–21, https://doi.org/10.1515/9783110638332-002, 2019.

Matthews, J.: The journey of Theophanes. Travel, Business, and Daily Life in the Roman East, Yale University Press, New Haven, USA, 2006.

Millar, F.: The Roman Near East, 31 BC–AD 337, Harvard University Press, Cambridge, MA, USA, 1993.

Mor, M.: The Second Jewish Revolt. The Bar Kokhba War, 132–136 CE, The Brill Reference Library of Judaism 50, Brill, Leiden, The Netherlands, 2016.

Pfeiffer, S.: Der römische Kaiser und das Land am Nil. Kaiserverehrung und Kaiserkult in Alexandria und Ägypten von Augustus bis Caracalla (30 v.Chr.–217 n.Chr.), Historia Einzelschrift 212, Steiner, Wiesbaden, Germany, 2010 (in German).

Reddé, M.: Mare nostrum. Les infrastructures, le dispositive et l'histoire de la marine militaire sous l'Empire romain, École française de Rome, Rome, Italy, 1986 (in French).

Redon, B.: Les circulations transversales dans le Delta égyptien – entre adaptation au paysage et nécessités pratiques, in: Landscape Archaeology, Egypt and the Mediterranean World, Proceedings of the Cairo Conference, Bibliothèque d'étude 169, edited by: Tristant, Y. and Ghilardi, M., Institut Français d'Archéologie Orientale, Cairo, Egypt, 151–172, 2018 (in French).

Salomon, F., Purdue, L., Goiran, J.-P., and Berger, J.-F.: Introduction to the special issue: Roman canal studies – Main research aims, Water History, Springer, Berlin, Germany, 1–9, 2014.

Schäfer, D.: Makedonische Pharaonen und hieroglyphische Stelen. Historische Untersuchungen zur Satrapenstele und verwandten Denkmälern, Studia Hellenistica 50, Peeters, Leuven, Belgium, 2011 (in German).

Schäfer, P.: Hadrian's policy in Judaea and the Bar Kokhba revolt: a reassessment, in A Tribute to Geza Vermes. Essays on Jewish and Christian Literature and History, Journal for the Study of the Old Testament Supplement Series 100, edited by: Davies, P. R. and White, R. T., JSOT Press, Sheffield, United Kingdom, 281–303, 1990.

Schäfer, P.: The History of the Jews in the Greco-Roman world, Routledge, London, United Kingdom, 2003.

Scheuble, S.: Inschriften aus Schedia, Chiron, 39, 463–503, 2009 (in German).

Schiestl, R.: Field Boundaries and Ancient Settlement Sites: Observations from the Regional Survey around Buto, Western Delta, in: Mitteilungen des Deutschen Archäologischen Instituts, Abteilung Kairo, 68, 175–190, 2012.

Sidebotham, S. E., Zitterkopf, R. E., and Helms, C. C., Survey of the Via Hadriana: The 1998 Season, J. Am. Res. Center Egypt, 37, 115–126, 2000.

Sijpesteijn, P. J.: Der ΠΟΤΑΜΟΣ ΤΡΑΙΑΝΟΣ, Aegyptus, 43, No. 1/2, 70–83, 1963.

Sijpesteijn, P. J.: A New Document concerning Hadrian's Visit to Egypt, Historia, 18, 109–118, 1969.

Silotti, A.: The Discovery of Ancient Egypt, Edizione White Star, Vercelli, Italy, 1998.

Stückelberger, A. and Graßhoff, G. (Eds.): Klaudios Ptolemaios. Handbuch der Geographie: griechisch-deutsch; Einleitung, Text und Übersetzung, Index/1: Einleitung und Buch 1–4, Schwabe, Basel, Switzerland, 2006 (in German).

Talbert, R. J. A.: Barrington Atlas of the Greek and Roman World, Princeton University Press, Princeton, USA, 2000.

Talbert, R. J. A.: Rome's World: The Peutinger Map Reconsidered, Cambridge University Press, Cambridge, United Kingdom, 2010.

Wikander, C.: Canals, in: Handbook of Ancient Water Technology, Technology and Change in History, Vol. 2, edited by: Wikander, Ö., Brill, Leiden, The Netherlands, 321–330, 2000.

Wittke, A.-M., Olshausen, E., Szydlak, R.: Historischer Atlas der antiken Welt, Der Neue Pauly, Supplemente, J. B. Metzler Verlag, Stuttgart, Germany, 2007.

Young, G.: Rome's Eastern Trade. International commerce and imperial policy, 31 BC–AD 305, Routledge, London, United Kingdom, 2001.

Yoyotte, J.: Tells oubliés de la region de Sân, in: Cahiers de Tanis I, Éditions Recherche sur les Civilisations, Paris, 107–112, 1987 (in French).

Zeller, T.: Driving Germany. The landscape of the German Autobahn, 1930-1970, Studies in German History 5, Berghahn Books, New York, USA, 2007.

Zimmermann, M.: Der Kaiser als Nil, in: Propaganda-Selbstdarstellung – Repräsentation im römischen Kaiserreiche des 1. Jhs. n. Chr., Historia Einzelschriften 164, edited by: Weber G., and Zimmermann, M., Steiner, Stuttgart, Germany, 317–348, 2003 (in German).

Zivie-Coche, C.: Statues et autobiographies de dignitaires, Tanis à l'époque Ptolémaique, Tanis, Travaux récents sur le Tell San El-Hagar, mission française des fouilles de Tanis 3, Éd. Noesis, Paris, France, 2004 (in French).

E&G Quaternary Sci. J., 70, 83–92, 2021
https://doi.org/10.5194/egqsj-70-83-2021

Open Access E&G Quaternary Science Journal

Research article

Significant depositional changes offshore the Nile Delta in late third millennium BCE: relevance for Egyptology

Jean-Daniel Stanley and Sarah E. Wedl

Mediterranean Basin (MEDIBA) Program, 6814 Shenandoah Court, Adamstown, Maryland 21710, USA

Correspondence: Jean-Daniel Stanley (stanleyjd0@gmail.com)

Relevant dates: Received: 28 July 2020 – Accepted: 17 December 2020 – Published: 22 February 2021

How to cite: Stanley, J.-D. and Wedl, S. E.: Significant depositional changes offshore the Nile Delta in late third millennium BCE: relevance for Egyptology, E&G Quaternary Sci. J., 70, 83–92, https://doi.org/10.5194/egqsj-70-83-2021, 2021.

Abstract: No environmental factor has been as critically important for Egypt's ancient society through time as sufficiently high annual flood levels of the Nile River, the country's major source of fresh water. However, interpretation of core analysis shows reduced depositional accumulation rates and altered compositional attributes of the sediment facies deposited seaward of the Nile Delta during a relatively brief period in the late third millennium BCE. These changes record the effects of displaced climatic belts, decreased rainfall, lower Nile flows, and modified oceanographic conditions offshore in the Levantine Basin, primarily from 2300 to 2000 BCE, taking place at the same time as important geological changes identified by study of cores collected in the Nile Delta. It turns out that integrated multidisciplinary Earth science and archaeological approaches at dated sites serve to further determine when and how such significant changing environmental events had negative effects in both offshore and landward areas.

This study indicates these major climatically induced effects prevailed concurrently offshore and in Nile Delta sites and at about the time Egypt abandoned the Old Kingdom's former political system and also experienced fragmentation of its centralized state. In response, the country's population would have experienced diminished agricultural production leading to altered societal, political, and economic pressures during the late Old Kingdom to First Intermediate Period at ca. 2200 to 2050 BCE.

Kurzfassung: Für die Gesellschaft des Alten Ägypten war im Laufe der Zeit kein anderer Umweltfaktor so entscheidend wie die ausreichend hohen jährlichen Hochwasserstände des Nils, der wichtigsten Süßwasserquelle des Landes. Allerdings deuten Bohrkernanalysen darauf hin, dass während eines relativ kurzen Zeitraums gegen Ende des 3.Jahrtausends v. u. Z. geringere Ablagerungsraten sowie Veränderungen in der Zusammensetzung der Sedimentfazies auftraten, die sich meerwärts des Nildeltas akkumulierten. Diese Veränderungen resultierten aus einer Verschiebung der Klimagürtel, geringeren Niederschlägen und Nilabflüssen sowie veränderten ozeanographischen Bedingungen im Levantinischen Becken um etwa 2300 bis 2000 v. u. Z., einer Zeit weiterer geologischer Veränderungen, deren Effekte sich ebenfalls in den Bohrkernen nachweisen lassen. Wie sich nun zeigt, helfen integrierte multidisziplinäre geowissenschaftliche und archäologische Untersuchungen im Umfeld archäologischer Stätten dabei, näher zu bestimmen, wann und wie sich solche bedeutenden Umweltereignisse negativ auswirkten, sowohl vor der Küste, als auch im Delta selbst.

Die Ergebnisse dieser Studie legen nahe, dass sich diese großen klimabedingten Effekte gleichzeitig vor der Küste und im Umland archäologischer Stätten im Nildelta nachweisen lassen, ungefähr im gleichen Zeitraum, als in Ägypten das politische System des Alten Reiches zerfiel und die Fragmentierung des zuvor zentralistischen Staates einsetzte. Eine mögliche Konsequenz daraus wäre der Rückgang der landwirtschaftlichen Produktion, was wiederum zu veränderten gesellschaftlichen, politischen und wirtschaftlichen Bedingungen für die Bevölkerung des Landes vom späten Alten Reich bis zur Ersten Zwischenzeit um ca. 2200 bis 2050 v. u. Z. geführt haben könnte.

1 Introduction

Climatic conditions evolved considerably during the Middle to Late Holocene as interpreted by study of the sedimentary record examined in Egypt, northeastern Africa, and the Levant (Said, 1993; Gasse, 2000; Bar-Matthews and Ayalon, 2011; Marriner et al., 2013; Kaniewski et al., 2018). The present survey focuses primarily on significantly decreased sediment accumulation rates and marked lithofacies changes seaward of the Nile Delta that became more pronounced after the African Humid Period (AHP), from about 5000 to 4000 years ago (Maldonado and Stanley, 1976; Krom et al., 2002; Stanley et al., 2003; Ducassou et al., 2009; Kholeif and Mudie, 2009; Blanchet et al., 2013; Revel et al., 2015). Stratigraphic, lithological, and compositional attributes of deposits accumulating in lower Egypt and the delta during that period record increased effects of aridity and desertification (Calvert and Fontugne, 2001; Stanley et al., 2003; Ducassou et al., 2009; Kholeif and Mudie, 2009; Kholeif and Ibrahim, 2010; Bernhardt et al., 2012; Blanchet et al., 2013; Marriner et al., 2013; Pennington et al., 2019). Altered monsoonal rainfall patterns and intensities induced erosional changes in Nile highland source terrains south of Egypt, including Ethiopia and the East African lakes region, which modified the hydrography of both the Blue Nile and the White Nile during the Holocene (Gasse, 2000; Blanchet et al., 2015; Woodward et al., 2015). These changes induced substantially lower Nile flows northward to and across the Sudan and Egypt and significantly reduced rates of fresh water and sediment discharged into the delta (Stanley, 2019). Interpreting possible climatic effects seaward of the delta in the Mediterranean during this period is of major consideration in the present study.

The millennium from ca. 5000 to 4000 years BP (before present) comprises Egypt's early dynasties (numbered I to XI). This time span includes the Early Dynastic Period and Old Kingdom to the First Intermediate Period as established archaeologically (Shaw, 2000; Bard, 2008). It was during pharaonic rule of the Old Kingdom that Egypt's civilization was already reaching stunning levels, including major phases of social and municipal expansion, monumental construction projects along the Nile, and impressive artistic development (Shaw, 2000). Toward the latter part of that millennium, however, some notable degradation occurred, such as of pyramids (see Fig. 5 herein for example) during Egypt's late Old Kingdom and First Intermediate Period. These took place at, or about, the time when environmental conditions were evolving extensively, not only in the Nile Delta but also offshore as highlighted in the present review. Whether the country's population could have been affected by such altered climatic conditions at that time will be considered herein.

2 General background

Depositional changes observed offshore are recorded between the outer continental shelf and more distal, deeper slope sectors north of the delta in the eastern Mediterranean (Ducassou et al., 2009; Kholeif and Ibrahim, 2010). Studies at sea here (Fig. 1a) in recent years have recorded altered attributes through time in radiocarbon-dated sediment core sections, including markers such as texture, mineralogy and isotopes, and biogenic components. Together, these reveal that after ca. 5000 years BP proportions of eolian sediment, derived from both proximal and more distal arid terrains and deserts, were increasing in both deltaic and offshore deposits. By ca. 4000 years BP observations indicate that desert conditions had fully reached Egypt's Sahara (Calvert and Fontugne, 2001; Krom et al., 2002; Marriner et al., 2013; Blanchet et al., 2013; Pennington et al., 2019). For the purposes here we define three periods: from $\sim 11\,000$ to ~ 8000 years BP is Early Holocene, from ~ 8000 to ~ 4500 years BP is Middle Holocene, and from ~ 4500 years BP to present is Late Holocene. The Middle to Late Holocene is a time of prime interest here that has experienced significant shifts in amounts of water and sediment derived from Blue Nile, and to a lesser extent White Nile, upland source areas that were dispersed downslope to lower Egypt, its delta plain, and offshore. For example, Revel et al. (2015) proposed that decreased proportions of clastic sediments from Ethiopia's Blue Nile were at times derived from ca. 6 to 3.1 ka. Such changes resulted from altered rainfall patterns in East African highland source areas and increased aridification (Marriner et al., 2013; Revel et al., 2015) that markedly reduced sediment discharged by Nile flows at the coastal margin. This resulted in lower proportions of fluvial terrigenous and volcanically derived material released over more limited deltaic and offshore areas (Stanley and Warne, 1993).

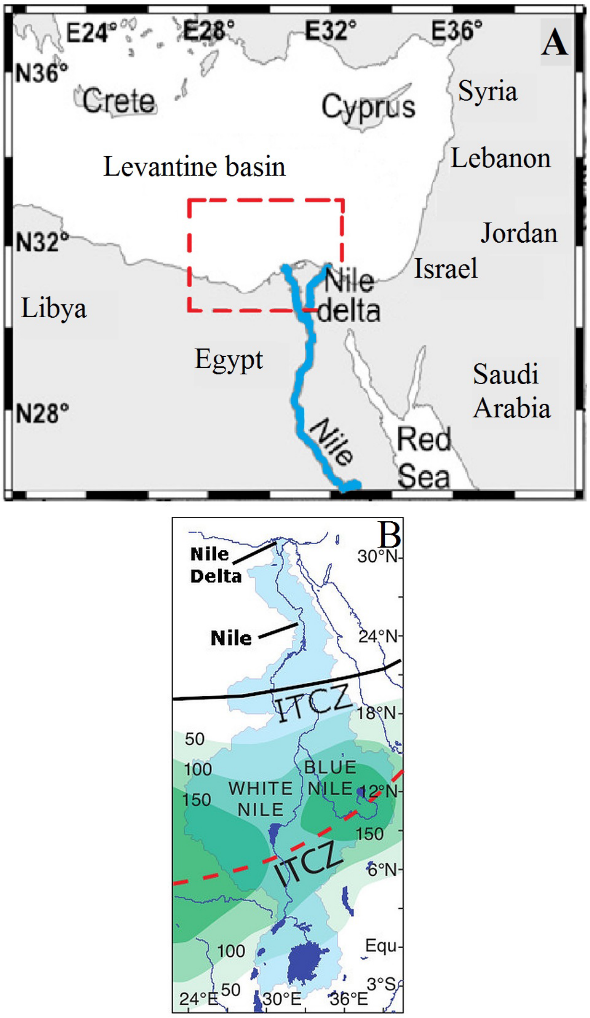

Figure 1. **(a)** Levantine Basin in the eastern Mediterranean showing the study area NW of Egypt's lower Nile River and delta. **(b)** Nile catchment basin (in blue) shows two approximate latitudinal positions of the June–July–August Intertropical Convergence Zone (ITCZ): solid black line denotes monsoonal shift to the north during Early to Middle Holocene; dashed red line denotes its Late Holocene move toward present position farther to the south. Numbers 50 to 150 are rainfall values (in mm), for the monsoon season (after Marriner et al., 2012, their Fig. 1b, modified here by authors of this article).

Egypt's then modest population along the Nile valley and lower river stretches had initially used a portion of deltaic plain terrains for pasturing and later for cultivation. The latter depended increasingly on channelization and diversion of water for irrigation from the Nile, that country's major source of fresh water (Butzer, 1976, 1984). Critical in this respect is the amount of freshwater discharge reaching the delta that responded largely to regional climate change induced by north–south latitudinal migration of the Intertropical Convergence Zone (ITCZ; Fig. 1b). Nile discharge fluctuations were also induced by more frequent and periodically intense El Niño–Southern Oscillation (ENSO) cycles that, at a centennial scale, affected water flow and sediment delivery to lower Egyptian sectors and its coast (Said, 1993; Krom et al., 2002; Marriner et al., 2012).

The focus here is on altered sediment databases recorded offshore Egypt that can be compared with those of similar age previously examined in the Nile Delta and farther inland. Data from dated sediment cores in the delta's northern sector and coastal area identify a period of markedly decreased depositional rates. This phase prevailed primarily during a 200- to 300-year period, between ca. 4300 and 4000 years BP (Stanley, 2019), and spans that of a climatically altered period generally termed the "ca. 4200 year BP event". This phase has been discussed by climatologists, geographers, sedimentologists, palynologists, and others, who have examined the Holocene record in different sectors of the eastern Mediterranean, Levant, and beyond (Weiss et al., 1993; Bar-Matthews and Ayalon, 2011; Kaniewski et al., 2018).

Other natural phenomena considered include neotectonic activity, as recorded by stratal deformation and offsets observed in seismic subbottom surveys that could have triggered some downslope displacement of sediment by gravitative flows such as turbidites and slumps during the Holocene. Near-surface displacement may have been set in motion by deep-seated underlying salt tectonics, isostatic readjustment of consolidated strata at depth, or shifts triggered by episodic shallow earthquake motion in the late Quaternary and continuing to the present (Ross and Uchupi, 1977; Kebeasy, 1990; Bellaiche et al., 1999; El-Sayed et al., 2004). Eustatic sea-level rise could also account for some changes in offshore sedimentation, especially during the period when the > 100 m rise in sea level occurred from the Late Pleistocene (ca. 18 000 years BP) to the Middle Holocene (ca. 7500 years BP). This rapid rate of rise then decreased markedly by about 7500 to 6000 years BP to an elevation of -8 to -6 m below present sea level and then further declined by ca. 4000 years BP, attaining a level of about -3 to -2 m beneath the present level (Fleming et al., 1998; Sivan et al., 2001). The shelf's once subaerially exposed surface was submerged as the shoreline retreated landward toward the south. The delta's coastal margin from ca. 6000 to 4000 years BP (Fig. 2) appears to have reached its northward position on what once had been near the mid-shelf (Stanley and Warne, 1993). It then continued its southward retreat as a function of coastal erosion and concurrent subsidence of the inner shelf to mid-shelf and low-lying northern delta substrate (Stanley and Clemente, 2017; Stanley, 2019).

2.1 Early to Middle Holocene Nile offshore sedimentation

Seafloor deposits of Holocene age seaward of the delta, examined in about 150 gravity and piston sediment cores by specialists in diverse fields, were recovered across extensive offshore areas. These are curated in marine research centers

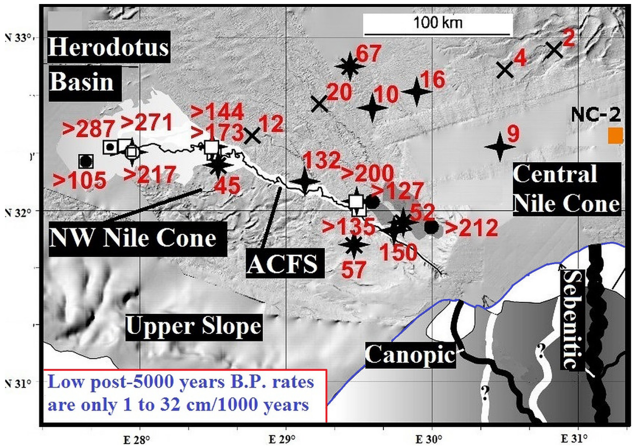

Figure 2. Study area off the NW Nile Delta (in lower right of figure) shows the Herodotus Basin (> 3000 m), NW and central sectors of the Nile Cone, Alexandria canyon–fan system (ACFS), corner of delta in northern Egypt, and positions of 23 cores offshore. Numbers in red: sedimentation rates in centimeters per 1000 years for lower core sections dated from ca. 10 000 to ca. 5000 years BP (data after Ducassou et al., 2009, their Figs. 13 and 14, modified here by the authors of this article). These record high rates of Nile sediment discharge during wetter climate. Different symbols at each core site identify major sediment types. In marked contrast, upper sections of the same cores, dated from ca. 5000 years BP to Late Holocene, record much lower rates of Nile discharge (only 1 to 32 cm per 1000 years; also after Ducassou et al., 2009) during the period of increased aridity.

and museum collections, including those in Egypt (Kholeif and Mudie, 2009), Europe (Ducassou et al., 2009), the United States (Maldonado and Stanley, 1976), and elsewhere. Core samples serve to compare dated Early (from ∼ 11 000 years BP) to dated Late Holocene lithofacies changes between Egypt's Nile continental shelf and deeper sectors. Focus here is on offshore slope deposits that accumulated on the upper surface of a large elongated bulge off Egypt, termed the Nile Cone, which extends seaward of the delta's shelf and upper slope. The study area is primarily on the pronounced cone sector that trends northwest of the delta's shelf edge (> 200 m depth) to the deep (> 3000 m) Herodotus Basin plain (Fig. 2). Seafloor isobaths in this area are shown in Ducassou et al. (2009) and are well defined on larger-scale charts such as the one compiled by the US Defense Mapping Agency Hydrographic Center (1972, N.O. 310) at a scale of 1 : 2 849 300.

The cone in this sector is ∼ 225 km long, increases in width downslope to ∼ 250 km at its base, and covers ca. 50 000 km^2. An elongate submarine canyon, traced on the surface of the NW cone, meanders downslope (Fig. 2); it extends from off-Nile mouths of the modern Rosetta and former Canopic branches to the lower cone. This Alexandria canyon–fan system (ACFS) actively distributed sediment seaward, primarily prior to ca. 5000 years BP during the Middle Holocene. Sedimentation patterns distributed on the Nile shelf, between the delta and its upper fan, have been defined by Summerhayes et al. (1978), Sestini (1992), and also Egyptian agencies including the Coastal Research Institute and the National Institute of Oceanography and Fisheries.

Shelf and upper-slope sediments record influences of the Late Holocene to recent wind- and wave-driven bottom current transport, the latter presently most active along the inner shelf and mid-shelf. These processes shift shallow seafloor sediment mainly eastward and, locally, seaward off the shelf (UNESCO/UNDP and Arab Republic of Egypt, 1978; Frihy and Dewidar, 2003; Kholeif and Mudie, 2009). Materials normally originating on the shelf and recovered in upper-slope and deeper Nile Cone cores indicate seaward displacement at times of intensified coastal margin circulation that swept the seafloor. Sedimentary structures and the composition of strata show that, once off the shelf, some sediments were shifted farther downslope by gravitative processes such as turbidity currents and mass flows. These mechanisms displaced clay and silt and, to a lesser extent, sand of fluvial Nile and eolian origin, along with shelf material of terrigenous, carbonate, and biogenic origin. Core analyses reveal transport of these components in varying proportions via the ACFS and NW cone's surface to more distal sectors primarily during the Early to Middle Holocene (Stanley and Maldonado, 1977; Ducassou et al., 2009; Kholeif and Ibrahim, 2010). It is also likely that some of the finer sediment components and low accumulation rates may indicate displacement from the NW-oriented cone eastward toward the central Nile Cone as well.

Sediments displaced from land to considerable distances offshore during that period were derived primarily from Nile flood discharge, which is strong in summer, across the delta's coastal margin and then seaward. These largely land-derived materials could be further shifted downslope and dispersed as they settled across climatically controlled, well-stratified intermediate and bottom water masses. One of these sediments distributed well offshore is sapropel, a depositional sequence typically comprising a dark gray to black, mostly silt and clay, organic-rich sediment unit of variable thickness (log in Fig. 3).

This dark unit accumulated beneath oxygen-deficient bottom water and reached euxinic seafloor conditions. High amorphic organic carbon content (58 %–72 %) indicates good preservation of autochthonous planktonic organic matter (Kholeif and Ibrahim, 2010). Stagnation in deep water, increases in primary productivity, and other associated oceanographic conditions are discussed by Rohling and Hilgen (1991) and Krom et al. (2002). Gray deposits, below and above the dark unit, were deposited on the seafloor in less well stratified water and only partially reduced oxygenated conditions.

The youngest sapropel sequence, termed S1, is dated to the AHP, from the Early to Middle Holocene (ca. 9500 to 6000 years BP). The climate during its deposition, one of ex-

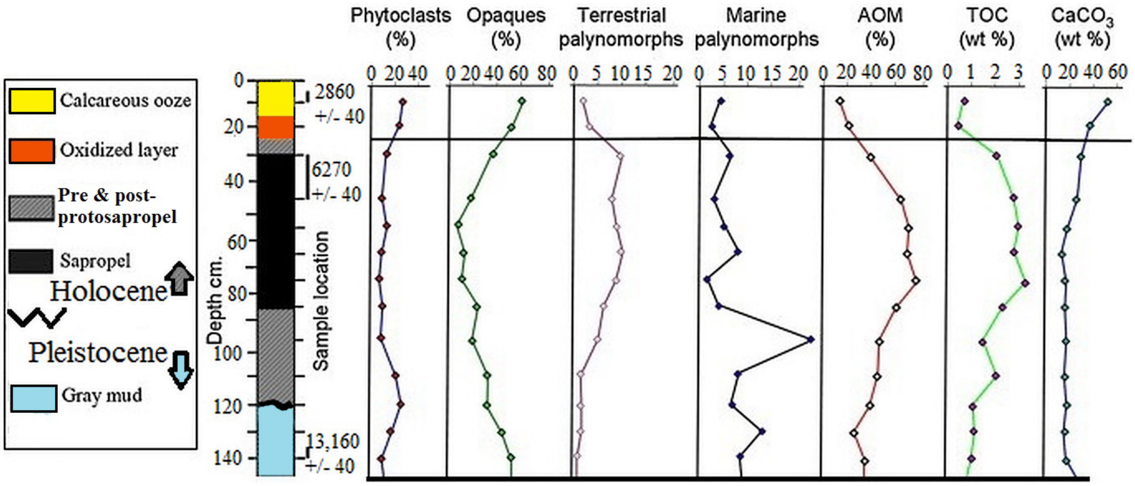

Figure 3. Stratigraphic log of core NC-2 (location shown in Fig. 2) records an Early to Middle Holocene sapropel S1 sequence formed during a period of ca. 3500 years and a much thinner Middle to Late Holocene upper core section of oxidized layer and calcareous ooze. Note proportions of compositional components that change markedly at about 25 cm from core top, at ca. late 4000 years BP (after Kholeif and Ibrahim, 2010). AOM is amorphous organic matter, and TOC is total organic carbon.

tensive to moderate rainfall, was in large part a response to northward displacement of the ITCZ (Fig. 1b; Said, 1993; Krom et al., 2002; Marriner et al., 2013). The S1 sequence is recovered at water depths usually greater than 500 to 600 m on the cone (Maldonado and Stanley, 1976; Ducassou et al., 2009). Complete S1 sequences can range from ~ 50 to > 200 cm in thickness. The gray deposits underlying and covering the dark gray to black unit usually include finely laminated silty clay and clayey silt mixes; their sedimentary structures indicate some were emplaced by bottom currents and others by fine-grained turbidity currents. The age and composition of these deposits indicate they were released beyond the delta's shelf during the AHP when East African source lake levels, Nile floods, and amounts of sediment discharge were at or near the optimum (Fig. 4a, b) and maximum aridity did not yet prevail (Gasse, 2000; Kholeif and Mudie, 2009; Revel et al., 2015; Pennington et al., 2017). Compositional analyses of both deltaic and offshore core facies indicate that the upper Blue Nile volcanic province in Ethiopia (Fig. 4c) was the major source of sediment released to and beyond the delta during that period.

2.2 Reduced depositional rates after 5000 years BP

Uppermost sedimentary sequences recovered in cores seaward of the delta and discussed here have received much less attention than the underlying sapropel sequences discussed in the previous section. Their lithofacies and compositional attributes differ significantly from the older S1 sequence. Notably, most sections are much thinner, generally only ~ 20 to 30 cm or less (Stanley and Maldonado, 1977). From the base upward, these present partially laminated silty clay and clayey silt layers that, in some cores, change upward and display a mottled tan, brown, or orange coloration, which is indicative of increasingly oxygenated water conditions above the S1 sequence (Fig. 3). These younger sections commonly evolve upward to a bioturbated silt and clay ooze, rich in calcareous carbonate content (up to 50 %), and grain size that can become coarser toward the core top. Although recovered at considerable water depth, some upper deposits include shallow seafloor components derived from the shelf; these became incorporated with deeper-water materials during downslope transport. Such strata may present sedimentary structures indicative of displacement by bottom currents or by relatively low density sand and silt to fine-grained turbidite flows. Uppermost sediments were released above older S1 sequences not only within the ACFS but also on adjacent cone surfaces (Fig. 2). Their lithologic attributes, much different from those of underlying S1 sequences, resulted from southern displacement of the ITCZ (Fig. 1b) and also from some effects of ENSO cycles during and after the Middle Holocene (Marriner et al., 2013; Pennington et al., 2017).

Average sediment accumulation rates in 23 cores recovered along the SE to NW trending Nile Cone were calculated for two age groups in each core based on sediment thickness and radiocarbon dates using planktonic foraminifera (Ducassou et al., 2009; Kholeif and Mudie, 2009; Kholeif and Ibrahim, 2010; Blanchet et al., 2013). An older group comprises lower core sections dated from ca. 10 000 to ca. 5000 years BP and usually includes the S1 sequence. Depositional rates for this Early to Middle Holocene period range from > 287 to 2 cm per 1000 years (Fig. 2). The average overall rate for all Early to Middle Holocene values in the 23 cores is ~ 106 cm per 1000 years. When examining the same offshore cores but using samples from the upper units dated from ca. 5000 years BP to the Late Holocene, measure-

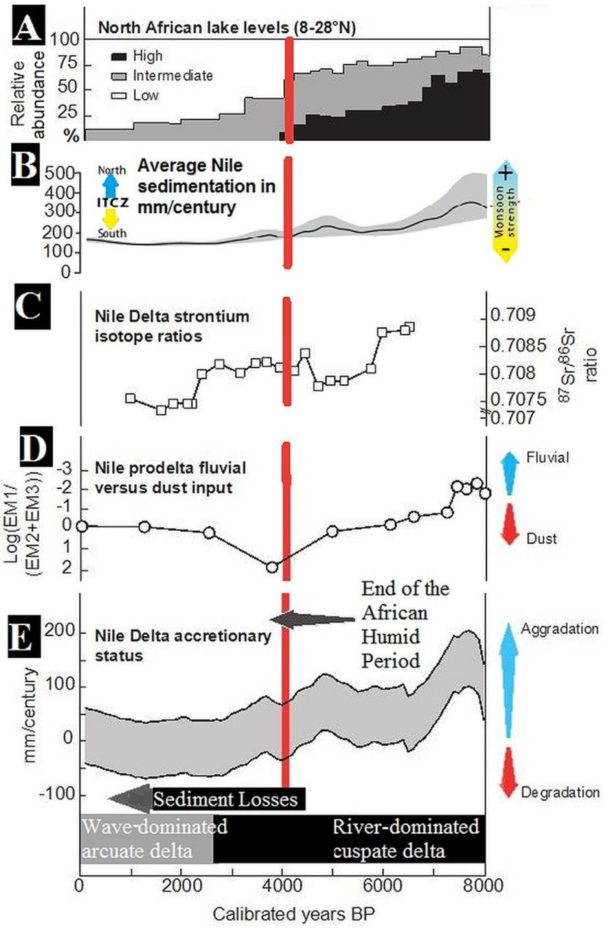

Figure 4. Sedimentation and compositional data respond to climatic change affecting **(a)** highland Nile source area, and **(b–e)** Nile Delta and offshore settings from ca. 8000 years BP to present (modified after Marriner et al., 2012, 2013). Changes in the Nilotic hydrological system and associated depositional responses during the Holocene include those before, at, and after ca. late 4000 years BP (vertical red time marker). These were induced largely by displacement of the monsoon system and associated climatic controls, including migrating ITCZ and ENSO events.

ments of their depositional rates are very much decreased (Fig. 2) and range from only 32 to 1 cm per 1000 years (data in Ducassou et al., 2009). The overall averaged value for all 23 upper core sections provides a much reduced average depositional rate of only ∼ 8.4 cm per 1000 years, or under ∼ 10 % of the average accumulation rate of underlying Early to Middle Holocene S1 sequences. This records that the former turbidite-rich downslope depositional system had decreased substantially largely as a function of the Nile's much-altered hydrology and reduced sediment dispersal seaward of the delta, responses largely due to markedly changing climatic conditions that were seriously affecting this region in the Late Holocene. It is also possible that a center of sedimentation was shifting toward the east.

2.3 Effects of increased aridity and lower Nile flows

Of note are a number of altered compositional and textural attributes recorded offshore in upper core sections (Fig. 3) that correlate with some of similar age identified in the Nile Delta (Fig. 4 and Stanley, 2019). Together these serve as proxies to help interpret regional environmental changes occurring after 5000 years BP and especially in late 4000 years BP. The much thinner accumulation of Late Holocene and younger oxidized mud and carbonate ooze (log in Fig. 3) was deposited under conditions of relatively low Nile input responding to the considerably modified climate (Kholeif and Mudie, 2009). Conditions had become increasingly arid, and sediment discharge by the Nile was much reduced during formation of the upper marl section (Calvert and Fontugne, 2001). The major increase in hyper-aridity occurred ca. 4200–4000 years BP, contemporaneously with the time when the whole of the Egyptian Sahara had become a desert as cited earlier (Pennington et al., 2019).

In contrast with underlying sapropel sequences, the uppermost sediment sections comprise markedly decreased amorphous organic matter (AOM), total organic carbon (TOC), terrestrial pollen, and spores (Fig. 3). Uppermost core units, on the other hand, are defined by their high $CaCO_3$ content (up to 50 %) closely associated with increasingly warm climate and decreasing moisture (Kholeif and Mudie, 2009). Moreover, increased quartz grain roundness and size and especially a peak in the Ca/Ti ratio at that time indicate an eolian influx linked to hyper-aridity (Zhao et al., 2017; Pennington et al., 2019). Upper core sections also record increased proportions of Mg calcite and illite (Calvert and Fontugne, 2001) and higher amounts of opaque fractions (Kholeif and Ibrahim, 2010). Such arid periods are typically characterized by a larger input of coarser particles due to reworking of older deposits (Ducassou et al., 2009) and also of kaolinite derived largely from desert source areas in North Africa (Calvert and Fontugne, 2001).

Also noted were periodic decreases in Ethiopian-derived Blue Nile clastic sediment dispersed between 6000 and 3100 years BP (Krom et al., 2002; Revel et al., 2015). This is recorded by a marked minimum in strontium isotopic ratios (Fig. 4c), an indication of decreased Blue Nile sedimentation offshore (Krom et al., 2002). Relative increases in White Nile runoff were measured at times when Blue Nile fluvial input decreased relative to that of higher eolian transport (Fig. 4d). Minimal Nile discharge occurred in the upper layer offshore during its deposition under oxic bottom water conditions and good ventilation within the water column (Fig. 4e; cf. Kholeif and Mudie, 2009; Kholeif and Ibrahim, 2010). A decrease in fluvial discharge from about 6500 to 2800 $m^3 s^{-1}$ and also in both flood frequency and intensity are estimated during the past 5000 years (Ducassou et al., 2009). These resulted in decreased sedimentation rates to less than 1 $mm\,yr^{-1}$ during some low-flood periods (Blanchet et al., 2013). Rather than primary responses to tectonic motion, eustatic sea-level rise, or human intervention, most lithofacies and compactional changes recorded by upper marine core sections were induced by the broad, powerful influences of regional climate shift.

3 Archaeological implications

Of prime consideration is whether the evolving natural events discussed in the previous sections would have had sufficient input to trigger societal changes in Egypt in late 4000 years BP, during the latter part of the Old Kingdom (ca. 2278–2181 BCE) and the First Intermediate Period (ca. 2181–2055 BCE) (dates after Shaw, 2000). Archaeologists tend to focus on the primary roles of evolving social, political, and/or economic factors during that timeframe and, to a lesser extent, on the potential effects of climate change. Their studies of this period tend to evaluate the role of environmental impacts on Egypt in one of three different ways: (1) little or no environmental changes occurred, were not influential, or had little societal effect at about this time (Moreno Garcia, 2015); (2) some environmental changes may have occurred but were not primarily responsible for triggering or activating major societal changes recorded during that period (Seidlmayer, 2000; Moeller, 2005); or (3) environmental conditions seriously impacted Egypt and were largely responsible for some extensive, and possibly traumatic, scenarios leading to social, political, and economic upheaval (the so-called "Dark Age" scenarios) then affecting the country such as those summarized by Vandier (1936), Bell (1971), and Hassan (2007).

For a recent example of archaeological support for the concepts of group (1) above, one can read the following: "Contrary to traditional interpretations of the end of the Old Kingdom, recent archaeological research shows no trace of climatic or subsistence crisis" (Moreno Garcia, 2015, p. 79). In contrast, it is noted that some historical documents previously cited by Egyptologists of group (3) to support arguments favoring major climate change and its dire effects on society at the end of the Old Kingdom are now recognized as having been documented long after the actual period that they describe. Moreover, others referring to documents used by group (3) to describe a major breakdown of the social order at that time have also indicated that considerable discretion should be used. For example, some suggest that Egyptian writings during those early years had a tendency to exaggerate the extent of damage and disorder and thus should be cautiously interpreted before using these as firm and accurate evidence of such past events (Freeman, 1996).

Archaeologists generally agree, however, that a centralized government long and firmly controlled by a sequential reign of pharaohs had all but ceased by the end of the Old Kingdom, and Egypt proceeded for a century, or perhaps somewhat longer, without such an authoritative leader as head of state. This occurred shortly after the lengthy reign of Pepy II, estimated at some time between $\sim$ 2284 BCE and $\sim$ 2184 BCE. Following closely, the pharaoh was replaced by a series of concurrent nomarchs, or governors, charged with organizing and directing many of the primary activities in Egypt's many nomes, or geographic districts. In addition to these major political alterations during the First Intermediate Period, it is proposed here that the country's stability would have been weakened by the powerful environmental factors triggered by major climate change at about the same time as recorded in this study. The quality of construction at this time, in some cases, may have decreased markedly (Fig. 5). In particular, a period of marked increased aridity and decline in moisture and rainfall leading to intermittent low Nile floods lasting a century or longer likely led to episodic conditions of diminished cultivation and reduced harvests. Additionally, such periods of decreased food supplies and their less-than-well-organized storage and equitable distribution to the population had the potential to last for several years at a time, some triggering serious societal consequences (Weiss and Bradley, 2001). These conditions, in turn, would probably have also given rise to some documented migration from the delta to areas in middle and upper Egypt, some of which were then perhaps less acutely impacted by the altered environmental factors in lower Egypt.

To help resolve whether the timing of environmental impacts on Egypt can be correlated with historic events at the end of the Old Kingdom and during the First Intermediate Period, it would be useful to encourage collections and detailed mineralogical and geochemical study of sediment drill cores recovered within, and also adjacent to, established archaeological sites of that time period. Collecting closely spaced core samples and dating where possible with plant fossils in delta and marine microfossils offshore using carbon-14 dating, along with other refined dating methodologies, coupled with detailed compositional analyses at the same stratigraphic levels are now necessary tasks of primary geoarchaeological importance. For example, it should be recognized that proportions of some sediment components in both offshore and deltaic samples would likely have been altered during transport, sometimes for long distances and over a considerable period of time, prior to their final deposition at a core's recovery site on land or at sea. At least some particles and isotopic components that comprise a sample would likely not have been displaced during one single short-period transport event from source to final depositional site but rather by what is termed a longer "stop-and-go" sedimentation process (Stanley, 2019). This displacement would have involved several downslope reworking phases by repeated deposition and storage–erosion and displacement–redeposition episodes over time. As a consequence, a date obtained by calibrated C-14 or other means may well record an age for sample particles that is likely to be older than the actual younger date of a sample's final deposition. Thus, some dates obtained in both Nile Delta and offshore cores can record a time that can be on the order of 50 to 100 or more years older than what is likely to be their actual younger dates of final deposition (see

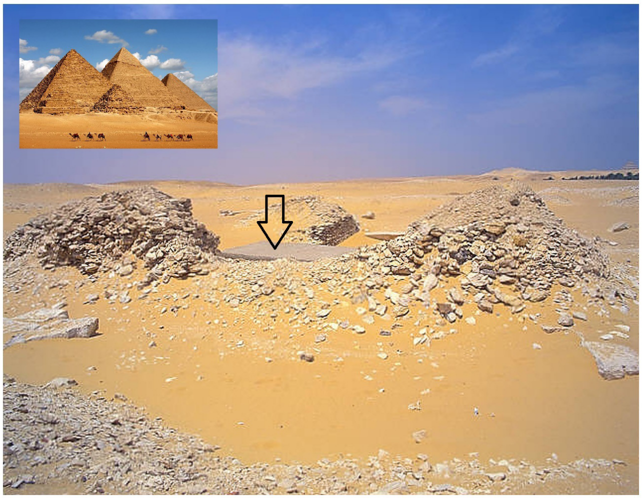

Figure 5. Pyramid of Ibi (Qakare) at South Saqqara, Egypt, built after the end of the Old Kingdom during the Eighth Dynasty of the First Intermediate Period. Ibi is little known and is believed to have ruled for about 2 years, from ca. 4109 to 4107 years BP. The structure includes a descending passage (see arrow) that leads to the burial chamber, and of its original height of ca. 21 m, only ~ 3 m now rests above the desert floor. Built largely of flat brick-size stones, it has been subject to destruction by weathering, structural failure, and theft of its rock material. In contrast, the upper inset shows the older, much larger, and better-constructed Old Kingdom Fourth Dynasty pyramids at Giza. From right to left are those of Khufu (ca. 4550 years BP), Khafre (ca. 4520 years BP), and Menkaure (ca. 4490 years BP). Khufu's pyramid, the highest (146 m), is formed of ~ 2 million large blocks of rock weighing 2.5 to 15 t. (Images publicly available as stock photographs.)

Dee, 2017). Caution is warranted particularly when interpreting sediment accumulation dates, especially in cases where a frequent reversal of sample ages (older dated samples above younger ones) occur as one proceeds upward from the base of a core study section.

4 Conclusions

The stratigraphic and sedimentological changes recorded both seaward of and in the Nile Delta proper during the Middle to Late Holocene examined herein resulted primarily from altered and reduced Nile flow conditions rather than from other natural factors and human intervention. It is proposed that marked climatic change led to intensified aridification, a decline in rainfall, diminished Nile flood levels, and a consequent periodic decline in agricultural production in late 4000 years BP. Such events would have negatively impacted Egypt's population toward the end of the Old Kingdom and in the early to middle First Intermediate Period. Of note in this respect is Herodotus (1987), who in his *The History* written in about 440 BCE, raised a pertinent question (Book II, Sect. 14): "If no rain falls in their land at all, and if the river cannot rise high enough to flood their fields . . . then . . . what will be left for Egyptians that live there, but starvation?" This commentary could pertain to an actual event that occurred prior to or during Herodotus' travel in Egypt or is perhaps meant as a predictor of future major climate changes such as increased droughts (Tabari and Willems, 2018; Nashwan et al., 2020) and of a substantial human-induced decreased-Nile-flow misfortune, such as by closure of the now near-completed Grand Ethiopian Renaissance Dam (GERD) placed across the Blue Nile in Ethiopia, the largest such structure in Africa (Stanley and Clemente, 2017). At the very least, these latter two factors alone warrant prompt and serious consideration that should lead to vital protection measures for Egypt. With its present population about 100 times greater than at the end of the Old Kingdom, the country cannot now readily withstand a 20 % to 30 % or more reduction in its present Blue Nile freshwater supply. Studies of this region's past history, such as those that integrate environmental and archaeological conditions in the late 4000 years BP, may provide some useful points serving as a basis to help interpret the present and also to better prepare for possible negative conditions in the years ahead.

Data availability. Information provided throughout the text is available in prior published studies by the first author (Jean-Daniel Stanley) and other authors cited throughout the text and listed in the references. These studies are readily available, and their data sets are publicly accessible therein. Data were gathered from prior original studies and are not stored in a separate database or website elsewhere.

Author contributions. This manuscript was prepared by JDS and SEW; conceptualization and project administration were completed by JDS, and visualization was completed by both SEW and JDS.

Competing interests. The authors declare that they have no conflict of interest.

Special issue statement. This article is part of the special issue "Geoarchaeology of the Nile Delta". It is a result of the workshop "Geoarchaeology of the Nile Delta: Current Research and Future Prospects", Würzburg, Germany, 29–30 November 2019.

Acknowledgements. The Smithsonian Institution's National Museum of Natural History, Washington, DC, is acknowledged for funding years of fieldwork seaward of and in Egypt's Nile Delta and for laboratory analyses that led to this study. Appreciation is expressed to Emmanuelle Ducassou, Université de Bordeaux, France; Suzan Kholeif, National Institute of Oceanography and Fisheries, Alexandria, Egypt; and Nick Marriner, Université de Franche-Comté, Besançon, France, for permission to use several of their published figures presented herein. Also thanked are Christopher E. Bernhardt, US Geological Survey; Paige Eager, Hood College; Adrienne N. Ellis, Adamstown, Maryland; and the two anonymous scholars for their useful reviews. The editors of this volume very kindly invited our contribution and assisted us in taking final steps for its publication.

Financial support. The article processing charge was funded by the Quaternary scientific community, as represented by the host institution of EGQSJ, the German Quaternary Association (DEUQUA).

Review statement. This paper was edited by Julia Meister and reviewed by two anonymous referees.

References

Bar-Matthews, M. and Ayelon, A.: Mid-Holocene climate variations revealed by high-resolution speleothem records from Soreq Cave, Israel and their correlation with cultural changes, The Holocene, 21, 163–171, https://doi.org/10.1177/0959683610384165, 2011.

Bard, K. A.: An Introduction to the Archaeology of Ancient Egypt, Blackwell Publishing, Maulden, Massachusetts, 400 pp., ISBN-13: 978-1405111485, 2008.

Bell, B.: The dark ages in ancient history, Am. J. Archaeol., 75, 1–26, https://doi.org/10.2307/503678, 1971.

Bellaiche, G., Zitter, T., Droz, L., Gaullier, V., Mart, Y., and Mascle, J.: Le cône sous-marin profound du Nil: principaux résultats de la campagne Prismed II du N.O. L'Atlante, Océanographie, 329, 727–733, https://doi.org/10.1016/S1251/8050(00)88492-X, 1999.

Bernhardt, C. E., Norton, S. P., and Stanley, J.-D.: Nile delta vegetation response to Holocene climate variability, Geology, 40, 615–618, https://doi.org/10.1130/G33012.1, 2012.

Blanchet, C. L., Tjallingii, R., Frank, M., Lorenzen, J., Reitz, A., Brown, K., Feseker, T., and Brückman, W.: High- and low-latitude forcing of the Nile River regime during the Holocene inferred from laminated sediments of the Nile deep-sea fan, Earth Planet. Sc. Lett., 364, 98–110, https://doi.org/10.1016/j.epsl.2013.01.009, 2013.

Blanchet, C. L., Contoux, C., and Leduc, G.: Runoff and precipitation dynamics in the Blue and White Nile catchments during the mid-Holocene: A data-model comparison, Quaternary Sci. Rev., 130, 222–230, https://doi.org/10.1016/j.quascirev.2015.07.014, 2015.

Butzer, K. W.: Early Hydraulic Civilization in Egypt, University of Chicago Press, Chicago, Illinois, 134 pp., ISBN: 0-226-08634-8, 1976.

Butzer, K. W.: Long-term Nile flood variation and political discontinuities in Pharaonic Egypt, in: From Hunters to Farmers: The Causes and Consequences of Food Production in Africa, edited by: Clark, J. D. and Brandt, S. A., University of California Press, Berkeley, California, 102–112, ISBN: 0520045742, 1984.

Calvert, S. E. and Fontugne, M. R.: On the late Pleistocene-Holocene sapropel record of climatic and oceanographic variability in the eastern Mediterranean, Paleoceanography, 16, 78–94, https://doi.org/10.1029/1999PA000488, 2001.

Dee, M. W.: Absolute dating climatic evidence and the decline of Old Kingdom Egypt, in: The Late Third Millenium in the Ancient Near East. Chronology, C-14, and Climate Change, edited by: Hoflmayer, F., University of Chicago, Oriental Institute Seminars no. 11, Chicago, Illinois, 323–331, 2017.

Ducassou, E., Migeon, S., Mulder, T., Murat, A., Capotondi, L., Bernasconi, S., and Mascle, J.: Evolution of the Nile deep-sea turbidite system during the Late Quaternary: influence of climate change on fan sedimentation, Sedimentology, 56, 2061–2090, https://doi.org/10.1111/j.1365-3091.2009.01070.x, 2009.

El-Sayed, A., Kerrat, I., and Hussein, H. M.: Seismicity and seismic hazard in Alexandria and its surroundings, Pure Appl. Geophys., 161, 1003–1019, https://doi.org/10.1007/s00024-003-2488-8, 2004.

Fleming, K., Johnston, P., Zwartz, D., Yokoyama, Y., Lambeck, K., and Chappell, J.: Refining the eustatic sea-level curve since the last Glacial Maximum using far- and intermediate-field sites, Earth Planet. Sc. Lett., 163, 327–342, https://doi.org/10.1016/S0012-821X(98)00198-8, 1998.

Freeman, C.: Egypt, Greece and Rome: Civilizations of the Ancient Mediterranean, Oxford University Press, Oxford, England, 784 pp., ISBN: 9780199651924, 1996.

Frihy, O. E. and Dewidar, K. M.: Patterns of erosion/sedimentation, heavy mineral concentration and grain size to interpret boundaries of littoral sub-cells of the Nile Delta, Egypt, Mar. Geol., 199, 27–43, https://doi.org/10.1016/S0025-3227(03)00145-2, 2003.

Gasse, F.: Hydrological changes in the African tropics since the last glacial maximum, Quaternary Sci. Rev., 19, 189–211, https://doi.org/10.1016/S0277-3791(99)00061-X, 2000.

Hassan, F. A.: Droughts, famine, and the collapse of the Old Kingdom: Re-reading Ipuwer, in: The Archaeology and Art of Ancient Egypt, edited by: Hawass, Z. A. and Richards, J., Publications du Conseil Suprême des Antiquités de l'Egypte, Cairo, Egypt, 1, 357–379, ISBN: I0977-437-241-7, 2007.

Herodotus: The History, translated by: Grene, D., The University of Chicago Press, Chicago, Illinois, 710 pp., ISBN: 9780226327723, 1987.

Kaniewski, D., Marriner, N., Cheddadi, R., Guiot, J., and Van Campo, E.: The 4.2 ka BP event in the Levant, Clim. Past, 14, 1529–1542, https://doi.org/10.5194/cp-14-1529-2018, 2018.

Kebeasy, R.M.: Seismicity, in: The Geology of Egypt, edited by: Said, R., A.A. Rotterdam, the Netherlands, Balkama, 51–59, ISBN: 978-9061918561, 1990.

Kholeif, S. and Ibrahim, M. I.: Palynofacies analysis of inner continental shelf and middle slope sediments offshore Egypt, southeastern Mediterranean, Geobios, 43, 333–347, https://doi.org/10.1016/j.geobios.2009.10.006, 2010.

Kholeif, S. and Mudie, P.: Palynological records of climate and oceanic conditions in the late Pleistocene and Holocene of the Nile Cone, southeastern Mediterranean, Egypt, Palynology, 33, 1–24, https://doi.org/10.2113/gspalynol.33.1.1, 2009.

Krom, M. D., Stanley, J.-D., Cliff, R. A., and Woodward J. C.: Nile River sediment fluctuations over the past 7000 years and their key role in sapropel development, Geology, 30, 71–74, https://doi.org/10.1130/0091-7613(2002)030<0071:NRSFOT>2.0.CO;2, 2002.

Maldonado, A. and Stanley, J.-D.: The Nile Cone: submarine fan development by cyclic sedimentation, Mar. Geol., 20, 27–40, https://doi.org/10.1016/0025-3227(76)90073-6, 1976.

Marriner, N., Flaux, C., Kaniewski, D., Morhange, C., Leduc, G., Moron, V., Chen, Z., Gasse, F., Empereur, J.-Y., and Stanley, J.-D.: ITCZ and ENSO-like pacing of Nile delta hydrogeomorphology during the Holocene, Quaterernary Sci. Rev., 45, 73–84, https://doi.org/10.1016/j.quascirev.2012.04.022, 2012.

Marriner, N., Flaux, C., Morhange, C., and Stanley, J.-D.: Tracking Nile Delta vulnerability to Holocene change, PLoS One, 8, 1–9, https://doi.org/10.1371/journal.pone.0069195, 2013.

Moeller, N.: The First Intermediate Period: A time of famine and climate change?, Egypt and the Levant, 15, 153–167, 2005.

Moreno Garcia, J.: Climatic change or sociopolitical transformation? Reassessing late 3rd millennium BC in Egypt, in: 2200 BC – A Climatic Breakdown as a Cause for the Collapse of the Old World, edited by: Meller, H., Arz, H. W., Jung, R., and Risch, R., Landesamt für Denkmalpflege und Archäologie Sachsen-Anhalt – Landesmuseums für Vorgeschichte, Halle, 79–94, 2015.

Nashwan, N. S., Shahid, S., and Chung, E.-S.: High-resolution climate projections for a densely populated Mediterranean region, Sustainability, 12, 23 pp., https://doi.org/10.3390/su12093684, 2020.

Pennington, B. T., Sturt, F., Wilson, P., Rowland, J., and Brown, A.: The fluvial evolution of the Holocene Nile Delta, Quaternary Sci. Rev., 170, 212–231, https://doi.org/10.1016/j.quascirev.2017.06.017, 2017.

Pennington, B. T., Hamdan, M. A., Pears, B. R., and Sameh, H. I.: Aridification of the Egyptian Sahara 5000–4000 cal BP revealed from x-ray fluorescence analysis of Nile Delta sediments at Kom al-Ahmer/Kom Wasit, Quatern. Int., 514, 108–118, https://doi.org/10.1016/j.quaint.2019.01.015, 2019.

Revel, M., Ducassou, E., Skonieczny, C., Colin, C., Bastian, L., Bosch, D., Migeon, S., and Mascle, J.: 20,000 years of Nile River dynamics and environmental changes in the Nile catchment area as inferred from Nile upper continental slope sediments, Quaternary Sci. Rev., 130, 200–221, https://doi.org/10.1016/j.quascirev.2015.10.030, 2015.

Rohling, E. J. and Hilgen, F. J.: The eastern Mediterranean climate at times of sapropel formation: a review, Geol. Mijnbouw, 70, 253–264, ISBN: 0016-7746, 1991.

Ross, D. A. and Uchupi, E.: Structure and sedimentary history of southeastern Mediterranean sea – Nile Cone area, AAPG Bull., 61, 872–902, https://doi.org/10.1306/C1EA4397-16C9-11D7-8645000102C1865D, 1977.

Said, R.: The River Nile: Geology, Hydrology, and Utilization, Pergamon Press, Tarrytown, New York, 320 pp., ISBN: 0-08-041886-4, 1993.

Seidlmayer, S.: The First Intermediate Period, in: The Oxford History of Ancient Egypt, edited by: Shaw, I., Oxford University Press, Oxford, England, 118–147, ISBN: 978-0-19-280458-7, 2000.

Sestini, G.: Implications of climatic changes for the Nile Delta, in: Climatic Change and the Mediterranean, edited by: Jeftic, L., Milliman, J. D., and Sestini, G., Edward Arnold, London, England, 535–601, ISBN: 0-340-55329-4, 1992.

Shaw, I. (Ed.): The Oxford History of Ancient Egypt, Oxford University Press, Oxford, England, 552 pp., ISBN: 978-0-19-280458-7, 2000.

Sivan, D., Wdowinski, S., Lambeck, K., Galili, E., and Raban, A.: Holocene sea-level changes along the Mediterranean coast of Israel, based on archaeological observations and numerical model, Palaeogeogr Palaeocl., 167, 101–117, https://doi.org/10.1016/S0031-0182(00)00234-0, 2001.

Stanley, J.-D.: Egypt's Nile Delta in late 4000 Years BP: Altered flood levels and sedimentation, with archaeological implications, J. Coastal. Res., 35, 1036–1050, https://doi.org/10.2112/JCOASTRES-D-19-00027.1, 2019.

Stanley, J.-D. and Clemente, P. L.: Increased land subsidence and sea-level rise are submerging Egypt's Nile Delta coastal margin, GSA Today, 27, 4–11, https://doi.org/10.1130/GSATG312A.1, 2017.

Stanley, J.-D. and Maldonado, A.: Nile Cone: Late Quaternary stratigraphy and sediment dispersal, Nature, 266, 129–135, https://doi.org/10.1038/266129a0, 1977.

Stanley, J.-D. and Warne, A. G.: Nile Delta: recent geological evolution and human impact, Science, 260, 628–634, https://doi.org/10.1126/science.260.5108.628, 1993.

Stanley, J.-D., Krom, M. D., Cliff, R. A., and Woodward, J. C.: Nile flow failure at the end of the Old Kingdom, Egypt: Strontium isotopic and petrologic evidence, Geoarchaeology, 18, 395–402, https://doi.org/10.1002/gea.10065, 2003.

Summerhayes, C., Sestini, G., Misdorp, R., and Marks, N.: Nile Delta: nature and evolution of continental shelf sediment systems, Mar. Geol., 27, 43–65, https://doi.org/10.1016/0025-3227(78)90073-7, 1978.

Tabari, H. and Willems, P.: More prolonged droughts by the end of the century in the Middle East, Environ. Res. Lett., 13, 104005, https://doi.org/10.1088/1748-9326/aae09c, 2018.

UNESCO/UNDP and Arab Republic of Egypt: Coastal Protection Studies, Project Findings and Recommendations, UNDP/EGY/73/063, Final Report, UNESCO, Paris, FNR/SC/OSP/78/230, 483 pp., 1978.

U.S. Defense Mapping Agency Hydrographic Center: Mediterranean Sea, Washington, D.C., Chart N.O. 310, 1972.

Vandier, J.: La Famine dans l'Egypte Ancienne, Recherches d'Archéologie, de Philologie et d'Histoire, Institut Français d'Archéologie Orientale, Cairo, Egypt, tome 7, 176 pp., 1936.

Weiss, H. and Bradley, R. S.: What drives societal collapse?, Science, 291, 609–610, https://doi.org/10.1126/science.1058775, 2001.

Weiss, H., Courty, M. A., Wetterstrom, W., Guichard, F., Senior, L., Meadow, R., and Curnow, A.: The genesis and collapse of 3rd millennium north Mesopotamian civilization, Science, 261, 995–1004, https://doi.org/10.1126/science.261.5124.995, 1993.

Woodward, J., Macklin, M., Fielding, L., Millar, I., Spencer, N., Welsby, D., and Williams, M.: Shifting sediment sources in the world's longest river: A strontium isotope record for the Holocene Nile, Quaternary Sci. Rev., 130, 124–140, https://doi.org/10.1016/j.quascirev.2015.10.040, 2015.

Zhao, X., Liu, Y., Salem, A., Marks, L., Welc, F., Sun, Q., Jiang, J., Chen, J., and Chen, Z.: Migration of the intertropical convergence zone in North Africa during the Holocene: evidence from variations in quartz grain roundness in the lower Nile Valley, Egypt, Quatern. Int., 449, 22–28, https://doi.org/10.1016/j.quaint.2017.06.036, 2017.

E&G Quaternary Sci. J., 69, 225–245, 2020
https://doi.org/10.5194/egqsj-69-225-2020

Open Access E&G Quaternary Science Journal

Research article

Mapping buried paleogeographical features of the Nile Delta (Egypt) using the Landsat archive

Tobias Ullmann[1], Leon Nill[2], Robert Schiestl[3], Julian Trappe[1], Eva Lange-Athinodorou[4], Roland Baumhauer[1], and Julia Meister[1]

[1]Institute of Geography and Geology, Physical Geography, University of Würzburg, 97074 Würzburg, Germany
[2]Geography Department, Humboldt-Universität zu Berlin, 12489 Berlin, Germany
[3]Faculty of History and the Arts, Department of Ancient History, LMU Munich, Geschwister-Scholl-Platz 1, 80539 München, Germany
[4]Institute of Egyptology, University of Würzburg, 97070 Würzburg, Germany

Correspondence: Tobias Ullmann (tobias.ullmann@uni-wuerzburg.de)

Relevant dates: Received: 29 June 2020 – Accepted: 12 October 2020 – Published: 9 December 2020

How to cite: Ullmann, T., Nill, L., Schiestl, R., Trappe, J., Lange-Athinodorou, E., Baumhauer, R., and Meister, J.: Mapping buried paleogeographical features of the Nile Delta (Egypt) using the Landsat archive, E&G Quaternary Sci. J., 69, 225–245, https://doi.org/10.5194/egqsj-69-225-2020, 2020.

Abstract: The contribution highlights the use of Landsat spectral-temporal metrics (STMs) for the detection of surface anomalies that are potentially related to buried near-surface paleogeomorphological deposits in the Nile Delta (Egypt), in particular for a buried river branch close to Buto. The processing was completed in the Google Earth Engine (GEE) for the entire Nile Delta and for selected seasons of the year (summer/winter) using Landsat data from 1985 to 2019. We derived the STMs of the tasseled cap transformation (TC), the Normalized Difference Wetness Index (NDWI), and the Normalized Difference Vegetation Index (NDVI). These features were compared to historical topographic maps of the Survey of Egypt, CORONA imagery, the digital elevation model of the TanDEM-X mission, and modern high-resolution satellite imagery. The results suggest that the extent of channels is best revealed when differencing the median NDWI between summer (July/August) and winter (January/February) seasons (ΔNDWI). The observed difference is likely due to lower soil/plant moisture during summer, which is potentially caused by coarser-grained deposits and the morphology of the former levee. Similar anomalies were found in the immediate surroundings of several Pleistocene sand hills ("geziras") and settlement mounds ("tells") of the eastern delta, which allowed some mapping of the potential near-surface continuation. Such anomalies were not observed for the surroundings of tells of the western Nile Delta. Additional linear and meandering ΔNDWI anomalies were found in the eastern Nile Delta in the immediate surroundings of the ancient site of Bubastis (Tell Basta), as well as several kilometers north of Zagazig. These anomalies might indicate former courses of Nile river branches. However, the ΔNDWI does not provide an unambiguous delineation.

Kurzfassung: Die Rekonstruktion der Paläotopographie und -hydrographie des Nildeltas spielt für landschaftsarchäologische Fragestellungen eine zentrale Rolle, da die antike Siedlungsaktivität stark von der Dynamik des antiken Flussnetzes beeinflusst war. Für viele Bereiche des Deltas ist die Lage antiker Flussarme jedoch unbekannt, da diese im Laufe der Zeit verlandet und heute nicht mehr eindeutig im Landschaftsbild erkennbar sind. In diesem Kontext erlauben moderne Fernerkundungsdaten eine flächendeckende Untersuchung und ermöglichen Anomalien der Landbedeckung und Diskontinuitäten der Oberflächenmorphologie zu identifizieren, wodurch wertvolle Hinweise zur paläogeomorphologischen Situation gewonnen werden können. Zur Detektion solcher Anomalien wird in diesem Beitrag das Landsat Archiv genutzt, wobei verschiedene spektrale und zeitlich-räumliche Metriken für das gesamte Nildelta (Ägypten) für den Zeitraum 1985 bis 2019 in der Google Earth Engine berechnet wurden. Die Merkmale der Merkmale der Tasseled Cap Transformation (TC), des Normalized Difference Wetness Index (NDWI) und des Normalized Difference Vegetation Index (NDVI) wurden analysiert und mit historischen topographischen Karten des Survey of Egypt, CORONA-Bildern, dem digitalen Höhenmodell der TanDEM-X-Mission und modernen Satellitenbildern verglichen. Die Ergebnisse der Zeitserienanalyse zeigen die Lage eines verlandeten Flussarms in der Nähe von Buto, der durch den Vergleich der Medianwerte des NDWI zwischen Sommer- (Juli/August) und Wintersaison (Januar/Februar) (ΔNDWI) deutlich zu erkennen ist. Der beobachtete Unterschied ist wahrscheinlich auf eine geringere Boden- und/oder Pflanzenfeuchtigkeit während des Sommers zurückzuführen, welche möglicherweise durch grobkörnige Ablagerungen im Untergrund bedingt wird. Ähnliche Anomalien wurden in der unmittelbaren Umgebung mehrerer pleistozäner Sandhügel (Geziras) und Siedlungshügel (Tells) des östlichen Nildeltas gefunden, was die Kartierungen der potentiellen oberflächennahen Fortsetzung ermöglichte. Weitere lineare und mäandrierende ΔNDWI Anomalien wurden im östlichen Nildelta in der unmittelbaren Umgebung der antiken Stätte von Bubastis (Tell Basta) sowie einige Kilometer nördlich der Stadt Zagazig gefunden. Diese Anomalien weisen vermutlich auf frühere Verläufe von Flussarmen des Nils in diesem Bereich des Deltas hin.

1 Introduction

The reconstruction of the paleo-topography and paleo-hydrography of the Nile Delta plays a central role in landscape-focused archeological investigations. Historical settlement activity was strongly linked to and influenced by the presence and dynamics of the ancient river network of the delta. The great importance of the river network for early settlements is underlined by the fact that larger cities were only found in the immediate vicinity of larger Nile branches, which were of outstanding importance for traffic and trade and met the basic need of water for agriculture and food security (Bietak, 1975). The earliest textual sources that allow, to a certain degree, the reconstruction of the branches of the Nile mainly date from the 5th century BCE to the 4th century CE and come from various Greek and Roman authors (including Herodotus, Diodorus, Strabo, and Ptolemy). These sources named and described the estuaries of the Nile and the landscape/riverscape of the delta in more or less detail; however, they generally do not allow clear localization in today's topographic context. Most records indicate seven main branches of the Nile, which were either named after the cities at their mouths or after an important city located on the respective arm (Bietak, 1975; Ginau et al., 2019).

Today's situation differs greatly, as only two main Nile branches still exist: the western Rosetta and the eastern Damietta arms. The fluvial landscape of the Nile Delta has, therefore, changed tremendously, indicating that the delta was a highly dynamic environment. The same is true for the time before the classical historiographers. In the time of ancient Egyptian culture, settlement patterns and overall economic, cultural, and religious processes were greatly impacted by changes to the hydrographic system of the alluvial plain (Butzer, 1976). Especially in recent decades, the importance of understanding the paleo-topographies and paleo-hydrographies of the Nile Delta at different times has been recognized, and several research projects have explored the topic. Geophysical and geoarcheological investigations have been carried out in different regions of the delta at various scales. Most of these surveys relied principally on the sedimentological analysis of core drillings (e.g., Sewuster and van Wesemael, 1987; Andres and Wunderlich, 1991; Wunderlich 1988, 1989; Stanley and Warne, 1993a, b; Stanley et al., 1996; Flaux et al., 2012; Marriner et al., 2012; Ginau et al., 2019) and/or geophysical measurements (El-Gamili et al., 1994; El Gamili et al., 2001; El-Mahmoudi and Gabr, 2009; Pennington and Thomas, 2016).

Additionally, remote sensing data, as well as topographic and historical maps, have been widely used as they allow area-wide investigation and sometimes even provide records on the past topographic situation that might not be visible today. Bietak (1975), for instance, reconstructed the course of some of the Nile branches of the delta based on the analysis of topographic maps and the location of ancient settlements. He mapped linear structures, which presumably represent natural embankments of former rivers (levees). Since the end of the 1980s, satellite images (e.g., Landsat, SPOT, Corona, RapidEye) have been increasingly used to detect old river courses in the Nile Delta (e.g., Wunderlich, 1989; Marcolongo, 1992; Moshier and El-Kalani, 2008; Wilson and Grigoropoulos, 2009; Trampier et al., 2013; Ginau et al., 2017). Along with this, digital elevation models (DEMs) from the Shuttle Radar Topography Mission (SRTM; Stanley and Jorstad, 2006), as well as high-resolution data acquired by the TanDEM-X mission, have been used (Ginau et al., 2019). Lately, Elfadaly et al. (2020) showed the use of various remote sensing sources (including Landsat) to identify potential former settlement areas in the northern delta.

The above-listed studies all use geospatial data to indicate features of the modern land surface (e.g., location and orientation of field boundaries, anomalies of land cover, discontinuities of surface morphology) that may be related to the paleogeomorphological setting. Although these datasets do not allow chronological information to be derived or remains of the paleo-landscape to be detected without ambiguities, they are very valuable to support geophysical research on the ground as they help to narrow down the survey area, or indicate new promising locations for fieldwork. However, this requires buried features to have a distinct surficial expression compared to their surroundings so they can be detected with remotely sensed imagery.

In many of the studies listed above, results on the location of former landform features were obtained using single images or a few remote sensing datasets. With the opening of the Landsat Archive in 2008, an extensive time series of multispectral satellite data has become available to the public, open and free of charge. This archive compiles all available Landsat data, beginning with the first acquisitions made by Landsat 1 in the early 1970s. However, analysis of the entire Landsat archive for a region of interest is difficult using an individual processing strategy and standard infrastructure. This is due to high storage and processing requirements that – considering the huge amount of data – must be undertaken automatically. New analysis methods can provide a solution here, e.g., cloud-based infrastructure and automated processing chains. Both are offered by the Google Earth Engine (GEE) (Gorelick et al., 2017), a free cloud-based service that grants access to the entire Landsat archive and offers comprehensive algorithms for data processing and feature derivation. This enables processing of the Landsat Archive for the entire Nile Delta, and therefore offers a new and still unexploited pool of remote sensing data that can indicate features and anomalies related to the paleogeomorphological setting. The high spatial resolution and the long temporal baseline offered by the archive make it possible to visualize and investigate even small changes and subtle differences in reflection properties

This contribution presents results on the analysis of the Landsat Archive for the entire Nile Delta between 1985 and 2019 in order to detect buried paleogeographical features. The focus of the research is on the detection of anomalies that might indicate hints of a former, potentially ancient, geomorphological setting. Special emphasis is on the identification of (partially) buried geziras and tells and on potential courses of former or abandoned Nile branches. Anomalies detected in the Landsat time series are compared to the TanDEM-X DEM, historical topographic maps of the Survey of Egypt, and to satellite imagery of the CORONA mission and recent high-resolution imagery.

2 Study area

The Nile Delta (Fig. 1), an alluvial plain in the north of Egypt, today covers an area of about 24 000 km^2 and is densely populated and intensively used for agriculture (Pennington et al., 2017; Fig. 1). It is the youngest in a long series of deltaic formations that probably date back to the Miocene (Butzer, 1976; Said, 1981). The landscape dynamics of the delta were controlled by natural factors such as tectonics and climate and sea level fluctuations up to the Middle Holocene, but human influences have played an increasingly important role since the Late Holocene (Pennington et al., 2017).

In detail, the geological structure and history of the Nile Delta are quite complex and show regional differences (cf. Andres and Wunderlich, 1991; see also the delta-spanning summary of Pennington et al., 2017). In simplified terms, the geology can be described as follows. At the beginning of the Holocene, the delta was largely covered by sandy to sandy-gravel deposits of the Mit Ghamr and Geziracover formations. The Mit Ghamr formation consists of numerous smaller units of different genetic origin of Pleistocene age, deposited during an earlier, interwoven Nile regime (Said, 1981). Up to ca. 8000 cal BP, the Nile arms eroded or redeposited this material. On some topographic heights known as "turtlebacks" or "geziras", an aeolian rearrangement of the fluvial sands forming the Geziracover formation often occurred (Wunderlich, 1989; Pennington et al., 2017). The formation of the Holocene alluvial delta plain began in the Middle Holocene. From about 8000 cal BP onwards, hydrological changes and increased sediment supply in the "African humid period" led to high accumulation rates in the Nile Delta and to the development of swampy wetlands.

The area was characterized by a widely ramified river network with extensive flood plains. The bluish-black, organic-rich, silty-clayey to clayey-silty deposits with intercalated peat horizons of this phase belong to the Bilqas 2 formation, which was deposited between ca. 8000 and 6000 cal BP in large parts of the delta. The relief of the delta was slightly hilly at this time, with topographic highs in many places, especially on the edges of the delta, extending several meters above the flood plain. The coastline was further inland than today, especially in the east (Goiran et al., 2005; Pennington et al., 2017). Between 6000 and 5500 cal BP, relative sea level rise decreased and conditions became increasingly arid. The accumulation rate in the delta therefore decreased strongly and the river landscape changed noticeably. In the southern and central part of the delta, the sediments of the Bilqas 1 formation (brown-gray in color, and less rich in organic material) were already present at this time, deposited in a deltaic landscape with much wider, well-drained flood plains and individual river courses (Pennington et al., 2017). By around

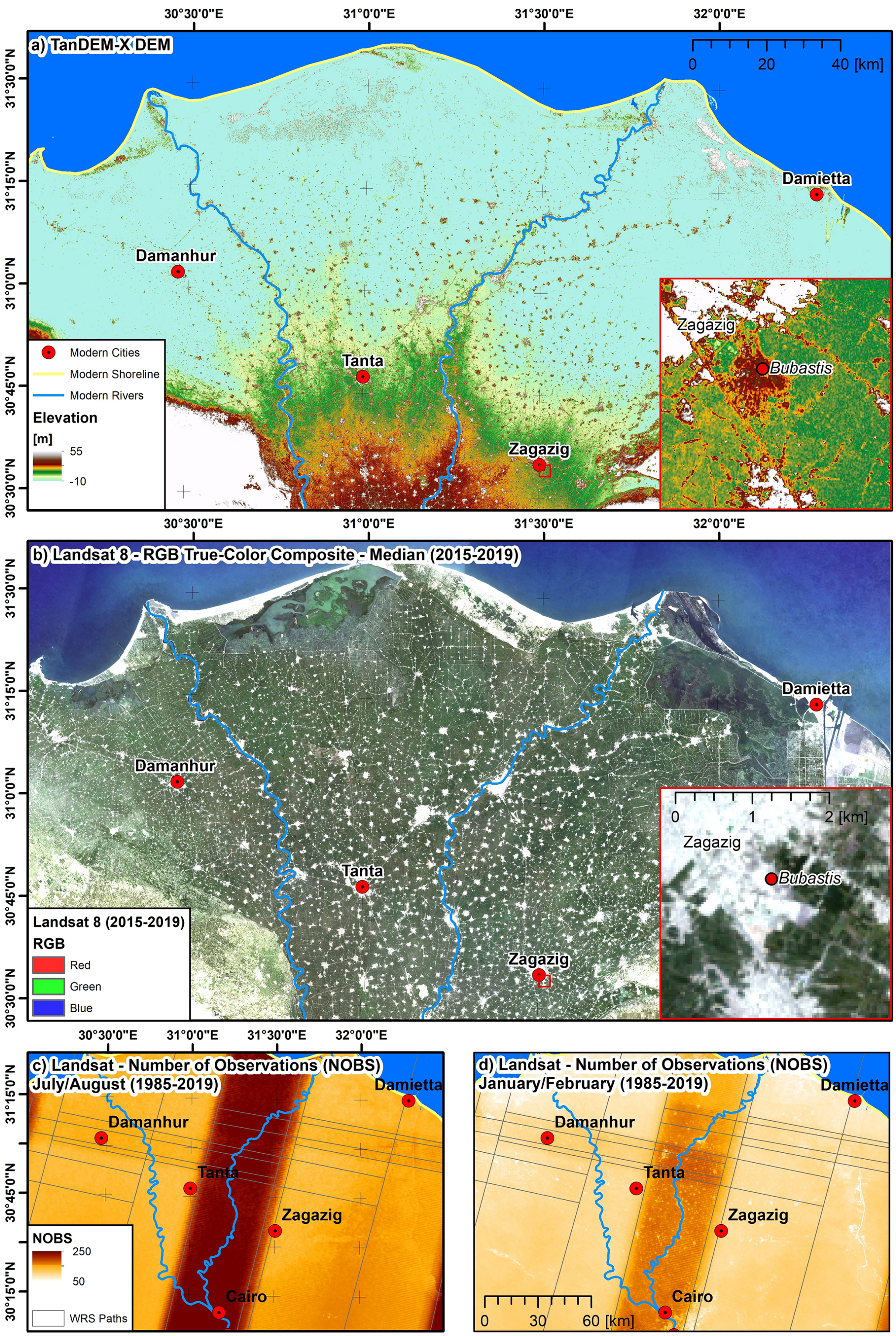

Figure 1. Study area and data availability: **(a)** TanDEM-X digital elevation model (DEM) with a resolution of 13 m by 13 m per pixel and **(b)** Landsat-8 true-color composite (RGB) for median surface reflectance between 2015 and 2019 and number of cloud-free Landsat observations between 1985 and 2019 for the months of **(c)** July and August and **(d)** January and February. Insets in **(a, b)** are centered on the excavation site of Bubastis (south of the modern city of Zagazig) and show the full resolution of the datasets. Landsat imagery courtesy of the US Geological Survey. TanDEM-X DEM courtesy of the German Aerospace Center (© DLR).

3500 cal BP, the sediments of the Bilqas 2 facies had almost completely disappeared and were spilled by sediments of the Bilqas 1 facies during the Late Holocene. The geziras, which were a typical landscape feature in the delta before 6000 cal BP, therefore gradually became rarer and smaller. From the perspective of cultural history, this dynamic environmental development played an important role in the formation of the ancient Egyptian state around 5050 cal BP (Pennigton et al., 2017).

3 Data and methods

The conceptual framework of the approach is illustrated in Fig. 2. The following sections provide information on the datasets, processing, and analysis.

3.1 Data

3.1.1 TanDEM-X digital elevation model

The DEM of the TanDEM-X mission was made available by the German Aerospace Center (DLR) (see Acknowledgments) for the entire Nile Delta (coverage of approx. 260 km × 180 km) (Fig. 1a). The elevation values are stored with single precision (i.e., submeter accuracy), and the vertical system refers to the height in meters above the WGS1984 ellipsoid. Note that the TanDEM-X DEM is a surface model. It therefore does not show the actual height of the terrain but the height of the land surface (including vegetation, buildings, etc.). The DEM was resampled to a resolution of 13 m × 13 m.

3.1.2 Landsat archive

The Landsat Mission provides the longest remote sensing archive of optical multispectral data with the earliest acquisitions dating back to the early 1970s. In this study, we used the imagery of Landsat-5, Landsat-7, and Landsat-8 obtained between 1985 and 2019. The (passive) optical sensors acquire multispectral information on the earth's surface and offer comparable temporal, spatial, and spectral resolutions (Figs. 1b and 3).

3.1.3 Reference data

The TanDEM-X DEM and the features processed using the Landsat archive (see below) were compared to historical topographic maps of the Survey of Egypt (SoE). The maps were surveyed between 1897 and 1911 and display the topographic setting of the Nile Delta at a scale of 1 : 50 000. Besides the typical topographic elements (e.g., location of roads, railways, canals), information on elevated areas inside the delta is also provided by a unique cartographic signature. From the maps, it becomes clear that this information is in relation to mounts (such as, for example, tells and geziras). However, a definition of this cartographic signature is missing.

Besides the SoE maps, CORONA imagery served as a reference. This high-resolution panchromatic satellite imagery was recorded in the late 1960s and early 1970s. It is available for the entire Nile Delta via the "CORONA Atlas of the Middle East" (Casana and Cothren, 2013). The datasets used in this study were acquired in the year 1968.

Finally, the high-resolution base maps provided in the geographic information system (GIS) software ArcMap served as a reference. These base maps are a compilation of recent high-resolution satellite imagery, and information is shown as true-color composites (i.e., RGB images). Most of the base maps used were recorded by the WorldView satellites, and images were acquired between 2017 and 2018 at a spatial resolution of less than 1 m.

3.2 Methods

3.2.1 Reference data georeferencing

The CORONA and the SoE datasets were georeferenced prior to the analysis using the Universal Transverse Mercator (UTM) projection at Zone 36 North and the WGS1984 ellipsoid. This was done by selecting a sufficient number (10–20) of ground control points (GCPs) for each sheet/image. The GCPs were found by comparing the datasets to the Esri base map and by identifying matching points. The root mean square error (RMSE) for both datasets was below 30 m after completing the georeferencing using an affine transformation function. The RMSEs were, therefore, sufficiently small for a comparison with the Landsat data. Finally, the georeferenced datasets were integrated into a GIS geodatabase along with the TanDEM-X DEM and the features derived from the Landsat time series.

3.2.2 Processing in the Google Earth Engine

In order to process the remotely sensed imagery, we made use of the cloud computing capabilities of the Google Earth Engine (GEE), which allows the processing and analyzing of large geospatial datasets (Gorelick et al., 2017). Processing the Landsat data and deriving the spectral-temporal metrics (STMs) relied on a GEE processing chain developed in preliminary work (Nill et al., 2019). This includes preprocessing the surface reflectance products, such as masking clouds and cloud shadows, and deriving STMs for specified features and time intervals. STMs describe the pixelwise spectral variance by reducing the temporal dimensionality into single statistical metrics such as the standard deviation. They enable the continuous coverage of large spaces.

3.2.3 Investigated features and seasons

The analyses focused on five widely used multispectral features: the Normalized Difference Vegetation Index (NDVI),

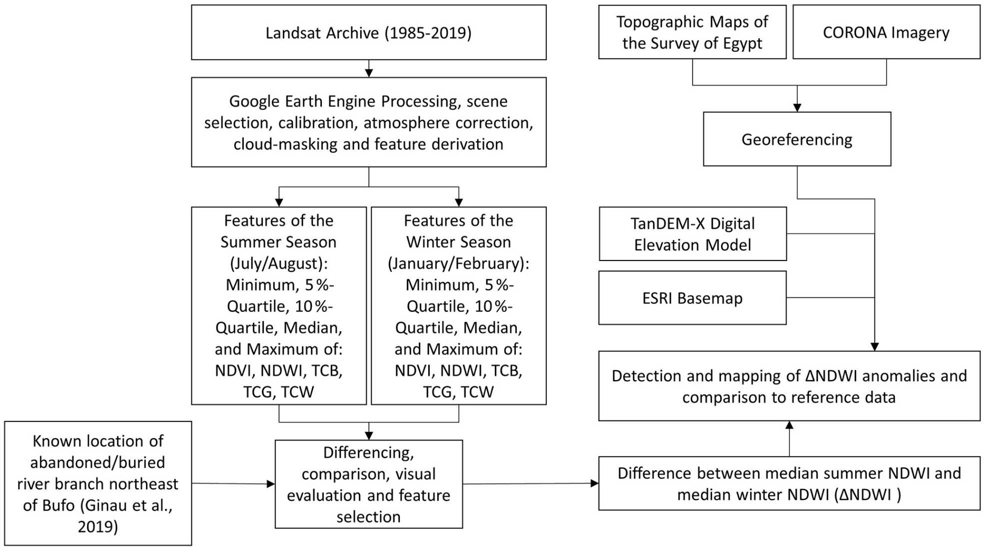

Figure 2. Conceptual framework of the data processing, feature selection, and analyses. Note: NDVI signifies Normalized Difference Vegetation Index, NDWI signifies Normalized Difference Water Index, and TCB signifies brightness, TCG greenness, and TCW wetness of the tasseled cap transformation.

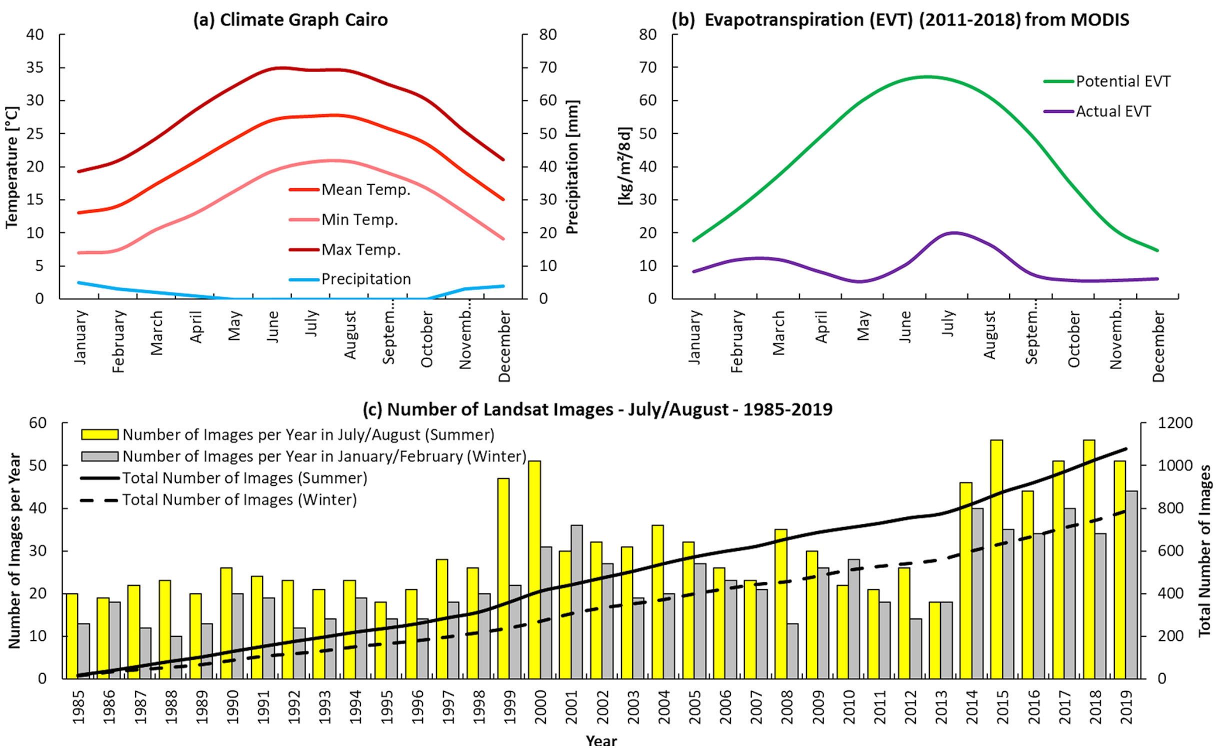

Figure 3. Study area and the number of Landsat images used in the analyses: **(a)** climate graph of Cairo, **(b)** potential and actual evapotranspiration (EVT) from the Moderate Resolution Imaging Spectroradiometer (MODIS) for selected vegetated areas in the central delta between 2011 and 2018 using the MODIS products MOD16A2-006, and **(c)** the number of Landsat images per year from 1985 to 2019 for July/August (summer) and January/February (winter).

the Normalized Difference Water Index (NDWI) (Eq. 1), and the brightness (TCB), greenness (TCG), and wetness (TCW) of the tasseled cap transformation (TC) (Kauth and Thomas, 1976).

$$\mathrm{NDWI} = (\mathrm{NIR} - \mathrm{SWIR1}) / (\mathrm{NIR} + \mathrm{SWIR1}) \tag{1}$$

The features were processed for July/August and January/February to represent the summer and winter seasons of the year. Figure 3 shows the data availability per season and year. The number of cloud-free images available per pixel for the summer and winter seasons is shown in Fig. 1c and d, respectively.

The split into winter and summer was intended to account for different situations in terms of water supply and potential water stress due to the large seasonal difference in potential and actual evapotranspiration (EVT) (Fig. 3b). EVT was estimated from the time series of the Moderate Resolution Imaging Spectroradiometer (MODIS) for selected vegetated areas in the central delta between 2011 and 2018. The processing of the MODIS products (MOD16A2-006) was carried out via the cloud-based processing service AppEEARS (Application for Extracting and Exploring Analysis Ready Samples), which is provided by the United States Geological Survey (USGS) and the National Aeronautics and Space Administration (NASA), among others.

Water stress is partially caused by the grain size composition of the substrate, in which infiltration rates are higher for coarser-grained deposits. Some of the features (e.g., NDWI, TCW) are known to be sensitive to the soil/plant moisture (e.g., Yan et al., 2014). As a result, locations with meaningfully different near-surface grain size compositions might be revealed through the different behavior of the STMs in winter and summer in the long run. Accordingly, the analyses and the presented results focus on the long-term differences (Δ) of the features for winter and summer, e.g., on the ΔNDWI (Eq. 2):

$$\Delta\mathrm{NDWI} = \mathrm{NDWI}_{\mathrm{Summer\ (JA)}} - \mathrm{NDWI}_{\mathrm{Winter\ (JF)}}. \tag{2}$$

The long-term differences were investigated for the five features listed above and for the following STMs: minimum, 5 % percentile, 10 % percentile, median, and maximum. These were processed in the temporal dimension of the stack for each feature (NDVI, NDWI, TCB, TCG, and TCW) and season (winter and summer). Therefore, the analysis investigated and compared five STMs of five multispectral features for two seasons for the entire Nile Delta using Landsat imagery acquired between 1985 and 2019.

3.2.4 Detection of anomalies

The investigations started with a proof of concept. Processing results of the GEE were compared to the results published by Ginau et al. (2019) on a buried/abandoned Nile branch in the northwestern delta close to the sites of Buto and Kom el-Arab. By using the location of the abandoned channel as a reference, all the processed Landsat features were analyzed. If and how the buried channel is revealed in the Landsat time series were then checked. This analysis aimed to select the feature that best indicates the channel in order to simplify and accelerate analysis on a delta-wide scale. Using the identified feature, anomalies (see below) were detected by visual inspection and by comparing the feature to the TanDEM-X DEM, the SoE maps, the CORONA imagery, and the Esri base maps. For all features that display the difference between summer and winter index values, e.g., the ΔNDWI, anomalies were defined by the mean and the standard deviation. In this definition, a feature value was assigned as anomalous if its value was significantly different from the mean. This significant difference, in turn, was defined by the range of 2 standard deviations centered on the mean value. For example, for ΔNDWI, the 2 standard deviation range is from -1.1 to $+1.1$. This means that values outside this range were defined as anomalies and were therefore of special interest. To support the visual analysis, the different images were displayed with a color bar from blue to white to red. Pixels are thus only colored (i.e., not white) if their value is outside the above-mentioned range (i.e., bluish colors for values < -1.1 and reddish colors for values $> +1.1$ for the ΔNDWI).

4 Results

4.1 Proof of concept

The processed Landsat features of both seasons are compared to the known location of the abandoned Nile branch proposed and described by Ginau et al. (2019). The branch is located several kilometers north of Buto and appears visibly in the TanDEM-X DEM as its levee is slightly higher than the floodplain (approx. 2 m) (Fig. 4). Coming from the south, the branch passes Kom el-Arab directly to the east and continues northwards towards Kom Alawi. There is no indication of this branch in the SoE maps, the CORONA imagery, or modern satellite imagery (i.e., it is just visible in the TanDEM-X data due to the aforementioned difference in elevation). At first glance, the median Landsat STMs (NDVI, NDWI, TCB, TCG, TCW) for this location do not provide information on the location of the channel. For TCB, TCG, and TCW, neither the summer nor the winter features display noticeable anomalies on the known course of the channel.

However, the channel location is visible via lower index values in the 5 % quantile (Fig. 4d), the 10 % quantile (Fig. 4e), and, to a lesser degree, in the median (Fig. 4f) of the summer NDWI. The difference between summer (Fig. 4c–g) and winter (Fig. 4h–l) NDWI features reveals that values of ΔNDWI (Fig. 4m–q) are strongly negative (i.e., index values are lower in summer) over the channel locations, showing significant differences of < -0.2. Ambiguities exist (especially towards the east where the SoE maps indicate a former inland water body), but the pattern of the ΔNDWI anoma-

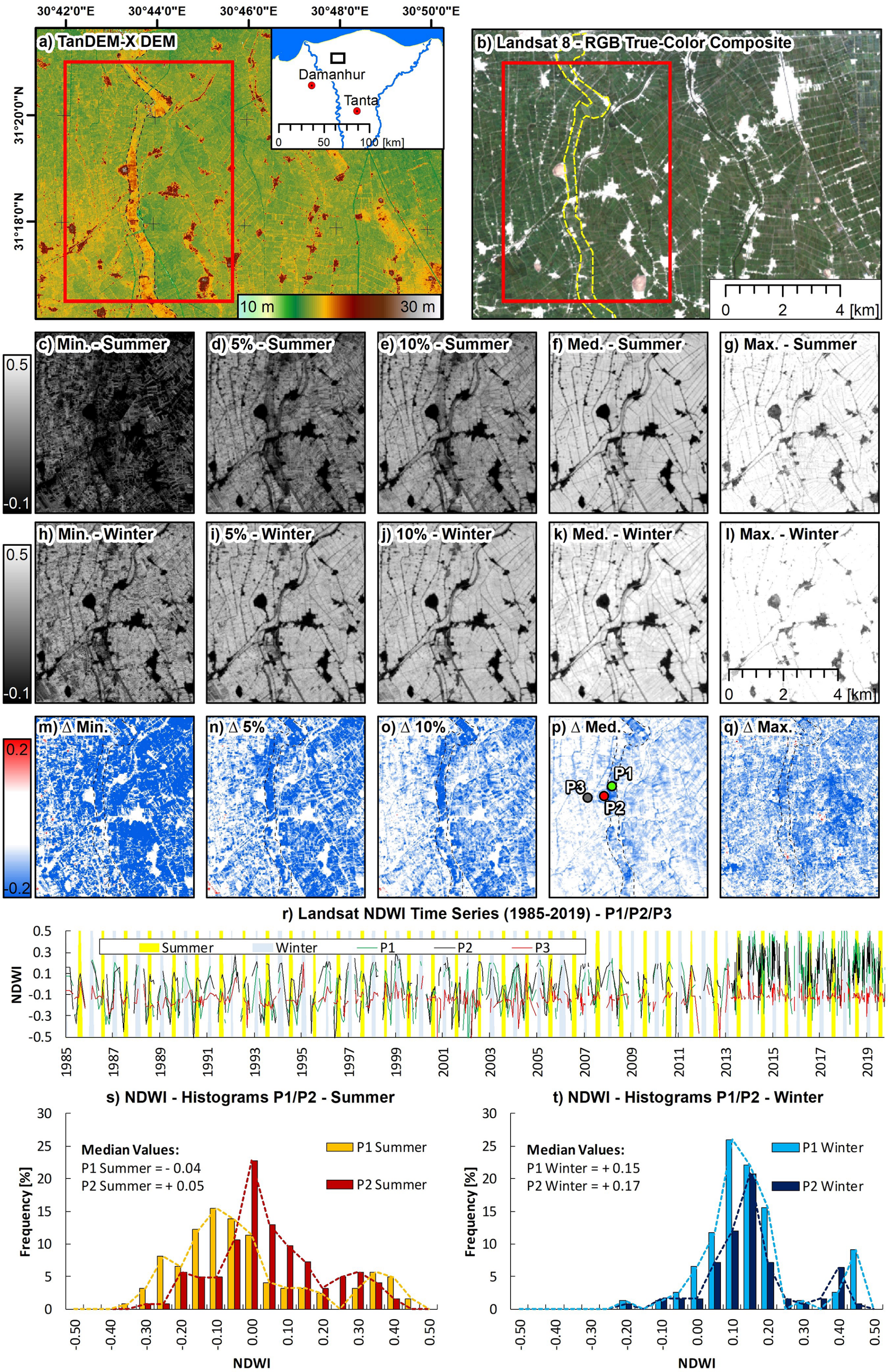

Figure 4. Comparison of the Landsat time-series features to a known abandoned/buried river branch northeast of Buto (location according to Ginau et al., 2019): **(a)** TanDEM-X digital elevation model (DEM), **(b)** Landsat-8 true-color composite (RGB) (see Fig. 1b), **(c–g)** minimum (Min.), lower 5 % percentile, lower 10 % percentile, median (Med.), and maximum (Max.) of the summer NDWI values of the Landsat time series (1985–2019), **(h–l)** Min., lower 5 % percentile, lower 10 % percentile, Med., and Max. of the winter NDWI values, **(m–q)** difference (Δ) between summer and winter STM values, **(r)** NDWI values of the sample points P1, P2, and P3 for all Landsat images ($n = 825$), **(s)** histograms of P1 and P2 for summer ($n = 123$), and **(t)** histograms of P1 and P2 for winter ($n = 80$); the ΔNDWI values are P1 = −0.19 and P2 = −0.12 accordingly. TanDEM-X DEM courtesy of the German Aerospace Center (© DLR).

lies matches the proposed location and extent of the channel. Among the differences between the respective summer and winter NDWI STMs (Fig. 4m–q), the channel is best visible as an anomaly in the difference between the NDWI medians of summer and winter (Fig. 4p). This feature provides fewer ambiguities than the different images calculated using the 5 % (Fig. 4d) or the 10 % (Fig. 4e) percentile features.

The complete time series of NDWI values is exemplarily displayed in Fig. 4r for three selected sample points around Kom el-Arab. Two points lie in agricultural fields over (P1) and outside (P2) the proposed course of the abandoned Nile branch and close to each other (Fig. 4q). The third point (P3) is located in the center of Kom el-Arab. For this region, 825 Landsat acquisitions are available from between 1985 and 2019. The respective NDWI values are rather stable over time for P3 but vary along with the vegetation phenology over the agricultural fields (P1 and P2). The time series show that both fields underwent a change in land use (e.g., in irrigation or plantation) between 2012 and 2013 as the NDWI signature changes.

A comparison of the histograms for P1 and P2 for the summer (Fig. 4s) and winter (Fig. 4t) seasons shows that, in the long run, lower NDWI values (i.e., indicating lower soil/plant moisture) are more frequently found over P1 than over P2 for the summer season. For both P1 and P2, NDWI values are similar for the winter season. The difference in the seasonal NDWI median values results in ΔNDWI vales of -0.19 (P1), -0.12 (P2), and -0.05 (P3).

A similar situation is found approx. 15 km to the east close to Kom el-Khawaled (Fig. 5). For this region, another levee of a former river branch is visible in the TanDEM-X data (Fig. 5a) connecting Kom el-Khawaled with Kom el-Garad and Kom el-Nashwia (Fig. 5c).

The levee is slightly more elevated than the floodplain. Again, median summer NDWI values (Fig. 5d) are found to be lower over the levee than the winter NDWI (Fig. 5e) values. This difference is displayed as ΔNDWI in Fig. 5f. Anomalies over the levee are significant with values of -0.15.

The ΔNDWI is further compared to the general ancient (approx. 4000 BCE) delta landscape/riverscape proposed by Butzer (1976). Figure 6 shows the ΔNDWI along with a georeferenced and digitized version of Butzer's map. The mismatch in spatial resolution does not allow a comparison of both datasets in detail. However, the upper central Nile Delta (towards the apex) is indicated by strong negative anomalies of the ΔNDWI, which somewhat matches the proposed location of "sands at or near the surface" in Butzer's map, for example, the locations between Tanta and Cairo, between the modern course of the Rosetta and the Damietta branches, respectively.

The border between strongly negative ΔNDWI values and values without significant difference (ΔNDWI around zero) is, for some locations, remarkably sharp, for example, between Tanta and Zagazig, where the Damietta branch marks a clear border in the ΔNDWI values. Most of the significant ΔNDWI anomalies are negative, indicating lower summer NDWI index values. For the inner fringes of the delta and for the desert, the ΔNDWI values are close to zero (i.e., no difference in NDWI between summer and winter is observed). Positive anomalies are found less frequently but exist, e.g., for larger patterns towards Lake Burullus and Lake Manzala.

4.2 Geziras and tells of the eastern Nile Delta

For the eastern delta, the region of interest lies between Bubastis (south) and Tanis (north) and between the northeastern desert margin (east) and the Damietta branch (west). Strongly negative local ΔNDWI anomalies are found in the direct vicinity of almost all larger tells and geziras in the eastern delta. This is exemplarily illustrated in detail for Geziret Sineita in Fig. 7 and for other locations in Figs. 8 and 9.

The ΔNDWI anomalies exhibit a clear and sharp border and differences between summer and winter NDWIs are < -0.2. Comparisons to the SoE maps, the CORONA imagery, and the modern satellite imagery indicate that these anomalies are not caused by differences in land cover (which would be visible in the modern high-resolution satellite imagery). These anomalies are also not related to former tell or gezira borders indicated in the SoE maps (i.e., almost all anomalies are found at some distance from the borders indicated in the SoE maps).

In addition, for almost all locations, the TanDEM-X DEM shows that anomalies are not caused by remarkable differences in elevation, but the terrain between the borders of the anomalies and the settlement, tell, or gezira borders is rather flat. This is exemplarily displayed in the profile lines in Fig. 7e for Geziret Sineita.

For Tell es-Sunayta (Fig. 8d), Geziret Umm Igrim, Tell Ibrahim Awad (Fig. 8e), and Geziret Abu Qeih (Fig. 8f), the ΔNDWI anomalies are asymmetric. Here anomalies are not found on both sides of the tell or gezira (i.e., one side of the tell is without a significant ΔNDWI anomaly).

The ΔNDWI anomalies are also found at smaller tells, which are indicated in the SoE maps but seem to have vanished over time. Figure 9d and e show two examples of small tells (diameters less than 250 m) in the eastern Nile Delta. These tells are indicated in the SoE maps but are not, or hardly, visible in the CORONA and the modern satellite imagery. They are, however, clearly displayed in the ΔNDWI by strong negative anomalies with values < -0.15.

The ΔNDWI anomalies, in some cases, even encompass two or more tells that the SoE maps indicate are separated. This is, for example, the case for Geziret Ziwilin and Tell Geziret Zuwelen (Fig. 9f) and also for Geziret Umm Igrim and Tell Ibrahim Awad (Fig. 8e). For more southward locations (towards the desert margin), the patterns of the anomalies are less clear, and generally fewer anomalies of smaller extent are found. An example is the Gezira Samana (Fig. 9g). Here the ΔNDWI anomalies mostly follow the border indi-

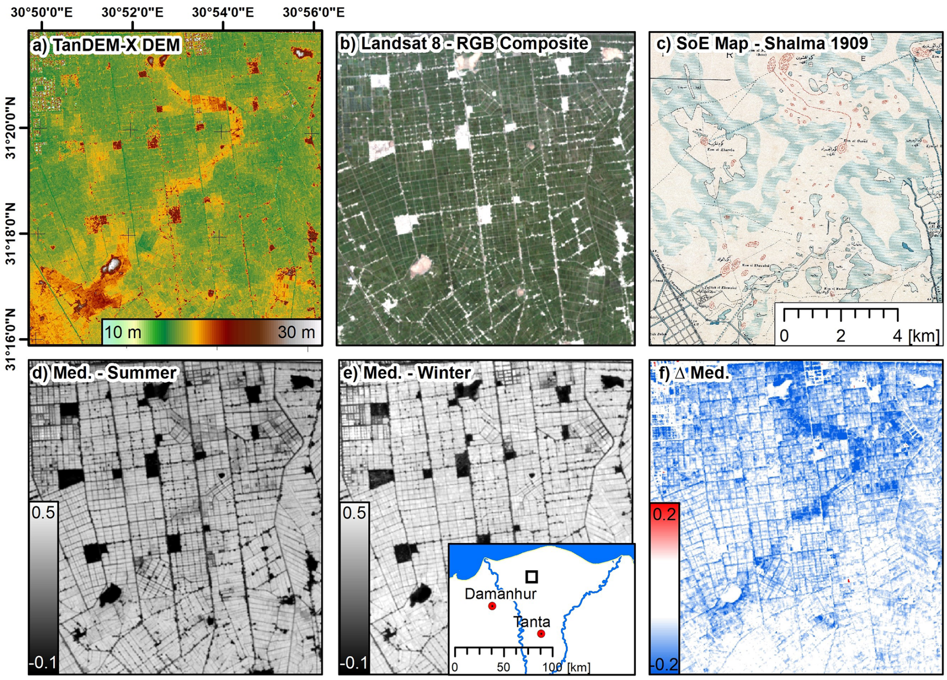

Figure 5. Comparison of the Landsat time-series features to a potential abandoned/buried river branch (location approx. 15 km east of Fig. 4) connecting Kom el Khawaled, Kom el Garad, and Kom el Nashwia (names according to the SoE Map): **(a)** TanDEM-X digital elevation model (DEM), **(b)** Landsat-8 true-color composite (RGB) (see Fig. 1b), **(c)** topographic map of the Survey of Egypt (SoE), **(d)** median (Med.) of the summer NDWI values of the Landsat time series (1985–2019), **(e)** median (Med.) of the winter NDWI values, and **(f)** difference (ΔNDWI) between summer and winter median NDWI values. TanDEM-X DEM courtesy of the German Aerospace Center (© DLR).

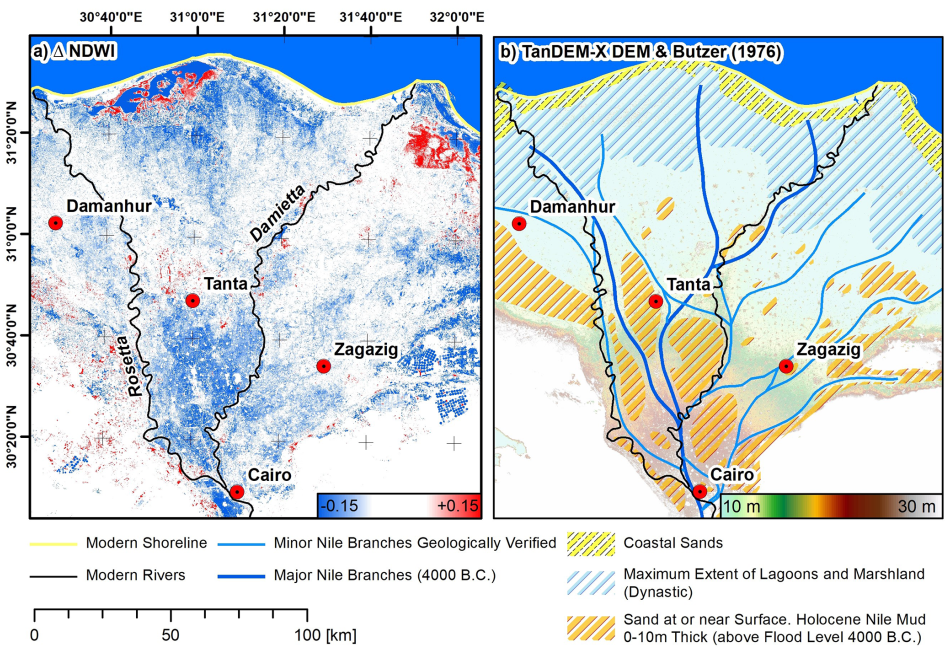

Figure 6. Comparison of Landsat time-series features to the general ancient delta landscape: **(a)** difference (Δ) between median summer Normalized Differences Water Index (NDWI) and median winter NDWI and **(b)** general landscape units of the Nile Delta around 4000 BCE according to Butzer (1976). TanDEM-X DEM courtesy of the German Aerospace Center (© DLR).

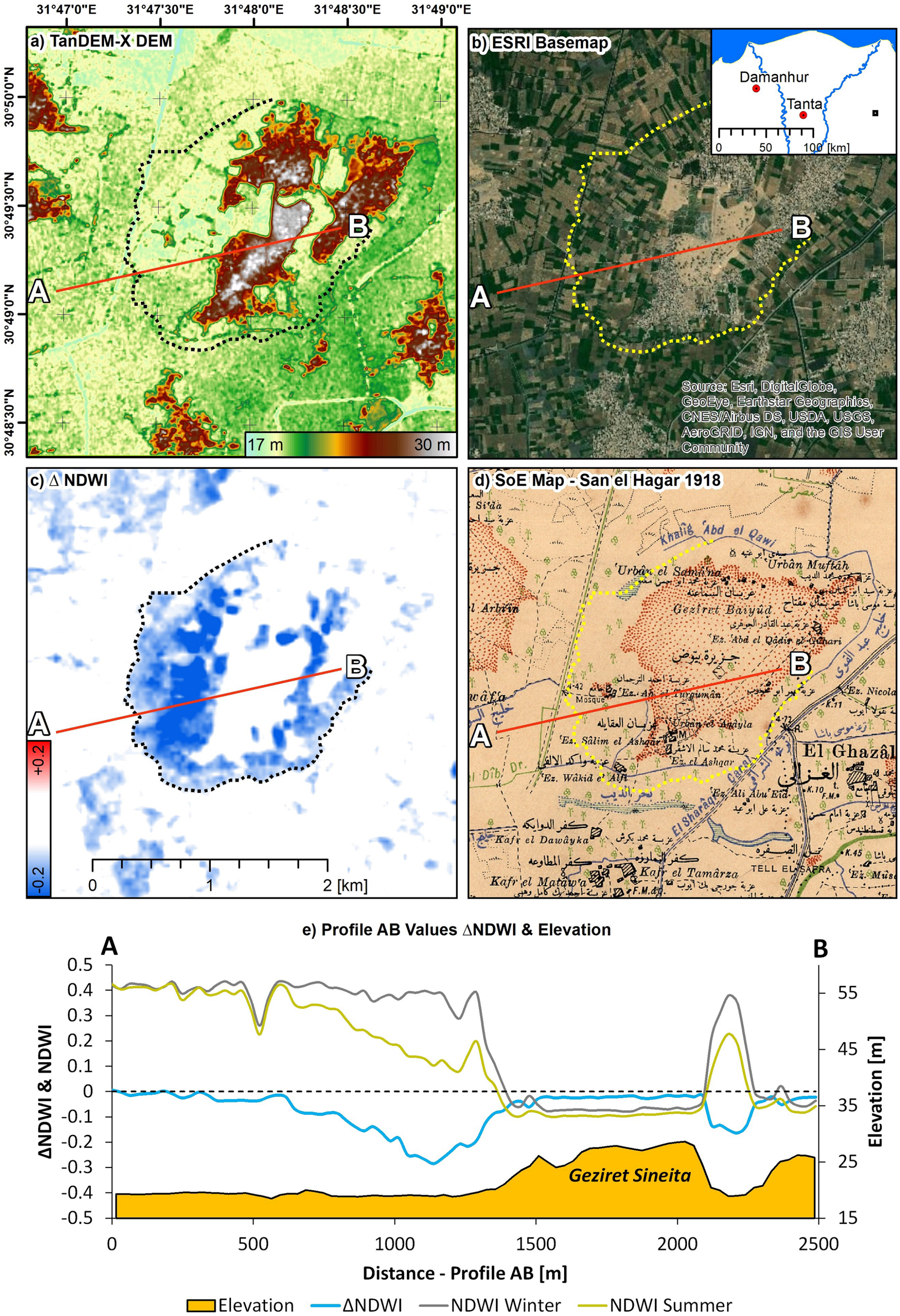

Figure 7. Processing results for the eastern Nile Delta for the example of Geziret Sineita (Tell es-Sunayta – SCA Sharqiya register 13120050, Sunaytah; EES 566 – but Geziret Bayud on SoE map – van den Brink, 1986, pp. 21, 24): **(a)** TanDEM-X digital elevation model (DEM), **(b)** Esri base map (2017/18), **(c)** difference (ΔNDWI) between summer and winter median NDWI values, **(d)** topographic map of the Survey of Egypt (SoE), and **(e)** values of summer and winter median NDWIs, ΔNDWI, and elevation of the DEM along profile AB. TanDEM-X DEM courtesy of the German Aerospace Center (© DLR).

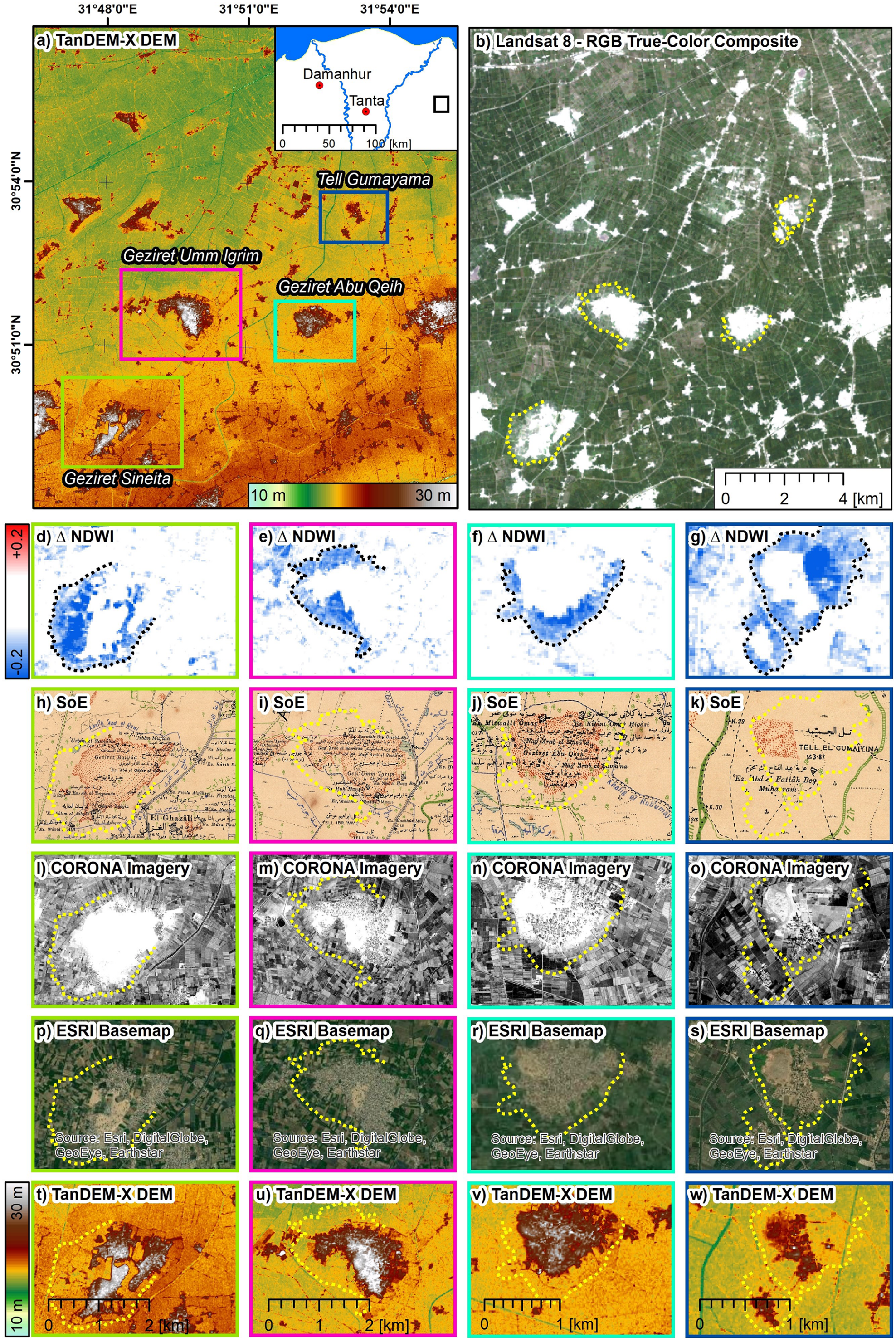

Figure 8. Processing results for the eastern Nile Delta: **(a)** TanDEM-X digital elevation model (DEM), **(b)** Landsat-8 true-color composite (RGB) (see Fig. 1b) and extent of the anomalies, **(d–g)** ΔNDWI (see Fig. 7) (1985–2019), **(h–l)** georeferenced maps of the Survey of Egypt (SoE) (ca. 1906–1912), **(h–l)** CORONA imagery (1968), **(p–s)** Esri base map (2017/18), and **(t–w)** TanDEM-X DEM (2012). Dashed black and yellow lines indicate the extent of ΔNDWI anomalies. Locations are, from left to right and including references, (i) Geziret Sineita, Tell es-Sunayta (SCA Sharqiya register 13120050, Sunaytah, EES 566) and Geziret Bayud on SoE map (van den Brink, 1986, pp. 21, 24), (ii) Geziret Umm Igrim/Agram (EES 569) and just south lies Tell Ibrahim Awad (SCA Sharqiya register 13120027, EES 535) (van den Brink, 1986, pp. 22, 24; van Haarlem, 2000, pp. 13–16; van Haarlem, 2019), (iii) Geziret Abu Qeih, and (iv) Tell Gumayama/Tell Gumaiyima (SCA Sharqiya register 13060032, EES 186) (Petrie, 1888, pp. 37–44; van den Brink, 1986, pp. 22, 24; Ashmawy, 2006, pp. 55–64). TanDEM-X DEM courtesy of the German Aerospace Center (© DLR).

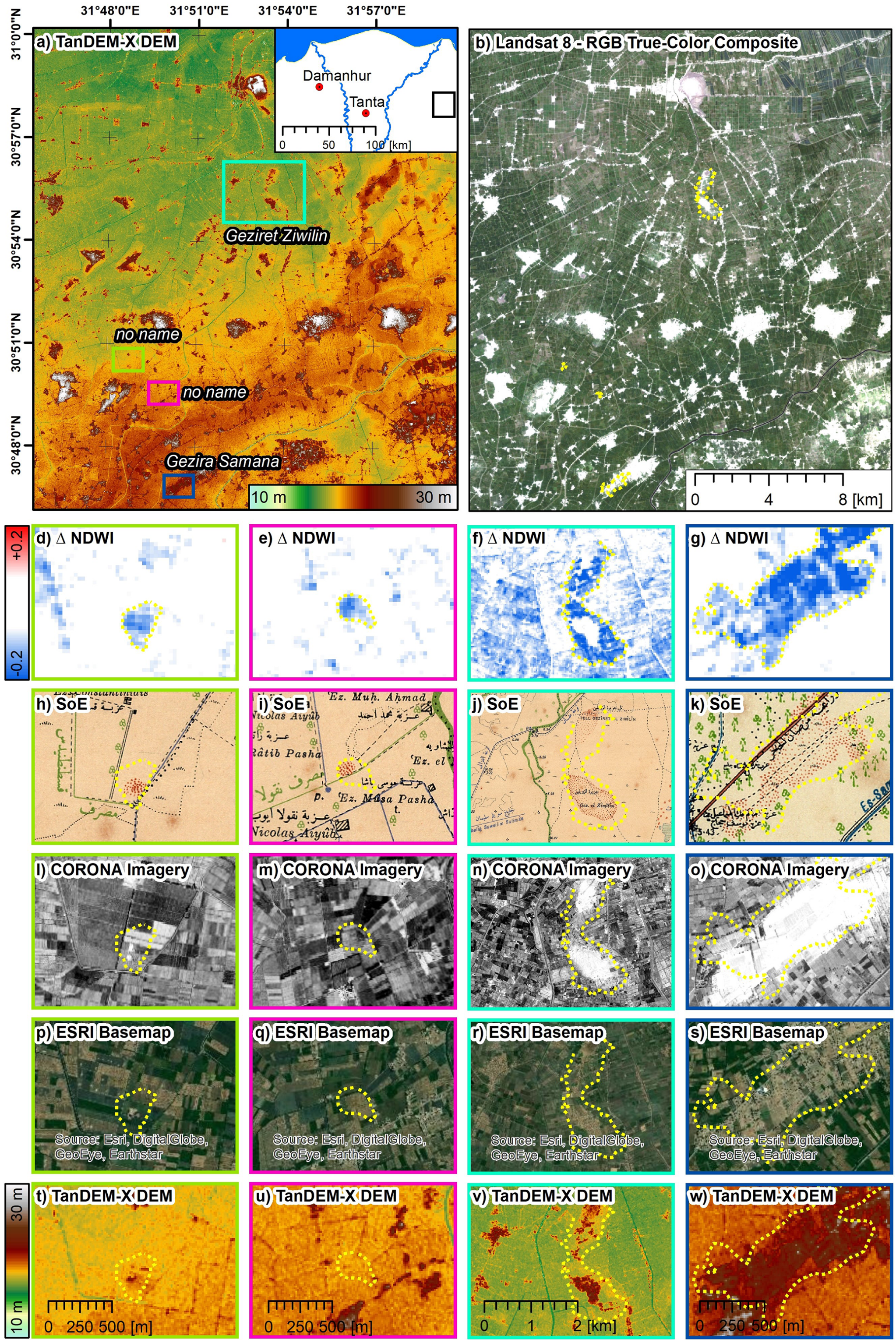

Figure 9. Processing results for the eastern Nile Delta: **(a)** TanDEM-X digital elevation model (DEM), **(b)** Landsat-8 true-color composite (RGB) (see Fig. 1b) and extent of the anomalies, **(d–g)** ΔNDWI (see Fig. 7) (1985–2019), **(h–l)** georeferenced maps of the Survey of Egypt (SoE) (ca. 1906–1912), **(h–l)** CORONA imagery (1968), **(p–s)** Esri base map (2017/18), and **(t–w)** TanDEM-X DEM (2012). Dashed black and yellow lines indicate the extent of ΔNDWI anomalies. Locations are, from left to right and including references, (i) no name, (ii) no name, (iii) Geziret Ziwilin, 1 km south of Tell Geziret Zuwelen/Tell Zuwelen/Tell Sueilin (SCA Sharqiya register 13060041, EES 324) (Petrie, 1885, pp. 29. Sect. 36; Griffith in Petrie, 1888, p. 46; Yoyotte, 1987, p. 107, n. 1; Favard-Meeks, 1999, p. 88, Fig. 1), and (iv) Gezira Samana (Habachi, 1954, pp. 479–489; Franzmeier, 2010, pp. 29–32). TanDEM-X DEM courtesy of the German Aerospace Center (© DLR).

cated in the SoE map (Fig. 9k). There also seems to be a relation to the topographic setting at this site (Fig. 9w) as the border of the anomaly follows the terrain discontinuities.

4.3 Tells of the western Nile Delta

While ΔNDWI anomalies appear in the immediate vicinity of most of the tells and geziras of the eastern delta, this is not the case for the tells of the western delta. In fact, no significant ΔNDWI anomalies are found for the tells indicated in the SoE maps. The investigated region is located north of Damanhur, several kilometers to the east and west of the Rosetta Branch.

For example, Fig. 10 shows the ΔNDWI along with the reference data for Kom el-Ghoraf/Ghuraf (Fig. 10d), Kom el-Sheikh Ismail/Kom Abu Ismail/Kom Ismail (Fig. 10e), Kom el-Nisf (Fig. 10f), and Buto (Tell el-Fara'in) (Fig. 10g). No ΔNDWI anomalies were found that are comparable in size or shape to those of the eastern Nile Delta, although the tells are comparable in size and shape.

4.4 Riverscape of the eastern delta

Focusing on potential former river courses, several linear and meandering anomalies are found in the eastern Nile Delta in closer proximity to Bubastis and Zagazig (Fig. 11). Local ΔNDWI anomalies are present to the west of the modern settlement of Dyarb Negm (Fig. 11c). The ΔNDWI anomalies, approx. < -0.12 and therefore of lesser magnitude than the anomalies found near the geziras, indicate several meanders that overall stretch from south-southwest to north-northeast (Fig. 11b).

For this location, the orientation of the field boundaries and the terrain (Fig. 11d) also give some evidence of a former branch of the Nile. A second linear ΔNDWI anomaly is found between Zagazig and Dyarb Negm, approx. 8 km west of the modern settlement of Hihya. The anomaly stretches from the southwest to the northeast (Fig. 11b), and anomalies are strong with a magnitude of < -0.15. None of the reference data provide further information on how this anomaly can be explained (i.e., neither the orientation of the field boundaries nor the TanDEM-X data indicate the potential location of the branch).

Finally, a third linear anomaly is found in the ΔNDWI data. It runs south of Zagazig, directly passing Bubastis, stretches from the southwest to the northeast, and therefore runs parallel to the lower reach of the more northern linear ΔNDWI anomaly (Fig. 11b). The ΔNDWI values are mostly significant, but they are of a lower magnitude with values < -0.12. From the visual interpretation, it seems clear that there is a linear anomaly. However, the connectivity of abnormal pixels is lower compared to the other two examples, and the course of the anomaly is, therefore, more ambiguous/speculative.

5 Discussion

5.1 Detection of anomalies via Landsat time series

The detection of anomalies relied on the analysis of the ΔNDWI calculated as the difference between the long-term median summer and median winter NDWI. In the analysis the features of the tasseled cap transformation (TCB, TCG, TCW) and their differences between winter and summer seasons were also investigated. However, these features were less suited to indicate the former location of the river channels. This may result from the fact that seasonal differences between tasseled cap features primarily display differences in the surface reflection caused by different lighting conditions (i.e., reflection in winter is generally reduced as the sun elevation is lower). In contrast, NDWI is a normalized (dimensionless) index. It is therefore not sensitive to differences caused by seasonally different lighting conditions, which makes the index comparable in all the seasons.

The differencing of winter and summer features in turn aims to investigate seasonal differences. It is therefore suited to cancel out land-cover classes with temporally stable index properties, e.g., such as permanent water bodies, (dry) desert surfaces, and urban areas. This limits the analysis to land-cover classes showing seasonal dynamics due to, for example, the phenological development of vegetation or to differing moisture conditions of the plants and/or the soil. Further, the interpretation of the seasonal differences must take into account the actual land cover and its spatial variability as some land-cover types inherently cause large seasonal differences in the NDWI (see below). The approach is therefore most promising/feasible over areas displaying the same coverage.

Anomalies were identified if ΔNDWI values were outside the 2 standard deviation range centered on the mean. Strong and connected ΔNDWI anomalies were found over the known location of the abandoned Nile branch proposed by Ginau et al. (2019). It is therefore likely that Landsat features are suitable for identifying surface anomalies (over vegetated areas of the same coverage) that may be related to subsurface anomalies. In this context, the assessment indicated that ΔNDWI anomalies result, in the long run, from lower summer NDWI values. This was revealed by comparing the NDWI signatures of locations over and beside the proposed channel location. This observation is most likely caused by lower soil/plant moisture. NDWI is sensitive to these parameters (Yan et al., 2014), and summer months are characterized by the highest evapotranspiration rates, which in turn make situations with water stress or reduced water supply more likely.

Following this line of argument, and considering that anomalies are not related to field boundaries or obvious differences in land cover, they must be caused by differences in the near-surface deposits and/or in the local morphology. These are likely, as the former levee offers better drainage

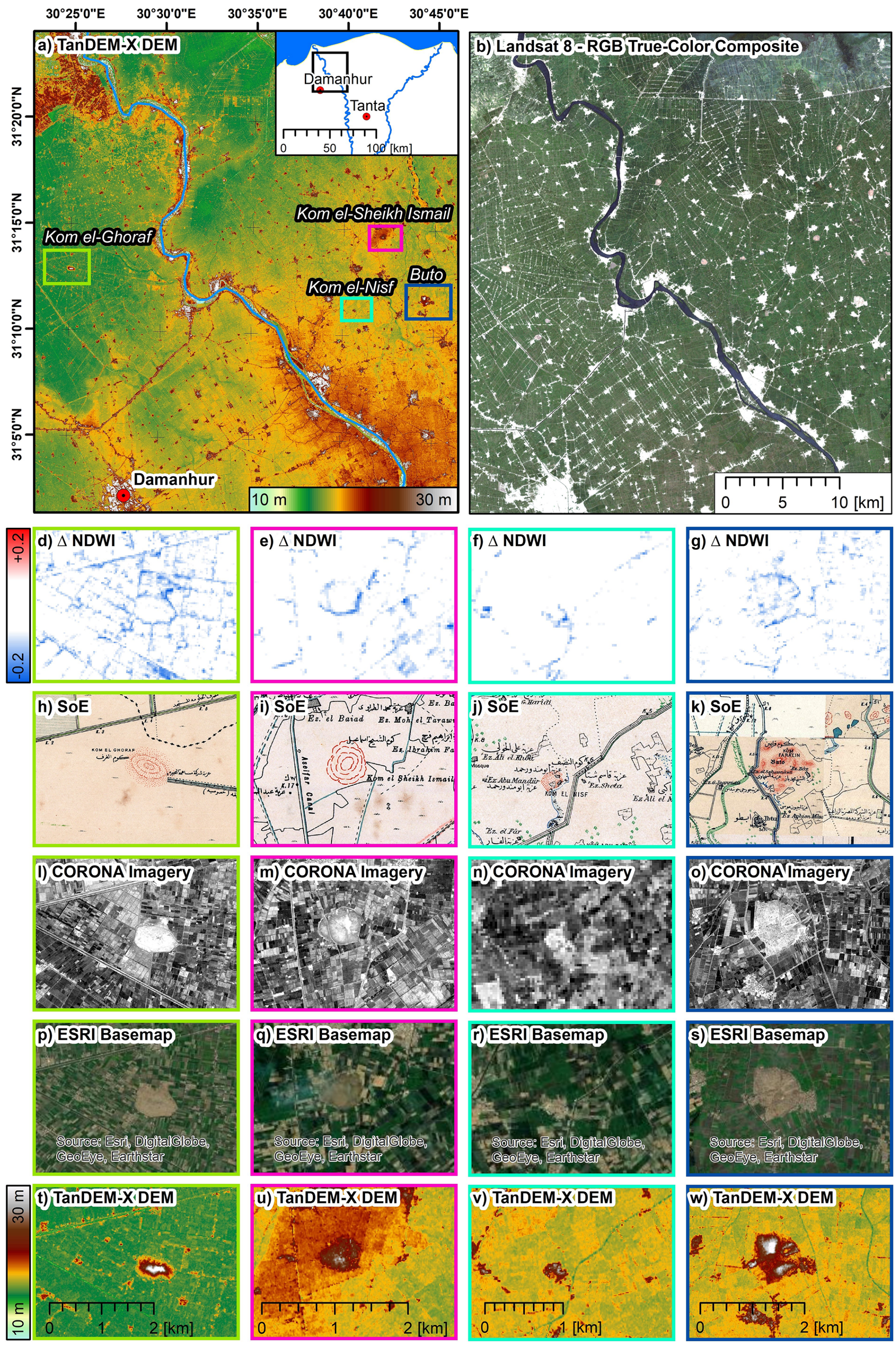

Figure 10. Processing results for the western Nile Delta: **(a)** TanDEM-X digital elevation model (DEM), **(b)** Landsat-8 true-color composite (RGB) (see Fig. 1b), **(d–g)** ΔNDWI (see Fig. 7) (1985–2019), **(h–l)** georeferenced maps of the Survey of Egypt (SoE) (ca. 1897–1912), **(h–l)** CORONA imagery (1968), **(p–s)** Esri base map (2017/18), **(t–w)** TanDEM-X DEM (2012). Locations are, from left to right and including references, (i) Kom el-Ghoraf/Ghuraf (SCA Beheira register 100164, EES 229) (Lanna, 2005, pp. 339–363; Sist, 2006, pp. 243–249; Wilson and Grigoropoulos, 2009, pp. 173–175; Kenawi, 2014, pp. 97–99), (ii) Kom el-Sheikh Ismail/Kom Abu Ismail/Kom Ismail (SCA Kafr es-Sheikh register 090168, as Kom Ismail, EES 251) (Ballet and von der Way, 1993, pp. 12–13; Wilson and Grigoropoulos, 2009, 215–218, no. 57; Ginau et al., 2019, Fig. 5), (iii) Kom el-Nisf (EES 2), and (iv) Buto (Tell el-Fara'in, SCA Kafr es-Sheikh register 090134, EES 4), adjacent in the north to Kom el-Dahab (SCA Kafr es-Sheikh register 090171) (Hartung et al., 2009, pp. 172–188; Ballet et al., 2011; Seton-Williams, 1969, pp. 5–22). TanDEM-X DEM courtesy of the German Aerospace Center (© DLR).

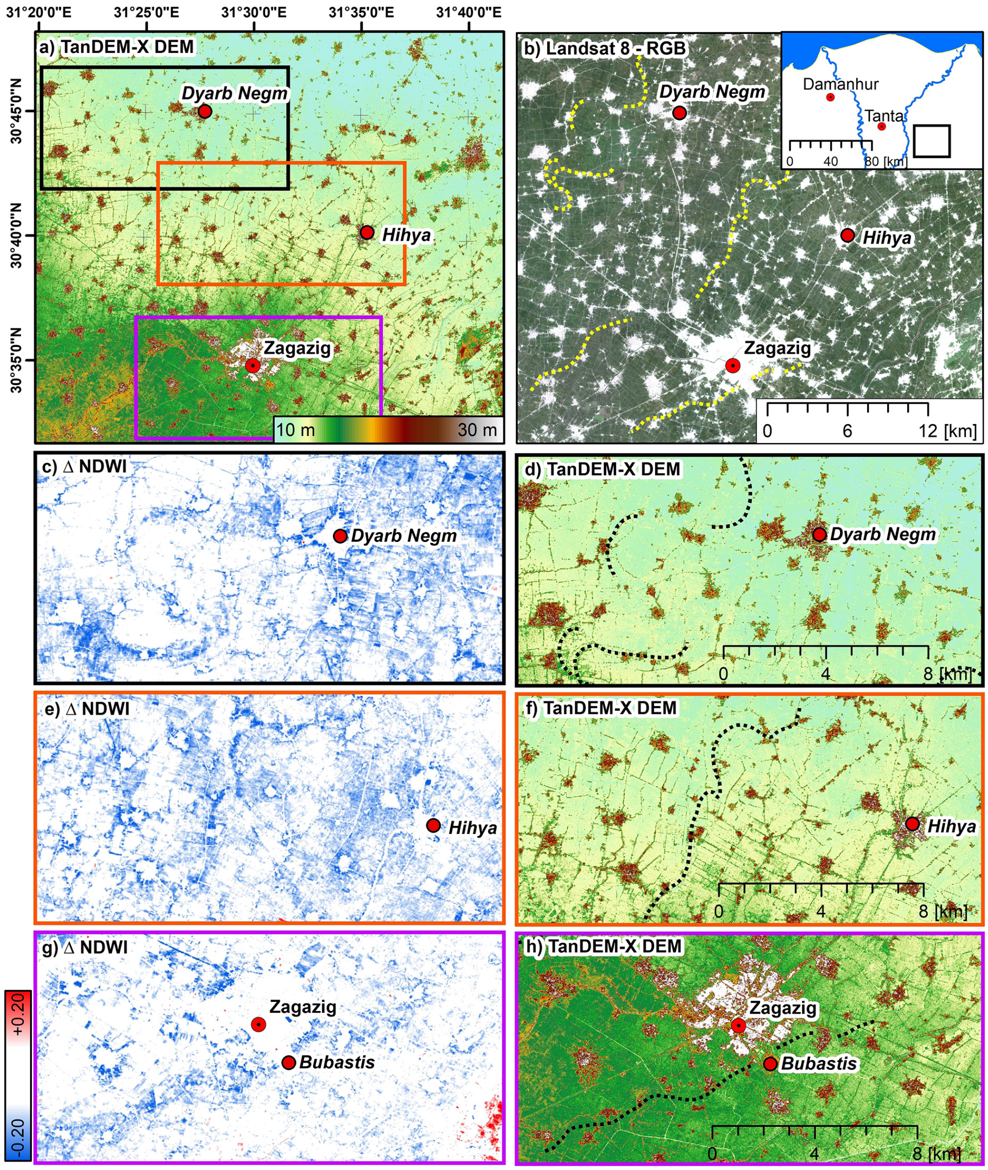

Figure 11. Processing results for the eastern Nile Delta: **(a)** TanDEM-X digital elevation model (DEM), **(b)** Landsat-8 true-color composite (RGB) (see Fig. 1b) and extent of the anomalies, **(c, e, g)** ΔNDWI (see Fig. 7), and **(d, f, h)** TanDEM-X DEM. Dashed black and yellow lines indicate the extent of ΔNDWI anomalies. TanDEM-X DEM courtesy of the German Aerospace Center (© DLR).

due to its slightly higher elevation than the floodplain. Further, the deposits are dependent on the flow velocity. They may therefore be coarser near the middle of the channel, while finer-grained deposits are expected in a more lateral position to the main channel (i.e., the surrounding floodplain) (Brown, 1997).

It is important to note that the observed seasonal differences in NDWI only become visible by investigating long timescales. A situation with reduced water supply or water stress is rather seldom for the (outer) delta also due to the irrigation. A long observation period and many acquisitions are therefore necessary to capture rather small differences in the NDWI between the two seasons. Thus, the course of the whole channel is not visible in a single image (i.e., a single NDWI), but it appears when all scenes of the time series are investigated and if summer and winter NDWIs are differenced.

However, comparisons of the ΔNDWI with the modern high-resolution satellite imagery of the Esri base map reveal that not all of the ΔNDWI anomalies can be explained by the model outlined above. There are several typical sources of ambiguities and their interpretation. Thus, ΔNDWI anomalies are frequently observed near small linear structures (e.g., roads, railroads, field boundaries) and at borders between different land-cover or land-use units (e.g., at the borders of cities). Such differences are believed to be caused by the spatial resolution of the Landsat system causing pixels with mixed coverage and by slightly different locations of the pixel footprints as the grid cells of the Landsat acquisitions are not necessarily congruent throughout the time series. Furthermore, some land-cover types and crop management practices will inherently cause large seasonal differences in the NDWI. This can be seen for plantations with broad-leaved woody vegetation, as far as this is detectable in the modern high-resolution imagery.

5.2 Anomalies of tells and geziras

Despite the limitations listed above, strong ΔNDWI anomalies were found in the surroundings of the tells and geziras of the eastern delta. The comparison to the Esri base map made clear that these are not caused by differences in the land cover as no obvious difference in coverage or usage was detected for these locations.

Considering the proposed evolution of the eastern Nile Delta (Andres and Wunderlich, 1991) it seems likely that these anomalies are related to the shallow subsurface continuation of the geziras and/or to the displaced tell and gezira material (e.g., investigated by Ginau et al., 2017, for the western delta also using Landsat imagery). Therefore, it is more likely that coarser-grained deposits are present near the surface, leading to better drainage and, on average, to lower NDWI index values in summer, as manifested by negative ΔNDWI anomalies. This is further supported as similar ΔNDWI anomalies are found over small tells that have vanished but were mapped in the SoE maps. These locations indicate that the ΔNDWI is, to some degree, sensitive to differences in the surficial substrate (Kalayci et al., 2019).

It was further observed that the ΔNDWI anomalies over the geziras in the eastern delta were asymmetric, which matches the general concept of their morphology and genesis, e.g., as demonstrated by El Beialy et al. (2001) (for Tell Tukh el-Qaramus), Andres and Wunderlich (1991) (schematic cross section for the western and eastern delta), and van Wesemael and Dirksz (1988) (for a schematic cross section of the eastern delta). This interpretation is also supported by the fact that no anomalies were found in the western delta that were similar in shape and magnitude. The tells of the western delta mostly have a different genesis and morphological setting (Andres and Wunderlich, 1991; Trampier, 2014). There are usually no large sandy bodies (i.e., geziras) or coarser-grained deposits, at least near the surface. In this context, Andres and Wunderlich (1991, p. 128) point out that fine-grained deposits in the eastern delta are embedded in a "[...] Pleistocene sand relief", while for the western delta "[...] Pleistocene sand is not found at the surface." While this conceptual model holds for the sites investigated by Andreas and Wunderlich (1991), later research by Wunderlich and Ginau (2016) indicated larger near-surface sand deposits at the site of Buto even though the authors note that these formations were covered by younger deposits.

Still, it is to be expected that tell material was displaced over time during the active periods (Ginau et al., 2017). Therefore, the absence/presence of ΔNDWI anomalies might finally be explained by the absence/presence of coarser-grained deposits at or near the surface whether the anomalies are due to rearranged tell material or an underground continuation of the landform.

Notwithstanding the above, the location and shape of the ΔNDWI anomalies provide interesting results for some of the tells. For example, the results suggest a linkage between Geziret Umm Igrim/Agram (EES 569) and the southern Tell Ibrahim Awad. Further, anomalies indicate a potential linkage between Geziret Ziwilin and Tell Geziret Zuwelen/Tell Zuwelen/Tell Sueilin. Favard-Meeks (1999) described the relationship of the two adjacent sites as a "double tell" with functional differences. There is a smaller settlement area in the north at Tell Geziret Zuwelen/Tell Zuwelen/Tell Sueilin and a very large cemetery area in the south at Geziret Ziwilin. The new results suggest that the two areas were connected. The northern site is much larger than previously thought, making both areas (settlement and funerary) roughly the same size. It has been observed for gezira sites that cemetery areas are located on the higher parts of geziras, while settlements are placed on lower sections (van den Brink, 1986). Possibly this is the case here, with large parts of the gezira sloping down towards the north. This may explain the reduced size in the north, which is either due to the easier leveling of this lower area or the lower parts continuing under the modern surface.

In this context, it is also interesting to note that ΔNDWI anomalies are of a smaller extent and magnitude for Gezira Samana. As indicated by Franzmeier (2010), this gezira is likely of different origin (e.g., compared to Geziret Sineita, Geziret Umm Igrim/Agram, or Geziret Abu Qeih). Surficial deposits are characterized by thin, shallower sandy deposits but more fine-grained material.

5.3 Anomalies of potential former river courses

For the western delta, the ΔNDWI anomalies were found over two abandoned river channels in the vicinity of Buto and Kom el-Khawaled. Both anomalies followed the courses of former levees. These courses were delineated using the TanDEM-X DEM as the levees are slightly more elevated than the floodplains. The observed ΔNDWI anomalies were caused by lower NDWI index values in summer, which indicate lower soil and/or plant moisture on average. This interpretation is supported, as the levees offer better drainage and are likely composed of coarser-grained deposits (Brown, 1997). Both sites display area-wide homogeneous land cover (as far as this is identifiable in modern high-resolution satellite imagery), which is an ideal setting for the detection of anomalies using the proposed approach.

The interpretation of the ΔNDWI anomalies suggests a connection between Kom el-Khawaled, Kom el-Garad, and Kom el-Nashwia and supports the proposed connection of Kom el-Arab and Kom-Alawi by a former river branch.

Similar linear, stretched ΔNDWI anomalies were found in the eastern Nile Delta in the direct vicinity of the ancient site of Bubastis and also north of Zagazig. These were interpreted as former branches of the Nile for this region, potentially of the Pelusiac or Tanitic Nile (Bietak, 1975; Tronchère et al., 2012). Compared to the anomalies found over the geziras, these were, however, less distinct (i.e., ΔNDWI anomalies were of lower magnitude), and no indication of former levees was found in the TanDEM-X DEM. The results of these anomalies therefore require more careful interpretation. They might indicate former branches of the Nile; however, the Landsat data do not allow further classification. Nevertheless, taking the information of the SoE maps into account, the potential channels have been abandoned for at least 100 years. The anomalies might indicate promising locations for future ground-based investigations, e.g., for drillings and electric resistivity surveying, which have been successfully applied to detect near-surface fluvial deposits across the delta on varying spatial scales (e.g., Andres and Wunderlich, 1991; El Gamili et al., 2001; El-Qady et al., 2011; Lange-Athinodorou et al., 2019).

6 Summary and conclusion

The paper investigated spatial-temporal metrics (STMs) of the Landsat system using remote sensing time-series data between 1985 and 2019 acquired over the Nile Delta. Comparisons to a formerly verified abandoned river branch in the northwestern delta close to Buto made clear that significant anomalies are present for some STMs over the proposed location of the former channel. The extent and location of this channel were best revealed by differencing the median NDWI values of the summer (July/August) and winter (January/February) seasons (ΔNDWI). The observed difference is likely due to lower soil/plant moisture during summer (i.e., months with high evapotranspiration). This may be caused by coarser-grained deposits and/or the morphology of the former levee. Further analyses of the ΔNDWI over the eastern Nile Delta showed similar anomalies (i.e., significantly lower summer NDWI values) in the immediate surroundings of several geziras and tells. This allowed, at least to some extent, the identification and mapping of the potential near-surface continuation of these landforms. Such anomalies were not observed for the surroundings of tells of the western Nile Delta. Additional, linear and meandering ΔNDWI anomalies were found in the eastern Nile Delta in the immediate surroundings of Bubastis, as well as several kilometers north of Zagazig. These anomalies might indicate former courses of Nile river branches (i.e., most likely of the Pelusiac and/or the Tanitic Nile). However, the ΔNDWI does not allow an unambiguous interpretation. The analyses have shown that the Landsat archive is promising for (geo-)archeological questions, especially in the context of landscape archeology. A transfer of the methodology to similar environments seems feasible considering the relatively simple approach, the global availability of the Landsat data, and the benefits that arise from the cloud processing in the Google Earth Engine. Future research will continue analyzing the ΔNDWI for the entire delta but will also investigate other spatiotemporal metrics that can be deduced from the Landsat time series (cf. Ginau et al., 2017). Furthermore, the benefit of including additional imagery from passive (e.g., MODIS, Sentinel-2) or active (e.g., Sentinel-1) remote sensing sensors will be assessed.

Data availability. The digital elevation model of the TanDEM-X mission is shown with the permission of the German Aerospace Center (DLR), Germany, © DLR 2015–2020. The data were requested via the proposal DEM_HYDR1426 (principal investigators: Andreas Ginau, Robert Schiestl, Jürgen Wunderlich, Eva Lange-Athinodorou, and Tobias Ullmann). A free version of the TanDEM-X digital elevation model with decreased spatial resolution is available via EOC Geoservice (https://download.geoservice.dlr.de/TDM90, last access: 30 November 2020, EOC Geoservice, 2020). Landsat images are provided freely by the U.S. Geological Survey (USGS) via Earth Explorer (https://earthexplorer.usgs.gov, last access: 30 November 2020, USGS, 2020). Landsat data were accessed via the Google Earth Engine (https://earthengine.google.com, last access: 30 November 2020, Gorelick et al., 2017, https://doi.org/10.1016/j.rse.2017.06.031). Imagery of the CORONA mission is available via the "CORONA Atlas of the Middle East" (https://corona.cast.uark.edu, last access: 30 November 2020, CAST, 2020).

Author contributions. The methodology was developed by TU, JT, and LN. Funding was acquired by TU and ELA. The project was administered by TU, RB, and ELA. The formal analysis was conducted by TU, JT, LN, and RS. All authors interpreted the results jointly. The manuscript was prepared by TU and JM with contributions from all authors.

Competing interests. The authors declare that they have no conflict of interest.

Special issue statement. This article is part of the special issue "Geoarchaeology of the Nile Delta". It is a result of the workshop "Geoarchaeology of the Nile Delta: Current Research and Future Prospects", Würzburg, Germany, 29–30 November 2019.

Acknowledgements. We warmly thank Katharine Thomas for proofreading the paper and the two anonymous reviewers for their valuable comments and suggestions on our paper.

Financial support. This research has been partially funded by the research fund of the Faculty of Philosophy of the University of Würzburg (Die Sakrallandschaft von Bubastis: Geoarchäologische Untersuchungen zu den heiligen Wasserkanälen des Tempels der Bastet).

This open-access publication was funded by Julius-Maximilians-Universität Würzburg.

Review statement. This paper was edited by Jan-Hendrik May and reviewed by two anonymous referees.

References

Andres, W. and Wunderlich, J.: Late Pleistocene and Holocene Evolution of the Eastern Nile Delta and Comparisons with the Western Delta, Erdkundliches Wissen, Düsseldorf, pp. 121–130, 1991.

Ashmawy, A. A.: Tell Gemaiyemi "Gomaimah", more than 100 years after Griffith's excavations, in: Timelines: studies in honour of Manfred Bietak, edited by Czerny, E., Hein, I., Hunger, H., Melman, D., and Schwab, A., Peeters, Dudley, Massachusetts, USA, 2006.

Ballet, P. and von der Way, T.: Exploration archéologique de Bouto et de sa region (époques romaine et byzantine), Mitteilungen des Deutschen Archäologischen Instituts, Abteilung Kairo, 49, 1–22, 1993 (in French).

Ballet, P., Lecuyot, G., Marouard, G., Pithon, M., and Redon, B.: Et la Bouto Tardive?, Bulletin de l'institut français d'archéologie orientale, 111, 75–93, 2011.

Bietak, M.: Tell el-Dab'a II, Der Fundort im Rahmen einer archäologisch-geographischen Untersuchung über das ägyptische Ostdelta, Untersuchungen der Zweigstelle Kairo des Österreichischen Archäologischen Instituts 1, Wien, 1975.

Bietak, M. and Goedicke, H.: Tell el Dab'a II: Der Fundort im Rahmen Einer Archäologisch-Geographischen Untersuchung Über das Ägyptische Ostdelta, Journal of the American Research Center in Egypt, 14, 115, https://doi.org/10.2307/40000374, 1975.

Brown, A. G.: Alluvial geoarchaeology: floodplain archaeology and environmental change, Cambridge University Press, Cambridge, New York, 1997.

Butzer, K. W.: Early hydraulic civilization in Egypt: a study in cultural ecology, Univ. of Chicago Press, Chicago, 1976.

Casana, J. and Cothren, J.: The CORONA Atlas Project: Orthorectification of CORONA Satellite Imagery and Regional-Scale Archaeological Exploration in the Near East, in: Mapping Archaeological Landscapes from Space, Springer New York, New York, 33–43, 2013.

Center for Advanced Spatial Technologies (CAST): Corona Atlas & Referencing System, University of Arkansas, U.S. Geological Survey, available at: https://corona.cast.uark.edu/, last access: 30 November 2020.

El Beialy, S., Edwards, K., and El-Mahmoudi, A.: Geophysical and palynological investigations of the Tell El Dabaa archaeological site, Nile Delta, Egypt, Antiquity, 75, 735–744, https://doi.org/10.1017/S0003598X00089249, 2001.

Elfadaly, A., Abate, N., Masini, N., and Lasaponara, R.: SAR Sentinel 1 Imaging and Detection of Palaeo-Landscape Features in the Mediterranean Area, Remote Sens., 12, 2878, https://doi.org/10.3390/rs12182878, 2020.

El-Gamili, M. M., Shaaban, F. F., and El-Morsi, O. A.: Electrical resistivity mapping of the buried stream channel of the Canopic branch in the western Nile Delta, Egypt, J. Afr. Earth Sci., 19, 135–148, https://doi.org/10.1016/0899-5362(94)90046-9, 1994.

El Gamili, M. M., Ibrahim, E. H., Hassaneen, A. R. Gh., Abdalla, M. A., and Ismael, A. M.: Defunct Nile Branches Inferred from a Geoelectric Resistivity Survey on Samannud area, Nile Delta, Egypt, J. Archaeol. Sci., 28, 1339–1348, https://doi.org/10.1006/jasc.2001.0761, 2001.

El Mahmoudi, A. and Gabr, A.: Geophysical surveys to investigate the relation between the Quaternary Nile channels and the Messinian Nile canyon at East Nile Delta, Egypt, Arab. J. Geosci., 2, 53–67, https://doi.org/10.1007/s12517-008-0018-9, 2009.

El-Qady, G., Shaaban, H., El-Said, A., Ghazala, H., and El-Shahat, A.: Tracing of the defunct Canopic Nile branch using geoelectrical resistivity data around Itay El-Baroud area, Nile Delta, Egypt, J. Geophys. Eng., 8, 83–91, https://doi.org/10.1088/1742-2132/8/1/010, 2011.

EOC Geoservice: TanDEM-X – Digital Elevation Model (DEM) – Global, 90 m, Earth Observation Center (EOC) Geoservice of the German Aerospace Center (DLR), available at: https://download.geoservice.dlr.de/TDM90/, last access: 30 November 2020.

Favard-Meeks, C.: Tell Sueilin, in Studies on Ancient Egypt in honour of H. S. Smith, edited by: Tait, W. J., Smith, H. S., Leahy, A., and Egypt Exploration Society, Egypt Exploration Society, London, 83–96, 1999.

Flaux, C., El-Assal, M., Marriner, N., Morhange, C., Rouchy, J.-M., Soulié-Märsche, I., and Torab, M.: Environmental changes in the Maryut lagoon (northwestern Nile delta) during the last ∼2000 years, J. Archaeol. Sci., 39, 3493–3504, https://doi.org/10.1016/j.jas.2012.06.010, 2012.

Franzmeier, H.: Ein Brunnen in der Ramses-Stadt: zur Typologie und Funktion von Brunnen und Zisternen im Pharaonischen Ägypten, Gebrüder Gerstenberg, Hildesheim, 2010 (in German).

Ginau, A., Schiestl, R., Kern, F., and Wunderlich, J.: Identification of historic landscape features and settlement mounds in the Western Nile Delta by means of remote sensing time series analysis and the evaluation of vegetation characteristics, J. Archaeol. Sci.-Rep., 16, 170–184, https://doi.org/10.1016/j.jasrep.2017.09.034, 2017.

Ginau, A., Schiestl, R., and Wunderlich, J.: Integrative geoarchaeological research on settlement patterns in the dynamic landscape of the northwestern Nile delta, Quatern. Int., 511, 51–67, https://doi.org/10.1016/j.quaint.2018.04.047, 2019.

Goiran, J.-P., Marriner, N., Morhange, C., Abd El-Maguib, M., Espic, K., Bourcier, M., and Carbonel, P.: Évolution géomorphologique de la façade maritime d'Alexandrie (Égypte) au cours des six derniers millénaires, Mediterranee, 104, 61–64, https://doi.org/10.4000/mediterranee.2132, 2005 (in French).

Google Earth Engine: https://earthengine.google.com/, last access: 30 November 2020.

Gorelick, N., Hancher, M., Dixon, M., Ilyushchenko, S., Thau, D., and Moore, R.: Google Earth Engine: Planetary-scale geospatial analysis for everyone, Rem. Sens. Environ., 202, 18–27, https://doi.org/10.1016/j.rse.2017.06.031, 2017.

Habachi, L.: Khatâana – Qantîr: Importance, Annales du Service des Antiquités de l'Égypte, 52, 443–562, 1954.

Hartung, U., Ballet, P., Effland, A., French, P., Hartmann, R., Herbich, T., Hoffmann, H., Hower-Tilmann, E., Kitagawa, C., Kopp, P., Kreibig, W., Lecuyot, G., Lösch, S., Marouard, G., Nerlich, A., Pithon, M., and Zink, A.: Tell el-Faracin – Buto: 10. Vorbericht, Mitteilungen des Deutschen Archäologischen Instituts, Abteilung Kairo, 65, 83–190, 2009.

Kalayci, T., Lasaponara, R., Wainwright, J., and Masini, N.: Multispectral Contrast of Archaeological Features: A Quantitative Evaluation, Remote Sens-Basel, 11, 913, https://doi.org/10.3390/rs11080913, 2019.

Kauth, R. J. and Thomas, G. S.: The Tasselled Cap – A Graphic Description of the Spectral-Temporal Development of Agricultural Crops as Seen by LANDSAT, in: LARS Symposium on Machine Processing of Remotely Sensed Data, 29 June–1 July 1976, Purdue University West Lafayette, Indiana, United States, Paper Number 159, 1976.

Kenawi, M.: Alexandria's Hinterland: Archaeology of the Western Nile Delta, Egypt, Archaeopress Publishing Ltd., Oxford, United Kingdom, 2014.

Lange-Athinodorou, E., El-Raouf, A. A., Ullmann, T., Trappe, J., Meister, J., and Baumhauer, R.: The sacred canals of the Temple of Bastet at Bubastis (Egypt): New findings from geomorphological investigations and Electrical Resistivity Tomography (ERT), J. Archaeol. Sci.-Rep., 26, 101910, https://doi.org/10.1016/j.jasrep.2019.101910, 2019.

Lanna, S.: Kôm el-Ghoraf: osservazioni per una ricostruzione storica del Delta occidentale nei periodi romano e bizantino, Aegyptus, 85, No. 1 /2, La pratica della religione nell'antico Egitto: Atti del X Convegno Nazionale di Egittoloia e Papirologia Roma, 1–2 febbraio 2006 (Gennaio–Dicembre 2005), 339–363, 2005 (in Italian).

Marcolongo, B.: Évolution du paléo-environnement dans la partie orientale du Delta du Nil depuis la transgression flandrienne (8000 BP) par rapport aux modèles de peuplement anciens, Cahiers Recherches l'Institut Papyrologie d'Egyptologie Lille, 14, 23–31, 1992 (in French).

Marriner, N., Flaux, C., Morhange, C., and Kaniewski, D.: Nile Delta's sinking past: Quantifiable links with Holocene compaction and climate-driven changes in sediment supply?, Geology, 40, 1083–1086, https://doi.org/10.1130/G33209.1, 2012.

Moshier, S. O. and El-Kalani, A.: Late Bronze Age paleogeography along the ancient Ways of Horus in Northwest Sinai, Egypt, Geoarchaeology, 23, 450–473, https://doi.org/10.1002/gea.20227, 2008.

Nill, L., Ullmann, T., Kneisel, C., Sobiech-Wolf, J., and Baumhauer, R.: Assessing Spatiotemporal Variations of Landsat Land Surface Temperature and Multispectral Indices in the Arctic Mackenzie Delta Region between 1985 and 2018, Remote Sens-Basel, 11, 2329, https://doi.org/10.3390/rs11192329, 2019.

Pennington, B. T. and Thomas, R. I.: Paleoenvironmental surveys at Naukratis and the Canopic branch of the Nile, J. Archaeol. Sci.-Rep., 7, 180–188, https://doi.org/10.1016/j.jasrep.2016.03.053, 2016.

Pennington, B. T., Sturt, F., Wilson, P., Rowland, J., and Brown, A. G.: The fluvial evolution of the Holocene Nile Delta, Quatern. Sci. Rev., 170, 212–231, https://doi.org/10.1016/j.quascirev.2017.06.017, 2017.

Petrie, W. M. F.: Tanis: Part I., 1883-4, Egypt Exploration Fund Memoir 2, Trübner & Co, London, United Kingdom, 1885.

Petrie, W. M. F.: Tanis: Part II., Nebesheh (Am) and Defenneh (Taphanes), Trübner & Co, London, United Kingdom, 1888.

Said, R.: The Geological Evolution of the River Nile, Springer New York, New York, 1981.

Seton-Williams, M. V.: The Tell El-Farâ'în Expedition, 1968, J. Egypt. Archaeol., 55, 5–22, https://doi.org/10.1177/030751336905500102, 1969.

Sewuster, R. J. and van Wesemael, B.: Tracing Ancient River Courses in the Eastern Nile Delta: a Geo-archaeological Survey in the Sarqiya Province, Egypt, University of Amsterdam, 1987.

Sewuster, R. J. E., van Wesemael, B., and Laboratorium, U. van A. F.-G. en B.: Tracing Ancient River Courses in the Eastern Nile Delta: A Geo-archaeological Survey in the Sarqiya Province, Egypt, University of Amsterdam, 1987.

Sist, L.: Kom el-Ghoraf. Indagine archeologica di un sito nel Delta, in: Imagines et iura personarum. L'uomo nell'Egitto antico per i novanta anni di Sergio Donadoni, Atti del IX Convegno Internazionale di Egittologia e Papirologia Palermo, 10–13 novembre 2004, Studi e Ricerche 48, edited by: Minà, P., Palermo, 243-249, 2006 (in Italian).

Stanley, D. J. and Warne, A. G.: Nile Delta: Recent Geological Evolution and Human Impact, Science, 260, 628–634, https://doi.org/10.1126/science.260.5108.628, 1993a.

Stanley, D. J. and Warne, A. G.: Sea level and initiation of Predynastic culture in the Nile delta, Nature, 363, 435–438, https://doi.org/10.1038/363435a0, 1993b.

Stanley, D. J., McRea, J. E., and Waldron, J. C.: Nile Delta drill core and sample database for 1985–1994: Mediterranean Basin (MEDIBA) Program, Sm. C. Mar. Sci., 37, 1–428, https://doi.org/10.5479/si.01960768.37.1, 1996.

Stanley, J.-D. and Jorstad, T. F.: Short contribution: Buried Canopic channel identified near Egypt's Nile delta coast with radar (SRTM) imagery, Geoarchaeology, 21, 503–514, https://doi.org/10.1002/gea.20117, 2006.

Trampier, J., Toonen, W., Simony, A., and Starbird, J.: Missing Koms and Abandoned Channels: The Potential of Regional Survey in the Western Nile Delta Landscape, J. Egypt. Archaeol., 99, 217–240, https://doi.org/10.1177/030751331309900110, 2013.

Trampier, J. R.: Landscape Archaeology of the Western Nile Delta, Vol. 2 of Wilbour Studies in Egypt and Ancient Western Asia, Lockwood Press, Atlanta, 2014.

Tronchère, H., Goiran, J.-P., Schmitt, L., Preusser, F., Bietak, M., Forstner-Müller, I. and Callot, Y.: Geoarchaeology of an ancient fluvial harbour: Avaris and the Pelusiac branch (Nile River, Egypt), Geomorphologie, 18, 23–36, https://doi.org/10.4000/geomorphologie.9701, 2012.

U.S. Geological Survey (USGS): "EarthExplorer", available at: https://earthexplorer.usgs.gov/, last access: 30 November 2020.

van den Brink, E. C. M.: A Geo-Archaeological Survey in the North-Eastern Nile Delta, Egypt; the First Two Seasons, a Preliminary Report, Mitteilungen des Deutschen Archäologischen Instituts, Abteilung Kairo, 43, 7–31, 1986.

van Haarlem, W. M.: Temple deposits in early dynastic Egypt: the case of Tell Ibrahim Awad, BAR Publishing, Oxford., 2019.

van Haarlem, W. M.: An Introduction to the site of tell Ibrahim Awad, Ägypten und Levante/Egypt and the Levant, 10, 13–16, 2000.

van Wesemael, B. and Dirksz, P.: The Relation between the Natural Landscape and the Spatial Distribution of Archaeological Remains, in: The archaeology of the Nile Delta, Egypt: problems and priorities? edited by: van den Brink, E. C. M., Netherlands Foundation for Archaeological Research in Egypt, Amsterdam, 1988.

Wilson, P. and Grigoropoulos, D.: The West Nile Delta Regional Survey, Beheira and Kafr el-Sheikh provinces, Egypt Exploration Society, London, 2009.

Wunderlich, J.: Investigations on the development of the Western Nile Delta in Holocene times, in The archaeology of the Nile Delta, Egypt: problems and priorities?, edited by: van den Brink, E. C. M., Netherlands Foundation for Archaeological Research in Egypt, Amsterdam, 1988.

Wunderlich, J.: Untersuchungen zur Entwicklung des westlichen Nildeltas im Holozän, Im Selbstverlag der Marburger Geographischen Gesellschaft, Marburg/Lahn., 1989 (in German).

Wunderlich, J. and Ginau, A.: Paläoumweltwandel im Raum Tell el Fara'in/Buto. Ergebnisse und Perspektiven geoarchäologischer Forschung, in Gedenkschrift für Werner Kaiser, edited by: Polz, D. and Seidlmayer, S. J., Mitteilungen des Deutschen Archäologischen Instituts, Abteilung Kairo, 485–498, 2016.

Yan, Y., Zhu, J., Yan, Q., Zheng, X., and Song, L.: Modeling shallow groundwater levels in Horqin Sandy Land, North China, using satellite-based remote sensing images, J. Appl. Remote Sens., 8, 083647, https://doi.org/10.1117/1.JRS.8.083647, 2014.

Yoyotte, J.: Tells oublies de la region de San, in Cahiers de Tanis I. Mission Française des Fouilles de Tanis, vol. 1, edited by Brissaud, P., A. D. P. F., Paris, 107–113, 1987.

E&G Quaternary Sci. J., 70, 129–143, 2021
https://doi.org/10.5194/egqsj-70-129-2021

Open Access E&G Quaternary Science Journal

Research article

Sandhills, sandbanks, waterways, canals and sacred lakes at Sais in the Nile Delta

Penelope Wilson[1] **and Hosni Ghazala**[2]

[1]Department of Archaeology, Durham University, Durham DH1 3LE, United Kingdom
[2]Geology Department, Mansoura University, Mansoura, Dakhalia Governorate, Egypt

Correspondence: Penelope Wilson (penelope.wilson@durham.ac.uk)

Relevant dates: Received: 30 July 2020 – Revised: 7 April 2021 – Accepted: 16 April 2021 – Published: 25 May 2021

How to cite: Wilson, P. and Ghazala, H.: Sandhills, sandbanks, waterways, canals and sacred lakes at Sais in the Nile Delta, E&G Quaternary Sci. J., 70, 129–143, https://doi.org/10.5194/egqsj-70-129-2021, 2021.

Abstract: The paper explores the relationship between the archaeological zones of the ancient city of Sais at Sa el-Hagar, Egypt, and the natural landscape of the western central Nile Delta and, in particular, the extent to which the dynamic form of the landscape was an element in the choice of settlement location. Furthermore, settlement at Sais has been determined to have existed at several locations in the immediate environs of the current archaeological zones from the Neolithic period, around 4000 BCE (Before Common Era), to the modern day, suggesting that the local environment was conducive to sustainable settlement, culminating in the establishment of a capital city in the 7th century BCE. The nature of the settlement, its immediate environs and waterway systems will, thus, be described, based on correlation of geological, geophysical, remote sensing and archaeological data, in order to establish if and when human interactions in the landscape can be determined to be reactive or proactive.

Kurzfassung: Der Beitrag untersucht die Beziehung zwischen den archäologischen Arealen der antiken Stadt Sais (heute: Sa el-Hagar, Ägypten) und der natürlichen Landschaft des westlichen Zentrums des Nildeltas und insbesondere, welche Rolle die dynamische Landschaftsentwicklung bei der Wahl des Siedlungsstandortes spielte. Dies geschieht vor dem Hintergrund, dass von der neolithischen Periode um 4000 v. Chr. bis in die Neuzeit verschiedene Siedlungsareale an mehreren Stellen in der unmittelbaren Umgebung der heutigen archäologischen Bereiche von Sais existierten, was darauf hindeutet, dass die lokale Umwelt dieses Ortes günstige Bedingungen für eine nachhaltige Besiedlung bot, ein Umstand, der in der Etablierung von Sais als Hauptstadt Ägyptens im siebten Jahrhundert v. Chr. gipfelte. Basierend auf der Korrelation von geologischen, geophysikalischen, Fernerkundungs- und archäologischen Daten wird dementsprechend im Folgenden der Charakter der Siedlung, ihrer unmittelbaren Umgebung und des zugehörigen Flussnetzes im Hinblick darauf beschrieben, ob eine auch zeitlich genauer zu fassende Bestimmung menschlicher Interaktionen mit der Landschaft als reaktiv oder proaktiv möglich ist. *(Abstract was translated by Eva Lange-Athinodorou.)*

Published by Copernicus Publications on behalf of the Deutsche Quartärvereinigung (DEUQUA) e.V.

1 Introduction

The archaeological site of Sais at Sa el-Hagar, Gharbiyah Governorate, Egypt (Fig. 1), has been studied since 1997, within its palaeo- and modern landscape, through a programme of archaeological survey and excavation combined with geoelectrical resistivity and magnetic survey as well as a manual drill coring programme (Wilson, 2006). The overall aim of the work was to understand the relationship and interactions between the archaeological settlement areas and the natural landscape features, in particular the waterways and buried sandbanks, from the period of the first human settlement at the site in Neolithic times, ca. 4000 BCE (Before Common Era), until the present day (Wilson et al., 2014). Furthermore, the dynamics of the landscape and human activity can be analysed for information about the extent to which the choice of area for settlement was dictated by naturally occurring favourable conditions, such as buried sand features and/or levees or levees, or by human political and economic choices connected with land and river management (Hritz, 2014, pp. 230–243). This paper will analyse the extent to which different types of data from geophysical, archaeological, remote sensing and ancient textual information can be combined to correlate and extend the interpretation of single data sets, in order to track waterways, buried sandhills, human settlement and other landscape interventions over the longue durée of 6000 years at Sa el-Hagar in a floodplain dominated by an ancient river system.

2 Methods

The study area is the floodplain the west of the Rashid (Rosetta) branch of the Nile where there are a number of towns and villages within a drain and canal network, mostly consolidated in the 19–20th century by the engineers of Muhammad Ali and the Ministry of Public Works (Barois, 1904, pp. 119–124). First, to reconstruct the palaeolandscape of the area, the University of Mansoura team made 19 deep-drill cores, up to 23 m deep, and six transects of 41 vertical electrical soundings (VESs; using a Schlumberger array) to trace the development of the landscape from the Pleistocene to the Holocene eras (Fig. 2; Ghazala, 2005; El-Shahat et al., 2005).

In addition, information from historical satellite imagery, such as CORONA and Google Earth, and from individual Landsat 5 images was also compared with the geophysical survey data to detect subsurface relict waterways (Abrams and Comer, 2013; see Pope and Dahlin, 1989; for Egypt, see Wunderlich, 1989). Then, from 1999 onwards, the geoarchaeological programme of the Durham–Ministry of Antiquities mission made over 300 shallow cores with a manual Eijkelkamp drill auger in the area (Wilson, 2006). The analysis of the core material showed that the human material culture layers usually do not extend beyond 6 to 7 m below the ground surface, except in some higher ground in the Kom Rebwa archaeological area. Deposits recorded in augers in the surface and buried archaeological zones included reworked primary settlement material, buried primary archaeological strata and, in some places, up to 8 m of continuous anthropogenic strata and layers of archaeological material apparently separated by alluvial sediments. Elsewhere, the augers contained purely geological sediments consisting of silts, hard compact clay and sandy-silt mixtures, as well as medium and fine sands (Wilson, 2006). Further data were collected from archaeological excavations (Ex's) in the Great Pit area (Ex 8) and in Kom Rebwa (Ex's 1–12), where fine-grained archaeological strata can be compared with drill auger data from the same place (Wilson, 2011; Wilson et al., 2014) to correlate the two sets of material more closely, to provide an understanding of anthropogenic material within drill cores and to integrate the geological and archaeological material. Finally, an ancient textual source was compared with the excavated and survey data to determine the limits of the source in answering specific questions without further topographical information. The correlation of the data can be used to refine chronological developments of human activity as it was played out in the dynamic floodplain environment.

3 The geological framework

Analysis of the underlying geology of the delta has identified the following four main phases and strata (Pennington, 2017; Pennington et al., 2017): at the base, the Mit Ghamr formation comprises Pleistocene medium coarse sands with an uneven surface, created by downcutting river systems (in some areas, the Mit Ghamr surface is covered by a layer of aeolian and reworked fluvial sand); next, and key to the period of human activity in the delta, is the deposition of the Bilqas 2 mud around 8000–7000 BP (Before Present) upon the surface of the Pleistocene fluvial sand, creating an undulating topography in the delta, with some sandhills, dynamic anastomosing channel networks, swampy floodplain and peat formation in some areas. Starting in the central and southern delta, there was a transition from the large-scale crevassing action of the river to the meandering river channels (Pennington et al., 2016) and from the Bilqas 2 muds to the Bilqas 1 layer around 6000–5500 BP, so that, by ca. 4500 BP, all of the delta was covered in Bilqas 1 sediments. This layer of brown silt clay ranged from 2 to 9.9 m thick and contains limestone nodules and gypsum rosettes according to periods of warm, arid conditions. The upper alluvial mud is essentially the layer in which human activity is detected.

In the Sa el-Hagar area, the detailed geological reconstruction of the area (Fig. 3) is based on the VES and deep-drill cores (Ghazala, 2005; Ghazala et al., 2005) and modelled scenarios of the main geologic strata from deep cores and the shallow-core drilling programme (Pennington, 2017, pp. 176–183). The analyses suggests that buried sandhills are located under the village of Kawady northeast of Sais, run-

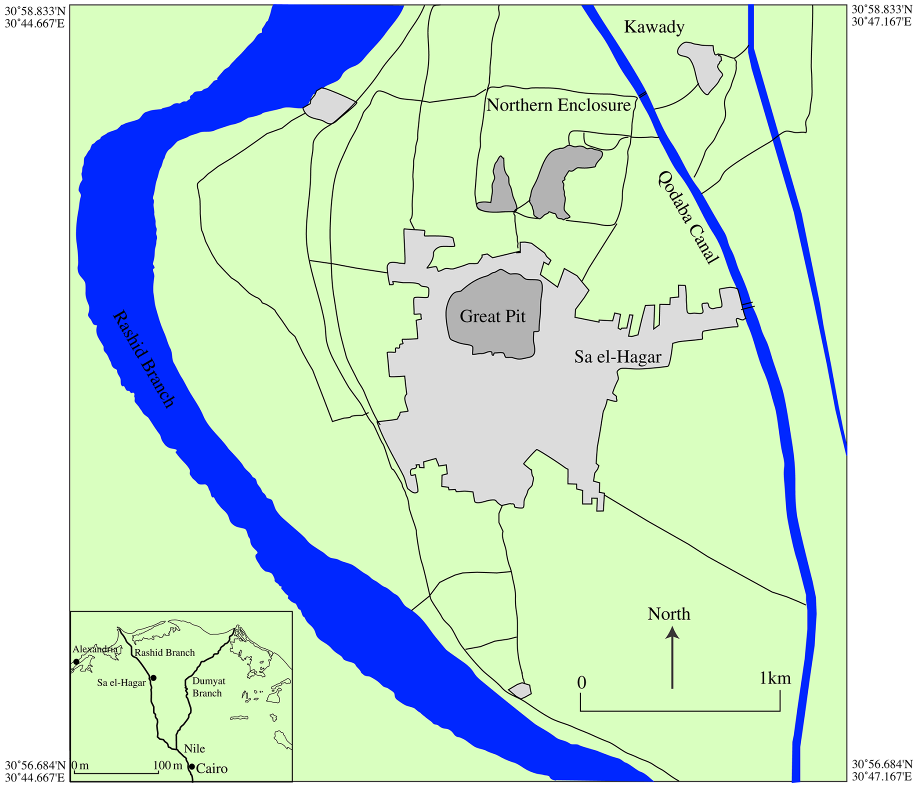

Figure 1. Map showing the location of the area of Sais, the archaeological zones and the modern town of Sa el-Hagar in the Nile Delta.

ning southward, and another sandbank runs along the eastern river bank on the western side of the area. In the region, other buried, elevated sands lie to the west of Basioun and in a large body running north to south to the east of the Sais area. The latter may have been a significant sand body separating the western river channels (the Canopic and Saitic branches) from the Sebennytic branch running through the centre of the delta.

The uneven Mit Ghamr surface also suggests that there were deep swampy basins north of Sais and, potentially, the course of a deep, older river channel to the east of Basioun flowing northward to Shubra Tana but with a distributary branching west, under what is now called the Great Pit, then turning in a meander back to the northeast and under what is now called the Northern Enclosure. A younger channel, mirroring the channel of the distributary but just a little south of it, has also been detected on the western side of the village of Sa el-Hagar and west of the Northern Enclosure. It seems likely that, over time, the river has continued this westward meander to its present location, leaving behind reworked sandbars on the inside of the bend of the modern Rashid or Rosetta branch at Sa el-Hagar. The environment in the period 4000–3500 BCE could be characterised as one of swamps and anastomosing river course, with higher land in isolated locations (Pennington, 2017, pp. 180–183), therefore making it ideal for settlement and river exploitation during the Neolithic period.

4 Data correlations

This section discusses the correlation of different types of data and their analysis.

4.1 Correlating geological survey and drill augers to the south of Sa el-Hagar

Shallow drill augers to the southeast of the village of Sa el-Hagar (Fig. 4), contained thick bands of bivalve mollusc shells, confirming the reconstruction of a series of channels or waterbodies here at one time, i.e. the cores labelled C107, C103, C102, C101 and C182 and C183 (Fig. 5). The thick shell bands were also associated with silts and sands that were blueish or turquoise in colour and were, thus, at the interface between the Bilqas 1 and Mit Ghamr formation. C119 and C120 to the east, and between the two transects above, are shown for comparison without the thick bands of shell material and only have a few fragments representing the floodplain of the channels. It can also be noted that C107 and C102 had pottery fragments underneath the shell layers, suggesting that prehistoric human activity had been interrupted by a new channel in the same location (see below).

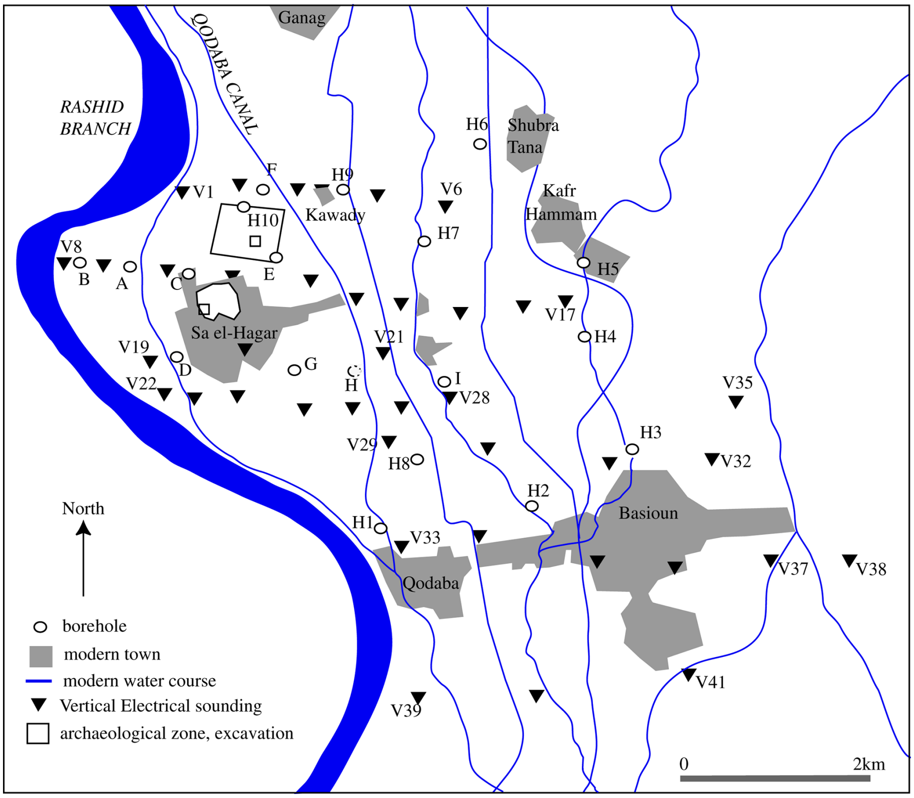

Figure 2. Area of Sa el-Hagar with the location of VES transects and deep-drill augers (after Ghazala, 2005).

4.2 Correlating the geophysical model, remote sensing data and drill auger data

The proposed younger channel has left a strong signal in satellite imagery and drill augers on the western side of the Northern Enclosure archaeological area. A Landsat 5 TM (thematic mapper) image of wavelength 5 (shortwave infrared; USGS, 2020) shows a dark band along the western side of the enclosure, almost parallel to it, due to relative water retention of sediments, and is most likely to be related to grain-size effects of buried river branches (see Ullmann et al., 2020; this Special Issue; Fig. 6). The band is an average of 200 m in width, similar to the narrow part of the modern Rashid branch bend at Sa el-Hagar.

A transect of the drill augers (C5, C191, C189, C63; Fig. 5) in the location of the band (Fig. 7) shows an upper 2.8 m of sediments with anthropogenic material in it, including broken limestone, orthoquartzites and pottery; then there are bands of finer silts and sands with broken bivalve mollusc shells (*Cyrenidae* family) in a 30 cm thick band, from 4 to 4.30 m below the ground surface in C189 and 3.5–4 m below the surface in C191. In the latter cores, the shell and sediment deposits continue for as much as 6.68 m belowground. But in C189, the core has a band of further anthropogenic material; apparently the channel cut into a previous area of human activity or deposition of material. In C189, there was especially dense anthropogenic material, and in fact, the core was stopped when the drill head hit a stone and could not proceed further at 7.25 m below the ground.

The pottery and other burnt material recovered from the lower part of the cores was potentially Predynastic in date, and this depth of material might well link with the prehistoric layers to the south in Ex 8 (see below). The satellite image, thus, seems to show the buried presence of a filled-in channel, with the sediments on top of the shell layer retaining more water than the sediments on either side. Such a strong signal cannot be detected in the satellite imagery elsewhere in the Sa el-Hagar area, and it may be that elsewhere the surface layers are too disturbed or built over by modern structures, as in the area to the south of Sa el-Hagar.

4.3 Correlating geological soundings and archaeological excavation

The river channel shift from the Great Pit area to the west can perhaps be detected in archaeological excavations in the Great Pit. A date can also be suggested for the movement of the channel. In Ex 8, the earliest level found was a fish midden of the Neolithic period, ca. 4300–4000 BCE, after radiocarbon dating and comparison of the pottery and lithics with other Neolithic sites in Egypt (Wilson el al., 2014). By correlating the archaeological section and drill augers (Fig. 8), it

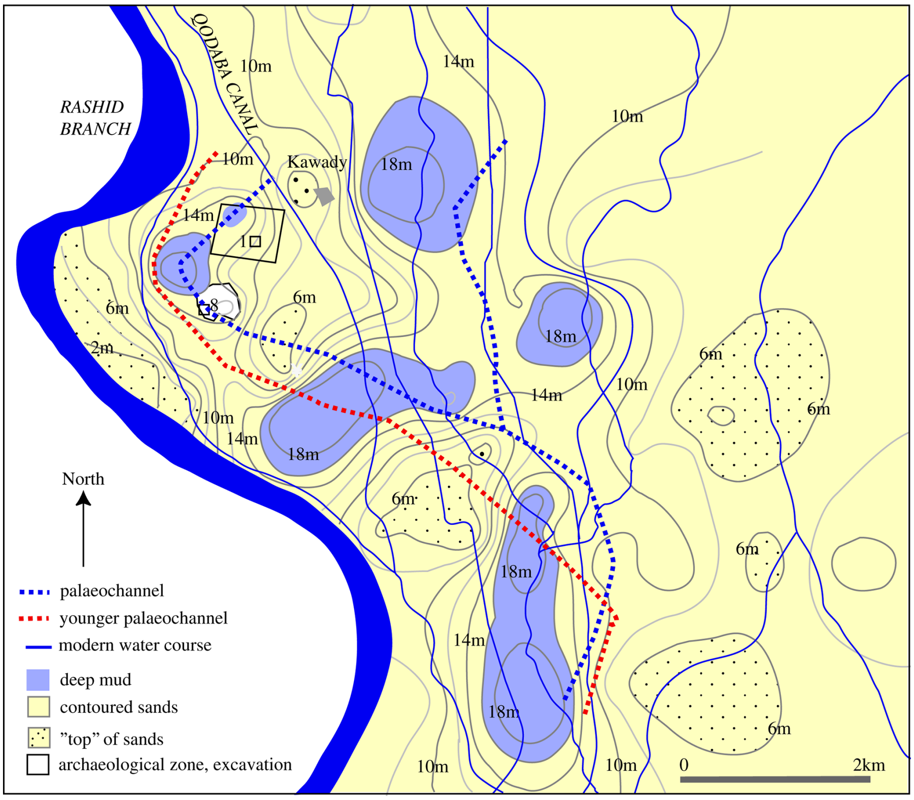

Figure 3. Map of the Sa el-Hagar area, with reconstructed subsurface sand contours up to 18 m below the ground, and the palaeochannel locations.

seems that the fish midden was situated on the western side of a riverbank (Mit Ghamr formation), which was then subject to flooding (Bilqas 1), and a settlement was established in the same location, which had evidence for semi-domesticated cattle, pigs and sheep goats. The area may have been subject to an arid period before the inundation increased to such an extent that the settlement area was abandoned and left to alluvial deposition (Bilqas 2) for some time until a reoccupation in the Buto–Maadi period, ca. 3500 BCE. The change in the alluvial regime could represent the shift of the river from the older channel to the younger channel, at which point human activity, if not settlement, resumed on the alluvium in the same place, at around 3500 BCE, until the Early Dynastic period around 3000 BCE, but was then situated on the eastern bank of a river channel.

The date of the change between 4000 and 3500 BCE seems to agree well with recent radiocarbon dates and pollen data from Sa el-Hagar (Zhao et al., 2020) that show the beginning of cultivated (domesticated) *Poaceae* cereal in the area during a period of warmer climate and expansion of the wetlands between 4750–3850 BCE (zone III), followed by a drier period with shrinkage of the wetland 3850–3550 BCE (zone IV) and then the recovery of the wetland from 3550–2250 BCE before the onset of a global, drier arid event 2250–2050 BCE. The key period of zones III to IV, when the older deep channel was abandoned through reduced water burden or a crevasse splay, was detected from coring at depths of 6.32 to 5.48 m below the ground (e.g. C41 in the north (Fig. 4) and C107 and C102 in the southeast; Fig. 5), consistent with reaching the Neolithic levels in Ex 8. In C107, there were blue-green coloured silts at the end of the core, and from this location, the bank of a possible water body would be on the same trajectory as the bank in Ex 8. Furthermore, C107 has a thick layer of settlement and anthropogenic material under the shell layer, but it is on top of coarse sands, at about 6.4 m below the ground surface, which may be redolent of the Pleistocene sand surface. The change in the river channel may have meant the replacement of human activities focussed on the exploitation of the river and water bodies in the Neolithic period, with humans settling on alluvial land with high areas and swampy backwaters that were attractive for settlement and exploitation of the agricultural, wetland and riverine resources in the Late Predynastic and Early Dynastic periods (ca. 3500–3000 BCE; Wilson, 2014).

The stratigraphic record, however, cannot be followed further in the Ex 8 area because, directly upon the Buto–Maadi period layers, is material from the destroyed structures dating to the Saite period at the end of the 6th century BCE. It seems likely that, in the Saite period, the area was cleared down to the sandy sediments for the purpose of founding new

Figure 4. Map of drill core transects discussed in the article in the area of Sa el-Hagar. This figure has been generated from QGIS (Quantum GIS) and satellite images. © Google Earth.

monumental structures in the area. Whatever happened there in the intervening 2800 years was removed by human action, demonstrating that, although riverine activity can have short-term and long-term impacts, human intervention on geological layers can also be substantial.

5 Analysing the archaeological data from drill cores

According to the scenarios above, the current configuration of the river to the west, and perhaps other channels to east, of Sa el-Hagar suggests that there has been little change since the beginning of the Dynastic period and that anthropogenic material occurs in the 6 m or so of alluvium after the Bilqas 1–Bilqas 2 transition. The identification of settlement layers and alluvial layers from drill cores alone, without contextual data, can be difficult. At Sa el-Hagar there are areas of positive archaeological settlement data, which can help in the analysis of core material where there are no other contextual data.

5.1 Northern Enclosure – monumentalised settlement

The Northern Enclosure area, although much flattened and denuded now, once contained massive mud brick and stone structures, including an enclosure wall some 700 m by 680 m in dimension, which is now reduced to a track (Wilson, 2006, pp. 99–115). The archaeological material in the enclosure has been extensively removed so that it is not even certain that this was the location of the famous temple of Neith. The drill augers have proved useful in the enclosure, not only identifying the depth of settlement and archaeological material but also, in some places, the nature of that material (Figs. 4, orange dots, and 9).

A transect across the Northern Enclosure (Fig. 9) shows the landscape in which the settlement is situated and the deep bands of human material culture (Wilson, 2006, pp. 180–202). C53 is the channel, and its in-fill is to the west of the Northern Enclosure described above. The area seems to be virgin land and has no anthropogenic material in it, i.e. archaeological material defined as pottery, stone, burnt mate-

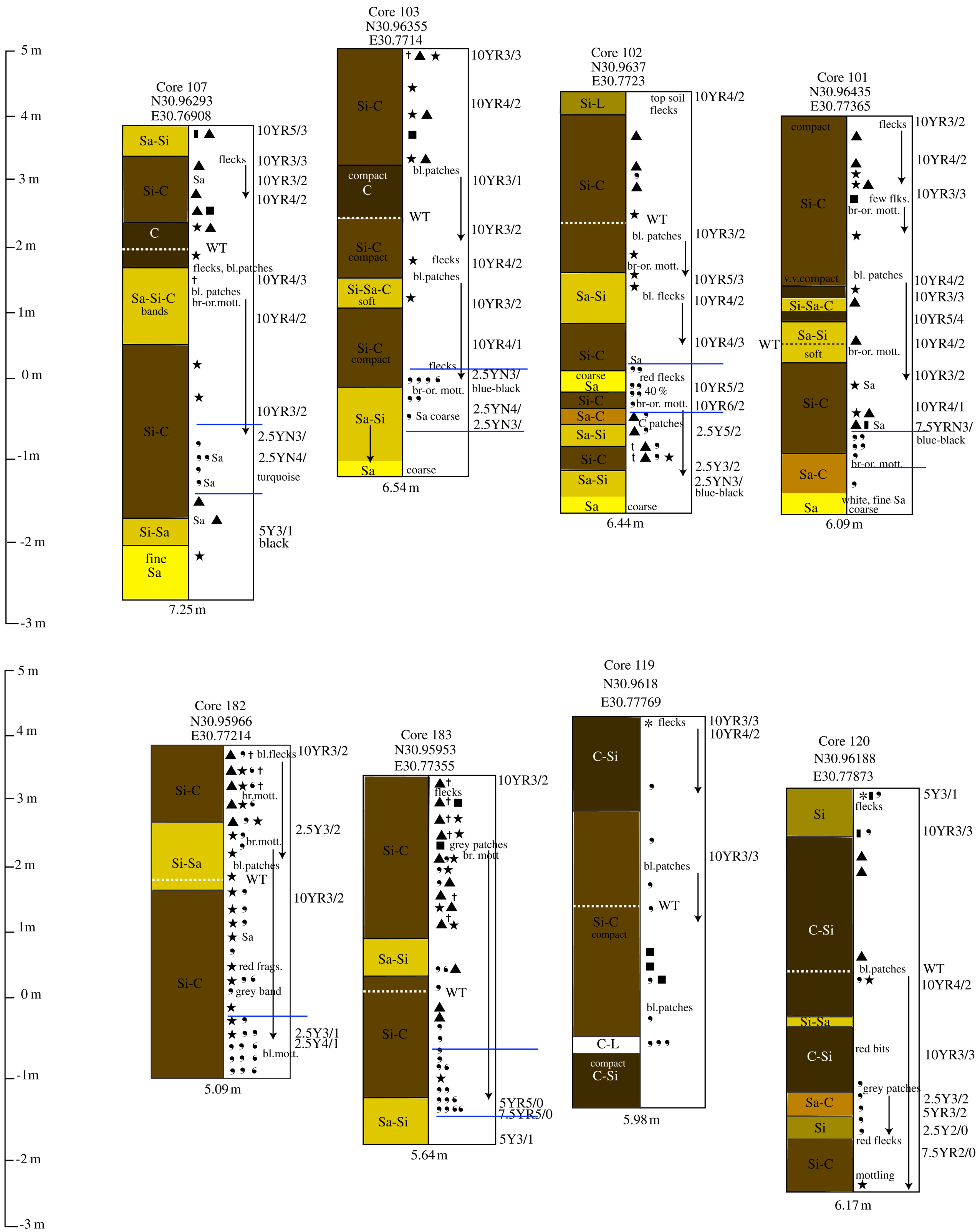

Figure 5. Transects southeast of Sa el-Hagar showing the following thick shell bands (blue lines): C107, C103, C102, C101 and C182 and C183, with C119 and C120 for comparison (see Fig. 13 for the key to cores).

Figure 6. Extract from Landsat 5 data, showing the subsurface water features west of the Northern Enclosure at Sa el-Hagar (water absorbs infrared energy and gives no return; thus, this detail appears to be greyish black). Base map source: USGS Landsat 5; 14 February 1998 (original image courtesy of the U.S. Geological Survey).

rial and bone concentrations. By contrast, C54, just inside the enclosure, shows dense stone fragment layers, which are the remains of destroyed stone structures in the top 5 m of the core. The stone fragments are of limestone, granite and orthoquartzite, especially in a band 4–5 m below the ground, and these were the standard materials used for monumental structures. The stone layer is directly situated upon compact clay, which could be a natural levee acting as a foundation or a mud brick construction, in turn, upon other settlement material. The sequence may suggest that there was a building or gateway in the western side of the enclosure built upon pre-existing settlement layers. Earlier human activity was evidenced within alluvial layers, to a depth of at least 8 m below the modern ground level in C54. C52, to the east of C54 inside the Northern Enclosure, has silt clay and clay upper material, and there is a stone debris layer between 4 and 5 m from ground level, perhaps the foundations of a stone structure, apparently upon clay mud, with a thin band of pottery at 6.25 m signalling an initial settlement layer upon compact clay river levee material. C50 in the northern wall of the enclosure also has thick layers of stone debris (limestone, granite and orthoquartzite) with pottery for a depth of almost 7 m, including a black gloss sherd, with brown and orange-red bands (3.5 × 2.7 × 0.4 cm; C50 and C43) that may be east Greek in origin, and this, thus, points to a date in the 7th–6th century BCE. The latter would directly suggest a Saite period date for some aspect of the stone structure, and its depth at 5.22 m below ground level shows the difficulties of dating archaeological layers in terms of the depth alone. There are also thick layers of stone material, for example in C57 between 4.5 and 6 m below the ground. But above the stone debris is a band of anthropogenic material, from 3.14 to 4.5 m, suggesting that the stone debris is from an earlier phase of monumental building in the eastern part of the enclosure. It may be that the stone structures were reorganised in a new phase of the site's history. In the eastern enclosure wall it is possible that the upper metre is the last part of the mud brick wall, which seems to have been founded on earlier settlement material, including an alluvial or mud band between and 2 and 3 m below ground. Other stone debris was recorded at the entrance to the Northern Enclosure in C47 and C48 (not illustrated), where the drill head could not penetrate the debris easily; this may suggest a gateway entrance to the enclosure or part of a monumental area.

As the enclosure is an identifiable archaeological zone with two low mound areas known that are protected Antiquities land, it is not unexpected to find considerable evidence of human activity, as detailed above. But the material from the cores can be directly compared with material from archaeological excavations, especially in Ex 1. Starting from datable layers and working downward through known archaeological features, the information from the drill cores can be contextualised, to some extent. C58 was drilled through a mud brick wall dating to the late Ramesside period (ca. 1189–1077 BCE) and was compared with subsequent excavation in this area (Wilson, 2011, p. 25; Fig. 25). The wall was known to have a height of over 1 m but was not completely excavated; in the core, the upper 1.64 m was a homogeneous mixture of silt clay with some pottery fragments, which is expected as walls were constructed by reusing settlement muds with pottery added for strength. The base of the wall seemed to be indicated by a layer of sand, possibly within a foundation trench or on top of earlier settlement debris to a depth of 2.76 m and aligned in the excavation section with the base of a series of ovens constructed in the area enclosed by the wall. The excavation ended after about 3 m of depth from the ground level due to reaching the water table and a layer of mud with blueish-black clay lumps in it, which was perhaps an alluvial layer. Pottery dating to the Old Kingdom had been found in this lower level. The drill core was able to proceed further, reaching the base of the alluvial layer at 3.64 m from its start, and another strong settlement layer was encountered, possibly topped by a burial ground due to the bones found between 3.64 and 4.9 m. The drill auger then continued through alluvial layers, including an apparent in-filled channel at 6.7–8 m, and through a compact clay levee down to 9.5 m. In archaeological terms, the presence of Old Kingdom layers within alluvial mud underlying the New Kingdom material is interesting. Little Middle Kingdom material has been found at Sais, and the period is regarded as having had high inundations (Vercoutter, 1966; Bell, 1975), which may have affected settlements adversely. The alluvial band between the two dateable settlement layers may thus

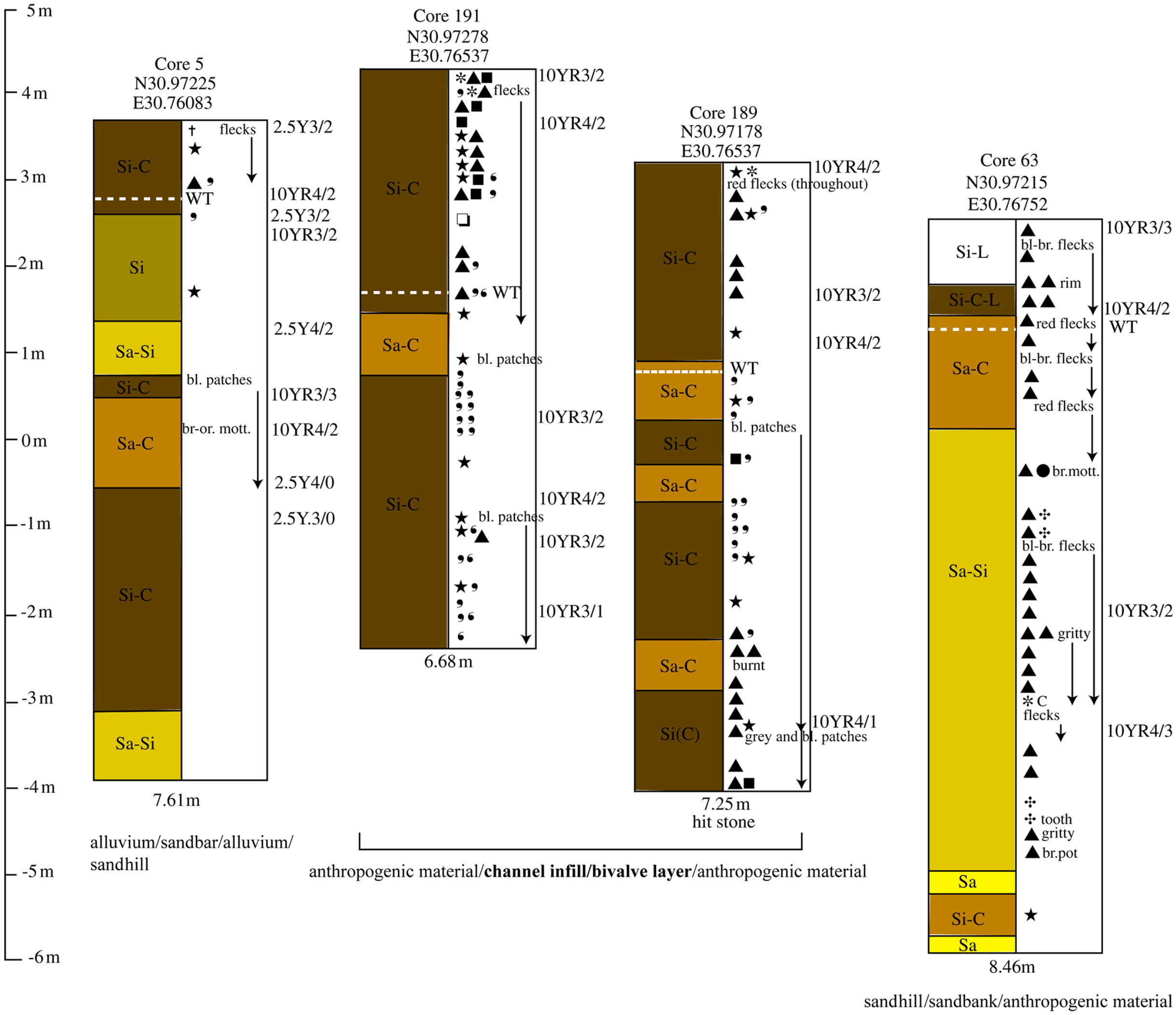

Figure 7. Transect (cores 5, 191, 189, 63) to the west of the Northern Enclosure, showing the channel and difference between alluvial and archaeological zones. Ground heights are taken from TanDEM-X data. (See Fig. 13 for the key to cores.)

be significant, implying that the old settlement area had been flooded. In the eastern side of the enclosure, C160 was made through Ex 5, and C161 was made through Ex 6. In Ex 5, upper levels dating to the Third Intermediate Period (TIP), ca. 1000–800 BCE, were found to be upon a cemetery, perhaps of the New Kingdom, and contained disturbed material from the late Second Intermediate Period, ca. 1500 BCE; Ex 6 had a similar stratigraphy but was closely dated by TIP structures lying over early New Kingdom burials (ca. 1400 BCE). In the drill cores, there were several phases of settlement material from the ground surface, with changes in the matrices perhaps indicating phases of activity. The drill core information is useful in pinpointing the depths of archaeological material that are otherwise not possible to access. With better typologies of the pottery, it may be possible to have more confidence in dating the small, but numerous, fragments that have been collected from the drill cores, as has been done at Buto (Hartung et al., 2009, pp. 172–188) and at Thebes (Toonen et al., 2017). In C161, there was almost constant settlement debris to a depth of 8.88 m below the ground, suggesting long-lived and continuous human activity over a long period, especially allowing for the fact that the upper level begins at about 800 BCE, because any later settlement material has been removed. The deepest hand-drilled core in the enclosure area is C8, to a depth of 10.51 m at the edge of the eastern side of the Antiquities land (not illustrated). This core has deep strata of possible reworked anthropogenic material – which means that the layers are not so well defined, but there is good deal of pottery and other material – to 4.75 m and then alluvial layers or solid mud material in bands upon a thin layer of degraded pottery fragments at 7.8 to 8 m and compact alluvial levee clay to 10.5 m. It seems, therefore, that below the 8 m limit there is no anthropogenic material at the site, and we may regard this as the Neolithic boundary. Similarly, Man-

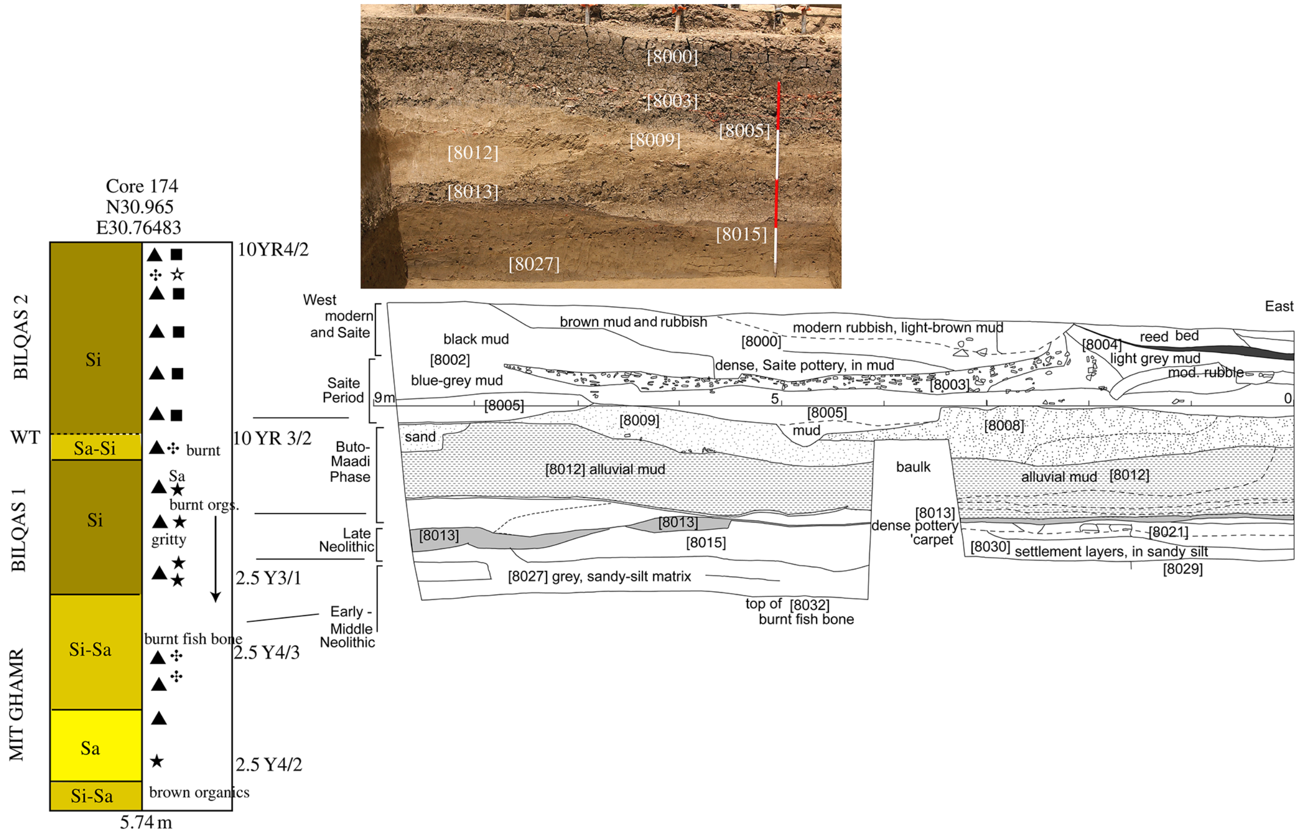

Figure 8. Correlation of archaeological strata in excavation 8 with drill core 174. Original data were taken from Angus Graham. (See Fig. 13 for the key to cores.)

soura cores E, to a depth of 11 m, and H10 (for location, see Fig. 2), to a depth of 16 m, detected anthropogenic material only in the upper 6 m of the cores.

5.2 Kawady sandhill and archaeology

A second archaeological zone is at Kawady (Ezbet Mohamed Ismail) to the northeast of the Saite area, where there is a buried sandhill (Figs. 2 and 3). According to theories of settlement patterns in Ancient Egypt, such a high-sand area should have provided an attractive place for settlement on the sides of the sandbank, with cemeteries being placed on the top to avoid the annual flooding. Excavations by the Egyptian Antiquities Service in 1961–1962 and 1965 discovered an elite cemetery area to the west of Kawady village, most likely consisting of a mausoleum structure that had contained limestone and basalt sarcophagi and a shrine to a local saint called Wahibre in the Saite period (Bakry, 1968). Drill cores in this area have located the sand lying relatively close to the surface, overlain by sandy silts that are often blue–black in colour (Fig. 11).

On top of these sands are strong anthropogenic signals from the ground level as far as the sand, suggesting that, indeed, this sandhill was an attractive area for human activity. In C20, C21 and C23, the stone debris in bands down to 1.5 m below the ground may correlate with the Saite elite cemetery area. Further work is needed on the identification of the pottery fragments to show whether this area was used from much earlier periods. The drill cores and vertical electrical soundings from villages further to the east at Shubra Tana, Kafr and Bahr el-Hamam also suggest that there is archaeological material at depth here. Although coring in all places has indicated human material culture in the upper layers, including observed Roman amphorae, deeper deposits have only been identified in Kafr el-Hamam C2 (G6) between 2 and 4 m, which may well be ancient, but it is unclear how ancient. The pattern of waterways, the positioning of settlements and the Roman–Late Roman material from some of the villages may suggest that this area was part of the irrigation system established during the Roman period in the area. As the system is visible in the current landscape, it cannot be very ancient, i.e. Late Roman or medieval at most, and is more likely from the 19th century during the irrigation projects from the Muhammad Ali era onwards.

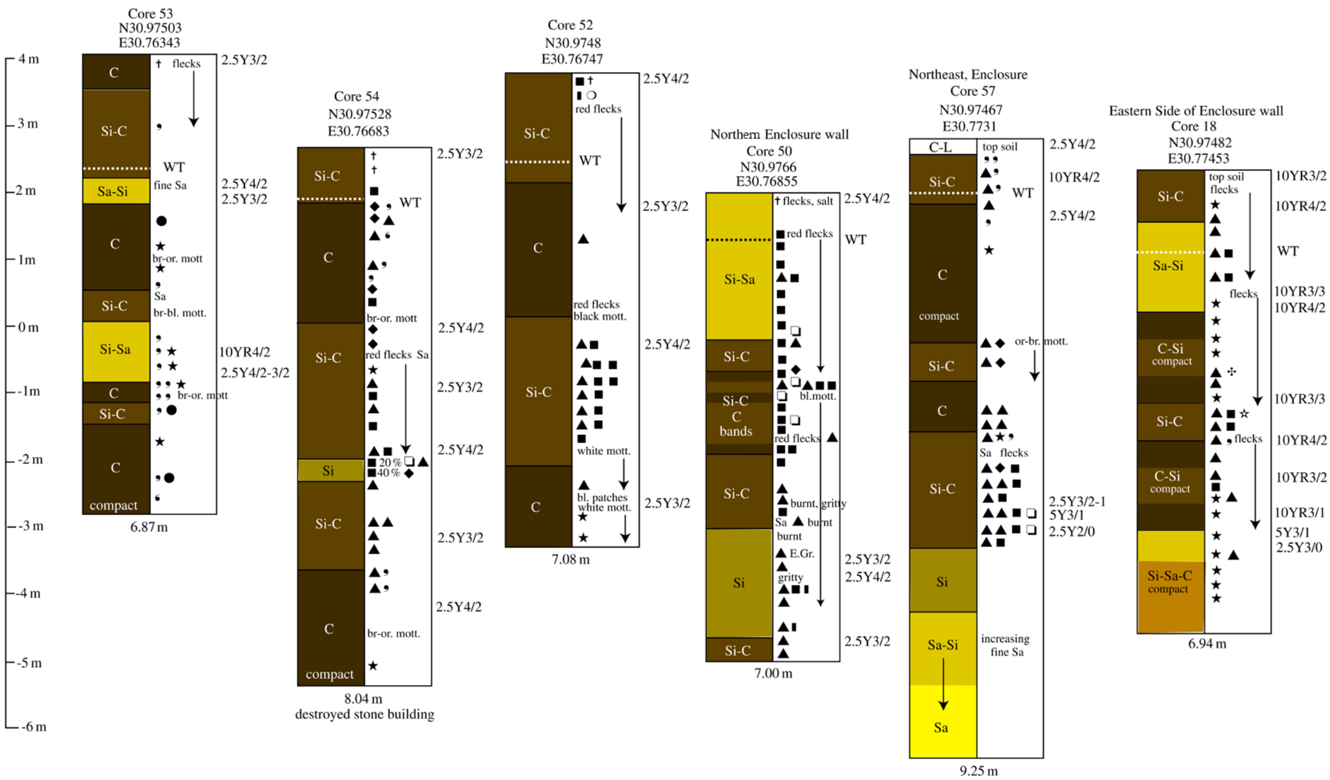

Figure 9. Transect of drill cores across the Northern Enclosure at Sa el-Hagar (C53, C54, C52, C50, C57 and C18) (see Fig. 13 for the key to cores).

5.3 A new southern settlement?

The geological reconstruction of the area to the southeast (Fig. 3) shows buried high ground that may also have been a focus for human activity that is no longer visible as an archaeological zone but can be detected in drill augers. Analysis of the core data has determined the following four types of core data at Sais: (1) human (anthropogenic) material culture (HMC) for the whole length of the drill core, with a high level of confidence that pottery, for example, had not dropped down into the borehole from the upper layers of the cores (Fig. 9, C50; Fig. 10, C161; Fig. 12, C155); (2) a layer of HMC at the top band, then a gap of alluvial material before a further buried band of HMC (Fig. 12, C143); (3) HMC in a strong or weak band in the top 1.2 m of the core (Fig. 12, C148); (4) strongly indicated HMC in the lower bands of the core. In the case of type (3), such cores can perhaps be taken cautiously as being the kind of archaeology they indicate. If the HMC content is weak and consists of top-soil-containing material from manuring or is in the modern town where settlement layers can be thick, then it may indicate relatively modern activity.

In the agricultural area south of Sa el-Hagar, type (2) drill auger cores, comprising two bands of HMC separated by alluvium, are evidenced by 25 drill cores in the area southeast of the village alone, mostly in the area that was flooded by the palaeochannel that moved to the west. In a transect across the area (Fig. 4 red dots; Fig. 12), the upper layers of human material culture, for example in C148, contain fired brick and sherds that may be from the Roman period and modern material. The settlement material in the lower core bands, for example C143 and C151, is overlain and on top of alluvium and channel deposits and is not easy to date due to the small size of the pottery fragments. The fact that the material is in dense bands, along with some charcoal and brown-orange mottling suggests that the anthropogenic material is a primary deposit, and it is also spread over a wide area. The presence of another archaeological zone at Sa el-Hagar raises questions about what would have been the settlement or even the urban constitution of ancient Sais. With areas in the north, in the Great Pit and under the modern village, and to the southeast and perhaps areas around Sais, the conurbation seems to be a loose federation of settlements, perhaps operating at slightly different chronological time frames, but suggesting a dynamic and changing urban catchment area that was responsive to changes in the alluvial character of the river and its branches.

6 Ancient topographies

There is a description of part of the topography of Sais from an inscription on a granite statue in the Greco-Roman

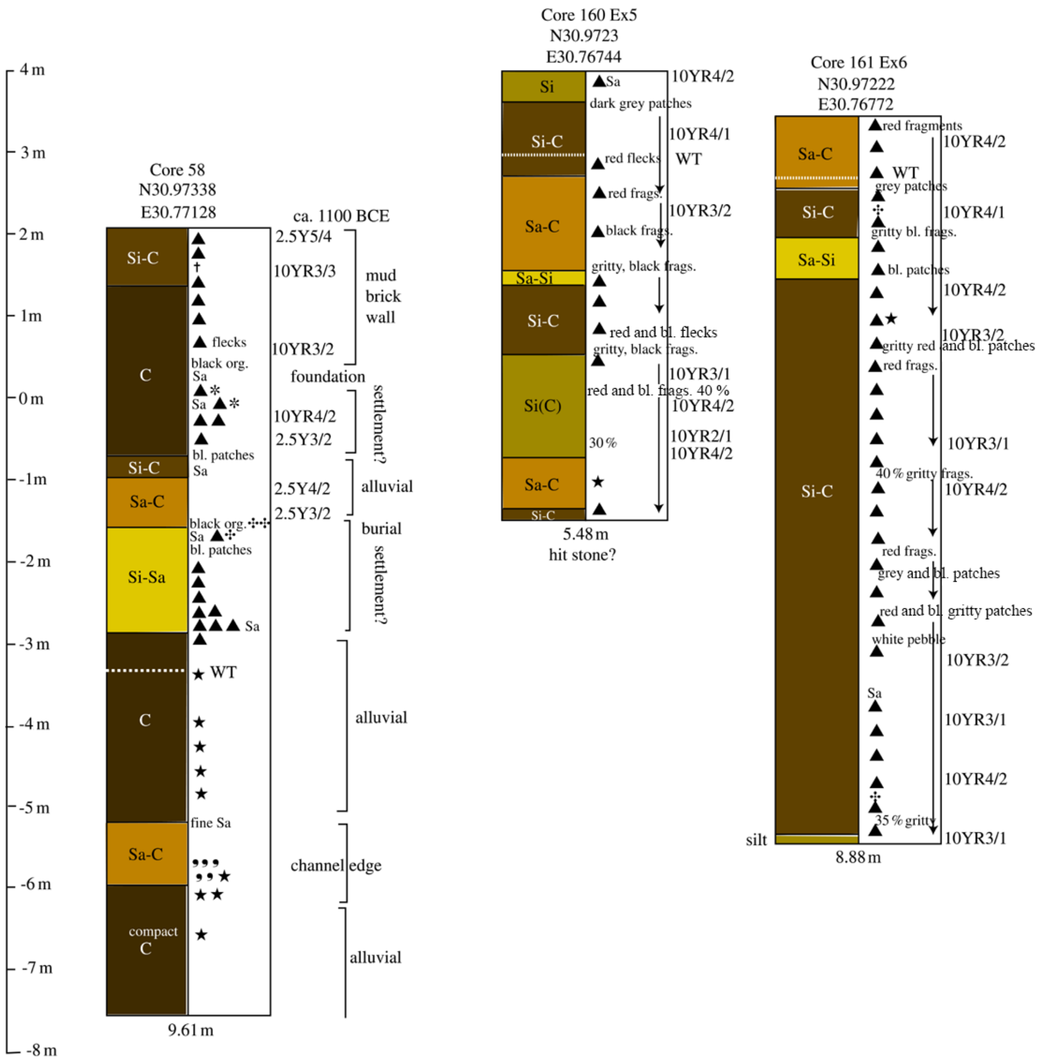

Figure 10. Drill cores in excavation trenches for Ex 1 (C58), Ex 5 (C160) and Ex 6 (C161) (see Fig. 13 for the key to cores).

museum in Alexandria (inventory no. 26532). The headless statue of man kneeling to present an offering table records the excavation of a lake at Sais by the "Administrator of the temples of Neith, Lector Priest, great Physician of Pharaoh, Royal Chancellor and Sole Companion Horkhebi" (Bakry, 1970; Geßler-Löhr, 1983, pp. 233–237). The decree from Ahmose II for the lake's construction was to enable water to be provided for purification purposes in the temple of Neith.

> I excavated the lake on the east side of the *Wuwu* Canal; its width was 68 cubits, its length of 65 cubits and built of [lime]stone, 8 stairways in it and walls around it.

The lake would have been a stone-lined structure with dimensions of around 34 by 32.5 m, perhaps like the sacred lake at the Dendera temple in upper Egypt, for example (it is about 25 by 35 m in size and lined with sandstone blocks). The location "east of the Double Canal" may suggest that a local canal system could feed water into the lake to keep the lake supplied. The writing with two quail chick signs between two canal signs has suggested the translation "Double Canal", but can the inscription be used to locate either the sacred lake or the "Double Canal"? And how does this fit within the geoarchaeological topography of Sais as a whole? The sacred lake should have been in the sacred enclosure area near the temple of Neith, which was most likely in the Northern Enclosure. In this case, the canal would be to the west of the enclosure and may have been in the channel noted there and described above. The lake would be somewhere in the area of the western part of the enclosure. Unfortunately, the inscription does not give enough information to be certain about where to look for the sacred lake, although the buried stone debris features noted above may, at some point in the future, prove to be indicators of some such feature. The ancient texts then provide details which cannot yet be verified

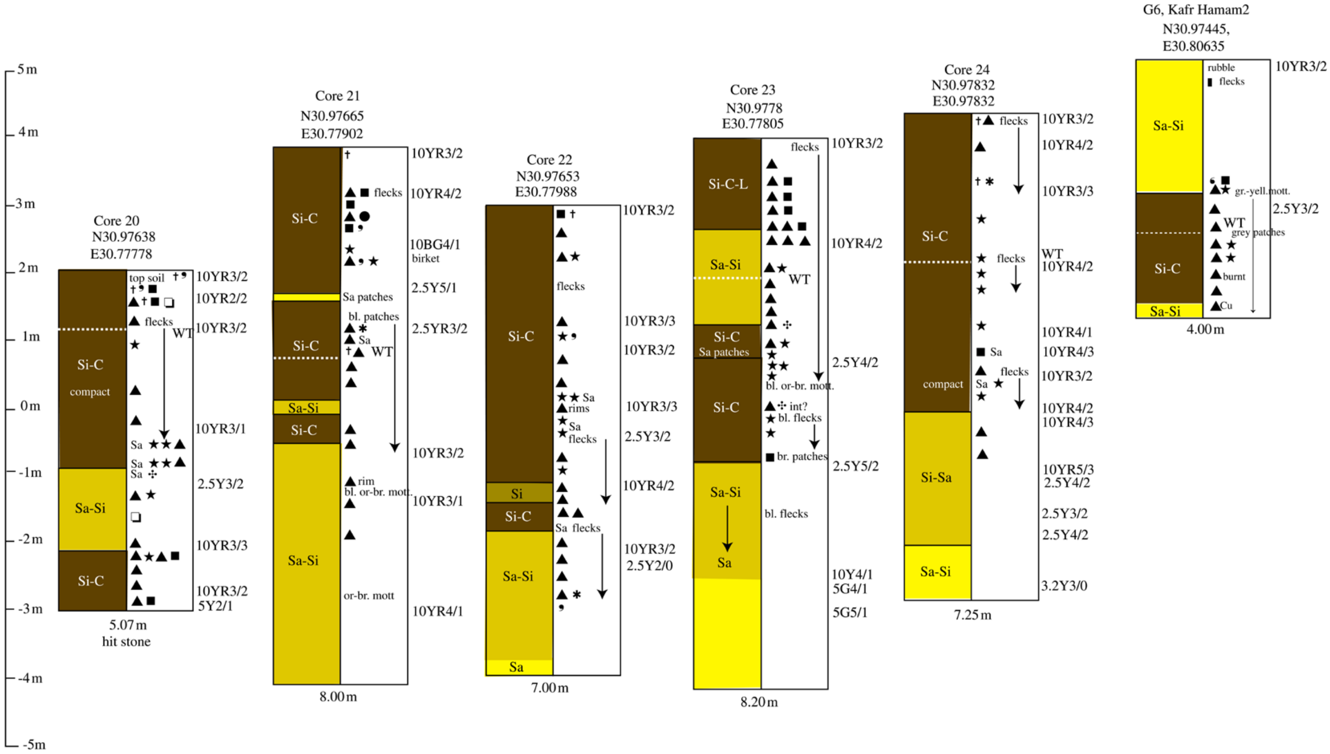

Figure 11. Transect in the Kawady elite cemetery area (C20, C21, C22, C23, C24 and KH2) (see Fig. 13 for the key to cores).

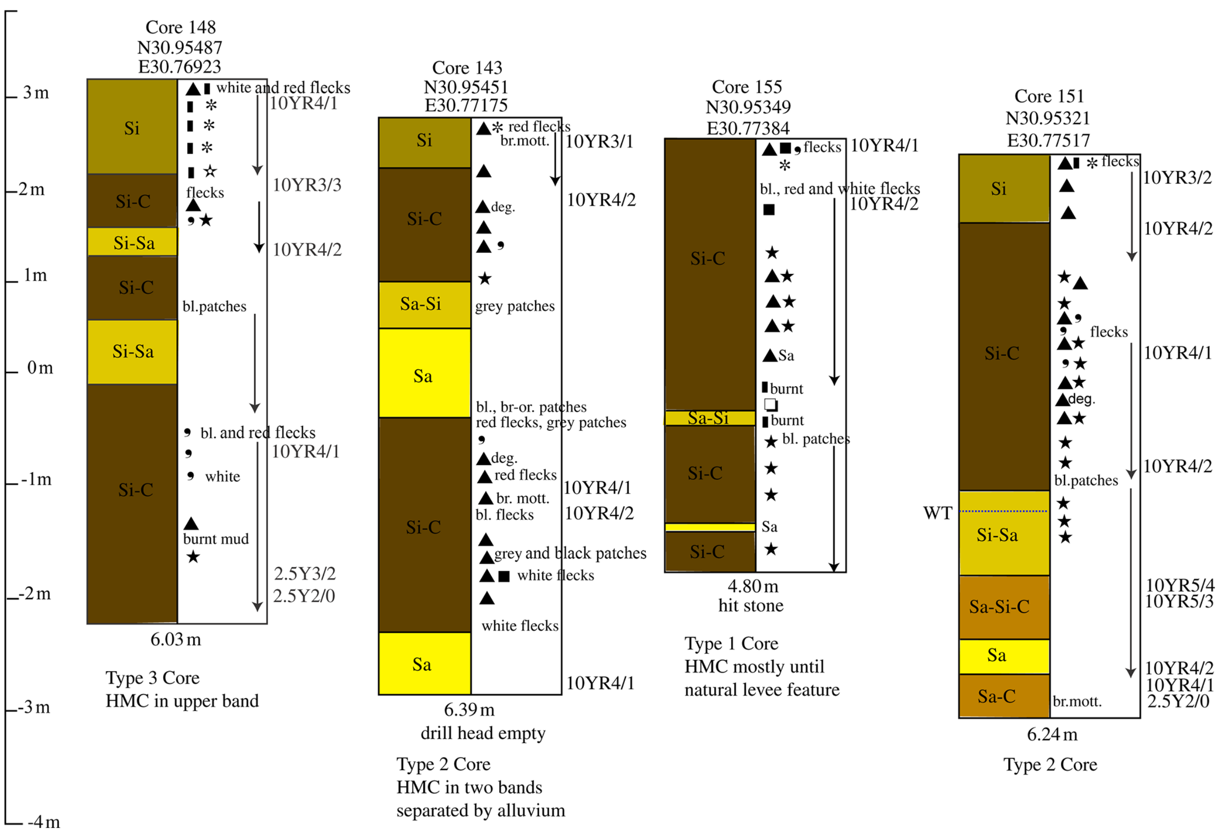

Figure 12. Transect south of Sa el-Hagar (C148, C143, C155 and C151) (see Fig. 13 for the key to cores).

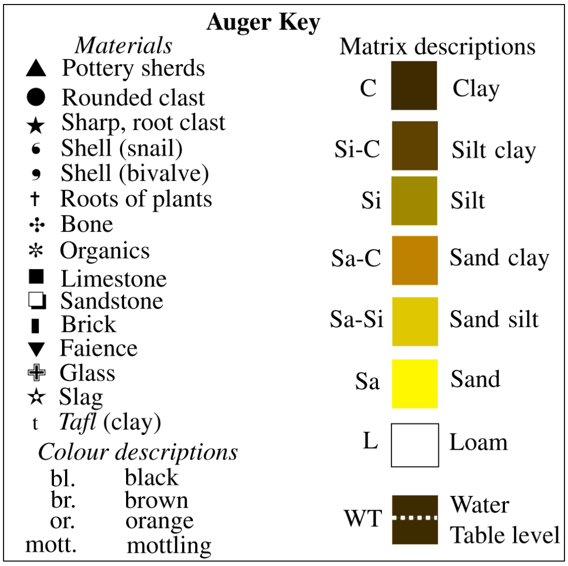

Figure 13. Key for the auger logs.

on the ground and, so, are limited in specific identifications of water features at Sais.

7 Summary

The analysis of the subsurface material contributes to understanding why the area at Sais area was suitable for sustained settlement. First, the underlying sand and channels of the meandering river system meant that there was always some high, non-flooded land available, either because it was naturally high or humanly managed so that it was high (settlement tell) and dry (mud brick enclosure), with high ground for a cemetery. Second, the period of the initiation of the deposition of the Bilqas mud was a decisive change in settlement and riverine exploitation at Sais. The old palaeochannel system with Neolithic settlement on the west bank of the channel was replaced by a more stable river system, with settlements on the east bank. Third, the Sais archaeological zone is extensive, with settlements changing their original locations in the area, being abandoned and then returning to previously inhabited places. The complex record therefore contains evidence of human reactions to larger environmental changes and proactive interventions in the construction of agricultural and settlement facilities.

By linking some of the archaeological material with geological data, it is possible to go some way towards understanding the components of a settled area, especially if it is buried under modern towns and agricultural land. A city like Sais may have consisted of, perhaps, numerous settlements at any one time that were distributed around the general area. In ancient times, such settlements may have been part of the estates controlled by Sais itself from the main temple zones, and together the settlements may have constituted an administrative unit. Further analysis of drill auger material, more targeted work in conjunction with floodplain geologists and dating and pollen analysis will yield significant information when collated and analysed. Most exciting is the potential for sites that have been mostly destroyed and removed to yield their information and further expand our knowledge of settlement patterns and the relationship with waterway dynamics in the Nile Delta floodplain.

Data availability. Data for the drill cores are available from the Archaeology Data Service at https://doi.org/10.5284/1081997 (Wilson, 2020).

The Landsat 5 imagery in Fig. 6 is part of the USGS Landsat 5 product (01198021202520009) from 14 February 1998, with 5 band wavelengths equal to 1.55 and 1.75. The radiometric gains and/or bias are equal to.0.1080784, −0.3700000.

Author contributions. PW compiled the article, maps and auger interpretations. HG carried out the deep-drill coring and VES work and interpretation.

Competing interests. The authors declare that they have no conflict of interest.

Special issue statement. This article is part of the special issue “Geoarchaeology of the Nile Delta”. It is a result of the workshop “Geoarchaeology of the Nile Delta: Current Research and Future Prospects”, Würzburg, Germany, 29–30 November 2019.

Acknowledgements. Thanks are due to the following people: the drill teams (Ahmed el Bishe, Esmaiein el Bishe and Ibrahim Darawy) and their supervisors (Daniel Lines, Joshua Trampier, Karen Exell, Shakira Christodoulou, Gregory Gilbert and Mohamed Gaber). The professors Adam El-Shahat, Hosni Ghazala, Mahmoud El-Gamili and Zeinab el-Sayed Belal and their teams from Mansoura University are thanked. For the discussions, we thank Benjamin Pennington, Angus Graham, Judith Bunbury, Willem Toonen and Israel Hinojosa-Baliño. For logistical support and local information, we extend our gratitude to the Ministry of Antiquities Tanta and Cairo, Inspectors Said el Assal, Emad el Shenawy and Fatma Ragab, the Egypt Exploration Society and Durham University.

Review statement. This paper was edited by Christopher Lüthgens and reviewed by Julia Meister and one anonymous referee.

References

Abrams, M. and Comer, D.: Multispectral and hyperspectral technology and archaeological applications, in: Mapping archaeological landscapes from space, edited by: Comer, D. C. and Harrower, M. J., Springer, New York, NY, 57–72, 2013.

Bakry, H. S.: A Family from Sais, Mitteilungen des Deutschen Archäologischen Instituts, Abteilung Kairo, 23, 69–74, 1968.

Bakry, H. S.: Two Saite Monuments of Two Master Physicians, Oriens Antiquus 9, 333–341, pl. XXXVIII–XL, 1970.

Barois, J.: Les irrigations en Égypte, first edn., librarie Polytechnique Ch. Béranger, Paris, 1904.

Bell, B.: Climate and the History of Egypt: the Middle Kingdom, Am. J. Archaeol., 79, 223–269, 1975.

El-Shahat, A., Ghazala, H., Wilson, P., and Belal, Z.: Lithofacies of the upper quaternary sequence of Sa el-Hagar area, Gharbiya Governorate, Nile Delta, Egypt, Journal of Geology and Geophysics, Mansoura University, 32, 79–110, 2005.

Geßler-Löhr, B.: Die heiligen Seen ägyptischer Tempel: ein Beitrag zur Deutung sakraler Baukunst im alten Ägypten, Hildesheimer Ägyptologische Beiträge, 21, Gerstenberg Verlag, Hildesheim, 1983.

Ghazala, H.: Landscape evolution during the Holocene at Sais Area based on the drilled boreholes and geoelectrical survey, unpublished report for the Sais Mission, 2005.

Ghazala, H., El-Shahat, A., Abdel Raouf, O., Wilson, P., and Belal, Z.: Geoelectrical investigations around Sa el-Hagar archaeological site, Gharbiya Governorate, Nile Delta, Egypt, Journal of Geology and Geophysics, Mansoura University, 32, 121–137, 2005.

Hartung, U., Ballet, P., Effland, A., French, P. G., Hartmann, R., Herbich, T., Hoffman, H., Hower-Tilmann, E., Kitagawa, C., Kopp, P., Kreibig, W., Lecuyot, G., Lösch, S., Marouard, G., Zink, A., Nerlich, A., Pithon, M.: Tell el-Fara'in – Buto. 10. Vorbericht, Mitteilungen des Deutschen Archäologischen Instituts, Abteilung Kairo 65, 172–188, 2009.

Hritz, C.: Contributions of GIS and Satellite-based Remote Sensing to Landscape Archaeology in the Middle East, J. Archaeol. Res., 22.3, 229–276, 2014.

Pennington, B. T.: Environmental Change in Deltaic Settings and the Emergence of Civilization. A study in palaeolandscape construction focussing on the mid-Holocene Nile Delta, available at: https://eprints.soton.ac.uk/424723/1/Ben_Pennington_PhD_Thesis_final_copy.pdf (last access: 13 May 2021), unpublished PhD Dissertation, Southampton University, Southampton, UK, 2017.

Pennington, B. T., Bunbury, J., and Hovius, N.: Emergence of Civilization, Changes in Fluvio-Deltaic Style and Nutrient Redistribution Forced by Holocene Sea-Level Rise, Geoarchaeology, 31, 194–210, 2016.

Pennington, B. T., Sturt, F., Wilson, P., Rowland, J., and Brown, A. G.: The fluvial evolution of the Holocene Nile delta, Quaternary Sci. Rev., 170, 212–231, https://doi.org/10.1016/j.quascirev.2017.06.017, 2017.

Pope, K. O. and Dahlin, B. H.: Ancient Maya Wetland Agriculture: New Insights from Ecological and Remote Sensing Research, J. Field Archaeol., 16.1, 87–106, 1989.

Toonen, W. H., Graham, A., Pennington, B. T., Hunter, M. A., Strutt, K. D., Barker, D. S., Masson-Berghoff, A., and Emery, V. L.: Holocene fluvial history of the Nile's west bank at ancient Thebes, Luxor, Egypt and its relation with cultural dynamics and basin-wide hydroclimatic variability, Geoarchaeology, 33, 273–290, 2017.

Ullmann, T., Nill, L., Schiestl, R., Trappe, J., Lange-Athinodorou, E., Baumhauer, R., and Meister, J.: Mapping buried paleogeographical features of the Nile Delta (Egypt) using the Landsat archive, E&G Quaternary Sci. J., 69, 225–245, https://doi.org/10.5194/egqsj-69-225-2020, 2020.

USGS: Fact Sheet 2015-3081, ver. 1.2, available at: https://pubs.usgs.gov/fs/2015/3081/fs20153081.pdf (last access: 18 May 2021), Landsat Earth Observation Satellites, 2020.

Vercoutter, J.: Semna South fort and the records of the Nile levels at Kumma, Kush: Journal of the Sudan Antiquities Service, 14, 125–164, 1966.

Wilson, P.: The Survey of Saïs (Sa el-Hagar), 1997–2002, Egypt Exploration Society, Excavation Memoir 77, Egypt Exploration Society, London, 2006.

Wilson, P.: Sais I: The Ramesside-Third Intermediate Period at Kom Rebwa, Egypt Exploration Society, Excavation Memoir 98, Egypt Exploration Society, London, 2011.

Wilson, P.: The Prehistoric Sequence at Sais: Temporal and Regional Connections, in: The Nile Delta as a centre of cultural interactions between Upper Egypt and the Southern Levant in the 4th millennium BC, edited by: Maczynska, A., Poznan Archaeological Museum, Poznan, Poland, 299–318, 2014.

Wilson, P., Gilbert, G., and Tassie, G.: Sais II: The Prehistoric Period, Egypt Exploration Society, Excavation Memoir 107, Egypt Exploration Society, London, 2014.

Wilson, P.: Royal City of Sais, York: Archaeology Data Service [distributor], https://doi.org/10.5284/1081997, 2020.

Wunderlich, J.: Untersuchungen zur Entwicklung des westlichen Nildeltas im Holozän, PhD thesis, Philipps-Universität, Marburg, West Germany, 1989.

Zhao, X., Thomas, I., Salem, A., Alassal, S., Liu, Y., Sun, Q., Chen, J., Fuwei, M., Finlayson, B., and Chen, Z.: Holocene climate change and its influence on early agriculture in the Nile Delta, Egypt, Paleogeography, Palaeoclimatology, Palaeoecology, 547, 109702, https://doi.org/10.1016/j.palaeo.2020.109702, 2020.

Geoarchaeology of the Nile Delta

https://www.eg-quaternary-science-journal.net/

ISSN 0424-7116